the power of

SPRINGS

to treat

SCOLIOSIS

The Power of Springs to Treat Scoliosis

Justin Vincent Christian Lemans

The Power of Springs to Treat Scoliosis

De Kracht van Veren voor het Behandelen van Scoliose

(met een samenvatting in het Nederlands)

Proefschrift

ter verkrijging van de graad van doctor aan de Universiteit Utrecht
op gezag van de rector magnificus, prof. dr. ir. W. Hazeleger
ingevolge het besluit van het college voor promoties
in het openbaar te verdedigen op

Donderdag 12 juni 2025
des middags te 2.15 uur

door

Justin Vincent Christian Lemans
Geboren op 6 mei 1993 te Utrecht

Eenvoud is niet het kenmerk van de beginner.
Het is de duur bevochten stempel van de meester.

Godfried Bomans

Table of Contents

Chapter 1
Introduction and Outline

J.V.C. Lemans

Early Onset Scoliosis

Scoliosis (from the Greek σκολίωσις meaning "a bending") is a three-dimensional (3D) deformity of the spine and trunk. The 3D deformity (Figure 1) is composed of a coronal component (i.e. lateral deviation), a sagittal component (i.e. flattening of the thoracic kyhosis) and an axial component (i.e. vertebral rotation).[1] The relation between these components, as well as the relation between the vertebral bodies and intervertebral discs (IVDs) in scoliosis as well as in the healthy spine, has been extensively studied and described by our group.[2–4] These studies provide important insights in the etiology of scoliosis, especially with respect to the adolescent type of idiopathic scoliosis.

A separate entity is Early Onset Scoliosis (EOS), which occurs when the diagnosis of scoliosis (defined as a coronal Cobb angle of ≥10°) is made before age 10. Whereas the etiology of Adolescent Idiopathic Scoliosis (AIS) is not completely known, EOS patients are classified based on the etiology of their disease, which can be roughly divided in 4 groups (Figure 1):

1. Neuromuscular EOS
Patients with neuromuscular EOS have an underlying disease that affects neurological- or muscle function. Many of these diseases (Duchenne muscular dystrophy, Spinal Muscular Atrophy, spinal cord injury) lead to paresis or paralysis, which result in long sweeping C-shaped curves that often include the pelvis, with high risk of pelvic obliquity. Untreated neuromuscular EOS has very high risk of progressing to severe curves. Since both skeletal- and respiratory musculature is often affected, many patients have compromised pulmonary function and are often wheelchair bound, with poor functioning before the onset of EOS. In contrast to these flaccid neuromuscular diseases, a subset of patients has spastic neuromuscular EOS, such as patients with cerebral palsy. The fragile health status of most neuromuscular EOS patients places them at great risk for developing complications (e.g. pneumonia or surgical site infections) when performing surgical procedures, which should therefore be kept to a minimum.

2. Congenital/Structural EOS
Congenital/Structural scoliosis is a spinal deformity that occurs during fetal development. In these patients, there is a failure of formation- or segmentation of one or more vertebrae, this is present at birth. This malformation leads to malalignment of the vertebrae over time. This in turn causes asymmetric loading, which results in progression of the curve during growth. Congenital defects are often seen in certain diseases such as Spondylocarpotarsal Synostosis Syndrome or the VACTERL association.

3. Syndromic EOS

Syndromic EOS occurs in the context of an underlying genetic or syndromic condition. In syndromic EOS, scoliosis is just one of the features associated with a broader genetic syndrome, and individuals affected may exhibit a combination of musculoskeletal, neurological, and other systemic abnormalities. According to the C-EOS classification, when a syndrome causes neuromuscular symptoms (e.g. Prader-Willi syndrome) or specific congenital spinal defects (e.g. Klippel-Feil syndrome), the EOS etiology is classified as either neuromuscular or congenital. Thus, syndromic EOS is only classified as such when the syndrome is not associated with neuromuscular symptoms, or congenital anomalies. Examples of such syndromes or genetic conditions include Ehlers-Danlos syndrome, Osteogenesis Imperfecta and Hurler syndrome.

4. Idiopathic EOS

Patients with idiopathic EOS lack any of the conditions of the previous groups. Like AIS, these patients are healthy and the etiology of the scoliosis is not completely understood. Since EOS presents earlier than AIS, EOS patients have a higher risk of progression than their AIS peers.

Figure 1: Radiographs of patients with different EOS etiologies
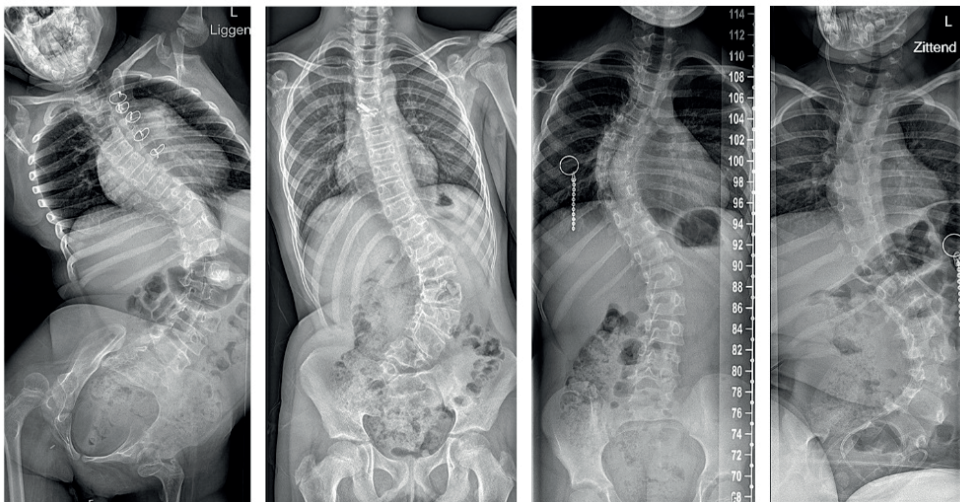
In the first picture, an example of neuromuscular EOS is seen, with a long, sweeping, C-shaped curve with substantial pelvic obliquity. The second picture shows a congenital EOS, with a hemivertebra in the distal lumbar spine. The third picture shows idiopathic EOS, with a thoracic curve that resembles AIS, and a compensatory curve in the distal spine. The last picture shows syndromic EOS, which can present as any of the other three etiologies.

Scoliosis and its effect on pulmonary function

The pediatric spine grows at different rates depending on a child's age. During the first 5 years of life, the thoracic spine grows around 1.3cm/year.[5,6] During this period, pulmonary development almost solely occurs through alveolar hyperplasia (i.e. increased number of alveoli). During age 5 through 10, spinal growth slows down to 0.7cm/year, picking up again to 1.1cm/year during puberty, which occurs around 2 years earlier in girls than in boys.[5,6] From age 5 onwards, the number of alveoli remains more or less constant, but pulmonary volume keeps increasing, due to alveolar hypertrophy (i.e. increased size of alveoli). This follows the increase of thoracic volume, which doubles in volume from 10 years old until adulthood.

Scoliosis in the growing child interferes with pulmonary volume in several ways, ultimately reducing a child's respiratory function. It limits thoracic growth, and thus volume, which decreases alveolar hyperplasia or -hypertrophy, depending on age. When the spinal deformity rotates into one of the hemithoraces, the space in which the convex lung can expand can be severely restricted. Simultaneously, the concave hemithorax is compressed, reducing its volume as well. Both phenomena can lead to asymmetric ventilation, meaning that one lung (in 60% the concave lung, in 40% the convex lung) has a much reduced function compared to the other lung (Figure 2). In severe scoliosis, the affected lung can have <20% of function compared to the contralateral side. In addition, the spinal intrusion into the thorax leads to bronchial narrowing by direct compression, which has been shown to correlate with pulmonary function loss in scoliosis.[10] The deformity also leads to reduced lung- and chest wall compliance, forcing the child to expend more energy for breathing.[11] When the thorax is unable to support cardiopulmonary growth, we speak of Thoracic Insufficiency Syndrome (TIS), a phenomenon first described by Robert Campbell and Melvin Smith, both of whom would work on the design of the innovative Vertical Expandable Prosthetic Titanium Rib (VEPTR) implant.[12,13] Dr. Redding, a renowned pediatric pulmonologist, describes the problem of TIS as follows:

> *"The child with TIS due to scoliosis can thus be described as someone with increased work of breathing, minimal chest wall excursion, who relies increasingly on one lung as the spine and chest wall deformity progress."*[11]

Figure 2: 3D CT reconstruction of thoracic insufficiency
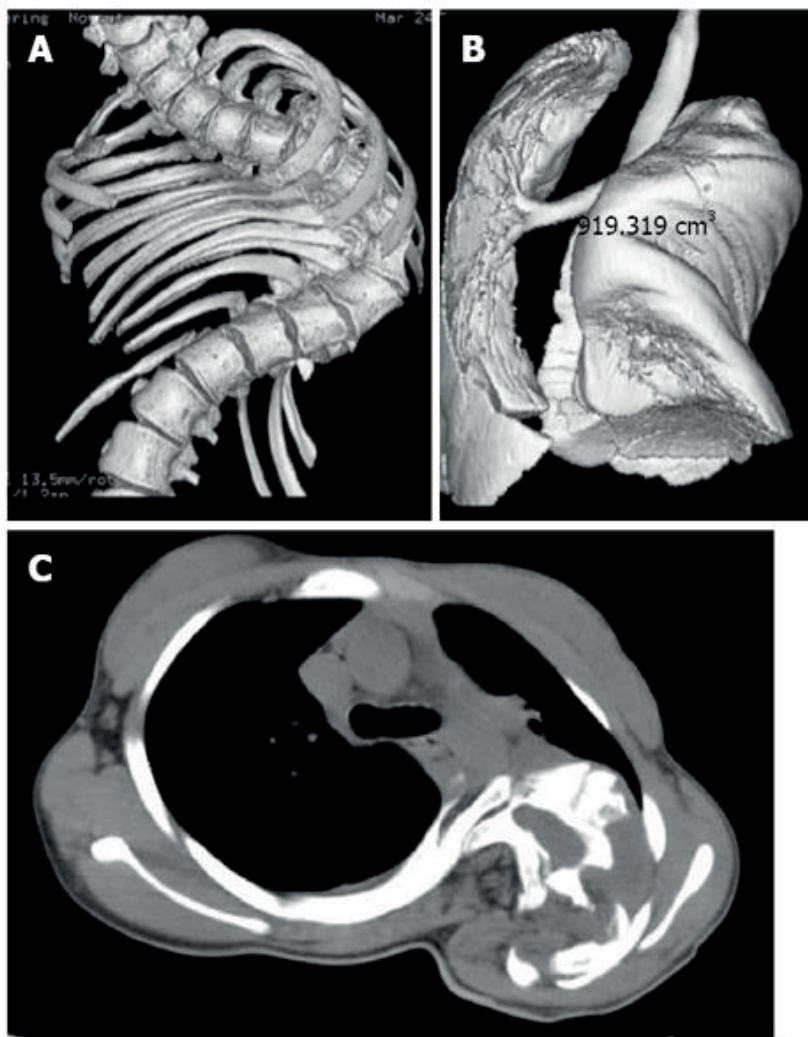
The convexity of the curve penetrates into the left hemithorax. Simultaneously, the concave hemithorax is compressed in the cranio-caudal direction.

Treatment dilemma

The previous paragraph shows that a main goal in EOS treatment is to maximize spinal- and thoracic height, so that the heart- and lungs have the chance to develop. One major part of maximizing thoracic volume is achieved by correcting the deformity, which reduces penetration of the spine within the thorax, and achieves increased spinal length. The other part is achieved by allowing the spine and thorax to continue growing. Any method that disrupts this growth, reduces pulmonary volume and is therefore at odds with the goals for treatment of EOS. This is why the classic spinal fusion is not a desirable treatment in children who have many years of growth left. While fusion is able to correct the deformity and reduce spinal penetration, it completely arrests all remaining growth in the fused segments, which will reduce further increase in pulmonary volume.[14,15] In addition, when using a posterior surgical approach, the remaining anterior spinal growth may lead to crankshafting of the spine, which leads to an increase in deformity over time.[16] Waiting for end of growth to do a spinal fusion is an alternative, although by then, the curve is often so large, that adequate correction cannot be achieved anymore.

Bracing is one method in which the curve can be reduced somewhat while the spine is allowed to grow. This can be especially effective in very young idiopathic EOS patients aged 0-3 (previously called infantile scoliosis) with continuous correction through plaster castings, also known as Mehta casting. In these patients, the continuous and strong correction has the potential to completely resolve the deformity.[17] However, in older children, such rigorous, long-term correction through a brace is generally not accepted, and thus, often ineffective.[18,19]

In the past, orthopedic surgeons thus faced the difficult dilemma in many EOS patients: Do we fuse (too) early, or do we fuse (too) late?

History of surgical treatment of Early Onset Scoliosis

During the first half of the 20th century, spinal deformities were mainly treated with physical therapy and braces. Surgical options were limited, the only surgical treatment at that time was a rudimentary spinal fusion, introduced and popularized by Russell Hibbs.[20,21] This was effected by creating a bony fusion mass near the spinous processes and facet joints of adjacent levels.

In the 1950s, Paul Harrington developed the Harrington instrumentation system to correct post-poliomyelitis spinal deformities. These neuromuscular deformities would continue to progress during life, gradually decreasing pulmonary function. Harrington already knew that control of the curve was essential to maintain pulmonary function and used the Harrington instrumentation system to try and keep the spine in a corrected position. Harrington described his technique initially without fu-

sion. He later stated that for adolescents, fusion was necessary but for younger and lighter patients that was not needed. His system allowed for segmental correction by using hooks which could distract and compress at different levels (Figure 3).[22] While effective, and the only option available, the system had several important drawbacks, including the need for 6 months of post-operative immobilization, the lack of the rod to be contoured and a high risk of hook failure and loss of correction.[23]

Figure 3: Harrington rod instrumentation
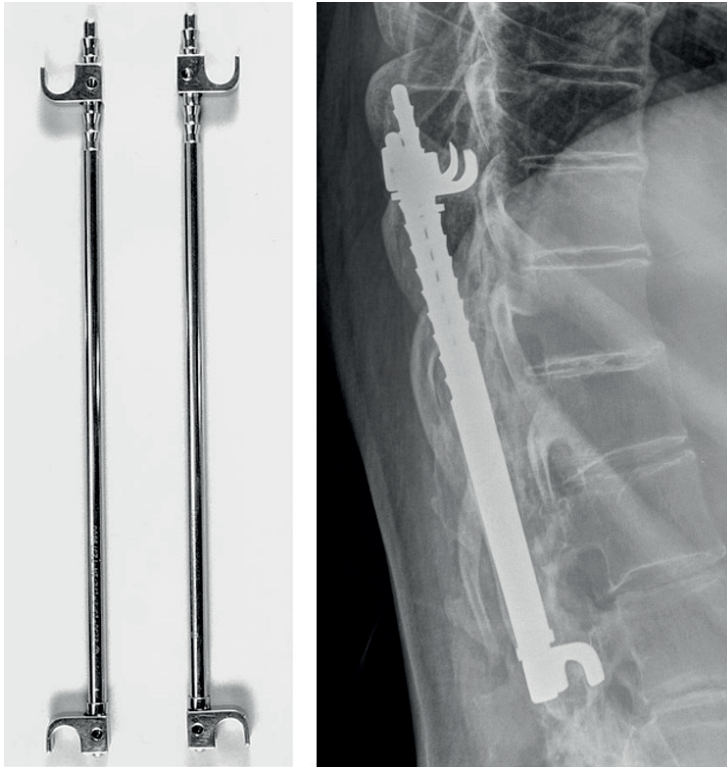
Straight notched rods were implanted in the spine, utilizing hooks to provide segmental correction of the deformity.

In the 1970s, Eduardo Luque took another approach to correct scoliosis. He developed a technique which he called segmental spinal instrumentation, where each vertebra was individually corrected towards a set of rigid rods using sublaminar wiring (Figure 4). Initially, his technique was aimed towards fusion, although Luque himself noted that some patients exhibited continued growth, while showing maintained correction.[24,25] This was caused by the fact that the sublaminar wires can slide across the rod, and thus can passively grow with the spine. This "growth-friendly" application of his initial technique was later named the Luque trolley.[26] Since no additional lengthenings take place, this is an example of a growth-guidance technique. Unfortunately, the Luque trolley technique is associated with high rates of implant failure and recurrence of the scoliosis possibly due to spontaneous lamina and facet fusions.[27,28] However, recent innovations have led to a novel trolley implant, which is a redesign of the original Luque trolley concept that aims to prevent these limitations.[29]

Figure 4: Luque trolley concept
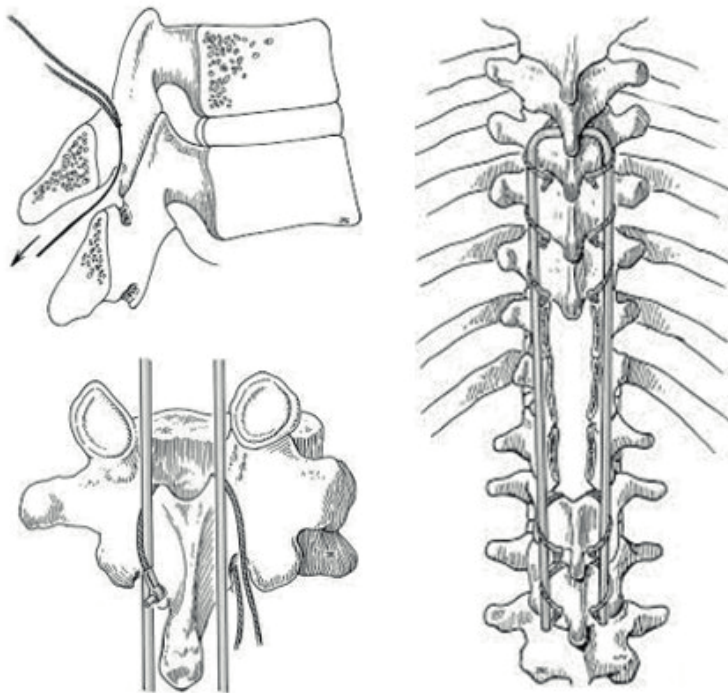
At several spinal levels, sublaminar wires are looped around one or more rods. This corrects the deformity while allowing the spine to grow.

Another growth-guidance technique is the Shilla technique, in which the apex is fused and the distal ends of the rods are mounted in pedicle screws that can slide along the rod (Figure 5). Unfortunately, this technique is also associated with a high rate of implant failure, and since many apical levels are fused, spinal growth is often disappointing.[30,31]

Figure 5: Shilla instrumentation
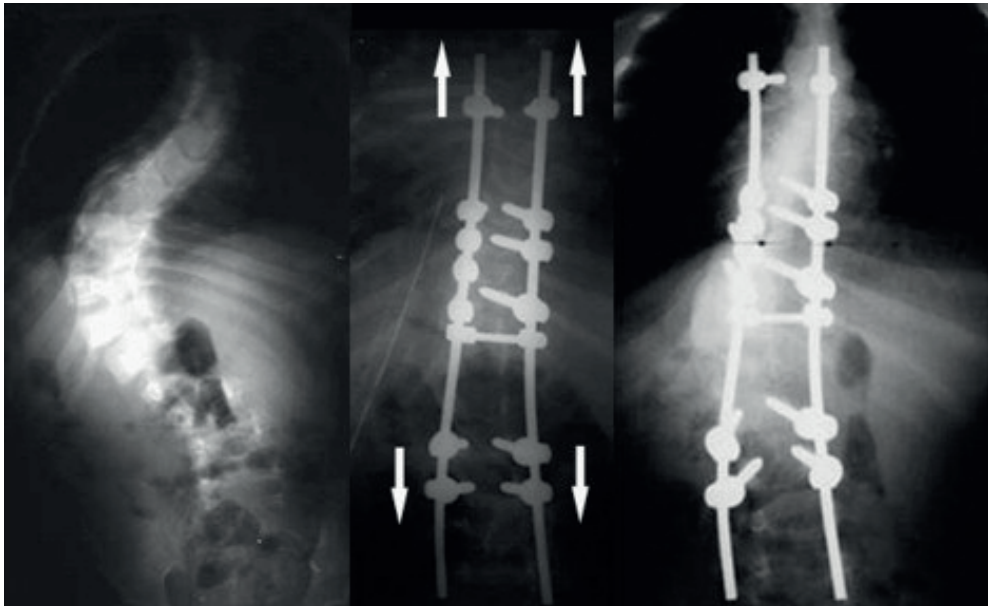
The apex is fused and the rods are able to slide through the proximal and distal screws

In contrast to growth-guidance techniques, several distraction-based techniques were developed, which not only accommodate spinal growth, but even stimulate it after the index surgery through repeated surgical or non-surgical lengthenings. One method is the traditional growing rod (TGR), wherein two sets of rods are implanted and fixated to the proximal and distal spine. These rods are then connected to one another through a side-to-side- or tandem connector (Figure 6). During growth, repeated surgeries are performed, where the connectors are unlocked, the rods are distracted and then fixated again. In this way, additional correction and spinal lengthening can be achieved with each lengthening. Correction- and growth results are generally good, but its major disadvantage is the requirement of repeated surgeries, generally one every 6 months.[32] This leads to high rates of wound-related complications; literature has shown that each lengthening procedure increases the risk of complications by 24%.[33] The treatment is an enormous burden for both the parents as well as the child, who will spend a substantial part of his or her growing life inside

the hospital. In addition, the many surgical lengthenings result in high anaesthetic stress, with potential negative neurodevelopmental consequences.[34] Finally, there is evidence that the repeated forceful lengthenings lead to damage of the spinal facet articulations, resulting in fusion and a decrease in spinal growth as the number of lengthenings increases, a phenomenon known as the "law of diminishing returns".[35]

Figure 6: Traditional growing rod
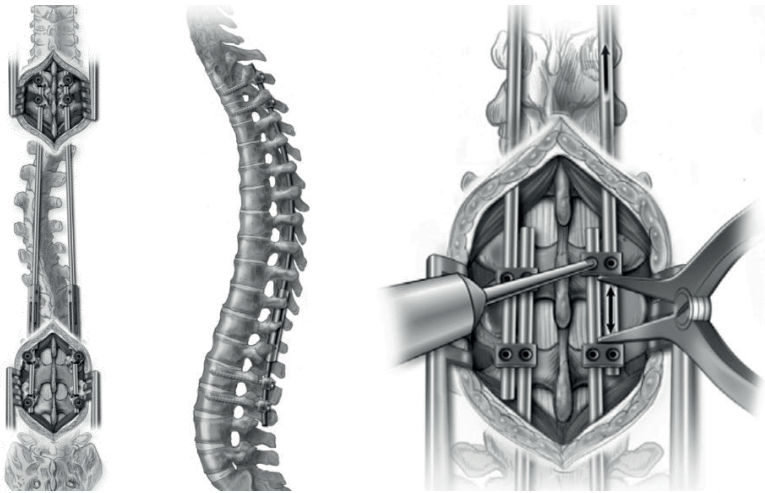
Rods are fixated to the proximal and distal spine, with pedicle screws or hooks. The rods are connected with tandem or side-to-side connectors. At regular intervals, the wound over the connector is opened and the connectors are unlocked. Then, the rods are distracted apart and the connectors are locked again.

The magnetically controlled growing rod (MCGR) was developed to combat TGRs main disadvantage; i.e. the repeated surgeries. The MCGR is a "growth-friendly" implant that uses a rod with a magnetic actuator to lengthen the spine (Figure 7). This actuator can be lengthened with an external rotating magnet without opening the wound. This innovation was met with great enthusiasm, as it eliminated the need for repeated surgeries, and allowed for more frequent lengthenings, while providing good correction and growth.[36–40] However, in the last couple of years, many studies have shown the vulnerability of MCGR. Its complex mechanism is prone to fail and may jam due to offset loading, which results in high friction, metallosis, and failure to lengthen.[41–45] The issues of metallosis have led to a temporary revocation of its CE-mark, as well as a temporary product recall in the UK and the USA.[46–48] It is currently recommended to replace the rods after 2 years of implantation.[49] Other disadvantages include its inability to be contoured, especially in the sagittal plane, and its high costs.

Figure 7: Magnetically controlled growing rod
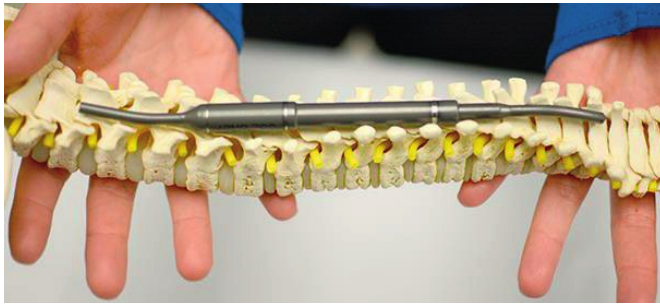
The magnetically controlled growing rod is implanted to the spine proximally and distally. It can be lengthened in the outpatient clinic with the electronic remote control.

A new philosophy

If we consider the shortcomings of current "growth-friendly" techniques and would have the opportunity to design a new and better system, this should embrace the following principles.

It should:

… aim to increase trunk height, in contrast to growth-restraining procedures.

… remove the spine from the hemi-thorax, or prevent it from dislocating there.

… retain chest and spine flexibility, thus avoiding stiffness, to preserve or improve pulmonary function.

… avoid rigid and intermittent distraction.

… be a single procedure, without repetitive surgical- or outpatient distractions.

… touch as few vertebrae as possible and allow for spinal motion to limit auto-fusion.

… allow load sharing with the spine to avoid stress shielding and anchor failure.

… allow for some mobility in the system to mitigate fatigue issues and bone loss.

… be easy to contour in all planes, especially the sagittal plane.

… promote further correction after insertion, without intervention.

… promote posterior lengthening. This is a crucial aspect because in all types of scoliosis, the system has to overcome a relatively increased anterior length.

… be easy to combine with standard implant systems.

… be able to be inserted less invasively.

Many of the above principles can be addressed if the advantages of both non-rigid growth-guidance systems (Luque/Shilla) and active distraction systems (TGR/MCGR) are combined into a single implant.

Our idea of something close to the ideal system would rely on a permanent internal distraction force. The key component of such a system is a (pre-tensioned) longitudinal helical spring that can deliver such a continuous distraction force.

History of springs in correction of scoliosis

The coil or helical spring is an ingenious human invention from the 15th century that is essential for many technological achievements where mechanics and energy transfer play a role.[50] Even using springs to aid in the correction of scoliosis is not a completely new concept. Already in the beginning of the 20th century, actually before the advent of the Harrington rods, Polish surgeon Adam Gruca experimented with the use of springs in the treatment of AIS.[51] He believed scoliosis was, in a large part, caused by muscle imbalances, and he added springs to the spine to resolve these imbalances. He created two types of spring implants, which could be attached to the spine or ribs with hooks (Figure 8). The first was a spring that would pull on the curve convexity with around 30N-50N. This was actually not unlike (but more advanced than) vertebral body tethering. Based on the size of the curve and the age of the patient, Gruca tried to calculate the total magnitude of required force (even taking into account the remaining growth of the spine), and combined multiple springs on several levels. When curves were large or stiff, he combined this spring with a concave pushing spring, to increase the corrective force. Both procedures were combined with extensive soft tissue (mainly muscle) releases and -transpositions. His initial results were promising, albeit somewhat unpredictable, with curve correction ranging between 10-100%. However, while his work was highly innovative, it was only picked up by a few surgeons.[52] This may be due to the fact that it was highly complex, both in terms of implant manufacturing, and also the extensive planning and calculation of forces that was needed. The advent of the Harrington instrumentation offered a much more accessible and predictable correction solution.

Today, coil springs can be designed and manufactured relatively easy in a wide range of materials, dimensions and forces. For the purpose of continuous distraction of the pediatric spine, the selection of the right materials and dimensions is relatively easy. The spring should be biologically inert (e.g. medical grade titanium) and the spring should fit around standard rods (e.g. 4.5mm or 5.5mm) and should allow for at least 5-7 cm of growth (~1cm/year). However, according to Hooke's law there is a linear (inverse) relation between distraction force (F) and length of the spring (L) described as

$$\Omega F = \Omega L \cdot k$$

Figure 8: Gruca's spring implants
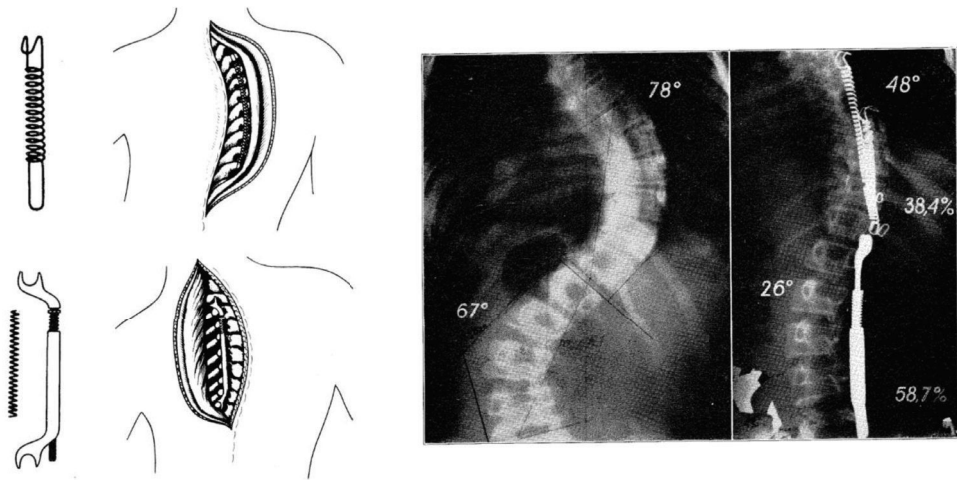
The top left shows the pulling spring used on the convexity of the curve. The bottom left shows the pushing spring used on the curve concavity. The right picture shows both systems combined, to correct what is likely a double major curve (Lenke type 3).

where k is the spring constant (in N/mm). This means that the longer the working length of the spring, the lower is the decrease in force per unit length of distraction. Variables that can be altered to change the spring dynamics include the spring material, the outer- and inner diameter, the number of coils, the coil width and the coil angle. One can imagine that many of these variables have to be constrained to a certain degree to accommodate implantation and fabrication. For example, the spring should be able to be mounted on a standard rod (and therefore has restrictions in diameter) and the entire compressed spring should fit between the anchors.

Spring Distraction System

Figure 9 shows the basic set up of what we will refer to as the Spring Distraction System. In essence, it consists of two sets of rods, that are connected with an oversized side-to-side connector that is only locked to one of the rods, so that the other rod can slide freely during growth. To provide a continuous distractive force, a spring can be tensioned on (one or both of) the sliding rods during surgery. During follow-up, the spring(s) push(es) both rods apart in the cranio-caudal direction. A spring can be added to both sides of the spine or only on the curve concavity.

Figure 9: Spring Distraction System concept
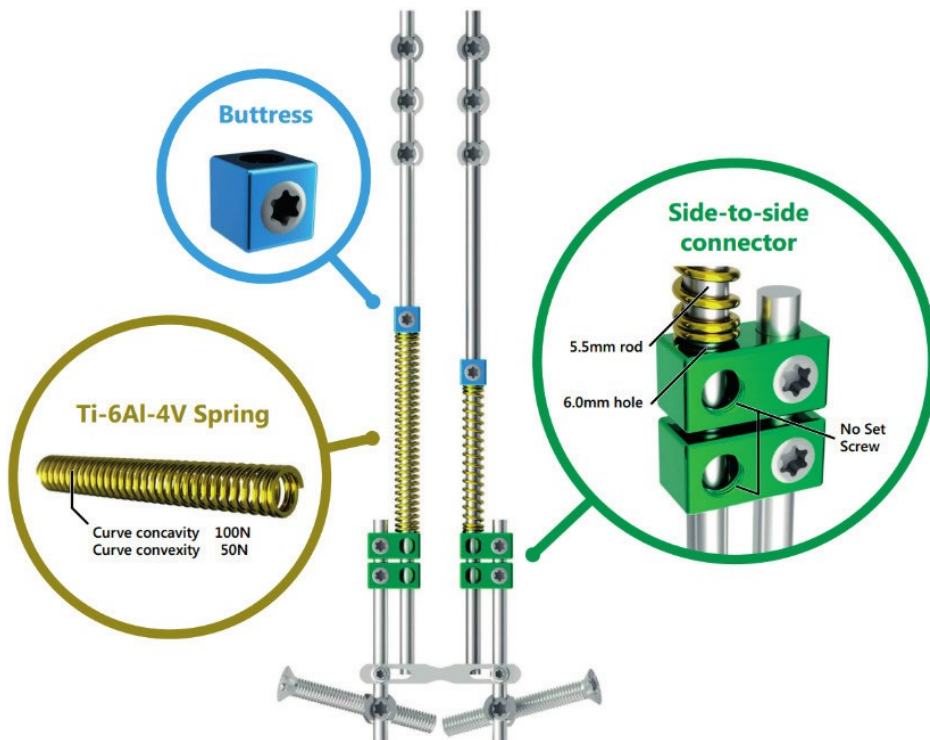
The SDS consists of standard instrumentation to which several components are added. Green: Two side-to-side connectors that have an oversized hole that can accommodate a sliding CoCr rod. Gold: Uni- or bilateral Ti6Al4V springs that are mounted on the rod and which can be compressed. Blue: A buttress block that compresses the spring against the side-to-side connector.

Initially, the SDS was designed to treat a severe progressive deformity in a patient with the spondylocarpotarsal synostosis syndrome, a rare disease. In this patient, the lamina were fused and would fuse again quickly after performing osteotomies and inserting standard distraction devices. Therefore, we were unable to treat the rapidly developing thoracic lordosis which would be fatal in time. We required a method to continuously distract the spine, to dynamically and continuously lengthen the immature fusion mass that would immediately recur after posterior spinal release. We based this on the same principle as distraction osteogenesis for limb lengthening. For that purpose, we designed relatively short 75N springs with a compressed length of 38mm that could expand to 72mm. This means that it would lengthen 34mm, and would lose 2.15N of strength with every millimeter of lengthening (75N/34mm, this parameter is identical to k, the spring constant). The patient was treated successfully

in 2015. As the concept appeared effective for these rare indications, we broadened the indications for use to different types of EOS. Since these patients have more room between the anchors, we could stack two springs which would not increase the total force, but doubled the lengthening potential to 68mm, thus halving k (i.e. the force lost per millimeter of lengthening). Using a 75N spring on both the concavity and convexity resulted in a doubling of force to 150N, while the spring constant remained the same. Using two different spring strengths, or using only a concave spring led to differential force application, which provided differential growth (i.e. lengthen the concave side more than the convex side). In subsequent years, these opportunities led to the design and manufacturing of many different spring types ranging from 50N to 150N, available in different lengths.

Currently, the SDS can be used for almost all EOS patients with an indication for surgical treatment while adopting many of the previously described principles for an ideal "growth-friendly" system:

- It actively stimulates 'growth'.
- It can address spinal penetration into the hemi-thorax.
- It ensures that distraction continues gradually over time.
- It minimizes the risk of spontaneous fusion by leaving the spine between the proximal and distal anchors untouched.
- It allows motion between the rods, especially in the axial plane, which may prevent auto-fusion.
- It allows for load sharing with the spinal segments bridged by the system. Due to this and the mobile connections, the implant is not stiff which may mitigate some of the stresses that cause (fatigue) failure. In addition, load on the spine itself prevent disuse osteoporosis.
- It allows for rod contouring in all planes, most importantly (but not exclusively) to address the sagittal plane.
- It promotes posterior lengthening which allows the spine to derotate back into the midline.
- It can be combined with almost any posterior instrumentation rod system.
- It can be inserted less invasively, like TGRs.

Anchor positions and configuration

After the indication for SDS has been made, the position of the proximal and distal anchors is chosen, which is according to the same considerations as in other "growth-friendly" techniques. If possible, only the primary curve is addressed with unilateral (concave) distraction and an additional convex sliding rod fixed to the apex.

In neuromuscular patients, the curve often extends to the pelvis which is a reason to include the lumbosacral joint.

Surgical Technique

A video showing the SDS surgical technique can be seen at https://youtu.be/pY1CL-ziKKmc. First, proximal and distal anchors are implanted via small midline incisions. Then, the distraction rod is carefully contoured and is mounted with a parallel connector fixed at least 5 cm from the end (this is the residual rod length for growth). This fixation is temporary and the parallel connector hole should be oversized (e.g. 5.5mm for a 4.5mm rod). The spring is slid over the rod from the other end against the connector and pre-tensioned between the connector and a buttress (Figure 10). This "loaded" rod is inserted subfascially from the receiving anchor to the other (push) anchor. Then the parallel connector is mounted on the receiving anchor rod using an appropriate hole size and then fixed permanently. The other end of the rod is mounted to the push anchor and then the temporary fixation of the parallel connector to the sliding rod can be released. Patients are allowed unrestricted activity, but one can choose to limit this in order to allow fusion of the anchor vertebrae which may increase their pull-out strength.

Figure 10: Tensioning the spring during surgery
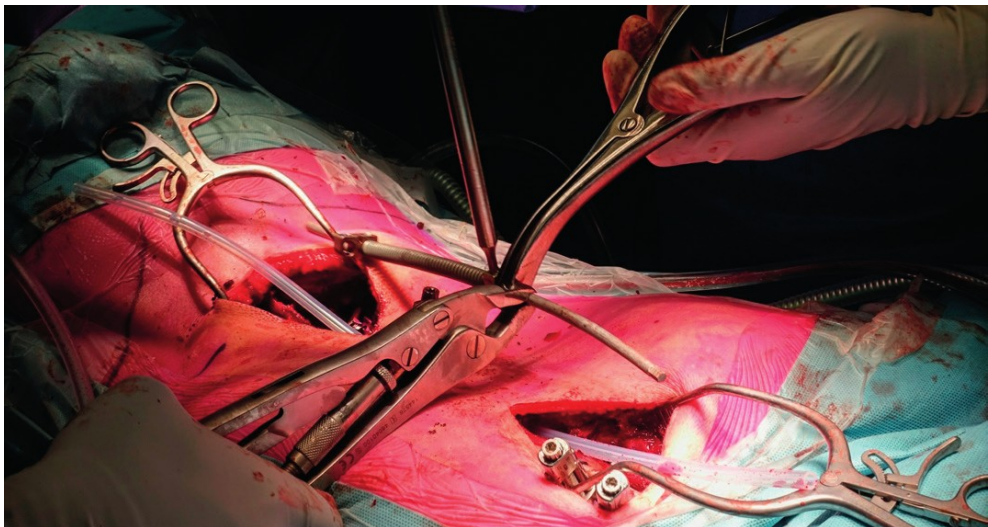
The anchors have been placed and the SDS spring is tensioned on the rod and fixated with a buttress block. When the rod is in place, the set screw in the hole of the side-to-side connector that houses the sliding rod is released and the spine will be under tension

Double Spring Reduction

Although SDS has shown its feasibility as a "growth-friendly" treatment of EOS, it cannot fully correct the scoliosis and therefore cannot be considered a curative treatment. We believe using springs in ingenious ways may also lead to innovative treatment of AIS. Only in very young patients can external forces, applied by serial casting, cure the spine while retaining spinal flexibility. In patients older than 3 years old, this external casting method is not possible anymore. Based on previous research, we hypothesize that inefficient force transfer from brace to spine and poor compliance are the causes of our inability to revert soft tissue changes, and the subsequent deformity, in older patients.[18] With current knowledge of the nature of the 3D deformity as provided by our group and with recent technological advances, there is potential for an early and complete 3D reduction of the deformity.[3,4,53] For that purpose, the concept of bracing should be harnessed in terms of strategic, continuous, corrective forces on the spine, but these forces must be applied much more efficiently and with 100% patient compliance. This may be possible by using a flexible internal brace that can continuously guide and direct the spine through the critical period of growth during which AIS develops to reverse the process and realign the spine.

   This is possible by combining the SDS technology with a derotational torque to the apex, using a torsional spring. Such a spring was designed in collaboration with Twente University. The Torsional Spring Implant consists of two in-line nickel-cobalt alloy (MP35N) torsion springs with titanium U-loops at the upper and lower ends that can slide through the upper and lower anchor bearings (Figure 11). This allows for spinal growth and even prevents loss of torque during the correction process. At the apex, the connector block between the two springs can be pre-tensioned and mounted to the apical anchor to deliver a continuous (de)rotational torque. The U-shaped loops are designed so that by spinal growth the torsional moment arm increases at the cranial and caudal anchors. This counteracts the decrease in torque that takes place due to spinal correction over time.

Figure 11: Double spring reduction
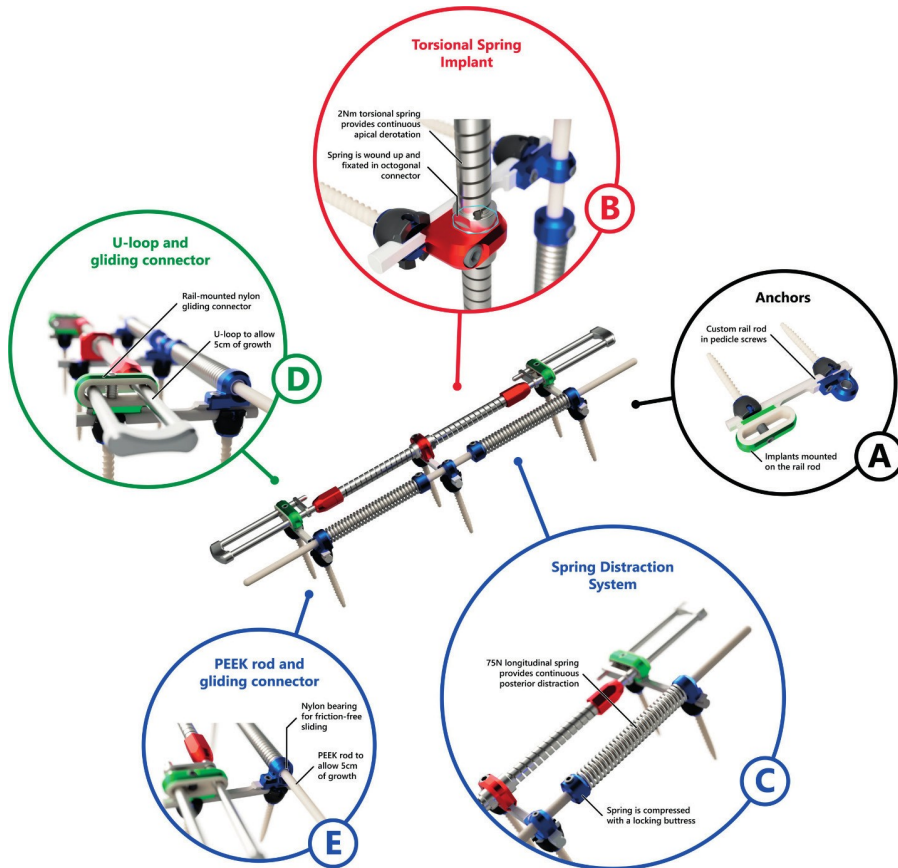
The Double Spring Reduction implant consists of two different springs that are mounted on top of custom rail rods (A). The torsional spring implant (TSI) is fixated to the curve convexity (B) and exerts a continuous axial torque to the apical level. The spring distraction system (C) is fixated to the curve concavity. Both the torsional spring implant (D) and spring distraction system (E) have sliding connectors that allow for spinal growth.

The aim of this concept, Double Spring Reduction (DSR), is to resolve the spinal deformity while the spine matures into a stable, non-scoliotic configuration. After treatment, the spine should be aligned, mobile and functional without loss of spinal height. This is essentially and principally different from current treatments, where the aim is to either stabilize the spine with an external, cumbersome brace, or where long segment fusions have to be performed. The option of DSR treatment, which can be considered as an internal dynamic brace, will change treatment perspectives entirely.

Outline of this thesis

The thesis that lies in front of you will take you through our scientific endeavour in which the SDS was developed and investigated. Starting with the requirements set forth previously and using the basic design from Figure 9, we begin by investigating several fundamental research questions in **Part I: A new philosophy**, where we address the following questions:

- **Chapter 2:** What is a safe distraction force that can be exerted on the pediatric spine?
- **Chapter 3:** Can we computationally simulate biomechanical differences between the SDS and conventional "growth-friendly" distraction systems?

A critical reader may (correctly) doubt whether these two questions are the only ones to answer before one can move from the drawing board, towards clinical studies in humans. Whilst not shown in this thesis, extensive technical, regulatory and ethical review was performed in the lead-up to the clinical studies. An extensive technical file was created together with the ISO 13485 certified department of Medical Technology and Clinical Physics of UMC Utrecht, which acted as the implant manufacturer. The technical file subsequently evolved into the Investigational Medical Device Dossier, which includes extensive information regarding spring- and manufacturing specifications, device classification, essential requirement checklist, risk analyses, user manual, quality control, and post-market surveillance and vigilance. Finally, before starting the clinical studies, ethical approval from the Institutional Review Board was granted.

Simultaneously, we had to keep in mind that the technology should ultimately become available for medical use outside of the clinical studies. This means that the implant needed to be registered according to the Medical Device Regulation (MDR) framework, which is an enormous time- and money consuming endeavour. It can only be accomplished with financial investments from industry. Therefore the intellectual property of the technique had to be secured with patents and a start-up company was created (Cresco Spine; www.cresco-spine.com).

With the above research and documentation, we were able to confidently move into **Part II: From bench to bedside**, wherein we started the clinical phase of testing. This clinical part had a hierarchical structure, starting with a small case-series of exceptional cases, to a larger prospective cohort, and finally to a randomized trial in a subset of EOS patients. In this phase, we aim to answer the following questions:

- **Chapter 4:** Is the SDS effective as a last-resort treatment in a small series of exceptional EOS patients with a severe congenital deformity?
- **Chapter 5:** Is the SDS safe and effective in a heterogenous EOS population with 2 year follow-up?
- **Chapter 6:** How can we design the world's first randomized clinical trial that compares two "growth-friendly" implants?
- **Chapter 7:** How does SDS treatment compare to treatment with a One Way Self-Expanding Rod (OWSER) in a randomized trial in neuromuscular EOS patients?

During the first phases of clinical research, several questions arose that required more in-depth analysis of specific techniques and outcome measures. These are answered in **Part III: Optimizing Spring Distraction System treatment**. The answer to the following questions allow us to continuously optimize and evaluate the SDS design:

- **Chapter 8:** What complications are common when using the SDS and how do these compare to complications seen in MCGRs?
- **Chapter 9:** How can we improve SDS design based on complications and vulnerabilities seen in previous chapters?
- **Chapter 10:** How does the SDS affect the Health-Related Quality of Life of EOS patients?
- **Chapter 11:** Are SDS outcomes different for different EOS etiologies?

Following our studies on SDS, we look ahead to the future. We believe it is possible to resolve AIS as well, by using two springs that work together to modulate spinal alignment in all dimensions. Using the results that were seen in SDS patients, **Part IV: Double Spring Reduction: The move towards two springs** paves the way for valorization of DSR, and provides pre-clinical data, which can form the basis of future clinical studies.

- **Chapter 12:** Is it possible to create an idiopathic-like scoliosis in minipigs using a combination of two springs?
- **Chapter 13:** Can we achieve 3D correction of scoliosis in growing minipigs using the DSR concept?
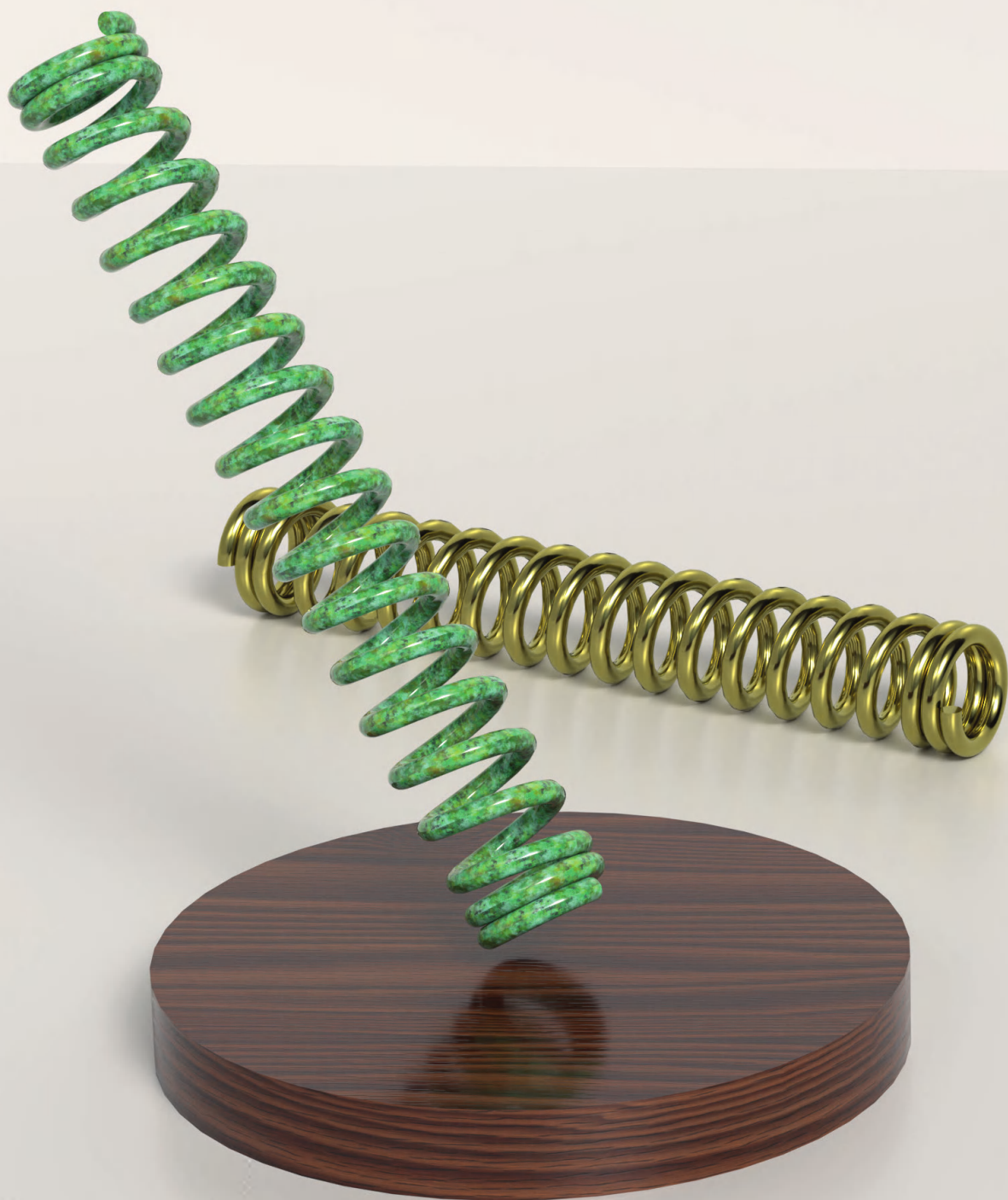
Chapter 2
Distraction Forces on the Spine in Early-Onset Scoliosis: A Systematic Review and Meta-Analysis of Clinical and Biomechanical Literature

J.V.C. Lemans
S.P.J. Wijdicks
I. Koutsoliakos
E.E.G. Hekman
A. Agarwal
R.M. Castelein
M.C. Kruyt

Abstract

Distraction-based growing rods are frequently used to treat Early-Onset Scoliosis. These use intermittent spinal distractions to maintain correction and allow for growth. It is unknown how much spinal distraction can be applied safely. We performed a systematic review and meta-analysis of clinical and biomechanical literature to identify such safety limits for the pediatric spine. This systematic review and meta-analysis was performed according to the Preferred Reporting Items for Systematic Reviews and Meta-Analyses (PRISMA) statement. Three systematic searches were performed including in-vivo, ex-vivo and in-silico literature. Study quality was assessed in all studies and data including patient- or specimen characteristics, distraction magnitude and spinal failure location and ultimate force at failure were collected. Twelve studies were included, 6 in-vivo, 4 ex-vivo and 2 in-silico studies. Mean in-vivo distraction forces ranged between 242 and 621 N with maxima of 422–981 N, without structural failures when using pedicle screw constructs. In the ex-vivo studies (only cervical spines), segment C0-C2 was strongest, with decreasing strength in more distal segments. Meta-regression analysis demonstrated that ultimate force at birth is 300–350 N, which increases approximately 100 N each year until adulthood. Ex-vivo and in-silico studies showed that yielding occurs at 70–90% of ultimate force, failure starts at the junction between endplate and intervertebral disc, after which the posterior- and anterior long ligament rupture. While data on safety of distraction forces is limited, this systematic review and meta-analysis may aid in the development of guidelines on spinal distraction and may benefit the development and optimization of contemporary and future distraction-based technologies.

Introduction

Distraction-based growing-rods are commonly used to surgically treat Early-Onset Scoliosis (EOS), a complex 3D spinal deformity. They aim to control the curve while allowing further spinal growth. Examples are the traditional growing rod (TGR) and the magnetically controlled growing rod (MCGR).[32,39] Although widely used, the magnitude and safety margins of the forces that are exerted during these distractions is still unknown. In MCGRs, the maximum force exerted by the actuator is about 200 N, although many MCGRs transmit only a fraction after several distractions.[54] TGR distraction force is determined by the surgeon that performs the distraction surgery, and these forces are rarely measured. Distraction forces are applied in a more controlled fashion with halo gravity traction (HGT), where forces up to 50% body weight are safely applied for several weeks.[55–57]

At our institution, we developed a dynamic growing-rod that exerts continuous distraction forces through a helical coil spring mounted around standard rods.[58,59] During implant design, we determined that there was a paucity of knowledge on which magnitude of distraction force can be tolerated by the pediatric spine. Pragmatically, we chose a relatively low initial force of 75 N, but higher forces may be much more effective. To aid in the development and optimization of this technology and its contemporary counterparts, a basic understanding on the safety of distraction forces in the pediatric spine needed to be established, a topic that has not yet been addressed in previous (systematic) reviews. Therefore, we performed a systematic review and meta-analysis of the clinical and biomechanical literature to identify the best evidence for upper safety limits of distraction forces on the pediatric spine.

Materials and methods

This systematic review was performed according to the Preferred Reporting Items for Systematic Reviews and Meta-Analyses (PRISMA) statement.[60] We systematically searched the literature for studies that investigated distraction forces on the pediatric spine or its components. The review consists of 3 separate sections: Section 1: In-vivo studies that clinically measure distraction forces in children. Section 2: Ex-vivo biomechanical tensile tests on whole pediatric spines or spinal sections. Section 3: In-silico models that investigate load-sharing of the spine and its components in either children or adults. Since these sections are heterogeneous in study design, the search strategy was different for each section (Table 1).

Table 1a. Search Strategy of In-vivo studies

	PubMed	Embase	Cochrane
1	force[tiab]	force:ab,ti	(force):ti,ab,kw
2	distract*[tiab]	distract*:ab,ti	(distract*):ti,ab,kw
3	spine[mesh]	'spine'/exp	mesh descriptor:[spine]
4	spine[tiab]	spine:ab,ti	(spine):ti,ab,kw
5	spinal[tiab]	spinal:ab,ti	(spinal):ti,ab,kw
6	#3 OR #4 OR #5	#3 OR #4 OR #5	#3 OR #4 OR #5
7	#1 AND #2 AND #6	#1 AND #2 AND #6	#1 AND #2 AND #6
	182 results	**215 results**	**14 results**

Date of Search: 14-01-2020

Table 1b. Search Strategy of Ex-vivo studies

	PubMed	Embase	Cochrane
1	pediat*[tiab]	pediat*:ab,ti	(pediat*):ti,ab,kw
2	paediat*[tiab]	paediat*:ab,ti	(paediat*):ti,ab,kw
3	*natal[tiab]	natal:ab,ti	(*natal):ti,ab,kw
4	child*[tiab]	child*:ab,ti	(child*):ti,ab,kw
5	adolesc*[tiab]	adolesc*:ab,ti	(adolesc*):ti,ab,kw
6	"year old"[tiab]	"year old":ab,ti	("year old"):ti,ab,kw
7	spine[ti]	spine:ti	(spine):ti
8	spinal[ti]	spinal:ti	(spinal):ti
9	vertebr*[ti]	vertebr*:ti	(vertebr*):ti
10	disc[ti]	disc:ti	(disc):ti
11	disk[ti]	disk:ti	(disk):ti
12	ligament[ti]	ligament:ti	(ligament):ti
13	physis[ti]	physis:ti	(physis):ti
14	epiphys*[ti]	epiphys*:ti	(epiphys*):ti
15	"growth plate"[ti]	"growth plate":ti	("growth plate"):ti
16	distract*[tiab]	distract*:ab,ti	(distract*):ti,ab,kw
17	tensi*[tiab]	tensi*:ab,ti	(tensi*):ti,ab,kw
18	failure[tiab]	failure:ab,ti	(failure):ti,ab,kw
19	biomech*[tiab]	biomech*:ab,ti	(biomech*):ti,ab,kw
20	force[tiab]	force:ab,ti	(force):ti,ab,kw

Date of Search: 14-01-2020

Table 1b. Search Strategy of Ex-vivo studies - Continued

21	#1 OR #2 OR #3 OR #4 Or #5 OR #6	#1 OR #2 OR #3 OR #4 OR #5 OR #6	#1 OR #2 OR #3 OR #4 Or #5 OR #6
22	#7 OR #8 OR #9 OR #10 OR #11 OR #12 OR #13 OR #14 OR #15	#7 OR #8 OR #9 OR #10 OR #11 OR #12 OR #13 OR #14 OR #15	#7 OR #8 OR #9 OR #10 OR #11 OR #12 OR #13 OR #14 OR #15
23	#16 OR #17 OR #18 OR #19 OR #20	#16 OR #17 OR #18 OR #19 OR #20	#16 OR #17 OR #18 OR #19 OR #20
24	#21 AND #22 AND #23	#21 AND #22 AND #23	#21 AND #22 AND #23
	1590 Results	**2083 Results**	**223 Results**

Date of Search: 14-01-2020

Table 1c. Search Strategy of In-silico studies

	PubMed	**Embase**	**Cochrane**
1	finite[tiab]	finite:ab,ti	(finite):ti,ab,kw
2	element[tiab]	element:ab,ti	(element):ti,ab,kw
3	"finite element analysis"[mesh]	'finite element analysis'/exp	mesh descriptor: [finite element analysis]
4	spine[mesh]	'spine'/exp	mesh descriptor: [spine]
5	spine[tiab]	spine:ab,ti	(spine):ti,ab,kw
6	spinal[tiab]	spinal:ab,ti	(spinal):ti,ab,kw
7	distract*[tiab]	distract*:ab,ti	(distract*):ti,ab,kw
8	tensi*[tiab]	tensi*:ab,ti	(tensi*):ti,ab,kw
9	failure[tiab]	failure:ab,ti	(failure):ti,ab,kw
10	#1 AND #2	#1 AND #2	#1 AND #2
11	#3 OR #10	#3 OR #10	#3 OR #10
12	#4 OR #5 OR #6	#4 OR #5 OR #6	#4 OR #5 OR #6
13	#7 OR #8 OR #9	#7 OR #8 OR #9	#7 OR #8 OR #9
14	#11 AND #12 AND #13	#11 AND #12 AND #13	#11 AND #12 AND #13
	436 results	**579 results**	**10 results**

Date of Search: 14-01-2020

Search strategy and eligibility criteria

For each section, the PubMed, Embase and Cochrane databases were systematically searched, with no restriction on publication date. We included English articles that investigated the spine or its components in distraction, and that measured or calculated distraction forces that were used. Reference screening and citation tracking was performed to find additional studies. As growth-friendly implants primarily transmit a pure distraction force (and will limit flexion/extension moments), studies investigating such moments without specifying the pure distraction component were excluded. Conference abstracts, letters and (systematic) reviews were also excluded. Additional eligibility criteria per section are outlined in Table 2.

Table 2. Eligibility Criteria

	Inclusion criteria	Exclusion criteria
Section 1: **In-vivo studies**	1. In-vivo study 2. Age < 18 years 3. Investigates spinal distraction	1. No quantitative force/stress data 2. No English language 3. Case reports, letters, reviews
Section 2: **Ex-vivo studies**	1. Biomechanical ex-vivo study of spine or spinal component 2. Age < 18 years 3. Investigates pure tension/distraction	1. Animal studies 2. Only reports data on implants 3. No quantitative force/stress data 4. No English language 5. Case reports, letters, reviews
Section 3: **In-silico studies**	1. In-silico study 2. Investigates the spine with at least 1 functional spinal unit 3. Investigates pure tension/distraction	1. Animal studies 2. Only reports data on implants 3. No quantitative force/stress data 4. Only gives results of single spinal component 5. No English language 6. Case reports, letters, reviews

Study selection and quality assessment

Title- and abstract screening was performed by two authors (JVCL and IK). Conflicts were discussed until consensus was reached. For clinical studies, quality was assessed with the Methodological Index for Non-Randomized Studies (MINORS) instrument.[61] A maximum score of 16 can be obtained for non-comparative studies, we arbitrarily defined low quality as a score below 8, moderate quality as a score between 8 and 12 and high quality as a score > 12. Since no metric to assess biomechanical- and finite element study quality was available at the time of this study, we prospectively created a quality assessment tool for each study type, based on reporting recommendations made by the US Food and Drug Administration.[62,63] All three quality assessment tools and their respective criteria are outlined in Table 3.

Table 3a. Study quality assessment for in-vivo studies (MINORS criteria)

Author(s)	Aim	Consecutive patients	Prospective data collection	Appropriate endpoints	Unbiased assessment	Appropriate follow-up	Loss to follow-up < 5%	Prospective study size calculation	Total
Waugh	2	0	1	1	1	2	2	0	9/16
Elfström and Nachemson	2	0	1	2	1	2	2	0	10/16
Dunn et al.	2	0	1	1	2	2	2	0	10/16
Noordeen et al.	2	2	2	2	1	2	2	0	13/16
Teli et al.	2	0	1	2	1	2	2	0	10/16
Agarwal et al.	2	2	2	2	1	2	2	0	13/16

Low Quality: 0–7; **Moderate Quality:** 8–12; **High Quality:** 13–16

Table 3b. Study quality assessment for ex-vivo studies

Author(s)	Aim	Protocol	Sample size	Specimens	Harvesting and treatment	Testing machine	Preconditioning and loading	Specimen accountability	Reporting force	Reporting failure	Total
Duncan	2	0	0	1	0	1	1	2	2	0	9/20
Ouyang et al.	2	2	1	2	2	2	2	1	2	1	17/20
Luck et al.	2	1	0	2	2	2	2	2	2	2	17/20
Nuckley et al.	2	1	0	2	2	2	2	2	2	1	16/20

2 points: Adequately reported. Enough information to replicate experiment. **1 point:** Reported but inadequate/unclear. Insufficient detail to replicate experiment. **0 points:** Not reported.

Low Quality: 0–10; **Moderate Quality:** 11–15; **High Quality:** 16–20

Aim: The research question of the investigation is explained, and this question can be answered through the proposed research. **Protocol:** A test protocol was prospectively created and all samples adhered to this protocol. **Sample size:** The number of included specimens was prospectively calculated and allows for valid comparisons between investigated groups. **Specimens:** A representative subset of the population is chosen to provide the specimens. Specimen characteristics (age, sex, weight) are reported. **Harvesting and treatment:** The condition under which the specimens were harvested, stored and prepared for the experiment are explained in detail and are identical for all specimens. **Testing machine:** The characteristics of the testing machine are reported, and the experimental set-up is explained in detail or is shown in a figure. **Preconditioning and loading:** Preconditioning steps and loading rate are reported. **Specimen accountability:** Data is reported for all specimens, including outliers/anomalous results. For specimens with failed measurements, a detailed explanation is provided. **Reporting force:** Force results are reported and detailed reporting is provided for each specimen explaining which structure(s) (if any) failed.

Table 3c. Study quality assessment for in-silico studies

Author(s)	Aim	Solver	Geometry and mesh	Material Properties	Assumptions and simplifications	Boundary- and loading conditions	Results	Mesh refinement	Validation	Total
DeWit and Cronin	2	2	2	2	1	2	2	2	1	16/18
Dong et al.	2	2	2	1	2	2	2	2	2	17/18

2 points: Adequately reported. Enough information to replicate experiment. **1 point:** Reported but inadequate/unclear. Insufficient detail to replicate experiment. **0 points:** Not reported.

Low Quality: 0–8; **Moderate Quality:** 9–13; **High Quality:** 14–18

Aim: The research question of the investigation is explained, and this question can be answered through the proposed research. **Solver:** The software package, version and type of simulation are reported. **Geometry and mesh:** The finite element geometry is presented in detail. This includes an explanation on how the geometry was obtained and includes details on elements and mesh used. **Material properties:** Material properties for all materials are included and referenced. **Assumptions and simplifications:** Differences with and simplifications of the model to the real-world situation are described (e.g. a rationale is provided for structures not included in the model). **Boundary and loading conditions:** Boundary conditions are explained. Initial conditions, pre-stresses and loading conditions are provided. **Results:** A relevant outcome measure was chosen and results were provided for several relevant regions in the finite element model. **Mesh refinement:** A mesh was chosen so that outcomes were not significantly influenced by element size. This was tested with mesh refinement or convergence analysis techniques. **Validation:** Results were validated to existing clinical or biomechanical data and were in accordance to that data.

2

Data extraction and statistical (meta-)analysis

Study characteristics and results regarding forces, displacement and tissue damage were extracted using standardized forms. The data of Section 2 was pooled and a meta-analysis was performed to determine relationships between age and ultimate force. Specimens were separated in three anatomical groups: C0-C2, C2-C5 and C5-T1. For each group, a least-squares second-order polynomial regression analysis was performed with age as the independent variable and ultimate force of each specimen as the dependent variable. Profile likelihood 95% confidence intervals were calculated for each regression equation and the adjusted coefficients of determination (R^2) were calculated. GraphPad Prism 8.4.1 (GraphPad Software Inc.) was used for statistical analysis.

Results

The literature searches of all sections yielded 5332 results. After title- and abstract screening, 64 studies remained for full-text screening. A PRISMA flowchart for each section is provided in Figure 1.

Figure 1. PRISMA diagram
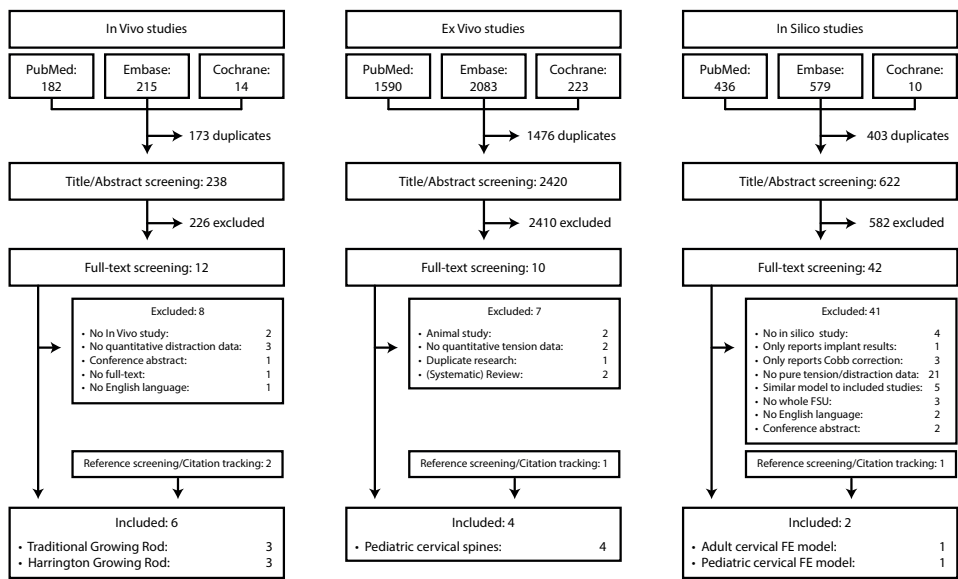
In-vivo studies: Study characteristics and -quality

Six articles were included, study characteristics and quality assessment are shown in Table 4a. Three studies investigated Harrington rod distractions,[64–66] three reported TGR distractions.[67–69] In one study, bilateral distraction was performed and mean

force was reported,[67] the others used unilateral distraction. Mean MINORS score was 10.8 (range 9–13) out of 16, indicating moderate to high study quality (Table 3a).

In-vivo studies: Force and failure results of Harrington rod distraction (Table 5a)
Waugh measured distraction force in 3 adolescent idiopathic scoliosis (AIS) patients from implantation to several hours postoperatively.[66] Maximum distraction force ranged from 177 to 373 N. In two patients, failures were observed; a laminar fracture at 373 N and several simultaneous transverse process (TP) fractures at 294 N. In the third patient, moments with high intra-abdominal pressure caused considerable increase of measured force (Coughing: 363 N, Vomiting: 677 N), although no failures were seen. Elfström and Nachemson used distraction force measurements in 8 AIS patients; maximum force was 422 N. There were two laminar fractures, at 235 N and 324 N.[65] Dunn et al. performed distraction in 12 patients in two steps; first with a slow continuous distraction outrigger, followed by the definitive, more forceful distraction.[64] Mean initial outrigger force was 332 N with a maximum of 608 N. During the forceful distractions, mean and maximum force increased to 627 N and 981 N respectively. During distraction, a laminar fracture in a patient with osteopenic bone occurred at 392 N. In all three studies, stress-relaxation was observed starting with a 40% reduction in residual forces during 30–60 min post-operatively. One study measured post-operative forces continuously for 2 weeks.[65] A further reduction in distraction forces took place so that only 40% of the force remained after 4 days. After 11 days, the unilateral residual force was relatively stable at 25% of the initial force, corresponding to around 100 N.

Table 4a. Study characteristics in-vivo studies

Author(s)	Year	Number of patients[a]	Patient type (N)	Mean age	Investigated spine location	Type of distraction	Proximal-distal anchors	MINORS score
Waugh	1966	3	AIS (3)	14.7±0.5	Thoracic–Lumbar	Harrington rod (unilateral)	1 Hook–1 Hook	9/16 (Moderate)
Elfström and Nachemson	1973	8	AIS (8)	14.0±1.6	Thoracic–Lumbar	Harrington rod (unilateral)	1 Hook–1 Hook	10/16 (Moderate)
Dunn et al.	1982	12	AIS (9), EOS (S:3)	14.7±4.3	Thoracic–Lumbar	Harrington rod (unilateral)	1 Hook–1 Hook	10/16 (Moderate)
Noordeen et al.	2011	26	EOS (I:4, S:3, NM:9, C:9)	6.5±2.3	Thoracic–Lumbar	TGR (unilateral)	3 Hooks–2 Screws	13/16 (High)
Teli et al.	2012	10	EOS (I:4, S:3, C:1, U:2)	8.3 (6–10)	Thoracic–Lumbar	TGR (unilateral)	2 Hooks–1 Screw + 1 Hook	10/16 (Moderate)
Agarwal et al.	2019	47	EOS (I:4, S:1, NM:2, C:40)	7.2±2.3	Thoracic–Lumbar	TGR (bilateral)	2 Hooks–2 Screws[b]	13/16 (High)

MINORS: Methodological Index for Non-Randomized Studies; AIS: Adolescent Idiopathic Scoliosis; EOS: Early Onset Scoliosis; TGR: Traditional Growing Rod; TP: Transverse Process; I: Idiopathic; S: Syndromic; NM: Neuromuscular; C: Congenital; U: Unknown.

[a]Only patients under age 18 were included.

[b]Used bilaterally.

Table 4b. Study characteristics ex-vivo studies

Author(s)	Year	Number of cadavers (specimens)	Specimen age (N)[a]	Investigated spine location (N)	Preparation of spine	Study method	Distraction system	Testing method and rate	Endpoint	Study quality
Duncan	1874	5 (5)	≤1 day (4) 0 yr (1)	C0-C7 (5)	Intact	Head fixed with rods at shoulders, weights added to ankles.	Manual adding of weight to pulley	Force controlled: Steps of several lbs every 30 s.	Complete severing of the cervical spine	9/20 (Low)
Ouyang et al.	2005	9 (9)	2 yr (2) 3 yr (2) 4 yr (1) 6 yr (2) 7 yr (1) 12 yr (1)	C0-T1 (9)	Removal of muscles, subcutaneous tissues.	Cranium and caudal vertebra potted and fixed to actuator in experimental frame. Then, non-destructive tests in flexion/extension and viscoelastic characterization. Then, tension until failure.	Mini-Bionix 858 MTS (MTS Systems Corp., Eden Prairie, MN, USA)	Displacement controlled: 5 mm/s.	Failure: 10% decrease in tensile load with increasing displacement.	17/20 (High)

Author(s)	Year	Number of cadavers (specimens)	Specimen age (N)[a]	Investigated spine location (N)	Preparation of spine	Study method	Distraction system	Testing method and rate	Endpoint	Study quality
Luck et al.	2013	23 (58)[b]	≤1 day (14) 0 yr (20) 1 yr (5) 6 yr (3) 7 yr (3) 9 yr (3) 12 yr (3) 14 yr (1) 16 yr (3) 17 yr (3)	C0-C2 (18) C4-C5 (21) C6-C7 (19)	Removal of muscles and subcutaneous tissues.	Cranial vertebra/ cranium and caudal vertebra potted and fixed to actuator in experimental frame. Then, tension until failure.	MTS (MTS Systems Corp., Eden Prairie, MN, USA)	Force controlled: 1000 N/s* scale factor based on T1 endplate size[c] Displacement controlled: 230 mm/s[d]	Failure: Load decrease with increasing displacement. Ultimate force: Maximum force in force–displacement curve.	17/20 (High)
Nuckley et al.	2013	8 (8)	2 yr (1) 3 yr (1) 5 yr (1) 8 yr (1) 9 yr (1) 11 yr (1) 13 yr (1) 16 yr (1)	C1-C2 (8)	Removal of muscles and subcutaneous tissues.	Cranial and caudal vertebrae potted, then non-destructive tests in compression, tension and bending. Then tension until failure.	MTS 318.10S (MTS Systems Corp., Eden Prairie, MN, USA)	Displacement controlled: 1000 mm/s.	Complete severing of the cervical spine	16/20 (High)

NR: Not reported

[a]Specified per year, 0–1 day old neonates reported separately.

[b]Several specimens included pre-term infants (>20 weeks gestation). These were counted as age ≤ 1 day.

[c]For specimens aged 0 days-5 months and 14 year old.

[d]For specimens aged > 5 months-9 years.

Table 4c. Study characteristics in-silico studies

Author(s)	Year	FEA program	Model	Included component	Material properties	Yield properties	Failure modelling	Tensile validation	Study quality
DeWit and Cronin	2012	LS-DYNA v.971 (LSTC, Livermore, CA,USA)	Male, adult, C4-C5	Cortical bone	E = 17,900 v = 0.3	σ = 190 ε = 1.8	Gradually removing elements as the critical failure stress was reached. Tie-break contacts were chosen for the disc-vertebra interface. These were broken as the failure stress was reached.	C4-C5[70]	16/18 (High)
				Cancellous bone	E = 55.6 v = 0.3	σ = 4.0 ε = 6.7			
				Bony endplate	E = 5967 v = 0.3	σ = 63.3 ε = 1.8			
				Cartilaginous endplate	E = 23.8 v = 0.4	σ = 53.3[b]			
				Annulus fibrosis	Shell elements in ground substance				
				Nucleus pulposus	K = 1720				
				ALL, PLL, LF, CL, ISL	Sigmoidal curves based on literature.[71,72]				

NA: Not applicable; NS: Not simulated

E: Young's modulus (MPa); v: Poisson's ratio; σ: Stress (MPa); ε: Strain (%); K: Bulk modulus

[a]Reported values were the used adult values, these were scaled down to pediatric values.

[b]Corresponding to a stress of 4.70 MPa across the entire disc and cartilaginous endplate.

47

Author(s)	Year	FEA program	Model	Included component	Material properties	Yield properties	Failure modelling	Tensile validation	Study quality
Dong et al.	2013	LS-DYNA v.971 (LSTC, Livermore, CA,USA)	Male, 9 years Head-T1	Cortical bone[a]	E = 13,400 v = 0.3	NS	Gradually removing elements as the critical failure stress was reached.	C4-C5[73] C6-C7[73] Head-T1[74]	17/18 (High)
				Cancellous bone[a]	E = 241 v = 0.3				
				Bony endplate[a]	E = 4480 v = 0.3				
				Cartilaginous endplate[a]	E = 23.8 v = 0.4	σ = 30			
				Epiphyseal plate	E = 25 v = 0.4				
				Annulus fibrosis[a]	Shell elements in ground substance				
				Nucleus pulposus	K = 1720				
				ALL, PLL, LF, CL, ISL[a]	Sigmoidal curves based on literature.[71,72,75]				

NA: Not applicable; NS: Not simulated

E: Young's modulus (MPa); v: Poisson's ratio; σ: Stress (MPa); ε: Strain (%); K: Bulk modulus

[a]Reported values were the used adult values, these were scaled down to pediatric values.

[b]Corresponding to a stress of 4.70 MPa across the entire disc and cartilaginous endplate.

Table 5a. In-vivo results of forces used and evidence of spinal failure

Author(s)	Year	Mean force	Maximum force[a]	Force at failure	Structural damage
Waugh	1966	242 ± 46 N	677 N	373 N	Proximal laminar fracture
				294 N	Multiple simultaneous transverse process #
Elfström and Nachemson	1973	288 ± 89 N	422 N	235 N	Proximal laminar fracture
				324 N	Proximal laminar fracture
Dunn et al.	1982	621 ± 251 N	981 N	392 N	Proximal laminar fracture
Noordeen et al.	2011	335 ± 170N[b]	645 N	NR	NR
Teli et al.	2012	331 ± 96 N	552 N	No failure	No failure
Agarwal et al.	2019	311 ± 114N[b]	578 N	455N[c]	Proximal laminar fracture

NR: Not reported; #: fracture

[a] Maximum force recorded during or after distraction.

[b] Mean force across all distraction episodes.

[c] No data for exact case, mean force at distraction episode during which damage occurred was taken.

Table 5b. Ex-vivo results of forces used and evidence of spinal failure

Author(s)	Year	Number of specimens	Segment tested (N)	Age group (N)[a]	Failure level (N)	Ultimate force[b]	Structural damage (N)
Duncan	1874	5	C0-C7 (5)	≤1 day (4)	C4-C5 (2)	405N-543N	NR (2)
					C5-C6 (1)	400N	NR (1)
					C6-C7 (1)	534N	NR (1)
				1 day-2 years (1)	C3-C4 (1)	654N	NR (1)
Ouyang et al.	2005	9	C0-T1 (9)	2–5 years (5)	C5-C6 (2)	494N-817N	# superior endplate C6 (2)
					C6-C7 (1)	570N	# inferior endplate C7 (1)
					C7-T1 (2)	531N-634N	# superior endplate T1 (1); # inferior endplate C7 (1)
				5–10 years (3)	C4-C5 (1)	892N	# superior endplate C5 (1)
					C6-C7 (1)	912N	# superior endplate C7 (1)
					C7-T1 (1)	765N	# superior endplate T1 (1)
				>10 years (1)	C7-T1	918N	# inferior endplate C7 (1)

Author(s)	Year	Number of specimens (N)	Segment tested (N)	Age group (N)[a]	Failure level (N)	Ultimate force[b]	Structural damage (N)
			C0-C2 (18)	≤1 day (4)	C1-C2 (2)	197N-275N	Atlanto-axial dislocation with Type III dens # (2)
					C2-C3 (2)	209N-242N	C2-C3 dislocation + multiple C2 # (1); Epiphyseal # inferior endplate C2 + multiple C3 # (1)
				1 day-2 years (7)	C1-C2 (3)	462N-1231N	Atlanto-axial dislocation with Type III dens # (2); Atlanto-axial dislocation + ossiculum terminale # of dens (1)
					C2-C3 (4)	174N-840N	C2-C3 dislocation + multiple C2 # (2); Epiphyseal # inferior endplate C2 (1); C2-C3 dislocation + type III dens # (1)
				5–10 years (3)	C0-C1 (1)	1761N	Basilar skull # + occipito-atlantal facet capsule disruption (1)
					C1-C2 (1)	1927N	Atlanto-axial dislocation + ossiculum terminale # of dens (1)
					C2-C3 (1)	1425N	C2 inferior vertebral body # + type III dens # (1)
				>10 years (4)	C0-C1 (3)	2703N-2970N	Occipito-atlantal + partial atlanto-axial dislocation + medial # of left condyle + avulsion of right alar ligament (1); Occipito-atlantal dislocation + C1 # in right anterior arch + right occipital condyle # (1); Occipito-atlantal dislocation (1)
					C2-C3 (1)	2350N	C2 inferior vertebral body # + bilateral spinous process (1)
Luck et al.	2013	58[b]	C4-C5 (21)	≤1 day (6)	C4-C5 (4)	174N-360N	Epiphyseal # superior endplate C5 (2); Epiphyseal # inferior endplate C4 + right neurocentral synchondrosis to posterior synchondrosis # C4 (1); Epiphyseal # inferior endplate C4 (1)
					C5-C6 (2)	57N-181N	Epiphyseal # inferior endplate C5 (1); Epiphyseal # superior endplate C6 (1
				1 day-2 years (9)	C3-C4 (3)	183N-631N	Epiphyseal # superior endplate C4 + bilateral C4 neurocentral synchondroses # + bilateral C5 lamina # (1); Epiphyseal # superior endplate C4 (2)
					C4-C5 (5)	167N-916N	Epiphyseal # inferior endplate C4 (4); Epiphyseal # superior endplate C5 (1)
					C5-C6 (1)	330N	Epiphyseal # inferior endplate C5 (1)

2

Author(s)	Year	Number of specimens (N)	Segment tested (N)	Age group (N)[a]	Failure level (N)	Ultimate force[b]	Structural damage (N)
				5–10 years (3)	C4-C5 (3)	700N–1214N	Epiphyseal # superior endplate C5 + C4 body fracture (1); Complete ligamentous and IVD disruption (1); Epiphyseal # superior endplate C5 (1).
				>10 years (3)	C4-C5 (3)	1732N–2444N	Complete ligamentous and intervertebral disc disruption + epiphyseal # inferior endplate C4 (1); C5 lamina and spinous process # + C4 vertebral body # and disruption endplate/IVD + complete ligamentous disruption (1); Epiphyseal # inferior endplate C4 (1)
				≤1 day (4)	C6-C7 (3)	154N–210N	Epiphyseal # superior endplate C7 (3)
					C7-T1 (1)	181N	Epiphyseal # inferior endplate C7 (1)
			C6-C7 (19)		C4-C5 (1)	735N	Epiphyseal # superior endplate C5 (1)
				1 day-2 years (9)	C5-C6 (4)	142N–800N	Epiphyseal # superior endplate C6 + unilateral right C6 neurocentral synchondrosis # (1); Epiphyseal # superior endplate C6 (3).
					C6-C7 (4)	152N–417N	Epiphyseal # inferior endplate C6 (1); Epiphyseal # superior endplate C7 (3)
					C6 (1)	864N	C6 vertebral body fracture (1)
				5–10 years (3)	C6-C7 (2)	814N–1758N	Complete ligamentous and IVD disruption (1); Epiphyseal # inferior endplate C6 (1)
				>10 years (3)	C6-C7 (3)	1570N–2185N	Complete ligamentous and IVD disruption + Epiphyseal # inferior endplate C6 (1); C6 lamina and spinous process # + C7 vertebral body # + C7 lamina and spinous process # (1); Epiphyseal # inferior endplate C6 (1)
Nuckley et al.	2013	8	C1-C2 (8)	2–5 years (2)	C1-C2 (2)	582–1102	Unspecified ligamentous failure (1) + type II dens # (1)
				5–10 years (3)	C1-C2 (3)	941–1543	Unspecified ligamentous failure (3)
				>10 years (3)	C1-C2 (3)	1588–1817	Unspecified ligamentous failure (3)

NR: Not reported, #: fracture, IVD: Intervertebral disc.

[a]Five groups were created: (1) ≤1 day, (2) 1 day-2 years, (3) 2–5 years, (4) 5–10 years, (5) >10 years.

[b]Several specimens included pre-term infants (> 20 weeks gestation). These were counted as age ≤ 1 day.

In-vivo studies: Force and failure results of TGR distraction (Table 5a, Figure 2)

Teli et al. investigated how forces increase during every subsequent millimeter of distraction during the first distraction episode.[69] After a threshold force of 133 N, there was a linear increase in force up to the 12th millimeter of distraction. The two other studies investigated overall increase in applied force with subsequent distractions.[67,68] Mean distraction force increased from 140 to 142 N during the first distraction to 515–555 N for the latest. Maximally applied forces ranged between 552-645 N. One TGR study reported a failure, a laminar fracture at around 450 N.[67]

Figure 2. Distraction force and failures in traditional growing rod studies
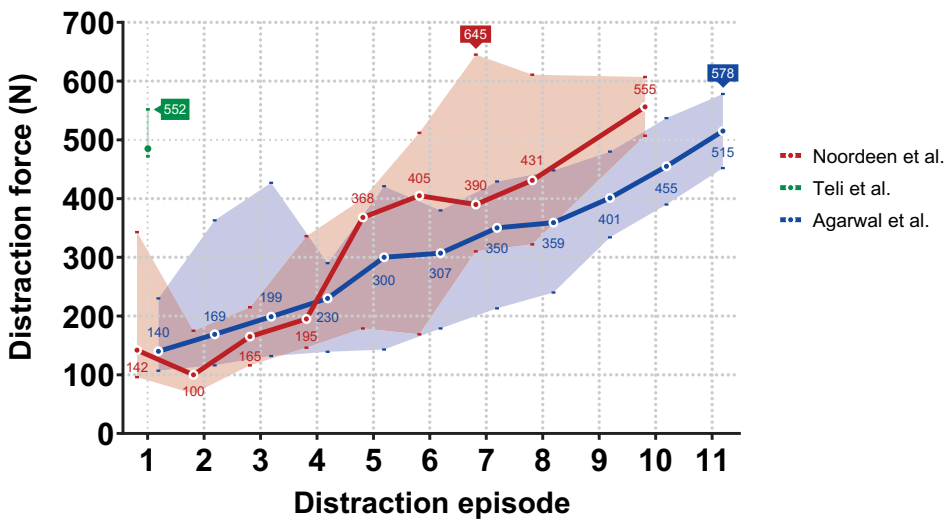
Mean[67,69] or median[68] forces with ranges are provided for each distraction episode.

Ex-vivo studies: Study characteristics and -quality

Four articles were included, study characteristics and quality assessment are shown in Table 4b. All investigated tension to failure in pediatric cervical spines. One study exclusively investigated neonatal spines,[76] the others investigated a range of age groups, from neonates to adolescents.[73,74,77] No studies investigated individual pediatric spinal components like the intervertebral disc (IVD), epiphyseal plate or spinal ligaments. Mean quality score was 14.8 (range 9–17) out of 20 (Table 3b). One study had low study quality,[76] while the other three had high study quality.

Ex-vivo studies: Force and failure results (Table 5b, Figure 3)

Already in 1874, Duncan investigated the force needed to sever the cervical spine in stillborn infants.[76] Increasing force was applied by weights through a pulley system. Mean force needed was 507 ± 95 N. All spines failed between C3 and C7, the struc-

ture that failed first was not reported. The other three studies tested ultimate force ($F_{ultimate}$) at different ages in displacement controlled experiments. Ultimate force was defined as the highest force recorded followed by a sudden decrease in reaction force with continued displacement and coincident with gross evidence of tissue damage (i.e. failure of the strongest spinal component). Luck *et al.* investigated the $F_{ultimate}$ of three different cervical levels in children of three different age groups (<2 years old, 6–9 years, 12–17 years).[73] In all age groups, C0-C2 showed the highest $F_{ultimate}$. In all levels, $F_{ultimate}$ increased non-linearly with age, with a 3–4-fold increase during the first 6–9 years and a 1.5–2.5-fold increase between 6 and 9 years and adulthood. For C0-C2, $F_{ultimate}$ increased from a mean of 436 ± 363 N in children < 2 to 2714 ± 230 N in adolescents. For C4-C5, $F_{ultimate}$ increased from 317 ± 198 N to 2030 ± 302 N. For C6-C7, these values were 292 ± 186 N and 1832 ± 259 N.

When correcting for vertebral cross-sectional area, ultimate tensile strength (UTS) also increased with age, albeit less sharply. For C6-C7, UTS was 2.7 ± 0.6 MPa for children < 2 years and 5.3 ± 1.2 MPa for adolescents. In the spines < 2 years old, failure occurred almost exclusively through the epiphyseal plate or through the cartilaginous synchondrosis. The two older age groups failed through the epiphyseal plate in half of the cases, in the other half, failure occurred at either the vertebral body or the IVD. Luck *et al.* also investigated yield force (F_{yield}), defined as the first point of lower force increase with continued displacement and coincident with visual spinal damage (i.e. failure of the weakest spinal component). Overall, F_{yield} was only slightly (~10%) lower than $F_{ultimate}$; C0-C2 showed an F_{yield} of 1016 ± 909 N versus $F_{ultimate}$ of 1116 ± 993 N. For C4-C5, these values were 652 ± 608 N and 705 ± 649 N respectively, and for C6-C7, they were 618 ± 576 N (3.0 MPa) and 694 ± 634 N (3.4 MPa). Ouyang et al. investigated $F_{ultimate}$ in entire cervical spines (C0-T1) in two age groups, 2–4 year olds and 6–12 year olds.[74] In the younger group, mean $F_{ultimate}$ was 609 ± 114 N. In older children, $F_{ultimate}$ was 872 ± 62 N. All failures occurred in the distal cervical spine, the exact structures that failed were not reported. Nuckley investigated $F_{ultimate}$ in level C1-C2 in two age groups, 2–8 year old children and 9–16 year old children.[77] In the younger group, mean $F_{ultimate}$ was 983 ± 265 N. For the older children this was 1669 ± 109 N. All failures were ligamentous failures.

Meta-analysis of the ex-vivo studies is shown in Figure 3. Residuals were normally distributed. Adjusted R^2 values of the cubic functions of different segments ranged between 0.82 and 0.86, indicating that most variation could be explained by age alone. In all segments, an increase in $F_{ultimate}$ was seen with increasing age. For C0-C2, this increase was largest during the first years, for the other segments, the increase followed a more linear trend. For the distal segments, increase in $F_{ultimate}$ was approximately 100 N/year. From infancy to end of adolescence, $F_{ultimate}$ increased from 341 N to 2453 N in C0-C2, from 342 N to 2190 N in C2-C5 and from 294 N to 1902 N in C5-T1.

Figure 3. Relation between age and ultimate force of the cervical spine
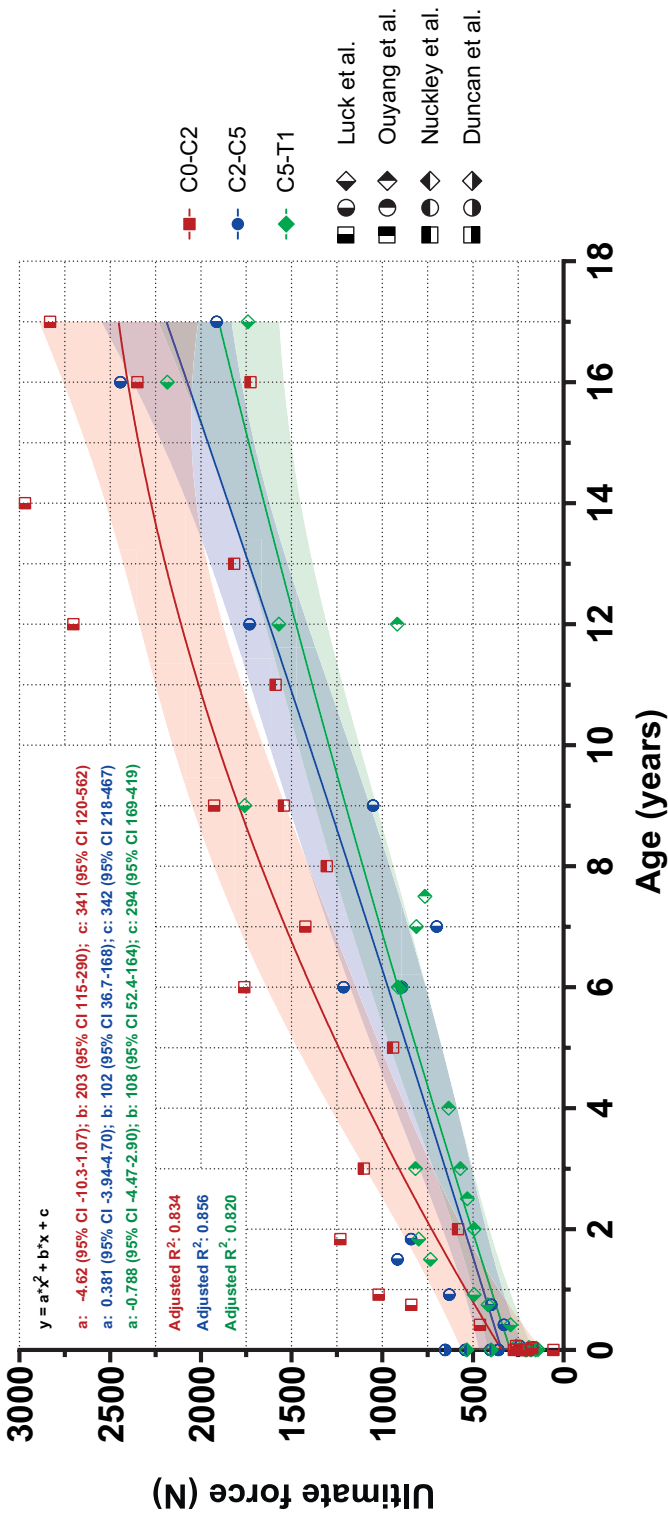
Meta-regression analysis was performed of all ex-vivo studies. For three cervical segments, the effect of age on ultimate force with adjusted R2 values are shown as well as polynomial regression curves (with 95% confidence intervals).

In-silico studies: Study characteristics and -quality

Two articles were included, study characteristics and quality assessment are shown in Table 4c. Dong et al. investigated tension to failure in an osseoligamentous FE model of a 10-year old cervical spine (Head-T1),[78] whereas DeWit and Cronin explored tensile failure in a single adult osseoligamentous functional spinal unit (C4-C5).[79] Both studies used models that included vertebral bodies, IVDs and (non-linear) ligaments. Dong et al. also included the epiphyseal plate. Both studies modelled failure, deleting elements of specific spinal components as they were loaded above their failure limit. This ensured a gradual reduction of the load-carrying capacity of the spine and permitted a detailed characterization of when and where failure occurred. Due to modelling constraints, DeWit and Cronin modelled the connection between cartilaginous endplate and IVD with tie-break elements, potentially reducing biofidelity of their failure modelling. Both studies validated their model to the respective adult or pediatric experimental literature. Mean study quality was 16.5 (range 16–17) out of 18, indicating high study quality (Table 3c).

In-silico studies: Distraction force, load sharing and failure results

The adult C4-C5 FE segment from DeWit and Cronin was validated against previous experimental tensile data.[70] During increasing displacement, several distinct peaks were seen where failure occurred (Figure 4). The first failure was a rupture between the posterior junction of the vertebral endplate and IVD at around 2600 N. With increasing IVD-endplate avulsion, the posterior long ligament (PLL; ~2500 N), anterior long ligament (ALL; ~2500 N) and anterior IVD-endplate junction failed (~1750 N). Dong et al. created an FE model that was validated against previous tensile pediatric cadaver experiments.[73,74] When simulating tension to failure at C4-C5, first failure occurred at the IVD-endplate junction at around 650 N. This is lower than the $F_{ultimate}$ or F_{yield} reported by Luck et al. However, at this point, only a small decrease in force was observed, indicating minor failure. With increasing distraction, larger decreases in force are seen indicating failure of the PLL (~890 N), followed by failure of the ALL together with the IVD-endplate junction (1060 N). For C6-C7, first failure occurred at the IVD-endplate junction (~1330 N) and $F_{ultimate}$ occurred with a PLL rupture (~1620 N). When simulating a whole cervical spine (Head-T1), first failure occurred at much higher displacement (as expected) and at a force of around 1025 N at the inferior IVD-endplate junction of C2.

Figure 4. Tension to failure results in the finite element method simulations
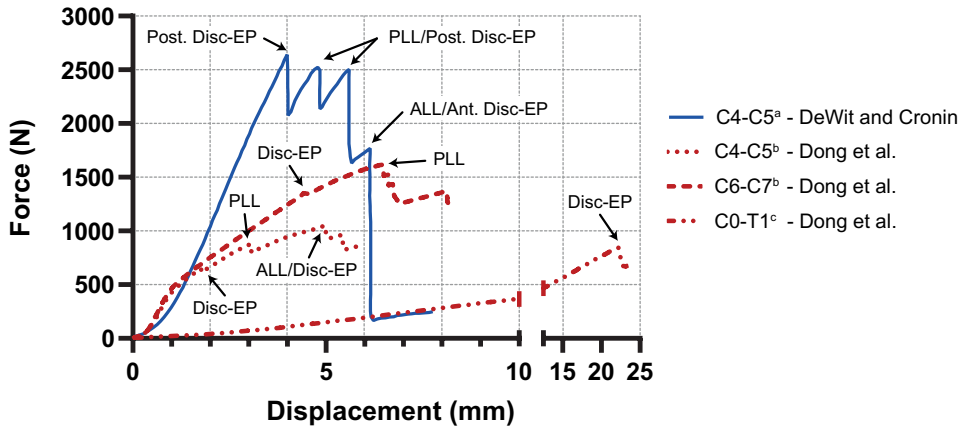
In the finite element studies, the simulated vertebrae were distracted until sequential failures occurred. The exact location of failure and the force and displacement at failure were calculated for several spinal levels. EP: Endplate (including epiphyseal plate in the pediatric model); ALL: Anterior long ligament; PLL: Posterior long ligament

[a]Material properties: Dibb et al.[70]

[b]Material properties: Luck et al.[73]

[c]Material properties: Ouyang et al.[74]

Discussion

Although distraction of the spine is often applied in deformity correction, we know little about its safety limits. Forces are generally applied based on previous experiences and common knowledge. The current study was an effort to get a better understanding of what forces can be applied safely for novel distractive implants.

In general, there was a paucity of literature on the pediatric thoracic spine where distraction implants are usually implanted. Relevant literature indicates that the force that can be applied to the pediatric spine is several times the force of body weight, much higher than forces used in HGT, TGR or MCGR. If spinal integrity fails, this is usually at or around the endplate. The resistance to failure of this structure increases with the increase in cross-sectional area during growth, but also independent of this, due to maturation.[73] As the maturation effect has also been observed quite similarly in animal species, this could enable future in-vivo research on distraction safety and efficacy.[80,81]

Since most studies investigated forces during only short periods of time, important phenomena like creep and stress relaxation were ignored. Creep properties of spinal components in tension have not been studied extensively, although its effect must take place as shown by HGTs effectiveness over time.[56,57] The included Harrington rod studies show that stress relaxation most certainly takes place during distraction surgery, where distraction forces decreased 60–75% during the first post-operative weeks. However, as distraction forces decrease non-linearly, even a micro-slippage in the Harrington rod itself could have resulted in substantial reduction of residual forces.

The FEM studies suggest that the epiphyseal plate fails first, followed by the PLL and subsequently the ALL. This pattern seems to be in accordance with those reported in the ex-vivo literature, although $F_{ultimate}$ in the FEM studies is lower.[73] It could be that micro-failures (apparent only through changes in the force–displacement diagram) are missed in the in-vivo and ex-vivo studies as they are not coincident with obvious visual changes. Potentially, such micro-failures of spinal tissues play an important role in autofusion of the spine and the "law of diminishing returns".[82,83] As micro-failures are hard to quantify in-vivo and were not subject of the current study, a safety margin should be adopted when choosing a maximum force that is to be applied. In addition, the results of the FEM studies must be interpreted with caution as many different pediatric spinal material and interaction properties are still unknown and had to be estimated from adult values.[78,79,84,85] Uncertainty margins of these estimations may cause large deviations in outcomes, as shown previously.[86,87]

Unfortunately, while an extensive search was performed, most studies that were identified focused exclusively on the cervical spine, while distraction-based therapy for EOS is primarily performed in the thoracic- and lumbar spine. Therefore, a de-

finitive answer to our research question cannot be given. Nevertheless, due to the increase in cross-sectional area of vertebral structures from cranial to caudal, these are likely stronger than cervical segments.[88–90] The observation that HGT complications almost exclusively occur in the cervical spine also suggests that the cervical structures are weakest and that the current results are therefore likely lower bounds of the true maximum, safe distraction force.[56,57] In addition, most included ex-vivo studies investigated the spine with all muscles and subcutaneous tissues removed, which has been shown to further reduce spinal strength by a factor of 2.[76,89] Taking this into account, we can make several inferences for clinical practice based on current literature. While speculative, they represent the best available evidence:

1. In-vivo literature shows that distractions of 300–400 N are common, without risk of macro-failure (when not using laminar or TP hooks).
2. Ex-vivo literature shows that $F_{ultimate}$ of spinal segments increases with age in a more or less linear fashion. This $F_{ultimate}$ is 300 N at birth, and increases around 100 N each year.
3. In-silico literature shows that first failure occurs at around 70–90% of $F_{ultimate}$ at the level of the endplate, followed by failure of the PLL and ALL.
4. Adjusting for these factors, the conservative $F_{ultimate}$ of the pediatric spine becomes approximately 800 N (age 5–6), 1000 N (age 7–8) and 1200 N (age ≥ 9).

Obviously, a margin of safety must be applied to account for individual variability and the fact that there is a paucity of data on several spinal regions. A reasonable safety factor of 4 will result in a potential maximum force of 200 N (age 5–6), 250 N (age 7–8) and 300 N (age ≥ 9) when using pedicle screw anchors. Anatomical structures at risk and bone- or soft-tissue weakness may require lowering distraction forces further. Special care must be taken to avoid excessive stress on the spinal cord and nerve roots, which have been associated with certain correction manoeuvres.[91] Whether these stresses are generated following axial distraction in growing-rod surgery is unknown, although neurological complications during spinal distraction are rarely seen.[56,67–69]

   The current study gives an approximation to the upper limit of corrective forces that can be applied to the pediatric spine. Whether maximum forces are also most effective has yet to be studied. There is evidence that frequent distractions with lower force improves curve correction, mitigates the "law of diminishing returns" and reduces complication rate.[92–94] Elucidation of these force-effects on different spinal components and implants could lead to optimization of both novel and contemporary growing-rod techniques.

   This is an attempt to review safety limits of spinal distraction forces across several clinical and biomechanical domains. This approach allows for the synthesis of data

from seemingly isolated research modalities which is useful in many fundamental and clinical sciences. Limitations include the low number of studies that could be included, and the fact that the ex-vivo and in-silico studies investigated only the cervical spine and not the thoracic and lumbar spine, which are most often instrumented. While this makes it difficult to draw definitive conclusions, the included studies are currently the best available evidence, which underscores the need for continued research on this important topic of spinal distraction.

Conclusion

Literature on safe distraction forces for the pediatric spine is limited. Clinically applied distraction forces of 300–500 N were frequently applied. Occasionally, this resulted in laminar- or TP fractures, but no study reported ligamentous disruptions or epiphyseal plate fractures. Ex-vivo cervical studies show that $F_{ultimate}$ is around 300 N at birth and increases 100 N each year, a 6–7 fold increase from birth to end of adolescence. In-silico studies show that yielding starts at 70–90% of $F_{ultimate}$ and that the junction between IVD and vertebral endplate fails first.
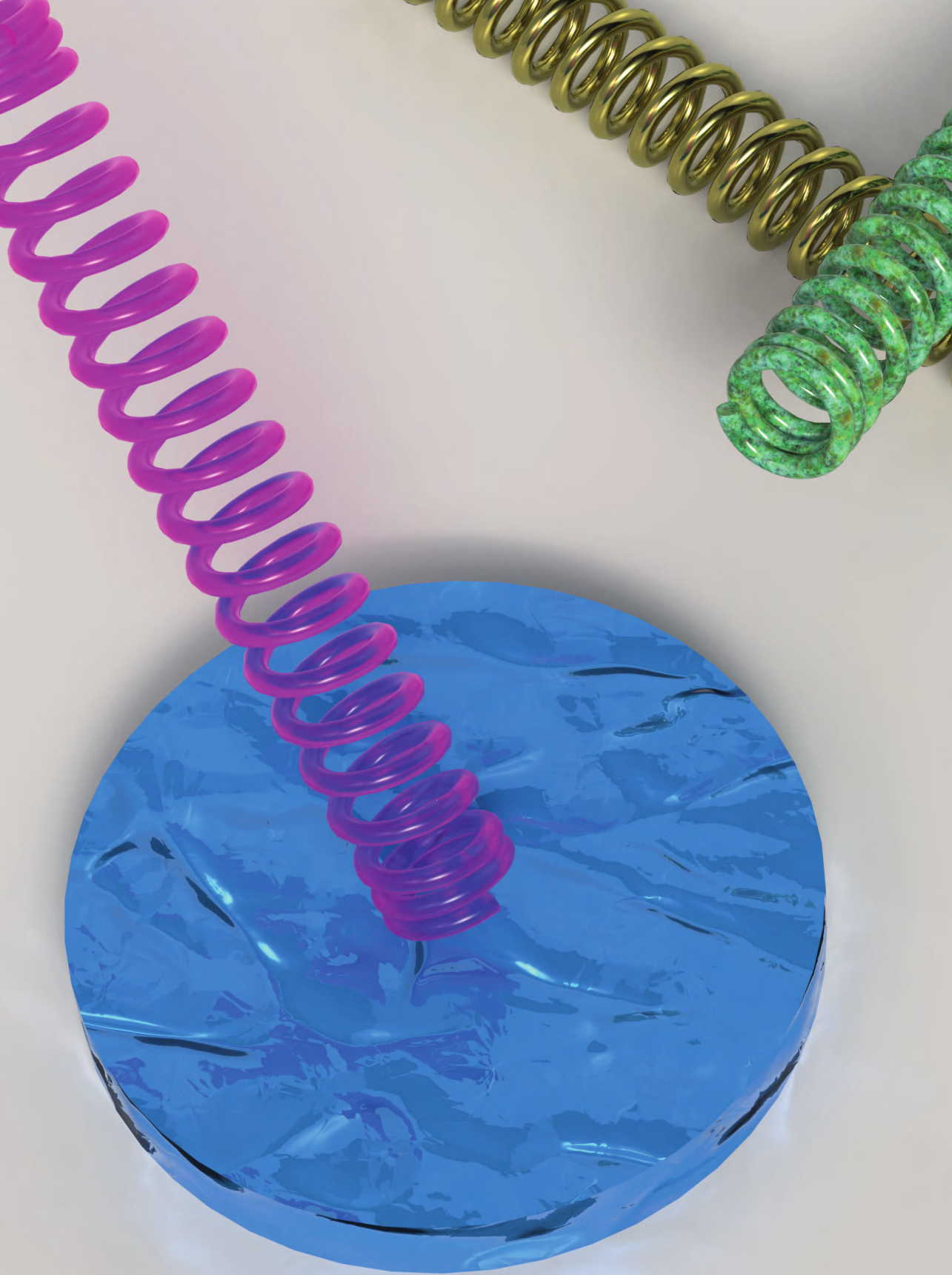
Chapter 3

Finite Element Comparison of the Spring Distraction System and the Traditional Growing Rod for the Treatment of Early Onset Scoliosis

J.V.C. Lemans

M.K. Kodigudla

A.V. Kelkar

D. Jayaswal

R.M. Castelein

M.C. Kruyt

V.K. Goel

A. Agarwal

Abstract

Study Design
Finite element analysis (FEA).

Objective
The aim of this study was to determine biomechanical differences between traditional growing rod (TGR) and spring distraction system (SDS) treatment of early-onset scoliosis.

Summary of Background Data
Many "growth-friendly" implants like the TGR show high rates of implant failure, spinal stiffening, and intervertebral disc (IVD) height loss. We developed the SDS, which employs continuous, dynamic forces to mitigate these limitations. The present FEA compares TGR and SDS implantation, followed by an 18-month growth period.

Methods
Two representative, ligamentous, scoliotic FEA models were created for this study; one representing TGR and one representing SDS. Initial implantation, and up to 18 months of physeal spinal growth were simulated. The SDS model was continuously distracted over this period; the TGR model included two additional distractions following index surgery. Outcomes included differences in rod stress, spinal morphology and IVD stress-shielding.

Results
Maximum postoperative von Mises stress was 249MPa for SDS, and 205MPa for TGR. During the 6-month TGR distraction, TGR rod stress increased over two-fold to a maximum stress of 417MPa, compared to a maximum of 262 MPa in the SDS model at 6-month follow-up. During subsequent follow-up periods, TGR rod stress remained consistently higher than stresses in the SDS model. Additional lengthenings in the TGR model led to a smaller residual curve (16.08) and higher T1-S1 growth (359 mm) at 18-month follow-up compared to the SDS model (26.98, 348 mm). During follow-up, there was less stress-shielding of the IVDs in the SDS model, compared to the TGR model. At 18-month follow-up, upper and lower IVD surfaces of the SDS model were loaded more in compression than their TGR counterparts (mean upper: +112 ± 19N; mean lower: +100 ± 17N).

Conclusion
In the present FEA, TGR treatment resulted in slightly larger curve correction compared to SDS, at the expense of increased IVD stress-shielding and a higher risk of rod fractures.

Introduction

In early-onset scoliosis (EOS), "growth-friendly" instrumentation aims to correct spinal deformities, whilst facilitating spinal and thoracic growth.[95] Distraction-based growing rods increase spinal and thoracic length using periodic implant lengthenings. One commonly used distraction-based implant is the traditional growing rod (TGR). [32] Its main disadvantage is the necessity for multiple lengthening surgeries. These require frequent anesthetic events (with potentially harmful neurodevelopmental effects) and increase the risk of wound complications.[33,34] To obviate the need for such lengthening surgeries, the magnetically controlled growing rod (MCGR) was developed, which allows for non-invasive magnetic lengthening. Although both implants are effective at controlling the deformity, they have certain disadvantages. Both systems exhibit the "law of diminishing returns," wherein later distractions do not reach the growth potential shown during earlier lengthenings.[35,67,68,96] In addition, implant complications such as screw pull-out, rod fractures and MCGR actuator failure are frequently observed.[33,42,43,45,97,98] Previous studies have implicated spinal stiffening and autofusion, which also necessitates higher periodic distraction forces, as a potential cause for both the "law of diminishing returns" and the high rate of implant complications.[82,93,99]

At our institution, a novel "growth-friendly" concept was developed that aims to circumvent both disadvantages by combining the strengths of both distraction-based- and guided-growth implants. This Spring Distraction System (SDS) employs helical springs to continuously distract growing rods that freely slide through open side-to-side connectors (Figure 1).[58,59] The continuous SDS force application removes the need for reoperations and the dynamic coupling of the rods should allow for residual spinal motion and could prevent stress-shielding of the spine, which may lower implant stresses, and prevent intervertebral disc (IVD) height loss.[100–102] Investigating these potential advantages in vivo is difficult, especially from an ethical point of view. However, in-silico comparisons between implants that use continuous distractive forces (e.g., SDS) and those that use intermittent forces (e.g., TGR) could be a second-best alternative. The present study aims to show differences between the SDS and TGR implants by simulating implantation and 18-month follow-up with physeal growth in a single, representative EOS finite element (FE) model. By performing two simulations, wherein everything but the used implant is kept identical, similarities and differences between the two strategies can be highlighted. The main investigated outcome is the magnitude and location of von Mises stresses (responsible for fatigue failure) in the rods during the course of treatment. Secondary outcomes are differences in spinal morphology during treatment (coronal Cobb angle, kyphosis/lordosis and T1-S1 height) and differences in IVD loading.

Figure 1. Spring Distraction System concept
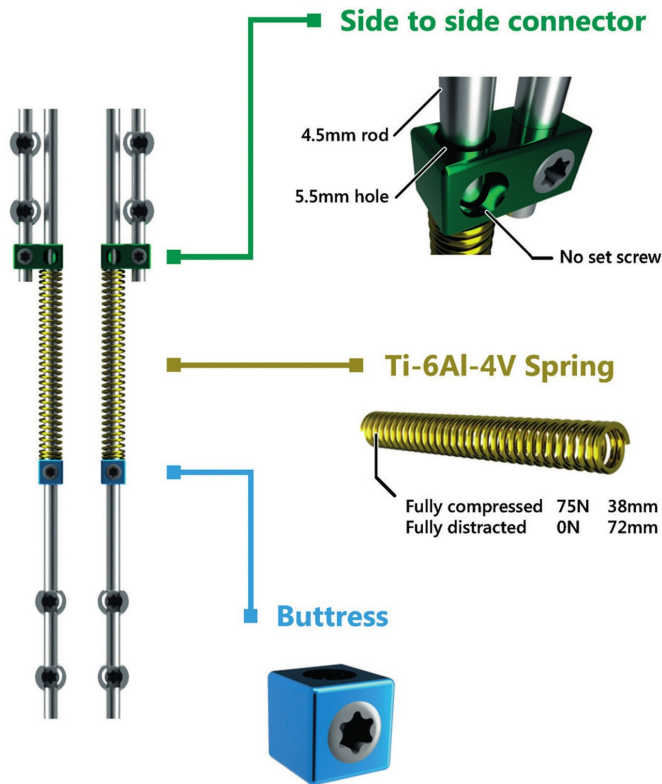
The Spring Distraction System consists of two long rods (4.5mm Co-Cr-Mo) that are able to slide through an oversized side-to-side connector (5.5mm Ti-6Al- 4V, green). A helical spring (Ti-6Al-4V, gold) with a maximum force of 75N is compressed against the connector proximally, and kept in a compressed state distally by a buttress (blue) that is mounted on the rod. During follow-up, the spring distracts the spine with attenuating force whilst lengthening from 38mm (compressed) to 72mm (uncompressed).

Materials and Methods

Finite Element Scoliotic Spine Model
A ligamentous, patient-specific, scoliotic FE model was used in this study. This was done by translating the nodes of a previously created, volumetric, ligamentous healthy spinal FE model until they matched the radiographic scoliotic curve of a real EOS patient (9-year-old female, C-EOS type I2N, T9 apex), both in the coronal (Cobb 44.8) and the sagittal plane (T5-T12 kyphosis: 25.8, L1-S1 lordosis: 52.8). The model was validated previously and has been used in several FE studies.[92,93,99,103–105]

Simulation of Surgery and Follow-up Growth

After successful creation of the curve, growing rod implantation surgery was modelled in several steps (Figure 2). Pedicle screws were inserted proximally (T2–4) and distally (L1-3). Mounting of two short rods was simulated on the proximal pedicle screws and mounting of two long rods was simulated on the distal pedicle screws. The proximal and distal rods were then connected with a side-to-side connector. The spine and implants were modelled to match the postoperative radiographic shape in both the coronal and sagittal plane. Two versions of the same model were created; one that mimicked TGR (side-to-side connector fixed to both rods after each distraction, bi-annual distraction) and one that mimicked SDS (free sliding side-to-side connector and 75N spring distraction). Except for the sliding connector and the addition of the SDS springs, both models were identical with respect to pre-operative curve morphology and intraoperative implant position. The connector was fixated to both rods in the TGR model through tie interactions, whereas in the SDS model, one rod was able to slide through the oversized connector through a sliding contact interaction (hard contact, friction coefficient: 0.1). The SDS spring was modelled as an analytical spring element between the inferior face of the side-to-side connector and a prespecified point of the rod 72 mm from the cross-connector (simulating an uncompressed spring). First, displacement control was used in both models to simulate distraction of 20 mm in the preoperative model. In the TGR model, the rods were then fixed In the connector. In the SDS model, after initial distraction, the distal end of the spring was displaced along the rod (while fixing the connector position) until a predefined length of 38 mm was reached (simulating a fully compressed spring). Then, the distal end of the spring was fixed, the connector piece released and spring distraction comenced. Spring length and stiffness (k = 2.15 N/mm) were identical to the parameters used clinically. Gravity and stabilizing muscle forces (i.e., post-surgical erect ambulation) were simulated through use of a follower load, following the sagittal spinal contour. The T1 vertebra was loaded with 14% of body weight, every subsequent vertebra was loaded with an additional 2.6% of body weight.[103,106] In the TGR model, during each distraction, the side-to-side connectors were uncoupled from the rods, and a bilateral force (130N per rod) was applied pushing the rods apart, after which the rods were both fixed to the side-to-side connector again.

Figure 2. Simulation timelines with measuring points
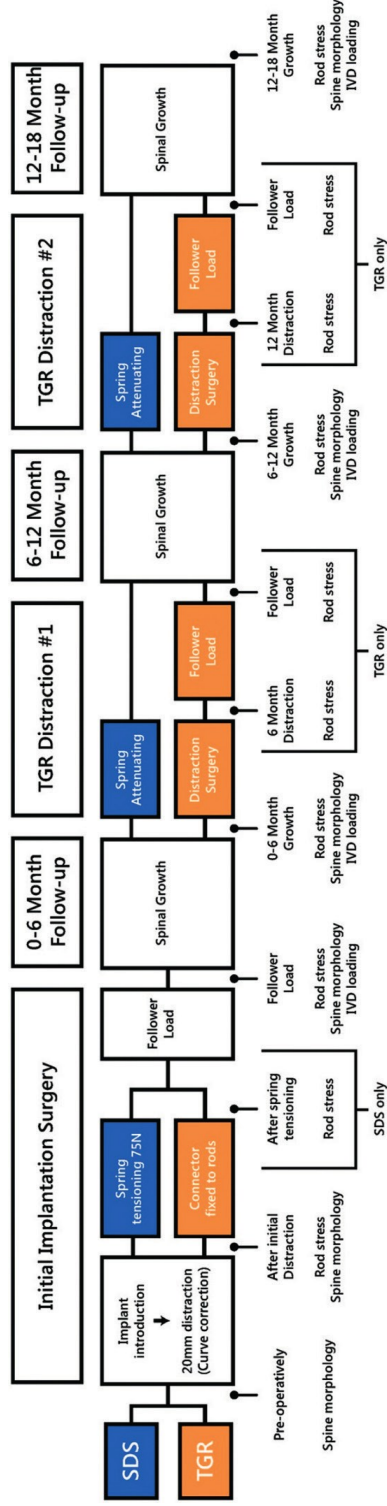
In both models, implantation surgery and 18 months of postoperative follow-up was simulated. For the SDS model, the simulation included spring tensioning and three periods of physeal growth with attenuating spring forces. For the TGR model, additional distractions were modelled at 6- and 12-month follow-up. The timepoints where rod stress, spine morphology and intervertebral disc loading were compared can be seen in the bottom of the figure for each model. IVD indicates intervertebral disc; SDS, Spring Distraction System; TGvR, traditional growing rod.

Material properties in the models were taken from the literature and were similar to values used in previously reported FE studies (Table 1).[107] The inferior surface of S1 was fixed in all degrees of freedom. Spinal growth was modelled using a previously employed method, in which the Hueter-Volkmann law describing physeal growth was emulated through the equation: $G=Gm"[1-β(σ-σm)]$ (G: The actual spinal growth strain, $Gm"$: The baseline spinal growth strain (0.035/6 months), σ: The actual compressive stress (MPa) on the spinal physis, $σm$: The baseline compressive stress (MPa) on the spinal physis, β: 1.5 MPa^{-1}).[108–110] These values were calculated during each simulation step, after which the physeal forces were converted to growth strains. These growth changes were then divided equally over the spanned vertebral body elements of the growth plates, increasing vertebral body size.

Design of the instrumentation was performed in Solidworks (Dassault Systémes, SolidWorks Corporation, Waltham, MA). The creation of the spine models, as well as the FE analyses were performed with Abaqus CAE v6.14 (Dassault Systémes, SIMULIA, Providence, RI).

Table 1. Element- and Material Properties

Material	Element used	Young's Modulus (MPa)	Poisson Ratio	Other Properties
Cortical bone	Linear hexahedral (C3D8)	75	0.29	Cortical bone
Cancellous bone	Linear hexahedral (C3D8)	75	0.29	
Posterior bone	Linear hexahedral (C3D8)	200	0.25	
Annulus fibrosis (ground)	Neo-Hookean hexahedral (C3D8)			C10 = 0.348 D1 = 0.3
Annulus fibrosis (fibers)	Rebar elements	357–550		
Nucleus pulposus	Linear hexahedral (C3D8H)	1	0.4999	
Apophyseal joints	Nonlinear soft contact, GAPUNI element	12,000		
Ligaments	Tension only truss elements (T3D2)	90% of adult values[107]		
Ti-6Al-4V	Linear hexahedral (C3D8)	115,000	0.30	
Co-Cr-Mo	Linear hexahedral (C3D8)	210,000	0.29	
Spring	Analytical Spring element			K = 2.15 Uncompressed length: 72 mm Compressed length: 38 mm

Co-Cr-Mo: cobalt-chrome-molybdenum; k: spring constant; NA: not applicable; Ti-6Al-4V: Medical grade titanium.

Analysis and Outcomes

In both models, we simulated distraction and physeal spinal growth until 18-month follow-up, just before (not including) the 18-month TGR distraction. The SDS continually distracts during this follow-up, where spring forces linearly decrease as they increase in length (75N at 38 mm; 0N at 72 mm). For the TGR model, two distractions after the index surgery (6- and 12-month distraction) were modelled according to current standard of care. The simulation steps and the evaluated follow-up points in the different models are shown in Figure 2. The primary outcome was von Mises stress in the rods. Maximum stress was identified in each of the four rods, excluding the interacting rod surfaces. Rod stress was compared intraoperatively, postoperatively after follower load introduction, and at 6-, 12-, and 18-month follow-up. For the TGR model, rod stresses before and after each distraction were determined. The size and location of maximum stress in every rod was evaluated and compared between both implants. Secondary outcomes were the coronal Cobb angles, T5-T12 kyphosis, L1-S1 lordosis and T1-S1 height, which were measured by measuring the length and angles between pre-specified elements across the relevant vertebral endplates. Loading of the IVD was measured for each IVD within the distraction construct (i.e., IVDs in the segment between the proximal and distal screws) by measuring compressive/tensile loads normal to the superior and inferior IVD surface using free-body diagrams. These values were graphed and compared at different time-points for both models.

Results

The final FE models included 589,466 (SDS) and 609,628 (TGR) nodes and 448,918 (SDS), and 466,164 (TGR) elements, respectively. The instrumented model is shown in Figure 3A-D. To find a balance between mesh accuracy and computational efficiency, a mesh convergence (h-refinement) study was performed on the rod meshes until rod stresses between three consecutive mesh densities varied <5%. Ultimately, this resulted in a rod element size of ~0.5 mm.

Figure 3. Instrumented finite element model
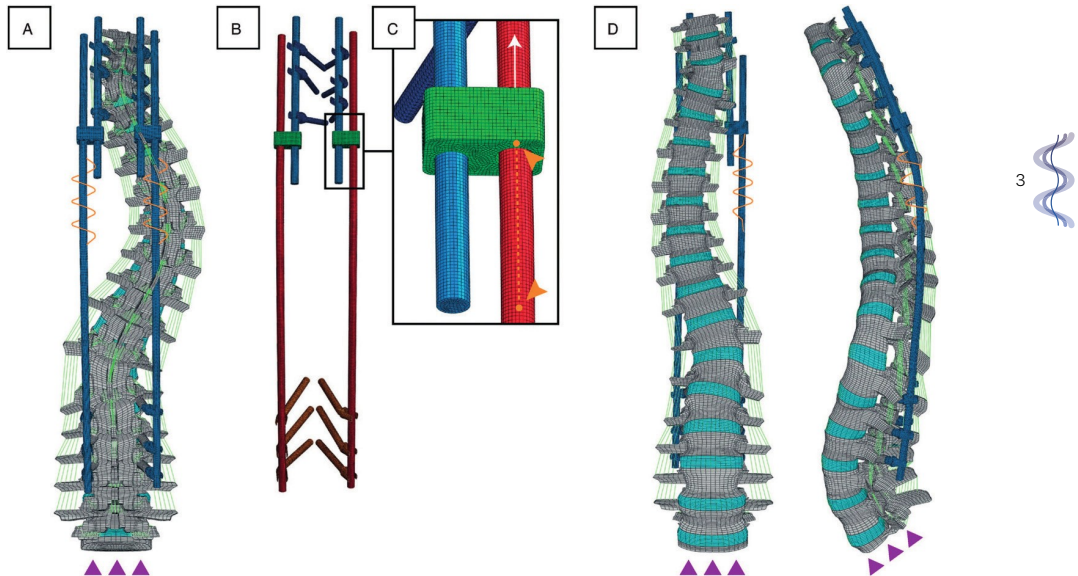
A: Posterior view of the model with implants (blue) and the SDS springs (orange). During simulation, the inferior side of S1 is fixed in all degrees of freedom (purple triangles). B: Rod and screw configuration. The proximal rods (blue) are tied to the proximal pedicle screws and to the side-to-side connector (green). The distal rods (red) are mounted on the distal pedicle screws and are either tied to the side-to-side connector (TGR) or are able to slide through it (SDS). C: The expanded view shows the sliding direction of the connector over the rod during growth (white arrow). The SDS spring is fixated on one side onto the inferior face of the side- to-side connector and on the other side onto the sliding rod after having been compressed (orange arrows). D: Anterior and sagittal view of the instrumented spine. SDS indicates Spring Distraction System; TGR, traditional growing rod.

Von Mises rod stress magnitude for the different models is shown in Figure 4 (SDS) and Figure 5 (TGR). Maximum Von Mises stress postoperatively (after follower load introduction) was 249 MPa for SDS and 205 MPa for TGR. At the end of the 6-month follow-up (before the first additional TGR distraction), maximum stress in the SDS rods was 30 to 89 MPa higher compared to the respective TGR rods. However, already during the first TGR distraction at 6 months, maximum von Mises stresses in the TGR rods increased over two-fold with a maximum of 417 MPa (bottom left rod), 59% higher than the maximum SDS rod stress (262 MPa). TGR rod stresses decreased somewhat as follower load was applied, decreased further during spinal growth but increased again during the next distraction. Overall, starting at the 6-month distraction, TGR von Mises stresses remained consistently higher than those in the SDS model, where a maximum of 296 MPa was seen at the end of 18- month follow-up. Stress plots with the location of increased rod stress are

shown in Figure 6 (TGR) and Figure 7 (SDS). There were characteristic differences in stress location between models that were already present after the initial surgery. For the TGR model, stress maxima were consistently present in the mid-construct section of the long rods, whereas in the SDS model, stresses were distributed near the rod-screw interface. During each TGR distraction, stresses shifted towards the vicinity of the distal anchor sites; then during spinal growth, the stress maxima returned to the mid-construct of the long rods. Overall, the TGR model had larger regions of increased stress compared to the SDS model.

Figure 4. Spring Distraction System von Mises stress over time
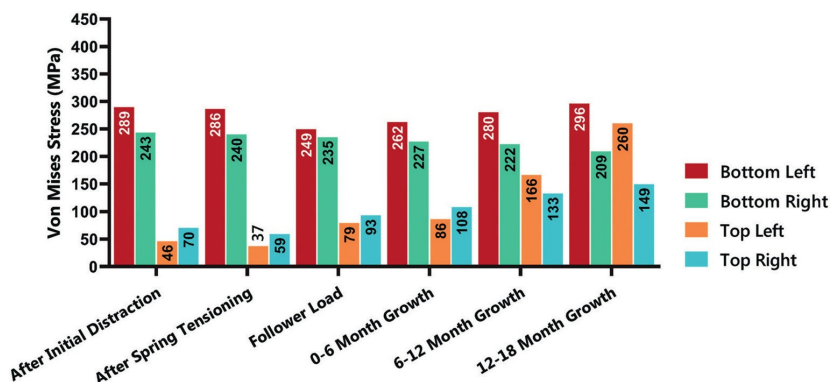
Each bar denotes a different rod used in the construct. Von Mises stress in MPa.

Figure 5. Traditional Growing Rod von Mises stress over time
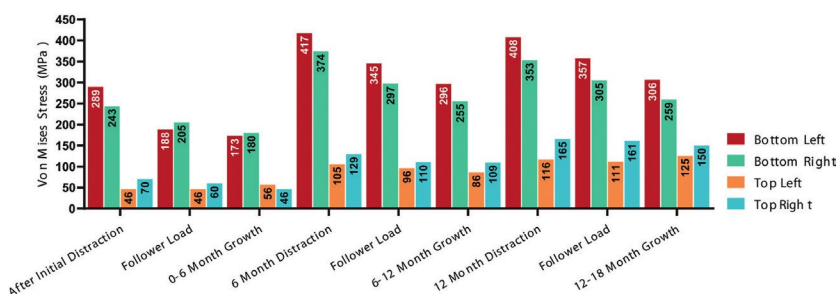
Each bar denotes a different rod used in the construct. Von Mises stress in MPa.

Figure 6. Von Mises stress plots in the Spring Distraction System model
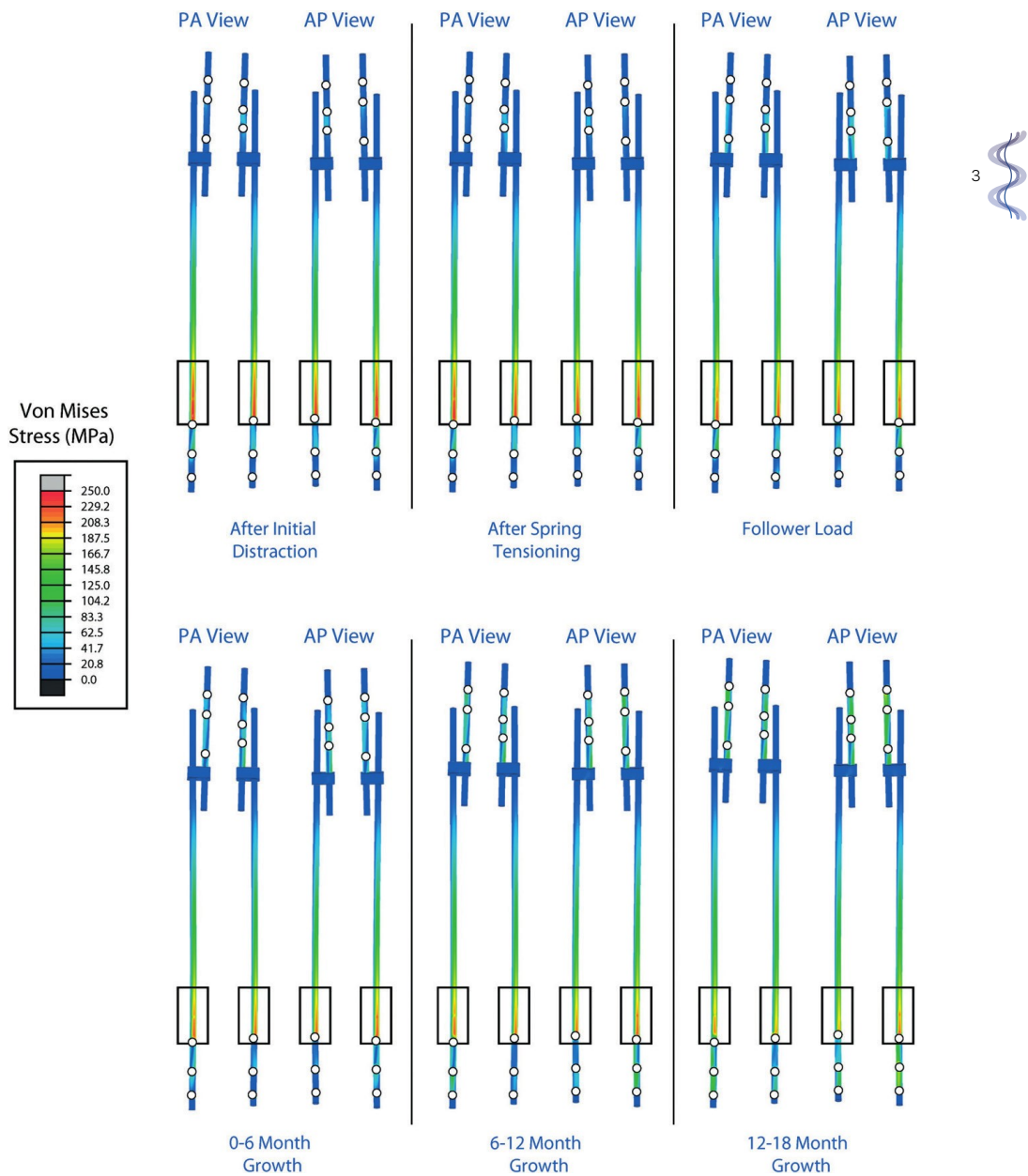
Stress magnitude and locations in each rod are shown in the PA and AP positions. Changes over time are shown from top left to bottom right. The regions of high stress are outlined in black. AP indicates anterior-posterior; PA, posterior-anterior.

Figure 7. Von Mises stress plots in the Traditional Growing Rod model
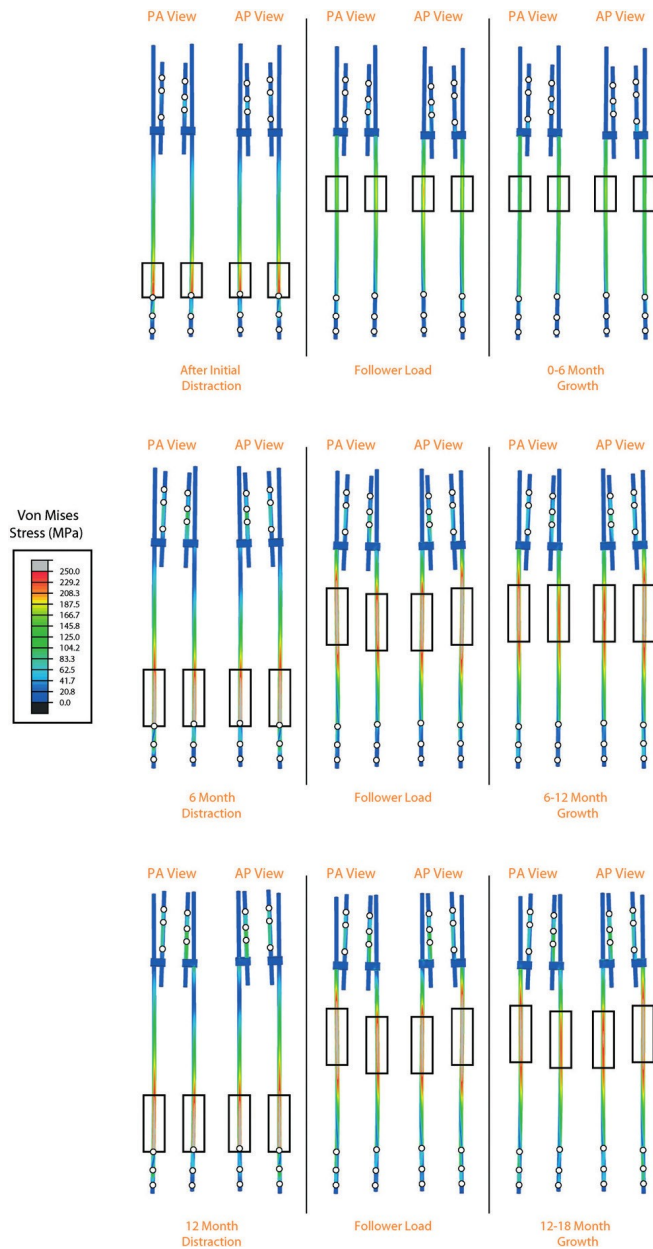
Stress magnitude and locations in each rod are shown in the PA and AP positions. Changes over time are shown from top left to bottom right. The regions of high stress are outlined in black. AP indicates anterior-posterior; PA, posterior-anterior.

Secondary outcomes are shown in Table 2. The initial main coronal curve of 43.9° decreased to 22.2° (SDS) and 23.0° (TGR) postoperatively. The additional lengthenings in the TGR model led to a smaller residual curve at 18-month follow-up compared to the SDS model (SDS: 26.9°, TGR: 16.0°). Sagittal profile was similar in both models, although the SDS was able to induce a stronger thoracic kyphosis at 18-month follow-up (SDS: 22.7°; TGR: 16.6°). T1-S1 height at 18-month follow-up was 347.5 mm for the SDS model compared to 359.2 mm for the TGR model.

3

Table 2. Spinal Morphology Over Time

	Timepoint	SDS	TGR
Main coronal Cobb angle (°)	Preoperative	43.9	
	Postoperative[a]	22.2	23.0
	0-6 mo Growth[b]	23.2	28.3
	6-12 mo Growth[b]	25.3	19.3
	12-18 mo Growth[b]	26.9	16.0
T5-T12 kyphosis (°)	Preoperative	25.1	
	Postoperative[a]	19.9	20.0
	0–6 mo Growth[b]	20.6	21.7
	6–12 mo Growth[b]	21.5	18.9
	12–18 mo Growth[b]	22.7	16.6
L1-S1 lordosis (°)	Preoperative	49.0	
	Postoperative[a]	47.4	48.2
	0–6 mo Growth[b]	47.5	48.2
	6–12 mo Growth[b]	48.3	47.6
	12–18 mo Growth[b]	48.9	47.4
T1-S1 height (mm)	Preoperative	323.5	
	Postoperative[a]	336.7	336.3
	0–6 mo Growth[b]	340.7	338.2
	6–12 mo Growth[b]	344.5	351.6
	12–18 mo Growth[b]	347.5	359.2

As the SDS and TGR model are the same until start of treatment, the preoperative values are identical for both implant systems.

[a]After follower load introduction.

[b]Represents the value at the end of the respective growth period (for TGR, this represents the value just before a distraction).

The compressive/tensile loads on the IVDs spanned by the growing construct can be seen in Figure 8. Although the SDS model initially showed lower relative compressive forces across the superior and inferior IVD surface compared to the TGR model, this reversed following the TGR distraction at 6 months. At 18-month follow-up, the upper IVD surfaces in the SDS model were all under higher compressive loads (mean difference: +112 ± 19N) than their TGR counterparts. For the lower IVD surfaces, the same pattern was seen with higher compressive loads in the SDS model (mean difference: +100 ± 17N).

Discussion

The present study demonstrated characteristic differences between the TGR and SDS in a representative, EOS FE model. An important difference was the overall higher implant stresses seen during the periodic TGR lengthenings, compared to the SDS. These additional lengthenings with higher force in the TGR model resulted in additional curve correction and higher T1-S1 growth compared to the SDS model. This continuously increasing curve correction in subsequent TGR lengthenings, however, contradicts clinical literature, where this phenomenon is rarely seen (when excluding length gain during final fusion).[31] This discrepancy can be explained by the fact that the current FE model did not take into account the effect of spinal stiffening and autofusion that takes place when using forceful distractions.

These have been linked to cause both the "law of diminishing returns" as well as the necessary increasing distraction forces in TGR treatment.[111,112] Ideally, a biofidelic model would include this effect. The present study did not attempt this for two reasons. First, it is unknown when, and to what extent, this stiffening occurs in vivo and in which structures and spinal levels it takes place. Second, it is yet unknown whether this effect also takes place in SDS patients, as these patients have relatively short follow-up. As this process is known to take place during TGR treatment, the outcomes reported in this manuscript thus represent a best-case scenario for the TGR model, as stiffening likely leads to reduced correction and spinal growth, and necessitates higher distraction forces which increase implant stresses further.[92,93,104]

As of yet, the SDS has been implanted in >70 patients as part of clinical studies. Two year follow-up results have shown that it was able to provide adequate curve correction that could be maintained at latest follow-up whilst providing T1-S1 growth exceeding 10 mm/year.[58,59] A recent complication analysis between SDS and (hybrid) MCGR patients showed that the SDS could not prevent rod fractures when 4.5 mm rods were used.[113] A review of these fractures showed similar points of failure to the locations highlighted by the present study. In several patients with bilateral springs, fractures occurred near the distal anchors, often close to the vicinity of the locking buttress, potentially due to set screw notches that act as stress con-

Figure 8: Forces on the intervertebral discs spanned by the construct
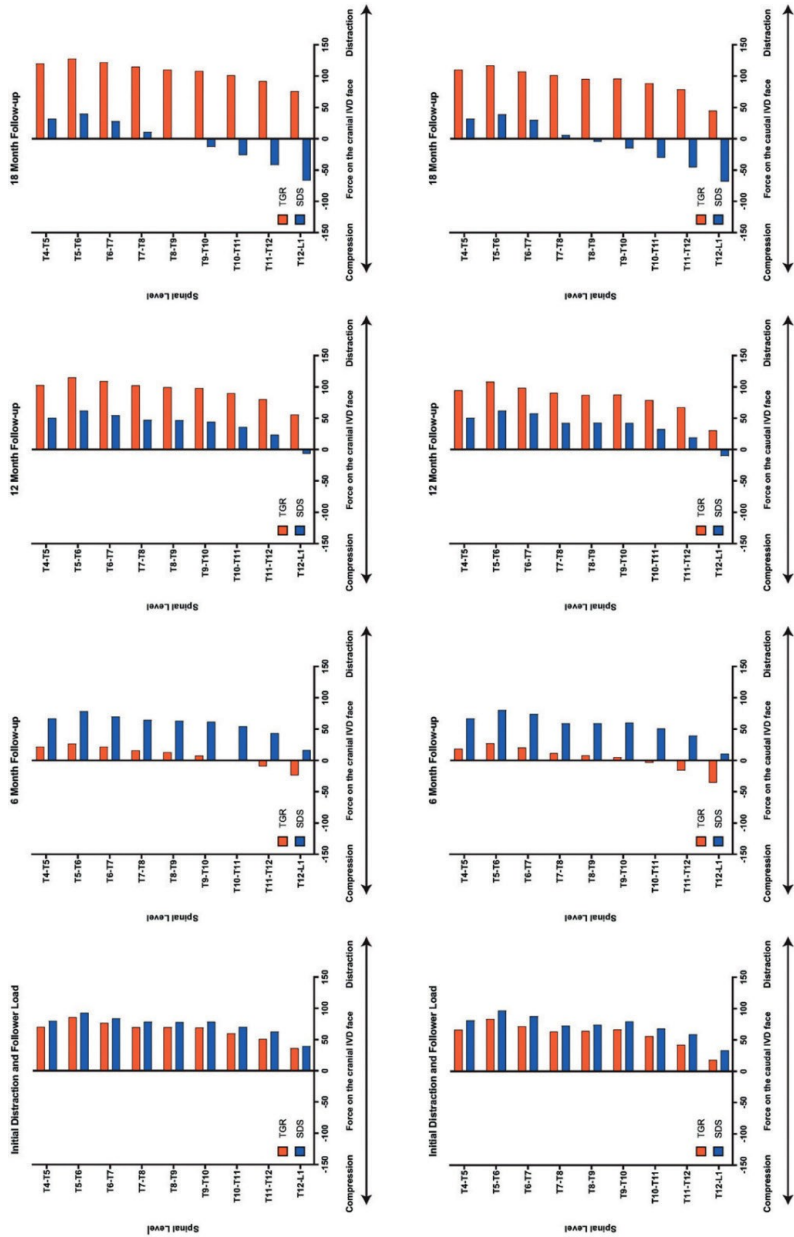
Normal forces on the upper IVD faces (top) and the lower IVD faces (bottom) extracted from the free-body diagrams. The evaluated IVDs were the ones spanned by the growing construct. Changes over time are shown from left to right. Positive forces denote distraction, negative forces denote compression. IVD indicates intervertebral disc; SDS, Spring Distraction System; TGR, traditional growing rod.

3
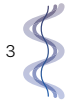
centrators.[114] These results of stress locations of growing rods are in line with recent studies on rod fractures and offer opportunities to prevent these complications.[97,105] Excessive rod bending in areas with high rod stress should be prevented (mid-construct for TGR, near the distal anchors for SDS), as this might introduce notches that weaken the rods.[115–117] Use of larger diameter rods may reduce overall rod stresses, although larger rods could mitigate these benefits by increasing construct stiffness, which has also been shown to be a risk factor for rod fractures.[118,119]

The use of the SDS springs allows for increased load-sharing of the IVDs during periods of increased loading. Recent studies on "growth-friendly" implants have shown that IVDs within a distraction construct show a decrease in height and volume over time coincident with degenerative changes seen on MRI.[101,102] In the present model, the SDS IVDs were under more distraction during the first 6 months. However, this effect reversed after the first TGR distraction, with the spanned IVDs in the TGR model under increasing amounts of distraction, whereas the IVDs in the SDS model were increasingly subjected to compressive forces again. This confirms the hypothesis that over time, the SDS allows for increased IVD load-sharing. Whether this also results in less IVD degeneration is unknown and will require clinical validation using 3D imaging.

The present study investigated one SDS configuration with bilateral 75N springs. While this configuration is still commonly used (e.g., for neuromuscular patients), for stiffer congenital or idiopathic curves, we now often combine a 100 N spring on the curve concavity with a sliding rod on the curve convexity (without a spring) that is fixated to the apex (for increased apical control). It is likely that this differential method of force application affects rod stress distribution, load-sharing of the spine, and spinal growth. Future FE studies should compare these new configurations to the present one to determine which one provides superior results with respect to curve correction and rod stress.

This is the first study investigating biomechanical differences between the TGR and the SDS. Strengths include the use of a previously validated, patient-specific, EOS FE model. In addition, representative modelling steps and implant configurations were modelled which ensured a fair comparison between both models. Limitations include the fact that several material properties had to be estimated from adult values and that certain effects such as spinal stiffening and autofusion were not present in the model. Future work will need to study how this phenomenon, in addition to different implant configurations, longer follow-up, and spinal motion affects implant biomechanics and spinal morphology.

Conclusion

During FE simulation of implantation and 18-month follow-up, several biomechanical and morphological differences were observed between TGR and SDS treatment. In the present models that did not model the effect of stiffening and autofusion of the spine, the additional TGR distractions resulted in better coronal curve correction and higher T1-S1 growth, but at the expense of increased stress-shielding of the IVD and increased propensity of rod fractures.

3

Acknowledgements
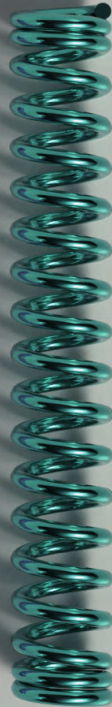
Chapter 4

The Potential of Spring Distraction to Dynamically Correct Complex Spinal Deformities in the Growing Child

S.P.J. Wijdicks
J.V.C. Lemans
G.J. Verkerke
H.J. Noordmans
R.M. Castelein
M.C. Kruyt

Abstract

Purpose
Current treatment of progressive early onset scoliosis involves growth-friendly instrumentation if conservative treatment fails. These implants guide growth by passive sliding or repeated lengthenings. None of these techniques provide dynamic correction after implantation. We developed the spring distraction system (SDS), by using one or multiple compressed springs positioned around a standard sliding rod, to provide active continuous distraction of the spine to stimulate growth and further correction. The purpose of this study was to determine feasibility and proof of concept of the SDS.

Methods
We developed a versatile, dynamic spring distraction system for patients who would benefit from active continuous distraction. This prospective case series evaluates four patients with exceptional and progressive congenital spine deformities.

Results
Four patients had a mean age of 6.8 years at surgery with a mean follow-up of 36 months (range 25–45). The mean progressive thoracic lordosis, which was the reason for initiating surgical treatment in two patients, changed from 32° lordosis preoperatively to 1° kyphosis post-operatively. During follow-up, this further improved to 32° thoracic kyphosis. In the two other patients, with cervicothoracic scoliosis, the main coronal curve improved from 79° pre-operatively to 56° post-operatively and further improved to 42°. The mean T1-S1 spine growth during follow-up for all patients was 1.3 cm/year. There was one reoperation because of skin problems and no device-failures.

Conclusion
These early results show the feasibility and the proof of concept of spring-based distraction as a dynamic growth-enhancing system with the potential of further correction of the deformity after implantation.

Introduction

Early onset spinal deformities can progress severely during growth. Especially in young children, this may result in thoracic insufficiency syndrome or untreatable spinal malformations.[12] When casts or brace treatment cannot control progression, implantation with internal growth-friendly systems is indicated.[32] Current growth-friendly systems can potentially stop curve progression while allowing the spine to maintain growth.[31] Some of these implants guide the reduced deformity by passive sliding, e.g., Shilla or Luque trolley techniques.[120,121] More commonly, implants that follow growth with repeated lengthenings are used, e.g., traditional growing rods (TGR), vertical expandable prosthetic titanium rib (VEPTR) or magnetically controlled growing rods (MCGR).[12,32,39] Although these techniques have dramatically improved our ability to treat early onset spinal deformities, some aspects can still be addressed to improve surgical outcomes: First, none of these systems dynamically stimulate growth and further reduction of the affected spinal segments. As a consequence, physiologic growth is not at all maintained.[31] Second, repeated anaesthesia and surgery, but also repeated outpatient visits and interventions have shown detrimental effects.[122–124] Third, due to the stiffness of current implant designs, the sagittal profile may be difficult to address, and autofusion often occurs, that potentially results in crankshafting and loss of spinal growth. Last, instrumentation failures are frequently observed.[33,82]

We were confronted with patients for whom we felt that the existing systems, even with the shortest possible distraction intervals, would have resulted in autofusion over a short period of time and therefore would not be effective. For these patients we developed and applied the spring distraction system (SDS). It uses the continuous distraction force of a compressed spring that is positioned around a traditional growing rod (4.5 mm) that is allowed to slide on one end (Figure 1). This paper reports on the first experience with SDS for the correction of severe spinal deformities.

Material and methods

Study design
Prospective case series of patients with progressive congenital spine deformities treated with the SDS. To prospectively investigate the SDS, institutional ethical review board approval was obtained (METC nr. 16–276).

Design and investigational medical device dossier
To our knowledge no papers exist that investigate spring distraction in humans or animals. Therefore, we had to rely on other literature that investigated the forces that

can be tolerated by the growing spine otherwise. For that purpose, we performed an extensive literature review that involved distraction forces in clinical, cadaver and finite element models.[125] In addition, we measured the distraction forces that we applied during traditional growing rod lengthenings. Based on these studies and expert evaluation by the medical engineers of the UMC Utrecht and University of Twente we concluded that a distraction force between 50 and 100 N on each side of the spine should be safe.

Based on the specifications from this research a medical grade Titanium (Ti-6AI-4V) spring was designed and manufactured. The ISO 13485 certified department of medical technology and physics of our hospital is competent to design and manufacture medical devices for custom use and clinical research in compliance with the European Medical Device regulations. During the design phase a risk analysis was performed through which Titanium (Ti-6AI-4V) was chosen mainly because this material is mostly bio-inert. The spring dimensions were chosen to fit around a standard 4.5 mm rod and to provide the predetermined distraction force over a specific distance. The following parameters were chosen for the spring: inner diameter of 5.16 mm, outer diameter of 7.70 mm, wire diameter of 1.27 mm, free length of 72.0 mm, compressed length of 38.0 mm, spring constant of 2.15 N/mm and maximum force of 75 N. The spring was manufactured by Lesjöfors (Karlstad, Sweden). Lesjöfors acted only as the provider of the springs as it has a quality management system ISO 9001 for producing springs, but not a quality management system for producing medical devices (ISO 13485), The ISO 13485 certified medical technology and clinical physics department, thus acted as the manufacturer of the spring, took lead in the design and manufacturing process and created the investigational medical device dossier (IMDD), consisting of: a spring description (including spring manufacturing process, sample control report and material inspection certificates), device classification, essential requirement checklist, risk analysis, user manual, processes of quality control, post market surveillance and vigilance. The investigational medical device dossier (IMDD) was approved after review of the medical technology and physics department (Project number 150310) and approved by the institutional ethical review board (METC nr. 16–276).

Surgical Techniques
After informed consent, patients received the SDS as an adjunct to conventional, pedicle screw based growing rods. For the lordotic patients we did posterior releases with Smith-Petersen osteotomies. For the mainly scoliotic patients, this included a convex hemi-vertebrectomy and hemi-epiphysiodesis. The SDS involves a distraction spring, placed around a conventional 4.5 mm rod that is not fixed but which is allowed to glide through an oversized parallel connector at its proximal anchor (Figure 1). A buttress that can be locked on the 4.5 mm rod is used to tension the

Figure 1. Three SDS configurations
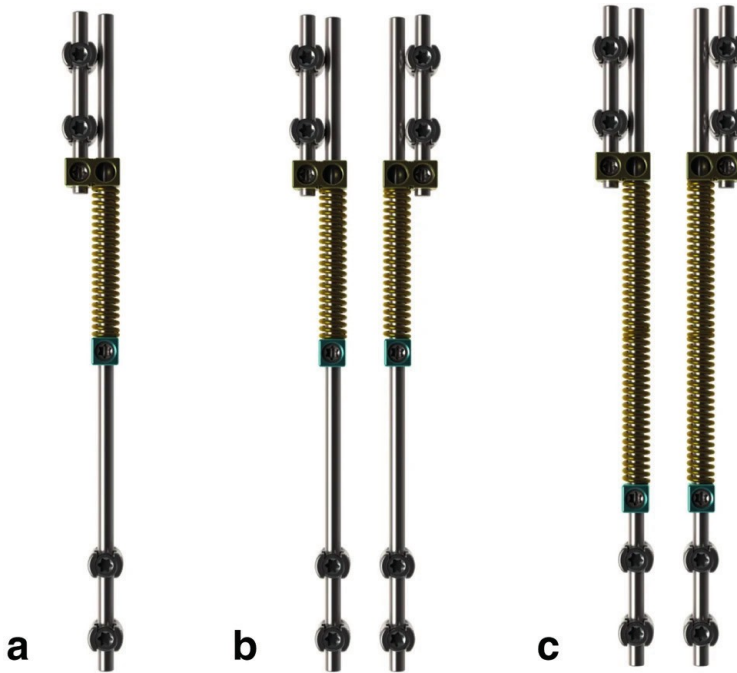
The SDS consists of a parallel connector (yellow) with an oversized medial 5.5 hole and lateral 4.5 hole, a 4.5 mm rod (silver) that can slide though the 5.5 hole of the parallel connector, a buttress (turquoise) used to tension or re-tension the spring and proximal and distal pedicle screws (silver). **a.** single concave SDS **b.** bilateral SDS and **c.** bilateral SDS with two springs in series.

spring. A single spring can provide a maximum force of 75 N and can lengthen 34 mm. Implanting bilateral SDS springs doubles this force to 150 N. Implanting two springs in series doubles the working length to 68 mm while keeping the force the same (Figure 1). When the spring is fully distracted, the rod can still glide through the parallel connector and function as a gliding system. Alternatively, the spring can be re-tensioned by adjusting the buttress through a small incision. The three configurations used in the 4 patients are shown in Figure 1. After surgery the patients were allowed normal activities with the exception of contact sports. No braces were used.

Patient cohort

The first patient, operated in 2015, was a 5-year-old girl that suffered from a rare skeletal dysplasia, spondylocarpotarsal synostosis (SCT) syndrome. A key feature of this syndrome is failure of segmentation of the posterior elements of the spine. The continued anterior growth results in a rapidly progressive lordosis which caused

thoracic insufficiency. Because we expected all currently available growth-friendly systems to fail for this specific case, we developed the posterior spring distraction system which we implanted bilaterally. Another girl with the same syndrome was first treated with bilateral MCGRs. Because the MCGRs could not reduce the deformity and fractured within 6 months, we decided to replace them with the SDS. Where the goal of treatment was primarily to create kyphosis for the SCT syndrome patients, a bilateral SDS was implanted. Because of the available space in the 2nd patient, we decided to increase the working length by using two springs in series. This doubled the working length, while the force remains the same (75 N). This was considered an advantage as the first patient already had a fully distracted spring after two years. The two other patients had high thoracic and cervical congenital anomalies with severe and progressive scoliotic deformity. The main goal was to correct the coronal deformity and a single concave SDS was implanted with a contralateral instrumented hemi-epiphysiodesis with sliding rods. In these patients we opted for the SDS approach to prevent the extensive procedure of hemivertebral resection. If treatment would fail, in terms of dynamic correction, hemivertebral resection can still be performed during definitive fusion surgery.

Data collection
Demographics, medical history, pre-, per- and post-operative clinical and radiographic parameters, as well as adverse events were prospectively recorded. Follow up was similar to TGR, with visits and radiographs at 1, 3 and 6 months and, if possible, every 6 months thereafter. Spinal lengths were measured after the x-rays were calibrated with the external diameter of the spring (7.70 mm). For height measurements (T1-T12 and T1-S1), the perpendicular distance between horizontal lines through midpoints of the chosen vertebral endplates was measured on coronal x-rays. For freehand measurements, we measured the curved mid-spinal line T1-S1 on coronal and sagittal x-rays. This freehand line, that is not affected by shape changes, was drawn through the exact midpoint of the upper and lower endplate of every vertebra. [31] Finally, the spring lengths on coronal and sagittal x-rays were measured on post-operative radiographs and at latest follow-up. The plane with the longest direct post-operative spring length was used for measuring spring length increase over time. All growth measurements were recorded from the first post-operative measurements to the latest follow-up measurements. To determine if further correction after surgery influenced spinopelvic balance, we measured apical vertebral translation, coronal balance, sagittal vertical axis (SVA) and pelvic obliquity. The measurements were performed with Surgimap Spine software (Nemaris Inc., New York, NY). All measurements were audited by an independent observer and discrepancies discussed until consensus was reached. Descriptive statistics were computed for the cohort, providing means and standard deviations.

Results

Patient demographics

All patients were referrals from other centers with already advanced deformities. The mean age at index surgery was 6.8 years (± 2.8) years. All patients were female. The mean age of first radiographical diagnosis of the scoliosis was 2.5 (± 2.2) years. The first patient was operated in 2015 and the mean follow-up time for all patients is 3.0 (± 1.2) years. Mean overall surgery time for the procedures was 191 min (range: 130–305). The instrumented segment involved 12 (range: 10–14) vertebrae with the lower instrumented vertebra varying from T10-L3. No intra-operative neuro-monitoring issues or complications occurred. Mean admission time was 6 days (range: 5–10). Mean estimated blood loss was 300 cc (range: 250–415).

Radiographic outcomes

The mean thoracic lordosis of the two SCT-patients could be reduced from −32° (lordosis) pre-operative, to a 1° kyphosis post-operative. During follow-up this dramatically improved further to a 32° thoracic kyphosis, despite our expectations that the lamina would fuse again (Figures 2 and 3). In the two mainly cervicothoracic scoliotic patients, the mean major curve reduced from 79° to 56° and further improved to 42° (Figure 4, Figure 5 and Figure 6). Apical vertebral translation improved from 45 mm pre-operative to 15 mm at latest follow-up. All (including individual) measurements are given in Tables 1, 2 and 3. The overall T1-S1 height increase that occurred after index surgery was 1.3 cm/year in the first 2 years. The T1-T12 height increased 0.8 cm/year (Table 2). The T1-S1 Freehand T1-S1 length growth in the coronal plane was 1.5 cm/year and 1.6 cm/year in the sagittal plane. The spring distraction was 1.1 cm/year (Figure 7).

Figure 2. Five-year-old girl with SCT syndrome
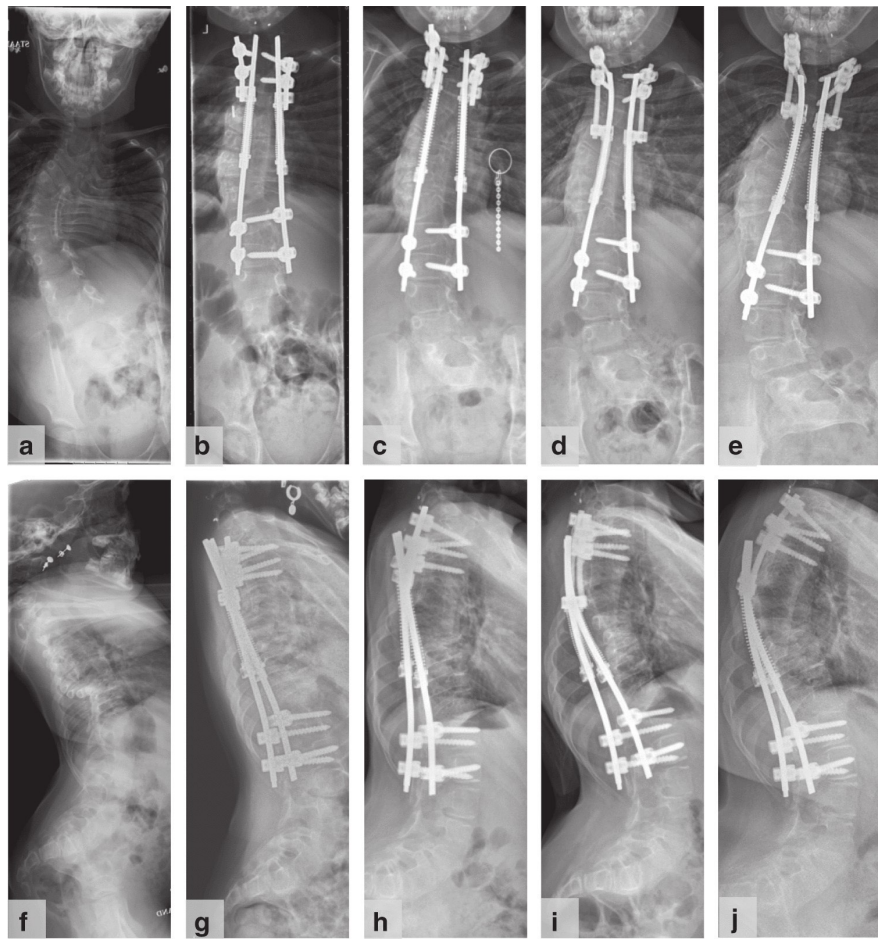
We performed Smith-Peterson osteotomies at Th7-Th11 and combined this with placement of a bilateral SDS (the springs were re-tensioned after 19 months). **a.** pre-operative **b.** post-operative **c.** at 19 months follow-up before re-tensioning **d.** after re-tensioning and **e.** at latest follow-up (3.9 years) frontal radiographs with corresponding sagittal radiographs **f–j.** The major coronal curve changed from 84˚ pre-operatively to 43˚ post-operatively and to 54˚ at latest follow-up. The thoracic lordosis of 43˚ changed to a kyphosis of 0.1˚ post-operatively to 43˚ at latest follow-up.

Figure 3. Nine-year-old girl with SCT syndrome
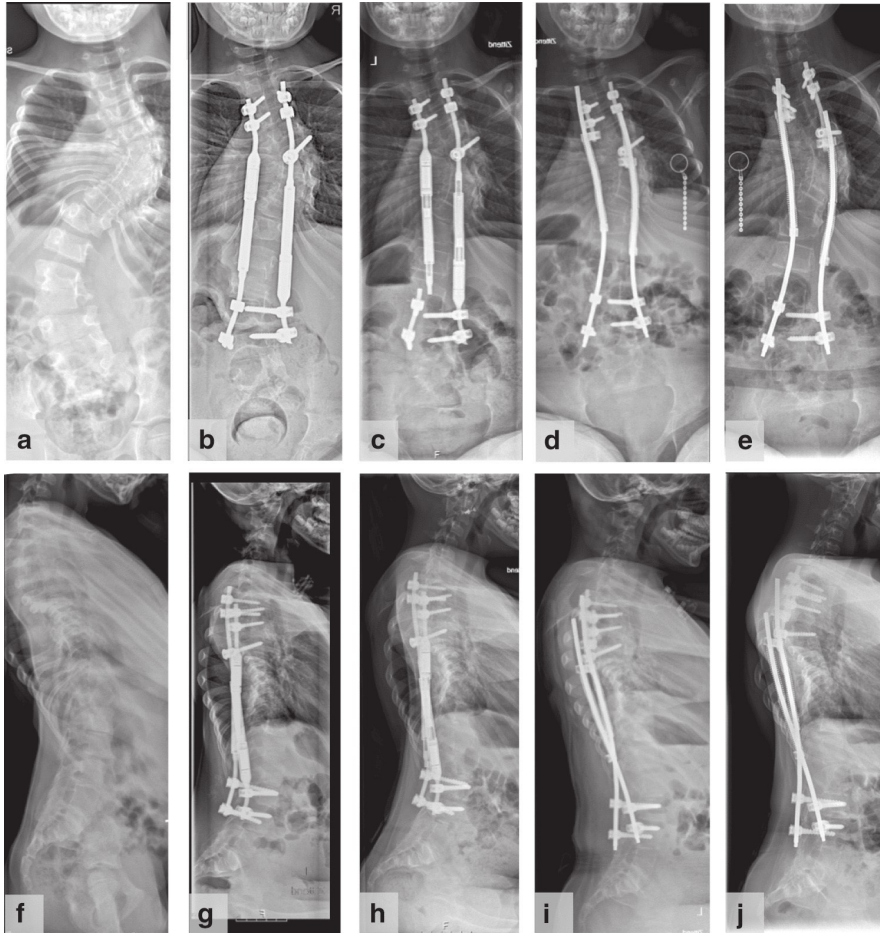
We performed dorsal Smith-Peterson osteotomies at Th6-Th11 and combined this with placement of a bilateral SDS (the dual MCGR broke after 6 months). **a.** pre-operative before MCGR surgery **b.** post-operative **c.** after broken MCGR and before bilateral SDS implantation **d.** post-operative and **e.** at latest follow-up (2.2 years) frontal radiographs with corresponding sagittal radiographs **f–j.** The major coronal curve changed from 57˚ pre-operatively to 58˚ post-operatively and to 59˚ at latest follow-up. The thoracic lordosis of 35˚ changed to a kyphosis of 3˚ post-operatively to 21˚ at latest follow-up.

Figure 4. Three-year-old girl with high thoracic scoliosis and severe clinical torticollis
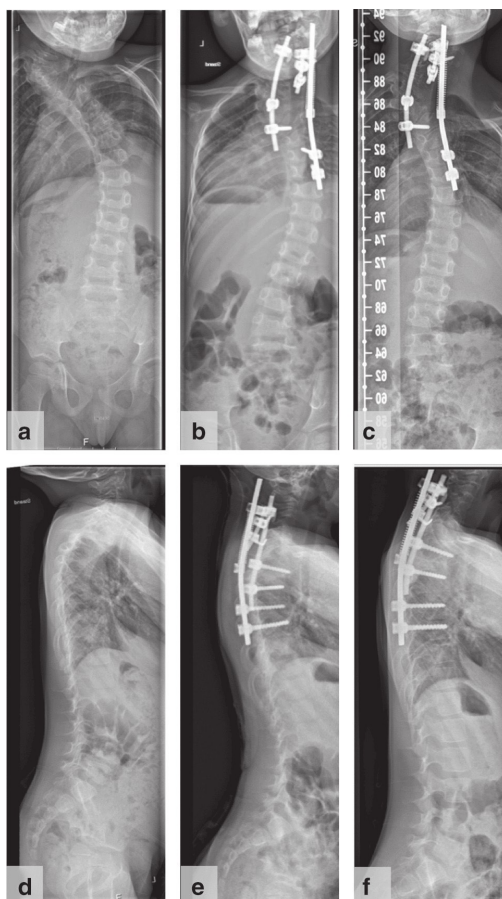
This patient underwent a convex posterior hemivertebrectomy and hemi-epiphysiodesis, combined with a concave SDS. **a.** pre-operative **b.** post-operative and **c.** at latest follow-up (2.1 years) frontal radiographs with corresponding sagittal radiographs **d–f.** The major coronal curve changed from 87˚ pre-operatively to 66˚ post-operatively and to 50˚ at latest follow-up.

Figure 5. Eight-year-old girl with high thoracic scoliosis and severe clinical torticollis
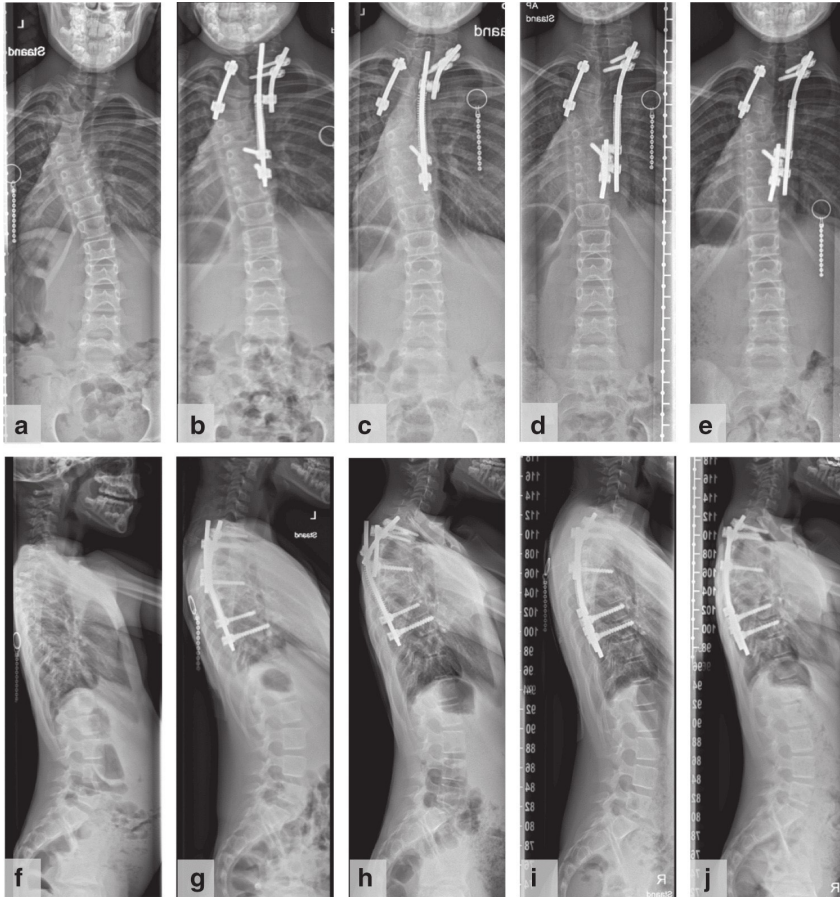
This patient underwent a posterior convex hemi-epiphysiodesis, combined with a concave SDS. **a.** pre-operative **b.** post-operative and **c.** at 19 months follow-up before implant exchange **d.** after implant exchange and **e.** at latest follow-up (1.9 years) frontal radiographs with corresponding sagittal radiographs **f–j.** The major coronal curve changed from 70° pre-operatively to 46° post-operatively and to 34° at latest follow-up.

Figure 6. Cobb angle (°) measured on serial x-rays
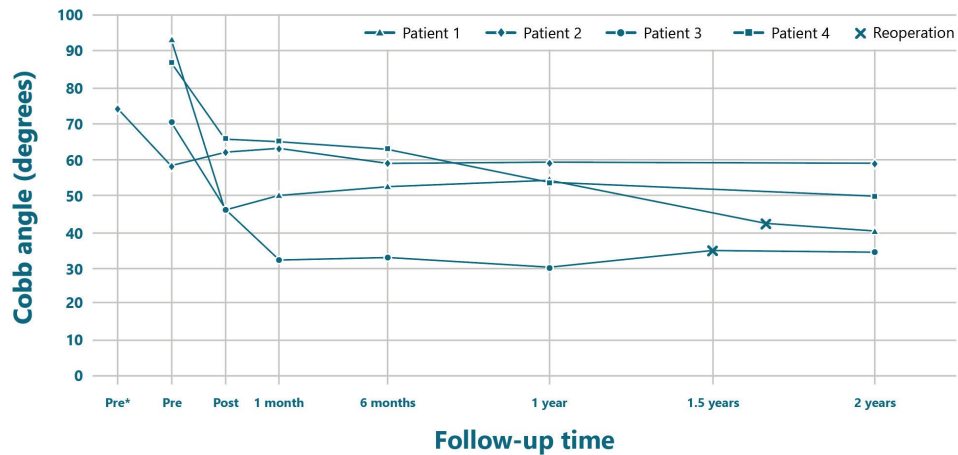
Pre* indicates the pre-operative x-ray before initial growth system implantation (in case of previous TGR or MCGR). **Pre** indicates the pre-operative x-ray before SDS implantation. **Post** indicates the post-operative x-ray directly after SDS implantation. The **X** indicates reoperation points at which the spring was re-tensioned.

Figure 7. Spring distraction (mm) measured on serial x-rays.
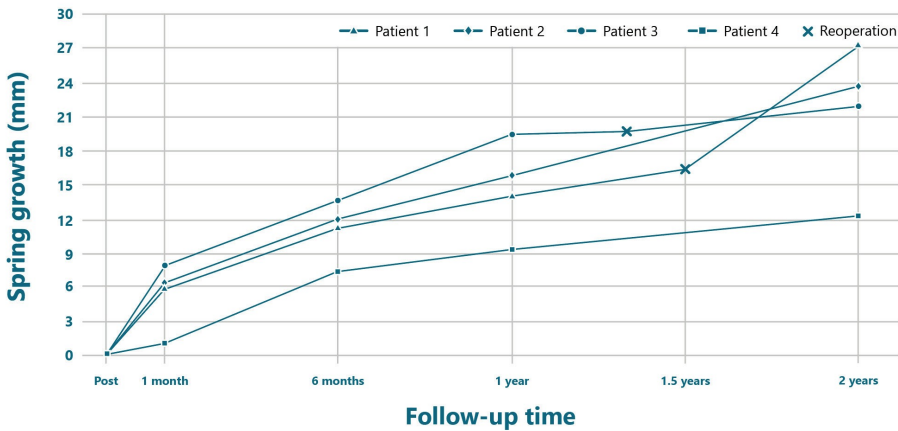
Post indicates the post-operative x-ray directly after SDS implantation. The X indicates reoperation points at which the spring was re-tensioned

Table 1. Major curve, kyphosis, T1-T12 height and T1-S1 height per patient

		Pre-op	Post-op	2-year follow-up	Latest follow-up
Coronal major curve	Patient 1	84°	43°	49°	54°
	Patient 2	57°	58°	60°	59°
	Patient 3	87°	66°	50°	50°
	Patient 4	70°	46°	34°	34°
Sagittal Kyphosis[a]	Patient 1	−43° (Lordosis)	0.1°	46°	43°
	Patient 2	−20° (Lordosis)	3°	20°	21°
	Patient 3	28°	29°	38°	38°
	Patient 4	14°	21°	38°	38°
T1-T12 height	Patient 1	111 mm	125 mm	134 mm	137 mm
	Patient 2	149 mm	146 mm	160 mm	163 mm
	Patient 3	109 mm	141 mm	162 mm	162 mm
	Patient 4	152 mm	151 mm	170 mm	170 mm
T1-S1 height	Patient 1	174 mm	233 mm	251 mm	254 mm
	Patient 2	267 mm	277 mm	290 mm	292 mm
	Patient 3	211 mm	244 mm	285 mm	285 mm
	Patient 4	268 mm	272 mm	305 mm	305 mm

[a]Negative numbers indicate a lordosis and positive numbers a kyphosis

Table 2. Coronal and sagittal parameters (Mean±SD)

		Pre-op	Post-op	2-year follow-up	Latest follow-up
Coronal	Major Curve	74±14°	53±10°	48±10°	49±11°
	Minor Curve	45±20°	27±16°	25±16°	23±15°
	Pelvic obliquity	9±9°	5±2°	4±3°	5±2°
	Coronal balance	25±18 mm	16±9 mm	9±7 mm	11±7 mm
	Apical vertebral translation	45±16 mm	22±19 mm	16±12 mm	15±10 mm
Sagittal	Kyphosis (T4-T12)[a]	−6±32°	13±14°	36±11°	35±10°
	Lordosis (L1-L5)	41±9°	53±21°	45±24°	34±8°
	Pelvic Tilt	5±8°	10±9°	6±7°	5±8°
	Sagittal vertical axis (SVA)	17±8 mm	13±38 mm	22±14 mm	14±17 mm

[a]Negative numbers indicate a lordosis and positive numbers a kyphosis

Table 3. Spinal growth (Mean±SD)

	Post-op–2-year follow-upb
T1-T12 height	0.8±0.3 cm/year
T1-S1 height	1.3±0.6 cm/year
T1-S1 freehand coronal	1.5±0.3 cm/year
T1-S1 freehand sagittal	1.6±0.4 cm/year
Spring distractiona	1.1±0.3 cm/year

aSpring distraction is the growth in spring length in cm between post-op and 2-year follow-up

Reoperations and complications
Due to successful elongation, we decided to re-tension the springs in the first SCT patient after 19 months when 1.6 cm of spring distraction had been gained. As expected, there was some wear debris present around the parallel connector. Histological analysis showed foreign body reaction (macrophages) without inflammation, consistent with the bio-inert nature of Titanium debris. In the second cervicothoracic scoliosis patient protrusion of the rod caused skin problems 19 months after implantation that required implant exchange. During the revision, the spring was changed and re-tensioned. Again, metal debris was observed without inflammation, the scar tissue that encapsulated the spring did not prevent it to expand. There were no deep infections, rod fractures, spring fractures or screw pull-outs in all 4 patients.

Discussion

This case series has shown that the feasibility of the spring distraction system (SDS) as a relatively easy and low invasive option for complex congenital deformities. In addition to maintaining correction and spinal growth, the SDS has shown the unique potential to further correct these rigid deformities after implantation, especially in the sagittal plane. The SDS was developed because we felt there were no other systems that could halt the progressive and life-threatening lordosis of the congenitally posteriorly fused spine in SCT syndrome. Although we performed posterior osteotomies, we expected that the available growth-friendly systems, even with the shortest possible distraction intervals, would have resulted in a rigid recurrence of bony fusion over a short period of time. In these cases, a continuous distraction force was needed that no other existing system could provide. There is only one case report that showed spinal deformity reduction after initial surgery using daily distractions with an MCGR. However, the MCGR was implanted without initial correction and was applied more like pre-operative halo gravity traction for a limited time.[37]

Our system is easy to contour in both the coronal and the sagittal plane unlike for instance the MCGR. Furthermore, the SDS is relatively mobile due to the sliding

connections at the proximal anchors. Theoretically, a more dynamic system is less vulnerable to fatigue failures as compared to static rods as demonstrated with finite element models.[93,126] Although wear debris is a serious concern, we saw no abundant debris nor did we observe adverse tissue reactions.

We realize that the use of a new device with active distraction is not without risks. Therefore, both the development and a thorough risk analysis of the distraction spring and components were done together with the engineers from the University of Twente (the Netherlands) and our department of medical technology and clinical physics (UMC Utrecht, the Netherlands). Having a department with a medical device certification (ISO 13485) inside the academic hospitals allows us to develop, manufacture and use hospital-specific medical devices for clinical research, which is especially important because of the upcoming Medical Device Regulation (MDR) laws in the European Union. We first looked at the forces delivered with the MCGR and traditional growing rods. The maximal distraction force of a single MCGR rod is 270 N and for a single standard traditional growing rod it may easily exceed 500 N.[68,69,127] When used as bilateral systems, these forces are doubled. However, these forces are applied as peak loads periodically and not continuously. In an attempt to calculate the optimal continuous force, we found a force between 25 and 150 N to be sufficient to gain 10 mm in a year. This was confirmed with finite element models of Agarwal et al. and Abolaeha et al.[104,128] Due to loss of force with distraction of the springs, we decided to develop a spring with a maximal force of 75 N that could be used bilaterally to deliver a total maximal force of 150 N. This spring was made from medical grade titanium alloy to minimize adverse tissue reactions.[129] The spring dimensions were guided based on the anatomical limitations of the first patient' small size, desired ratio between compressed and expanded version of the spring, ability to fit around a standard spinal rod and available wire thickness of medical grade Ti-6Al-4V.

Since we treated very rigid congenital deformities, the 38% major coronal curve correction and maintenance was at the lower range of the results reported in the literature of MCGR (32–58% correction).[36,130–132] Despite the rigidity of these patients, the correction improved over time and the T1-S1 spinal growth even approached natural growth during the same period.[31]

Although the gradual and spontaneous correction obtained in all dimensions compares favorably with other systems, springs lose distraction force when they expand. This can be mitigated by using a longer spring for certain indications. Based on Hooke's law this will decrease the spring constant but not the maximal force.[133] Consequently, by using two springs in series the maximum force will be the same (75 N) but the length of travel doubles (68 mm). Therefore, after 2 cm growth, the single spring has a remaining force of about 25 N whereas the double spring still delivers 50 N. Another concern may be overcorrection, especially in the sagittal

plane despite the fact that many scoliotic deformities are longer anteriorly. For the sliding anchors we used standard oversized connectors in an off-label manner, they can be improved to slide better and cause less debris. We are currently designing better alternatives that also minimize frictional forces and von Mises stresses on the instrumentation.

Limitations

This study is only a prospective case series with a relatively short follow-up period and without a control group. The patients had very specific deformities which may not represent the majority of early onset deformity patients. Pulmonary function tests are not routinely performed at our institute and therefore we did not measure all patients. For the corrections that we observed after insertion of SDS, especially for the scoliosis cases, the individual effect of distraction and the hemi-epiphysiodesis could not be determined. Nevertheless, we believe that this limited data does show feasibility and proof of concept of the SDS, similarly as was shown for the first 2 magnetically controlled growing rod patients reported in 2012.[39] To further study the possibilities and limitations, we have initiated a prospective clinical trial, where a broader range and less complex growing spine indications are included.

Conclusion

This is the first report of spring-based distraction to treat complex spinal deformities in the growing child. The early results of four patients show the potential of the innovative Spring Distraction System (SDS) to reduce the deformity and maintain growth after insertion, without additional lengthening procedures. Obviously, improvement of this in-house developed device, its long-term results and research on broader applications are our next step.

Chapter 5

Spring Distraction System for Dynamic Growth Guidance of Early Onset Scoliosis: Two-Year Prospective Follow-up of 24 Patients

J.V.C. Lemans

S.P.J. Wijdicks

R.M. Castelein

M.C. Kruyt

Abstract

Background
Current surgical treatment options for early onset scoliosis (EOS), with distraction- or growth-guidance implants, show limited growth and high complication rates during follow-up. We developed a novel implant concept, which uses compressed helical springs positioned around the rods of a growth-guidance construct. This spring distraction system (SDS) provides continuous corrective force to stimulate spinal growth, can be easily contoured, and can be used with all standard spinal instrumentation systems.

Purpose
To assess curve correction and -maintenance, spinal growth, complication rate, and health-related quality of life following SDS treatment.

Study Design
Prospective cohort study.

Patient sample
All skeletally immature EOS patients with an indication for growth-friendly surgery and without bone- or soft tissue weakness were eligible to receive SDS. For this study, all included patients with at least 2-year follow-up were analyzed.

Outcome measures
Coronal Cobb angle, sagittal parameters, T1-T12, T1-S1, and instrumented (ie, bridged segment) spinal height and freehand length, complications and re-operations, and the 24-Item Early Onset Scoliosis Questionnaires (EOSQ-24) score.

Methods
All primary- and conversion patients (conversion from failed other systems) with SDS and ≥2 years follow-up were included. Radiographic parameters were compared preoperatively, postoperatively and at latest follow-up. Spinal length increase was expressed as mm/year.

Results
Twenty-four skeletally immature EOS patients (18 primary and 6 conversion cases) were included. There were five idiopathic, seven congenital, three syndromic, and nine neuromuscular EOS patients. Mean age at implantation was 9.1 years (primary: 8.4; conversion: 11.2). Major curve improved from 60.3° to 35.3°, and was maintained at 40.6° at latest follow-up. Mean spring length increase during follow-up was

10.4 mm/year. T1-S1 height increased 9.9mm/year and the instrumented segment height showed a mean increase of 0.7 mm/segment/year. EOSQ-24 scores dropped after surgery from 75.6 to 67.4 but recovered to 75.0 at latest follow-up. In total, 17 reoperations were performed. Ten reoperations were performed to treat 9 implant-related complications. In addition, 7 patients showed spinal growth that exceeded expected growth velocity; their springs were retensioned during a small reoperation.

Conclusion

The 2-year follow-up results from this prospective cohort study indicate that the concept of spring distraction may be feasible as an alternative to current growing spine solutions. Curve correction and growth could be maintained satisfactory without the need for repetitive lengthening procedures. However, as in all growth-friendly implants, complications and reoperations could not be prevented, which emphasizes the need for further improvement.

Introduction

Early onset scoliosis (EOS), if left untreated, can cause severe cardiopulmonary dysfunction.[13,134,135] Different "growth-friendly" implants have been developed that aim to control the scoliotic curve whilst allowing for continuous spinal growth, thereby supporting truncal development. Current distraction-based implants are lengthened intermittently, either with repeated surgical procedures (traditional growing rod; TGR) or with a magnetic actuator (magnetically controlled growing rod; MCGR).[32,39] While these systems are widely used for the surgical treatment of EOS, they are not without disadvantages. First, as these systems are distracted at intervals, they do not mimic continuous physiological spinal growth.[31] Second, these implants are stiff which may contribute to autofusion of the spine, leading to the "law of diminishing returns" seen in both TGR and MCGR.[33,35,82,96] Third, the rigid nature of these implants leads to increased implant stresses and subsequent implant failures.[92,93,99,103] The MCGR in particular is complex, is difficult to contour, and has many components that can fail. Recent studies have shown that less than one in five retrieved MCGRs still function as intended.[43,44,54] It is also an expensive device, precluding its use in large parts of the world. To address these drawbacks, we developed the Spring Distraction System (SDS), which employs the continuous distraction force of a compressed helical coil spring that is positioned around a standard rod that is allowed to slide at the proximal- or distal foundation (Figure 1).[58] The system does not require periodic lengthenings (unlike TGR and MCGR), and can be built into any given configuration, utilizing the advantages of both guided-growth and distraction-based systems.

We aimed to assess curve correction, growth and complication rate following SDS treatment during a minimum of 2-year follow-up. Secondary aims were to assess health-related quality of life (HRQoL) and to compare outcomes between patients undergoing SDS as their first growth-friendly implant (primary cases) and patients that were revised to SDS after another (failed) system (conversion cases).

Materials and Methods

Ethical review and eligibility criteria
The current single-center prospective cohort study was approved by the Institutional Review Board of the UMC Utrecht (METC 16/276). All skeletally immature (ie, open triradiate cartilage on radiography) EOS patients from 2016 onward with a progressive curve >45° with an indication for growing-rod surgery were eligible and included after informed consent. Patients whose current "growth-friendly" system had to be revised (eg, because of implant failure) were also eligible for inclusion. Exclusion criteria were the presence of connective tissue diseases (eg, Marfan- and Ehlers-Danlos syndrome, neurofibromatosis) or severe bone pathology like osteogenesis

Figure 1. Spring distraction system concept
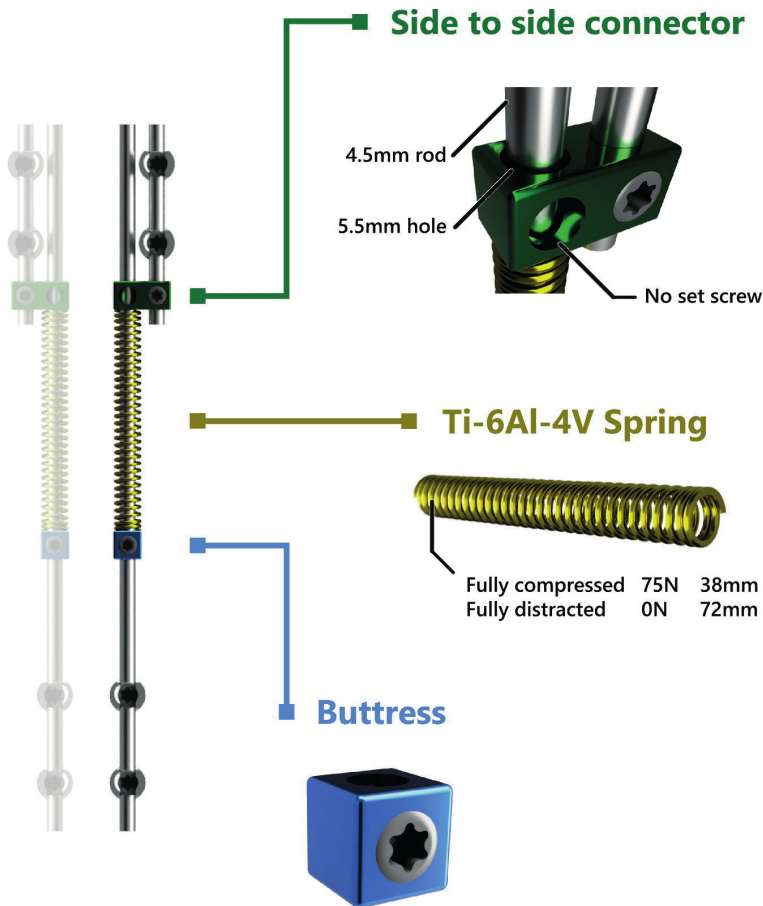
imperfecta. For the current analyses, only patients with at least 2 years of follow-up were included. This study followed the STROBE guideline for reporting observational studies.[136]

Investigational medical device

The key component of the experimental device (SDS) consists of a custom-made helical coil spring that was designed after extensive literature reviews to determine force safety limits and spinal growth.[125] We chose a maximum spring force of 75 N, which is much lower than the distraction force of a single MCGR rod (around 200 N), and forces applied in TGR lengthenings (which may easily exceed 500 N).[54,67,68] The medical grade titanium (Ti-6Al-4V) spring was manufactured by Lesjöfors AB (Karlstad, Sweden) to fit around a 4.5 mm rod, with an uncompressed length of 72.0

mm, compressed length of 38.0 mm, spring constant of 2.15 N/mm and maximum compressed force of 75 N.[58] Since Lesjöfors AB does not have a quality management system for producing medical devices, the ISO 13485 certified department of Medical Technology and Clinical Physics of the UMC Utrecht acted as the manufacturer of the spring, took lead in the design and manufacturing process and created an Investigational Medical Device Dossier, including quality control, risk analysis and postmarket surveillance and vigilance.

Spring distraction system

The SDS consists of three components (Figure 1): (1) A side-to-side connector with one oversized hole, (2) The spring that can be compressed, and which provides a distraction force, and (3) A locking buttress that is used to compress the spring over the rod during surgery. The spring and locking buttress are placed over the 4.5 mm sliding rod that has 4-6 cm of residual length. This rod bridges the scoliotic curve on its concavity and joins the short anchor rod in the parallel connector with an oversized hole to allow for sliding. By moving the buttress across the rod toward the parallel connector, the spring can be compressed. Implanting bilateral springs doubles the distraction force to 150 N, while implanting two springs in series doubles the working length to 68 mm while the force remains unaltered. The convexity of the curve can either receive a similar distraction construct, or, when apical control is preferred, a passive sliding rod, fixed to the apex as described previously for MCGRs [37,38]. To maintain distraction when full expansion has taken place, the spring can be retensioned by repositioning the buttress in a small surgical procedure. Figure 2 shows multiple SDS configurations that can be used depending on EOS type and surgeon preference.

Surgical technique

Surgery was performed through a posterior midline skin incision, using separate small transmuscular exposures for the foundations. Pedicle screws (Legacy, Medtronic, Dublin, Ireland) were placed with the freehand technique, the rods were passed subfascially. The sliding rods were cobalt-chromium (CoCr) to prevent titanium-on-titanium friction with the side-to-side connectors (K2M, Leesburg, VI, USA) and were contoured into the desired shape in both the coronal and sagittal plane. After surgery, patients were allowed normal activities without restrictions or braces.

Outcome parameters

The radiological outcomes were coronal Cobb angles, T5-T12 kyphosis, L1-S1 lordosis, height and freehand length of T1-T12, T1-S1 and the Instrumented segment (i.e., all vertebrae bridged by the instrumentation) as well as length of the springs. Segment heights were measured as the perpendicular distance between horizontal

Figure 2. Spring distraction system configurations

Idiopathic/Syndromic

Congenital

Neuromuscular
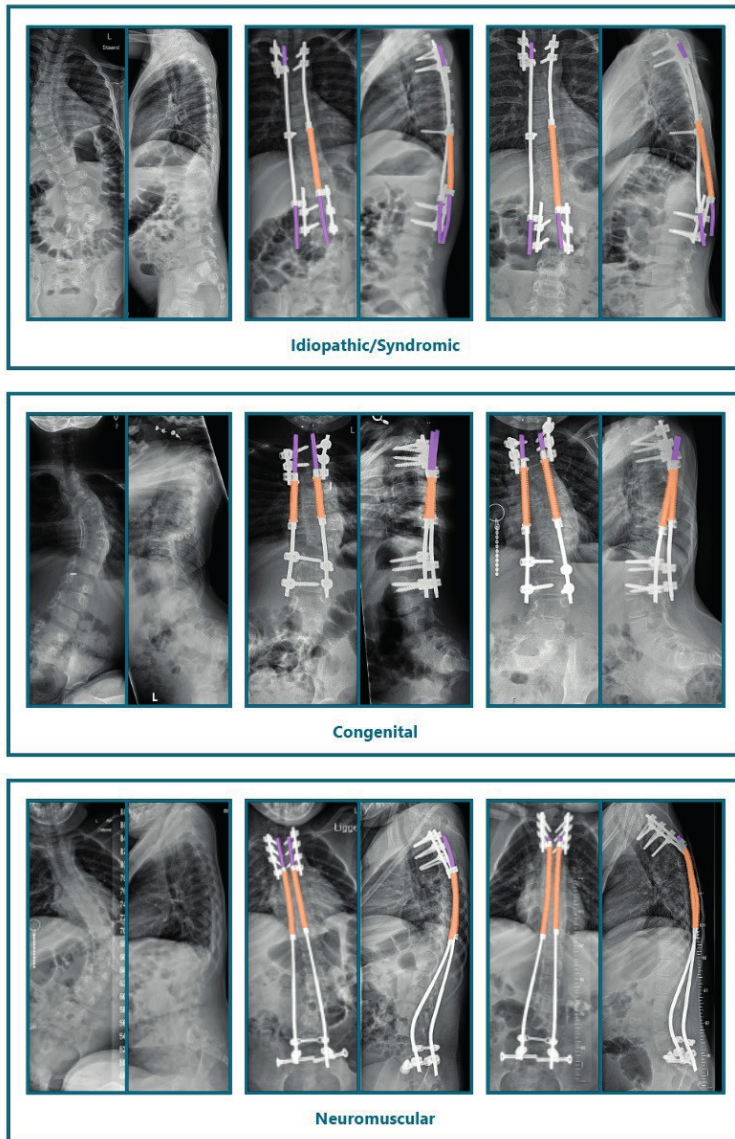
Left: Preoperative, **Middle:** Immediately postoperative, **Right:** Latest follow-up. Spring is colored orange, sliding rods are colored purple. For idiopathic and syndromic cases, a hybrid of the SDS on the curve concavity was often combined with a sliding rod with apical control on the convexity. For congenital cases, a concave SDS was implanted and combined with a sliding rod, hemi-epiphysiodesis or no instrumentation on the curve convexity. Neuromuscular cases were instrumented with bilateral springs that were fixated distally with iliosacral screws and proximally with pedicle screws.

lines going through the midpoints of the vertebral endplates (Figure 3). To determine spinal length gain in these segments, the freehand method was used by drawing a curved line through the midpoint of the upper and lower endplate of all involved vertebrae.[31,137] All measurements were performed on the pre- and postoperative radiographs, and on the radiographs at latest follow-up. Growth rates (mm/year) were calculated based on the difference between the postoperative and latest follow-up radiograph, thus excluding the length gain from initial surgery and definitive spinal fusion.[31] All measurements were performed on calibrated radiographs using Surgimap v.2.3.1.1 (Nemaris Inc, New York, NY, USA). Surgical outcomes such as skin-to-skin surgery time, estimated blood loss and occurrence of complications and reoperations were prospectively recorded. Patient-reported outcomes were measured using the validated Dutch EOSQ-24 questionnaire filled out preoperatively, 6 weeks postoperatively and at 1- and 2-year follow-up.[138]

Statistics

Descriptive statistics was performed on baseline characteristics and outcome parameters were reported as means with standard deviation. Differences in characteristics between primary- and conversion cases were compared with independent t tests for continuous variables, and with Pearson Chi-squared tests for categorical variables. Intrapatient differences in outcomes were analyzed with paired sample comparisons, either paired t tests (parametric) with 95% confidence interval (CI), or Wilcoxon Signed-Rank tests (nonparametric) with Hodges-Lehmann estimator and 95% CI, depending on whether the paired differences were normally distributed. Significance for all tests was set at $p < .05$. Statistical analysis was performed with IBM SPSS Statistics 25.0.0.2 (IBM Corp. Armonk, New York, NY, USA).

Results

Patient demographics

From 58 SDS patients, all patients who had at least 2 years of follow-up (N=24) were included and analyzed; 18 primary SDS patients and 6 conversion patients (3 TGR; 3 MCGR). Patient characteristics and comparison between primary- and conversion cases are shown in Table 1. All EOS etiologies were represented with 5 (21%) idiopathic cases, 7 (29%) congenital cases, 3 (13%) syndromic cases and 9 (38%) neuromuscular cases. The mean number of instrumented segments was 12.8±3.3. Mean follow-up was 2.4±0.3 years.

Figure 3. Spinal growth measurements.
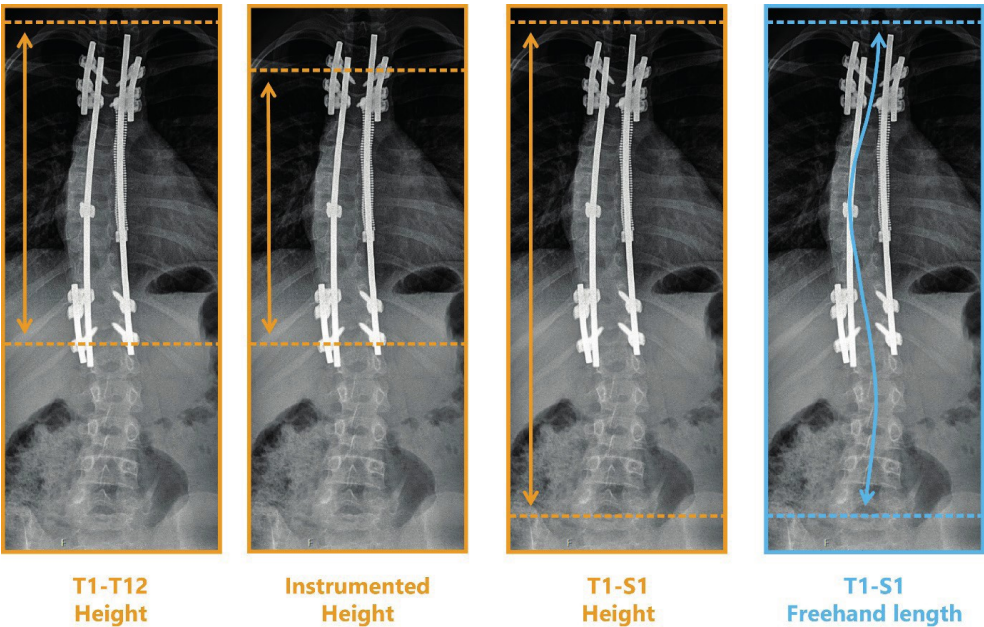
The first three panels show the different segment heights (T1-T12, Instrumented, T1-S1). The fourth panel show the T1-S1 segment measured with the freehand method. Note the difference in length compared to the third panel.

Table 1. Baseline characteristics

	Primary SDS (N=18)	Conversion SDS (N=6)	P value	All patients (N=24)
Age at surgery (years)	8.4±2.0	11.2±2.0	0.006	9.1±2.3
Gender (Male, %)	9 (50%)	2 (33%)	0.478	11 (46%)
EOS etiology			0.179	
Idiopathic	3 (17%)	2 (33%)		5 (21%)
Congenital	4 (22%)	3 (50%)		7 (29%)
Syndromic	2 (11%)	1 (17%)		3 (13%)
Neuromuscular	9 (50%)	0		9 (38%)
Previous growing system			NA	
TGR	NA	3 (50%)		3 (13%)
MCGR	NA	3 (50%)		3 (13%)
Preoperative primary curve (°)	65.0±16.2	45.9±21.9	0.032	60.3±19.3
Preoperative T5-T12 kyphosis (°)	18.6±21.0	33.4±26.2	0.173	22.3±22.7
Preoperative L1-S1 lordosis (°)	47.8±13.4	52.5±15.2	0.473	48.9±13.7
Surgery skin to skin time (min)	230±62.6	123±34.3	0.001	203±73.5
Estimated blood loss (mL)	372±148 (N=17)[a]	167±60.6	<0.001	318±159 (N=23)[a]
Instrumented levels	13.7±3.1	10.3±2.7	0.027	12.8±3.3
Time to discharge (days)	6.9±2.1	4.0±1.3	0.004	6.2±2.3

Mean and standard deviation are provided and differences were analyzed with the independent samples t test.

SDS: spring distraction system

[a]For one patient, estimated blood loss data was unavailable.

No significant differences were seen between primary and conversion cases with respect to sex, EOS etiology, sagittal profile, and follow-up length. As expected, primary patients were significantly younger (8.4 vs. 11.2 years). They also had larger primary curves at time of SDS surgery (65.0° vs. 45.9°) and had a higher number of instrumented segments (13.7 vs. 10.3). Surgery was also significantly longer (230 vs. 123 minutes), with higher blood loss (372 vs. 167 mL) and they were discharged later (6.9 vs. 4.0 days).

Radiographic outcomes

For primary SDS patients, the main curve corrected from a mean of 65.0° to 33.2° (49% reduction), which was maintained at 35.6° at latest follow-up (Table 2). Conversion cases started with a mean primary curve of 45.9°, which was reduced to 41.6° (9% reduction), and increased again to 55.8° at latest follow-up. Primary curve

development for each patient is shown in Figure 4. Nine patients showed additional curve correction during follow-up, seven patients showed a progression of the curve >10° compared to postoperatively. For secondary curves, similar trends were seen.In primary cases, thoracic kyphosis decreased from a mean of 18.6° to 16.7° postoperatively. During follow up, a significant increase was seen to 27.0° (p=.001). Two patients with a congenital thoracic lordosis of >20° due to posteriorly fused segments improved to a modest (5°–10°) thoracic kyphosis during follow-up. Conversion cases increased from a mean kyphosis of 33.4° to 36.3° postoperatively which increased significantly to 46.0° at latest follow-up (p=.028). Lumbar lordosis showed a similar pattern as thoracic kyphosis.

Table 2. Curve correction and sagittal profile

		Pre-operative	Post-operative	Latest follow-up	Change during follow-up[a]
Primary curve (°)	Primary	65.0±16.2	33.2±11.8	35.6±15.6	+2.4 (−3.4 to +8.1); p=0.401[b]
	Conversion	45.9±21.9	41.6±22.8	55.8±22.8	+14.2 (−0.1 to +28.5); p=0.051[b]
	All patients	60.3±19.3	35.3±15.1	40.6±18.1	+5.3 (−0.14 to 10.8); p=0.056[b]
Secondary curve (°)	Primary (N=16)[d]	34.3±15.2	21.6±14.3	23.1±13.5	+1.5 (−1.9 to +4.9); p=0.363[b]
	Conversion	24.4±7.86	21.0±9.66	23.9±6.80	+3.7 (−2.2 to +7.3); p=0.173[c]
	All patients (N=22)[d]	31.6±14.1	21.4±13.0	23.3±11.9	+1.9 (−0.8 to +4.5); p=0.152[b]
T5-T12 Kyphosis (°)	Primary	18.6±21.0	16.7±13.2	27.0±15.1	+9.7 (+4.0 to +16.3); p=0.001[c]
	Conversion	33.4±26.2	36.3±26.2	46.0±27.7	+9.8 (+4.5 to +12.7); p=0.028[c]
	All patients	22.3±22.7	21.6±18.8	31.7±20.2	+9.6 (+5.8 to +13.0); p<0.001[c]
L1-S1 Lordosis (°)	Primary	47.8±13.4	41.2±10.4	49.6±19.4	+8.5 (+0.4 to +16.5); p=0.041[b]
	Conversion	52.5±15.2	51.2±14.2	58.5±13.8	+7.0 (−3.7 to + 18.8); p=0.043[c]
	All patients	48.9±13.7	43.7±12.0	51.8±18.3	+8.2 (+1.9 to +14.4); p=0.013[b]

[a]A positive number indicates an increase during follow-up.

[b]Parametric distribution of differences. Paired t test was performed and mean and 95% CI are provided.

[c]Nonparametric distribution of differences. Wilcoxon-Signed Rank test was performed and Hodges-Lehmann estimator and 95% CI are provided.

[d]Two patients did not have a secondary curve and were not evaluated.

Figure 4. Coronal Cobb angle over time
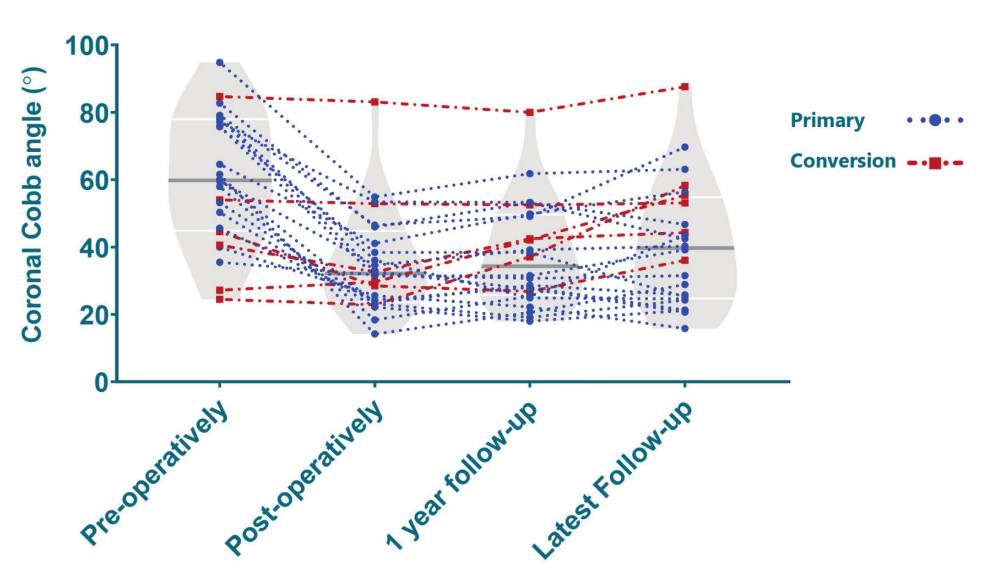
Cobb angle change over time is plotted for each patient and distribution of data is shown as a violin plot (showing the probability density of the data at different Cobb angles).

Spinal height and length values are reported in Table 3 and spring length values are shown in Table 3 and Figure 5. Mean T1-T12 height gain during follow-up was 7.9 mm/year (primary: 8.7, conversion: 5.7). For T1-S1 height, the mean gain was 9.9 mm/year (primary: 11.6, conversion: 4.8) and for the instrumented segment, the mean gain was 0.7 mm/segment/year (primary: 0.8, conversion: 0.4). The mean free-hand length gain was 9.7 mm/year for T1-T12, 13.6 for T1-S1 and 0.8 mm/segment/year for the instrumented segment, with only small differences between primary and conversion cases.

Table 3. Spinal growth

		Pre-operative	Post-operative	Latest follow-up	Post-operative growth (mm/year)[a]
T1-T12 height (mm)	Primary	172±29.4	191±26.8	212±28.3	+8.7 (+6.5 to +10.8); p<0.001[b]
	Conversion	200±33.9	205±35.0	218±41.7	+5.7 (+1.3 to +10.1); p=0.046[b]
	All patients	179±32.2	194±28.9	213±31.2	+7.9 (+6.0 to +9.8); p<0.001[b]
T1-T12 freehand length (mm)	Primary	192±26.7	199±24.9	222±28.4	+9.8 (+7.6 to +12.0); p<0.001[b]
	Conversion	209±28.6	214±30.6	235±35.9	+9.3 (+4.8 to +13.9); p=0.011[b]
	All patients	196±27.6	202±26.6	225±30.1	+9.7 (+7.8 to +11.5); p<0.001b
T1-S1 height (mm)	Primary	288±43.1	319±40.5	346±42.5	+11.6 (+7.9 to +15.3); p<0.001[b]
	Conversion	329±33.3	341±36.3	354±39.7	+4.8 (−2.1 to +11.8); p=0.137b
	All patients	298±44.0	324±39.9	348±41.1	+9.9 (+6.7 to +13.1); p<0.001[b]
T1-S1 freehand length (mm)	Primary	319±41.4	330±37.8	362±44.4	+13.4 (+9.6 to +17.2); p<0.001[b]
	Conversion	344±34.1	356±34.6	390±46.5	+14.2 (+3.7 to +24.7); p=0.029[b]
	All patients	325±40.6	336±38.1	369±45.7	+13.6 (+10.2 to +17.0); p<0.001[b]
Instrumented height (mm)[c]	Primary	NA	250±65.3	272±72.0	+0.8/segment (+0.5 to +1.1); p<0.001[b]
	Conversion		207±33.3	220±37.7	+0.4/segment (−0.1 to +0.9); p=0.069[b]
	All patients		239±61.3	259±68.3	+0.7/segment (+0.5 to +0.9); p<0.001[b]
Instrumented freehand length (mm)[c]	Primary	NA	259±65.0	286±75.1	+0.9/segment (+0.6 to +1.2); p<0.001[b]
	Conversion		220±39.0	241±41.0	+0.6/segment (+0.3 to +1.0); p=0.018[b]
	All patients		249±61.3	274±70.2	+0.8/segment (+0.6 to +1.1); p<0.001[b]
Spring length (mm)	Single spring (N=9)	NA	40.9±3.7	56.3±9.3	+6.5 (+3.6 to +9.4); p=0.001[b]
	Double spring (N=15)		83.7±7.6	113±15.3	+12.7 (+9.8 to +15.6); p<0.001[b]
	All patients		67.7±22.1	91.6±30.9	+10.4 (+8.0 to +12.7); p<0.001[b]

[a] A positive number indicates an increase during follow-up.

[b] Parametric distribution of differences. Paired t test was performed and mean and 95% CI are provided.

[c] For instrumented postoperative growth rates, the growth per segment spanned by the instrumentation is reported.

Figure 5. Spring lengthening over time
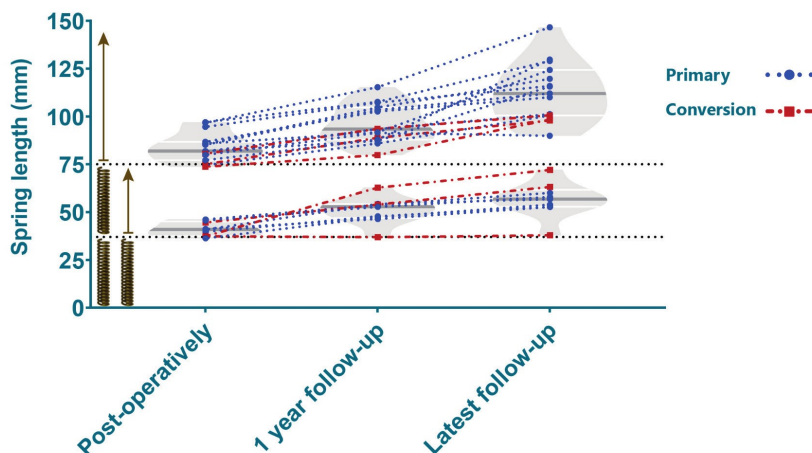
Spring length increase over time is plotted for each patient and distribution of data is shown as violin plots (showing the probability density of the data at different spring lengths). The dotted lines denote the length of one (bottom) or two (top) fully compressed spring(s) and the tip of the right and left arrow denote the fully distracted length of one and two springs respectively. Note that some springs had already distracted somewhat at the time of first erect radiograph.

Complications and reoperations

There were no intraoperative complications, patients recovered well and could be discharged after a mean of 6.2±2.3 days. The springs did not show any failures in terms of fracture or dysfunction due to tissue encapsulation. During ≥2 years of follow-up, 17 reoperations were performed in 13 patients. Ten reoperations were performed for 9 implant-related complications in 8/24 patients (33%). Implant prominence was the most common complication, and occurred in 3 patients. One patient needed two re-operations for a deep surgical site infection. The other complications are listed in Table 4. In addition to the complications, 7/24 patients (29%) needed a (small) reoperation for retensioning of the spring, after a mean of 1.9±0.6 years. This was due to unexpected high length gain immediately after insertion of the system (tissue relaxation/creep), and/or a spinal growth rate that exceeded expectations.

Health-related quality of life

Twenty patients filled out the EOSQ-24 questionnaire during all follow-up moments and were analyzed (Table 5). Mean preoperative EOSQ-24 score patients changed from 75.6±7.6 (out of 100) preoperatively, to 67.4±10.6 postoperatively (with decreases in pain/discomfort, physical function, fatigue/energy, and emotion domains) and increased again to 75.0±7.7 after 2 years.

Table 4. Reoperations and complications

Patient	Number of reoperations	Reason for reoperation	Treatment
P-01	0		
P-02	0		
P-03	0		
P-04	0		
P-05	0		
P-06	2	High growth rate; rod grew out of connector	Implantation of longer rod and re-tensioning of spring
		Distal iliosacral screw failure	Implantation of new iliosacral screw
P-07	0		
P-08	1	High growth rate; spring fully distracted	Re-tensioning of spring
P-09	3	Deep Surgical Site Infection	Irrigation and debridement (2x)
		Distal iliosacral screw failure	Implantation of new iliosacral screw
P-10	1	Rod fracture	Implantation of new rod
P-11	0		
P-12	1	High growth rate; spring fully distracted	Retensioning of spring
P-13	1	High growth rate; spring fully distracted	Retensioning of spring
P-14	0		
P-15	1	Protrusion of instrumentation	Additional bending of rod
P-16	1	High growth rate; spring fully distracted	Retensioning of spring
P-17	0		
P-18	1	Protrusion of instrumentation	Additional bending of rod
C-01	1	Connector failure	Definitive fusion
C-02	2	Protrusion of instrumentation	Additional bending of rod
		High growth rate; spring fully distracted	Re-tensioning of spring
C-03	1	Rod-connector slippage	Implantation of new set screw in connector
C-04	1	High growth rate; spring fully distracted	Retensioning of spring
C-05	0		
C-06	0		

P-XX denote primary patients, C-XX denote conversion patients.

5

Table 5. Health-related quality of life (N=20)[a]

	Pre-op	Post-op	1 year follow-up	2 year follow-up
General health	72.5±18.3	70.0±21.0	74.0±20.1	72.5±20.3
Pain/discomfort	71.3±23.8	57.0±19.8	72.6±17.7	77.0±19.3
Pulmonary function	85.6±19.7	83.2±21.3	79.5±24.2	84.5±20.2
Transfer	75.5±23.8	61.1±29.4	70.5±27.8	68.0±27.1
Physical function	72.7±30.6	58.5±30.7	66.4±34.0	69.7±32.6
Daily living	61.1±31.1	59.2±30.6	64.9±31.7	64.0±35.3
Fatigue/energy level	71.0±24.5	56.5±18.9	71.5±23.2	71.0±21.9
Emotion	82.5±18.5	65.8±24.3	75.0±24.8	76.5±22.8
Parental burden	76.3±23.3	70.0±26.8	73.5±23.1	76.6±23.3
Financial burden	90.0±14.8	91.0±17.3	87.0±21.2	93.0±13.1
Overall satisfaction	73.2±20.7	69.4±17.3	71.0±16.7	72.0±21.8
Mean domain score	75.6±7.6	67.4±10.6	73.3±5.8	75.0±7.7

Five-point Likert scale scores were converted to a score ranging from 20 (minimum) to 100 (maximum). Higher scores denote better patient outcomes.
[a]Only patients with filled out questionnaires at all 4 timepoints were included (N=20).

Discussion

The current study investigated the feasibility and safety of the SDS for surgical tre-atment of many types of EOS. The concept of distraction itself is not new and dates back to the early use of Harrington rods.[64–66] Springs were even used at that time to treat adolescent idiopathic scoliosis, but that technique never fully matured, probably due to the emergence of pedicle screw fixation and its potential for powerful cor-rection.[51] In the current study, postoperative Cobb angle correction with the SDS was 50% for primary patients, and this correction was maintained during ≥2 year follow-up. This is similar to contemporary systems that rely on repetitive distractions.[130] In the primary patient group, T1-S1 height increase was 11.6 mm/year; which seems to be higher than reported for other growth-friendly systems.[31,130] In general, patients tolerated the SDS well and although HRQoL decreased initially after sur-gery, patients recovered fully and experienced little to no discomfort of the SDS.

The complication rate necessitating reoperation was relatively low (9/24; 0.38 complications/patient) when compared to other systems (TGR: 1.48–2.30, MCGR: 0.43–0.90),[42,139,140] although the number of reoperations was still relatively high, owing to the considerable number of retensioning surgeries (7/24, 29%). These were caused by unexpectedly fast length gain in the system and subsequent loss of

distraction force. Although ideally, only a single SDS surgery is performed without reoperations, the rapid spinal growth can be considered a sign of treatment efficacy. By using two springs in series, spring forces can be spread out over a longer distance, and the risk of rapid force loss (and thus the need for retensioning) is reduced, although the cranial or caudal rod extensions must be left longer. When regarding only complications, implant prominence was the most frequent reason for reoperation, which can be related to the increase in thoracic kyphosis that is enforced by the posterior distraction. Currently, we use two stacked side-to-side connectors instead of just one to prevent this excessive kyphosis in the implant.

We observed several differences between primary cases and conversion cases; a main difference was the amount of postoperative curve correction which was substantially lower in the conversion group (49% vs. 8%). In addition, conversion cases had a tendency to exhibit somewhat lower segment height growth, although these differences disappeared when comparing freehand length instead. Since the freehand measurements are much less influenced by coronal curve changes (evidenced by the fact that pre- and postoperative freehand length values are similar), this provides a more accurate measure of true spinal growth. Freehand length parameters showed that both groups exhibit similar spinal growth, close to or exceeding normative values found in literature.[6,141]

Technical advantages of the SDS include the fact that it is easy to contour and that the system is relatively mobile due to the sliding connections. Theoretically, a dynamic system is less vulnerable to fatigue failures as compared to static rods which has also been demonstrated in recent finite element models.[126] The simplicity of the technique is also advantageous, we observed excellent distraction in all springs despite considerable tissue ingrowth. This is in contrast to MCGR, where failure to distract is common due to component failure of the driving mechanism.[43–45,54,139]

Strengths of the current study include the relatively large patient cohort that was prospectively followed for at least 2 years. In addition, the diverse patient group represents a varied EOS population, as observed by the considerable variation in baseline EOSQ-24 domain scores. Limitations of this study include the absence of a control group. Although we always offer MCGR as a standard treatment to our patients (SDS is only implanted as part of a clinical trial), only one patient opted for this. With the increasingly disappointing results of MCGR (in our own experience and also observed in the literature), we foresee difficulties including and randomizing patients to that treatment arm when performing a randomized controlled trial, but obviously, such studies should be performed when SDS is registered for medical use.[45,139,142,143] Another limitation is that the majority of patients have only short- to medium-term follow-up. It is possible that as follow-up increases, additional complications will manifest. Also, while we did include HRQoL results with the EOSQ-24, we did not specifically investigate pulmonary function in the SDS patients. Future

5

studies should correlate the radiographical and HRQoL outcomes of SDS patients to changes in pulmonary function. Finally, the SDS is not yet fully optimized. It is composed of a custom-made spring and uses several components in an off-label manner. Especially the CoCr on titanium sliding through the side-to-side connector is a concern, because of metal debris and lack of kyphosis control. We are currently optimizing the SDS design, while simultaneously pursuing medical registration, although the latter will be a laborious process, especially with the impending new European Medical Device Regulations.

Conclusion

The SDS appears to be a promising technique for surgical treatment of EOS. Curve correction in primary patients was 50% and could be maintained for at least 2 years. Mean T1-S1 height gain during follow-up was 11.6 mm/year, which compares favorably to contemporary systems that need intermittent distractions. Complications and reoperations could not be prevented, but the complication rate seems modest compared to contemporary systems, and there are opportunities to decrease this further. Improvement of this in-house developed implant and medical registration are our next steps.
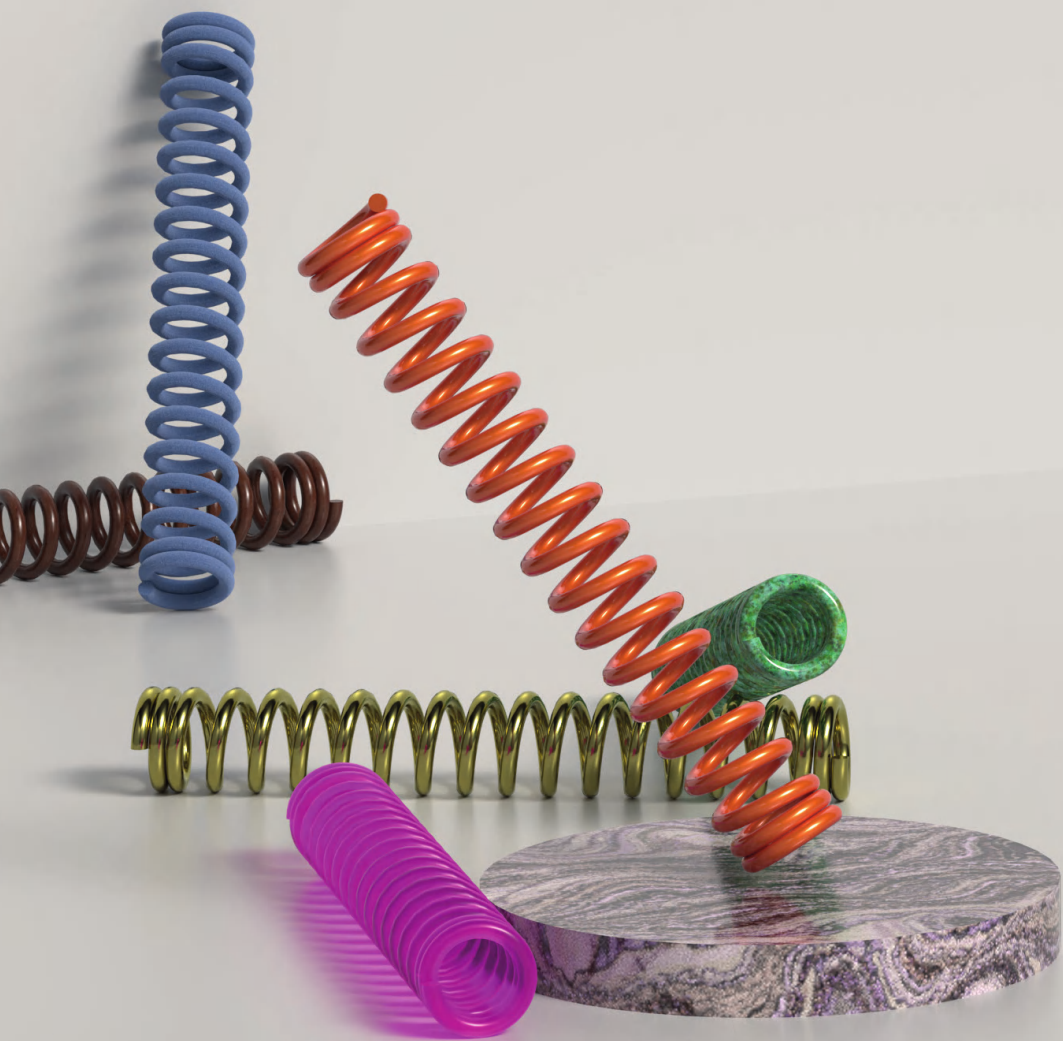
Chapter 6

Surgical Treatment of Neuromuscular Early Onset Scoliosis with a Bilateral Posterior One-Way Rod Compared to the Spring Distraction System: Study Protocol for a Limited-Efficacy Randomized Controlled Trial (BiPOWR)

J.V.C. Lemans
C.S. Tabeling
E.P. Scholten
H.W. Stempels
L. Miladi
R.M. Castelein
M.C. Kruyt

Abstract

Background
Early Onset Scoliosis (EOS) is a progressive spinal deformity in children, and a potentially life-threatening disease. "Growth-friendly" surgical techniques aim to control the deformity, while allowing the spine and trunk to maintain growth. Current "growth-friendly" systems such as the traditional growing rod (TGR) and magnetically controlled growing rod (MCGR) have limitations that reduce their efficacy and cost-effectiveness. Recently, two "growth-friendly" systems have been developed that mitigate many of these limitations, the Spring Distraction System (SDS) and the One Way Self-Expanding Rod (OWSER). The purpose of the multicenter BiPOWR trial is to investigate, describe and compare the 1-year limited-efficacy and -safety of both strategies in the treatment of neuromuscular EOS.

Methods
After informed consent, 28 neuromuscular EOS patients will be randomized to receive either the SDS or the OWSER. Patients and caregivers will be blinded to allocation until after surgery. Primary outcome will be maintenance of coronal curve correction and the occurrence of serious adverse events. In addition, spinal growth, implant lengthening, and perioperative findings are recorded systematically. At each follow-up moment, the Early Onset Scoliosis Questionnaire (EOSQ-24) will be used to assess health-related quality of life. All outcomes will be compared between groups.

Discussion
The BiPOWR trial is the first randomized controlled trial that compares two specific "growth-friendly" implants in a specified EOS population. It will determine the 1-year limited-efficacy and safety of the SDS and OWSER implants.

Trial registration
Clinicaltrials.gov: NCT04021784 (13-06-2019). CCMO registry: NL64018.041.17 (06-05-2019).

Introduction

Early Onset Scoliosis (EOS) is a complex three-dimensional deformity of the spine and trunk, which, if left untreated, can result in severe cardiopulmonary compromise or even death.[13,144] The early onset of the deformity carries with it a high risk of progression, which places importance on early treatment to preserve pulmonary function. This is even more important in patients with neuromuscular diseases such as spinal muscular atrophy or Duchenne muscular dystrophy. In these patients, respiratory muscles that are necessary for normal in- and expiration weaken, which, together with altered chest wall compliance, leads to further respiratory compromise. [145,146] Whilst a spinal fusion is able to correct the deformity, doing this in the growing spine arrests all further growth, which limits pulmonary function even more. [14] In addition, continued anterior spinal growth after posterior fusion may result in worsening of the curve, a phenomenon known as crankshafting.[16] To circumvent these problems, "growth-friendly" techniques have been developed, which control curve progression while allowing for the spine and trunk to grow. Currently, the most common "growth-friendly" systems are the traditional growing rod (TGR) and the magnetically controlled growing rod (MCGR).[32,147] While both systems can control the scoliotic deformity, they have important limitations. For the TGR, the most obvious limitation is the need for repetitive surgical lengthenings (generally every 6 months), which exposes patients to high anesthetic stress at a young age, which may negatively influence neurodevelopment.[34] For the MCGR, lengthenings are non-invasive, but they still require patients to come to the outpatient clinic on a regular basis, more often than in TGR, which imposes a psychological burden on these patients and their parents.[148] In addition, both TGR and MCGR have high mechanical (i.e. implant-related) complication rates which result in reoperations and diminished length gain. [33,35,45,96,139,149] The high rate of MCGR dysfunction recently resulted in a temporary suspension of CE certification and the advice to limit MCGR implantation in several countries.[46,47]

To overcome these limitations, two new systems were developed: the Spring Distraction System (SDS) that uses a compressed spring around standard rods to generate distraction and the One Way Self-Expanding Rod (OWSER, CE-marked as Nemost®; Euros, SAS, La Ciotat, France) which is a one-way sliding rod with split retaining ring system. Both systems are designed to facilitate growth of the spine without interventions, while maintaining curve correction. Previous publications have shown the feasibility of both systems.[59,150] However, patient populations and surgical strategies were heterogeneous, and the case series design could have led to selection bias. To determine clinical efficacy, identify early mechanical failures, and to generate level 1 evidence for potential differences between the techniques, a single-blinded, prospective randomized trial was considered the ideal strategy.

Methods

Study aims

The primary aim of the BiPOWR trial is to prospectively describe and compare efficacy (coronal and sagittal curve maintenance) and –safety (occurrence of Serious Adverse Events; SAEs) of two innovative implant systems in neuromuscular EOS patients. Due to the relatively short follow-up of participants (1 year), with intermediate instead of final outcomes, the study is regarded as a limited-efficacy and -safety study.[151] A secondary aim is to describe and compare spinal- and implant growth, peri-operative parameters and Health-Related Quality of Life (HRQoL).

Study design

The BiPOWR trial is a prospective, multicenter, randomized, surgical trial with two parallel groups and a 1:1 allocation ratio. Ethical approval was provided by the Institutional Review Board of the UMC Utrecht (METC 18-179). Following inclusion, patients undergo "growth-friendly" scoliosis surgery with one of two implants, the SDS or the OWSER. Which implant they receive is decided by randomization. Following implantation, the patients are followed until 12 months post-operatively, during which their radiographic- and clinical outcomes will be described and compared. The analysis at 12 months provides a point for interim analysis in the short follow-up, to determine whether one or both implants show short-term technical malfunctions, and to ascertain whether early detectable differences are present in other outcome domains. After the 1 year analysis, both patient cohorts are followed bi-yearly for several more years, until after skeletal maturity, to show efficacy and safety in the long-term. A SPIRIT table showing a detailed follow-up timeline for the first year of follow-up is shown in Table 1.

Table 1: SPIRIT Table

STUDY PERIOD

	Enrolment	Allo-cation	Surgery	Post-allocation				
TIMEPOINT	$-t_2$ Before -2 weeks	$-t_1$ -2 weeks	t_0 Day of surgery	t_1 +1 week	t_2 +4 weeks	t_3 3 months	t_4 6 months	t_5 12 months
Enrolment								
Eligibility screen	X							
Informed consent	X							
Allocation		X						
Interventions								
Spring Distraction System			**Implant in Situ**					
One Way Self-Expanding Rod			**Implant in Situ**					
Outcomes								
Main coronal Cobb angle	X			X	X	X	X	X
Serious Adverse Events			X	X	X	X	X	X
Implant length				X	X	X	X	X
EOSQ-24 questionnaire	X			X	X	X	X	X

6

Eligibility criteria

Inclusion criteria are:

- Neuromuscular or syndromic EOS (i.e. diagnosis before age 10)
- Progressive EOS with an indication for bipolar fixation extending to the pelvis
- Non-ambulant patients
- Age <12 years.

Exclusion criteria are:

- Closed triradiate cartilage
- Main curve proximal end vertebra at or above T3
- Presence of skeletal dysplasia affecting growth
- Presence of disease that severely influences bone quality or is associated with soft tissue weakness
- Presence of active systemic disease (other than neuromuscular disease)
- Congenital spinal anomaly of >5 vertebrae
- Previous instrumented spinal surgery
- Patients who cannot be followed for 1 year post-operatively

Recruitment and informed consent

The treating physician identifies potential eligible patients, and asks the patient and their caregiver(s) whether they would like to receive additional study information. Upon agreement, the principal investigator is consulted for approval and the research team subsequently sends the study information. After at least two weeks, a consultation with the research team takes place where the in- and exclusion criteria are assessed, the study is explained in detail and patients' questions are answered. Care is taken to ensure that the study design (in particular blinding and randomization) and the similarities and differences of the two treatment arms are understood. If willing to participate, the informed consent form is signed in duplicate and the consent is noted in the electronic patient record.

Randomization and blinding

After inclusion, the patient is randomized into one of two treatment groups. Before the start of the trial, a randomization sequence was created using a computer-generated random number sequence, which was used to create a permuted block design with random block sizes. A random number of blocks with random block sizes of 2, 4, 6 and 8 created the final sequence containing 28 randomized patients. The sequence was converted into allocation notes, which were stored in opaque, sealed envelopes. Each allocation envelope was sealed into a second, sequentially numbered, opaque envelope. The use of two envelopes prevents the use of trans-illumination to unblind allocation. Two weeks before surgery, the next numbered study envelope is retrieved

by two members of the study team. The envelopes, the seals in particular, are visibly examined for tampering. The allocation is confirmed by both research team members, and the pseudonymized patient number is written on the allocation note and the study envelopes. The treating physician is then notified of the outcome of the allocation, to order the required implants.

The patient and caregiver(s) remain blinded to the result of allocation until after surgery to prevent selection bias through termination from the study before surgery commences, which is a possibility if they have a strong preference for one treatment arm.[152] After surgery has taken place, the allocation outcome is shared with the patient and caregiver(s). While blinding patients during the entire study period is theoretically possible, enforcing this would require extreme effort, as it would preclude the treating physician of showing any of the follow-up radiographs to the patient and caregiver(s) as these clearly show the different implants. Since these radiographs often provide a wealth of information to the patient and caregiver(s), denying them these raises ethical concerns and would likely decrease enrolment rate.

6

Surgical procedure and treatment arms

All surgical procedures will be performed using a less invasive bipolar posterior approach with somatosensory and motor-evoked potential monitoring.[153] The distal anchor is created with iliosacral screws (Tanit®; Euros, SAS, La Ciotat, France). The proximal anchor for SDS consists of bilateral pedicle screws at 3 consecutive levels, typically T2-T4. For the OWSER, a series of laminar- and pedicle hooks spanning 5 vertebrae is applied (T2-T6).

The SDS (Figure 1) is an adjunct to standard 5.5 mm cobalt-chromium (CoCr) rods. It consists of three components: (1) a titanium (Ti6Al4V) spring placed over the rod, (2) two stacked oversized parallel connectors and (3) a buttress used to tension the springs (Stryker, Leesburg, VI, USA). In neuromuscular EOS, the SDS is placed bilaterally. The concave rod receives a strong 100 N spring (spring constant (k) = 1.32 N/mm), the convex rod receives a weaker 50 N spring (k = 0.68 N/mm). Around 6-7 cm of residual rod length is left for growth. The parallel connectors are secured to the distal anchor rods and the rod containing the spring is allowed to slide in the connector.

The OWSER (Figure 2) consists of two titanium components: (1) a 5.5 mm titanium long rod with a notched end, and (2) a sliding domino that passively migrates only one way across the notched rod segment. The long rod is connected to the proximal anchor with the notched end facing distally. The connector is fixated with a short rod to the distal anchor. Implant growth potential (i.e. the notched segment of the long rod) can be 50 or 80 mm. In neuromuscular EOS, the OWSER is also placed bilaterally.

Figure 1: Spring Distraction System

Buttress

Side-to-side connector

5.5mm rod

6.0mm hole

No Set Screw

Ti-6Al-4V Spring

Curve concavity   100N
Curve convexity   50N

The SDS consists of three components that are added to standard growing rods. It provides a continuous distraction force during follow-up, without the need for repeated lengthenings. In the BiPOWR trial, the distal anchors are iliosacral screws instead of pedicle screws. Green. A side-to-side connector with one oversized hole through which a CoCr rod can slide freely. Gold. Ti6Al4V springs which can be compressed over the rod. Blue. The buttress compresses the spring against the side-to-side connector.

Figure 2: One Way Self-Expanding Rod

The OWSER is a growing rod that passively lengthens one way as the spine grows. In the BiPOWR trial, the distal anchors are iliosacral screws instead of pedicle screws. Blue. the proximal fixation consists of hooks positioned in a claw configuration. Two crosslinks are added for torsional stability (green). Red. The growing domino, combined with a rod that is serrated across its distal length, allows for lengthening. The reserve length can be 50mm or 80mm long. Movement in the other direction is prevented by a split retaining ring system inside the domino.

The implant configurations are shown radiographically in Figure 3. All patients treated by either SDS or OWSER are allowed unrestricted physical activities postoperatively. We do not routinely perform manual axial trunk traction in the outpatient clinic for these most vulnerable of OWSER patients. For OWSER implant lengthening, we instead rely only on passive lengthening due to spinal growth, in combination with normal traction and bending generated through daily activities.

Figure 3: Implant configuration
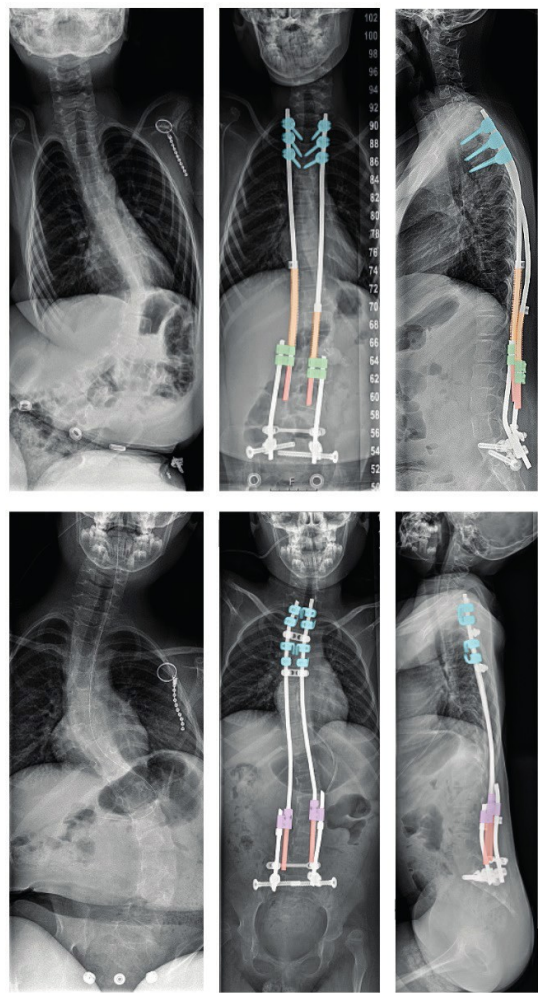
Representative implant configurations of the SDS (top) and the OWSER (bottom) are shown. Top. A proximal foundation of 3 pedicle screws is placed (blue). The distal foundation consists of iliosacral screws. CoCr rods are placed through open side-to side connectors (green). Around these rods, 2 springs

(orange) are positioned, which push against these connectors and a proximal locking buttress. The gliding parts of the rods (red) become shorter as the spine grows. Bottom. Here, the proximal foundation consists of 2 claws (blue), created with hooks. The distal foundation consists of iliosacral screws. The Ti6Al4V OWSER rods are inserted with the dominos placed distally (purple). The notched part of the rods (red) can only lengthen one-way through the domino's.

Outcomes

The primary outcomes include coronal Cobb angle – measured on radiographs – and occurrence of SAEs (defined as unplanned medical events which (could) result in permanent disability/damage, or which requires (lengthening of) hospitalization, a re-operation, or inpatient medical managing). SAEs will be categorized as either device/surgery related (e.g. rod fracture, post-operative neurological deficit), or as disease-related (e.g. pneumonia, pain) according to a previously created complication classification system for use in EOS treatment.[154] In addition to SAEs, complications that do not meet the criteria for an SAE, but which are device/surgery related (e.g. superficial infections, proximal junctional kyphosis) will also be recorded.

Secondary radiographic measurements include parameters such as T1-T12, T1-S1 and instrumented height, T5-T12 kyphosis, L1-S1 lordosis, and pelvic obliquity. In addition, implant length will be calculated at each timepoint for both groups (SDS: Spring length, OWSER: Notched rod length) so that implant growth velocity over time can be graphed and calculated. The number of outpatient axial traction events of OWSER patients, if these are performed, will also be reported. All radiographic measurements will be performed by a trained assessor. To ensure data quality, radiographic measurements are performed semi-automatically in Surgimap v2.3.2.1 software (Nemaris, New York, USA), after which all measurements are audited by the assessor. At the end of the data collection phase, all radiographic measurements are re-assessed by a second trained assessor who is blinded to the first assessors' measurements. Measurements are compared and disputed measurements are discussed until consensus is reached. If differences are believed to be caused by random measurement variation, the arithmetic mean of both assessors' measurement is taken.

HRQoL will be measured with the validated Dutch version of the EOSQ-24 which consists of 24 questions in 10 domains, from which a domain- and total score is calculated.[138,155] All outcome parameters are measured pre-operatively, immediately post-operatively, and at 1, 3, 6, and 12 months follow-up.

Sample size calculation and statistical methods

The sample size calculation is based on potential differences between groups in maintenance of the coronal curve between the post-operative situation and 1-year follow-up. A difference in Cobb angle ≥5° is considered clinically relevant and can be reliably measured.[156] In our previous MCGR cohort studies, we found a change

in Cobb angle between post-operatively and 1 year follow-up of 1° (SD 5.1°).[143] To determine differences in curve maintenance between groups ≥5° with a power (1-β) of 0.8, α=0.05, and SD=5.1°, we calculated a sample size of n=28, with a repeated measures ANOVA between factors design (comparing 2 timepoints). With an allocation ratio of 1:1, this means that 14 patients have to be included in each experimental group.

If all assumptions for performing repeated measures ANOVA are met, both systems will be compared with respect to coronal curve maintenance; age and sex will be included as covariates. For the other continuous variables, repeated measures ANOVA will be used, with the same covariates, but including all evaluated time points. If the assumptions for performing repeated measures ANOVA are not met (e.g. due to missing data), repeated measurement multilevel modelling will instead be performed, with patient, age, sex and treatment group as level 2 variables, and follow-up time as level 1 variables.

A Kaplan-Meier survival analysis will be performed comparing both groups. The survival curves showing SAE-free survival of both groups will be statistically compared with the Log-Rank test. Analysis of EOSQ-24 scores will be performed using repeated measures ANOVA. In case there are missing EOSQ-24 item scores or questionnaires, multiple imputation with parcel summary scores will be performed using a previously published statistical method.[157] For all statistical tests, statistical significance will be set at $p < 0.05$. All statistical analyses will be performed in IBM SPSS statistics v.26.0.0.1 (Chicago, USA).

Discussion

Current treatment of EOS is largely based on opinion and physician's experience. This low level of evidence has many reasons, which start with the broad definition of EOS. Currently, any scoliosis that initiated before age 10 is regarded as EOS. Since many curves only become problematic during the growth spurt, these can often be treated through spinal fusion and do not require "growth-friendly" surgery. Patients that may be eligible for "growth-friendly" surgery likely had a curve onset much earlier and therefore are a distinct subgroup. Another issue is that most data comes from combined registries which include patients with heterogeneous etiologies (varying from severely disabled children to completely heathy), surgical indications and implant types. In addition, most treatment strategies are just being discovered and promising techniques such as MCGR appear much more vulnerable to failure than expected.[45] Therefore, long-term follow-up of large groups is simply absent. Finally, if results are reported, these studies are often inconsistent, incomparable, and of poor methodological quality, as reflected in a previous systematic review.[31]

To investigate "growth-friendly" implants or strategies that are typically used in small numbers, we believe a prospective study on a specific population with a specific technique is essential, preferably with follow-up until after final fusion. Such a design demands a lot of effort, even before including patients, starting with a rigorous protocol, installation of a dedicated research team and IRB approval. The BiPOWR trial is the first surgical randomized trial to be performed in children with EOS, designed to investigate the limited-efficacy and safety of two novel "growth-friendly" systems.

Although the study will generate high level evidence, there are several limitations to consider. First, this study does not investigate if growth friendly surgery is actually better than continuing conservative treatment, as we only compare surgical treatments. Also, this study does not have a control group, as we compare the SDS with the OWSER, instead of a 'gold standard' surgical treatment – i.e., TGRs and/or MCGRs. We chose this design deliberately as we experienced many problems with current standard therapies, from which we conclude that there simply is no accepted 'gold standard'. In fact, many of our patients are referred to our center because we have the possibility to offer these novel treatments. It would be unethical to ask these patients to be randomized to a treatment of which we know it has serious disadvantages. Obviously, the patient can always choose not to be included in the study and opt for conventional treatments such as TGR or MCGR that we perform regularly. Second, the primary endpoint is at only one year follow-up. It is possible and likely that complications manifest after this period as is also seen with conventional "growth-friendly" systems.[33,45,113] The primary endpoint is, in that sense, a short-term interim analysis to look at early mechanical failures and short-term efficacy, hence the limited-efficacy nature of the study. After completion of the 1-year analysis, both cohorts of patients will be followed for several years until (and even after) skeletal maturity. Only at that point, definitive conclusions regarding efficacy can be drawn. For practical reasons, we did not incorporate the long-term analysis into the primary aim of the BiPOWR trial. Third, although randomization is obviously a strong method to minimize bias in comparative studies, this carries the risk of being too artificial and not representative.[158–160] One way to mitigate this, is a multicenter approach and sufficient learning curve for both treatments. We recognize, however, that the investigated techniques are new, and only practiced by a selective group of surgeons. This means that the outcomes of the BiPOWR trial should only be used as an initial indication of efficacy and safety. These findings should be confirmed with larger observational studies and registry data.

6
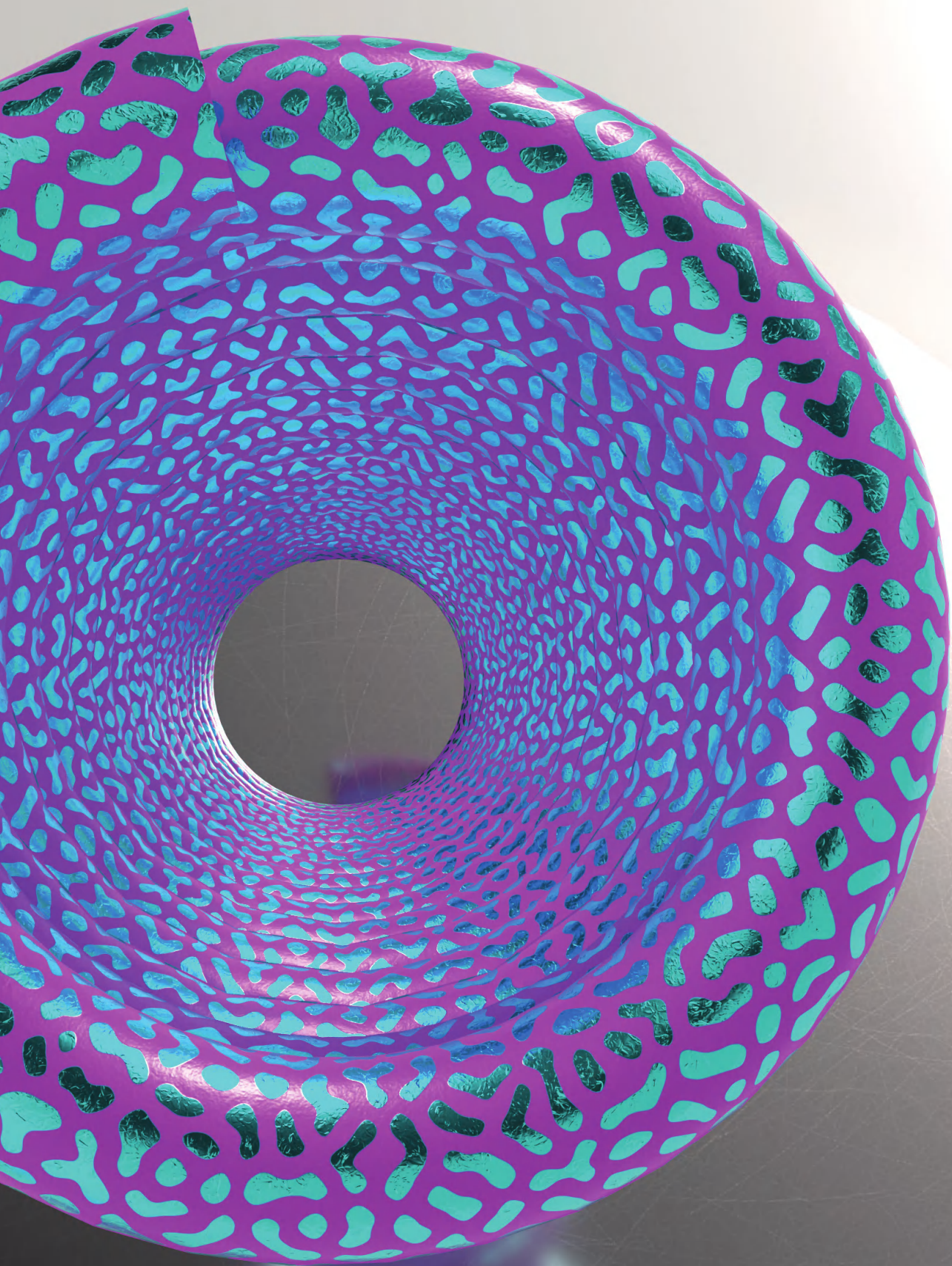
Chapter 7

One Year Results of the Randomized BiPOWR Trial Comparing the Spring Distraction System (SDS) and the One Way Self-Expanding Rod (OWSER) for the Correction of Neuromuscular and Syndromic Early Onset Scoliosis

J.V.C. Lemans

C.S. Tabeling

A. Stadhouder

J.J.M. Renkens

E.P. Scholten

H.W. Stempels

L. Miladi

R.M. Castelein

M.C. Kruyt

Abstract

Study Design
RCT

Objectives
To compare the 1-year efficacy and -safety of the Spring Distraction System (SDS) and the One Way Self-Expanding Rod (OWSER) in the treatment of neuromuscular/syndromic EOS.

Methods
Non-ambulant, neuromuscular/syndromic EOS patients were included in 3 academic hospitals. They were randomized to treatment with SDS or OWSER and were blinded until after surgery. Outcomes were coronal curve, spinal growth and the occurrence of (serious) adverse events ((S)AEs). In addition, spinal growth and implant lengthening was calculated. Data were collected pre-operatively, immediately post-operatively, and at 1, 3, 6 and 12 month follow-up.

Results
Thirty patients were included. Two patients passed away during follow-up, these patients were replaced, all collected data was used for analysis. Mean age at surgery was 9.0 years, 20/30 patients were male. Mean coronal curve decreased from 74.9° pre-operatively, to 37.6° post-operatively, remaining stable at 37.7° at 1 year follow-up, with no group differences. T1-T12 length increased 18 mm/year for SDS and 9 mm/year for OWSER. For T1-S1 length, this was 26 mm/year (SDS) and 18 mm/year (OWSER). Five (S)AEs occurred in the SDS group and 11 (S)AEs in the OWSER group. Two SDS patients passed away, unrelated to the surgery or implant. One (S)AE in the SDS group and 6 (S)AEs in the OWSER group were implant-related.

Conclusions
The SDS and the OWSER achieved coronal curve correction of 50%, which was maintained at 1-year follow-up. Spinal length increase was excellent for both systems. The (S)AE rate was 30%/patient/year for SDS and 78%/patient/year for OWSER.

Introduction

Early onset scoliosis (EOS) represents a complex deformity of the spine and trunk. Deformities can cause significant health problems, particularly pulmonary compromise, which places importance on early intervention.[144–146] Successful management relies on preventing progression of the spinal deformity, allowing growth of the spine and trunk and lung development to maximize pulmonary function with a minimal amount of complications.[145] Conservative treatment such as casting or bracing are commonly used for early intervention.[161] However, especially in neuromuscular or syndromic EOS, these techniques are at best able to delay surgery and have many drawbacks.[162,163] Surgical treatment of the growing spine is complex. In the past, the standard approach was a long-segment spinal fusion, often to the pelvis, resulting in growth arrest with the risk of underdevelopment of the lungs.[14] In addition, posterior fusion alone may lead to progression of the spinal deformity secondary to the remaining anterior growth of the spine, known as the "crankshaft" phenomenon.[16]

   To address these issues, growth-friendly procedures have been developed such as the traditional growing rod (TGR) and magnetically controlled growing rod (MCGR).[32,147] While both are able to control the spinal deformity and allow spinal growth by distraction, the complication rate is high and results can still be improved.[164,165] For the TGR, the most obvious limitation is the need for repetitive surgical lengthenings (generally every 6 months), increasing both the risk of complications and the anesthetic burden on the child.[33,34] The MCGR allows for more frequent lengthening without surgery. However, more frequent returns to the outpatient clinic imposes a psychological burden on the patients and their parents.[148] Besides these inherent limitations, both systems have high mechanical (i.e. implant-related) complication rates which lead to many unplanned reoperations and diminished length gain.[33,35,45,96,139,149] For MCGR, rod metallosis due to high frictional forces were a reason to temporarily withdraw it from the market and currently, the FDA has approved its use for no longer than two years of implantation, although many devices are implanted for much longer.[49,166–168] Another important disadvantage of the 'traditional' systems is that lengthening is intermittent, rigid and abrupt.[35,82,94] An ideal system would provide continuous, dynamic lengthening of the spine without further interventions.

   To combat the limitations of TGR and MCGR while utilizing their advantages, two new growth-friendly systems were developed: the Spring Distraction System (SDS) and the One Way Self-Expanding Rod (OWSER). The SDS (not yet FDA approved) uses a compressed spring around a conventional rod to generate distraction forces. The OWSER (FDA approved and CE-marked as Nemost®; Euros, SAS, La Ciotat, France) uses a notched rod that can lengthen one-way with a split-ring retaining system. The most important advantages of the SDS and OWSER are that they can

7

expand continuously, while maintaining deformity correction, without the necessity for surgical or outpatient clinic interventions. This, in combination with the less invasive method of implantation is especially useful for EOS patients with neuromuscular or syndromic etiologies, as these patients have increased risk of suffering from wound- and pulmonary complications following surgery.[169,170] The feasibility of both systems has been shown in previous studies, however, the patient populations and surgical strategies were quite heterogeneous.[59,113,150,171] Moreover, the case series design in these studies may have led to selection bias. We therefore performed a randomized trial (BiPOWR) to compare 1 year efficacy and safety of both the SDS and OWSER in a similar group of neuromuscular or syndromic EOS patients.

Methods

Trial protocol and ethical review
The current study was approved by the Institutional Review Board of all three participating centers and was prospectively registered (Clinicaltrials.gov: NCT04021784). In addition, an elaborate study protocol was published previously.[172] This study conformed to the CONSORT statement.[173] All patients and parents/caregivers provided written informed consent before they were included into the trial.

Study Design
The current study is a prospective, multicenter, randomized limited-efficacy trial comparing the SDS and the OWSER in 3 academic hospitals in The Netherlands. Non-ambulatory, neuromuscular or syndromic EOS patients were eligible for inclusion. Additional eligibility criteria are reported in Table 1. After inclusion, patients were randomized into either the SDS or OWSER group in a 1:1 ratio and their outcomes with respect to efficacy and safety were evaluated and compared during the first year of follow-up. A previous power calculation showed that fourteen patients in each arm were necessary to identify a 5° difference in coronal Cobb angle after 1 year with a power of 80% and an α of 0.05.[172] Patients in each group were evaluated pre-operatively, immediately post-operatively, and at 1, 3, 6 and 12 months post-operatively.

Randomization and blinding
Before the trial commenced, a pseudorandom sequence of 28 numbers was created using a computer-generated permuted block design with random block sizes. This sequence was converted into allocation notes kept in double sealed, opaque envelopes, which were sequentially opened after the surgery date was planned. The patient and his/her caregivers remained blinded until after surgery. This prevented the potential scenario in which patients/caregivers could withdraw from the study

Table 1. Eligibility criteria

Inclusion criteria
1. Neuromuscular or syndromic early onset scoliosis (diagnosis before age 10)
2. Progressive early onset scoliosis with an indication for bipolar fixation extending to the pelvis
3. Non-ambulant patients
4. Age <12 years

Exclusion criteria
1. Closed triradiate cartilage
2. Main curve proximal end vertebra at or above T3
3. Presence of skeletal dysplasia affecting growth (such as achondroplasia or spondyloepiphyseal dysplasia congenita)
4. Presence of disease that severely influences bone quality (such as osteogenesis imperfecta) or is associated with soft tissue weakness (such as Marfan syndrome, neurofibromatosis or Ehlers-Danlos syndrome)
5. Presence of active systemic disease
6. Congenital spinal anomaly of >5 vertebrae
7. Previous instrumented spinal surgery
8. Patients who cannot be followed for 1 year post-operatively

7

before surgery, if they were disappointed by the randomization result. Unblinding after surgery prevents this type of (selection) bias.

Surgical procedure and treatment arms

All surgical procedures were performed using a less invasive bipolar posterior approach and instrumentation with neuromonitoring when appropriate.[153] To minimize surgical heterogeneity between centers, the senior author was present during all surgeries in all participating centers. Before the start of the study, the senior author had multiple years of experience using both the SDS implant as well as the OWSER implant. The distal anchor was created using iliosacral screws (Tanit®; Euros, SAS, La Ciotat, France).[174] The proximal anchor for SDS consists of bilateral pedicle screws at 3 consecutive levels, typically T2-T4. For the OWSER, a series of proximal laminar- and pedicle hooks spanning 5 vertebrae was created (T2-T6).

The SDS (Figure 1) is an adjunct to 5.5 mm cobalt-chromium (CoCr) rods. It consists of three components: (1) a titanium (Ti6Al4V) spring placed over the rod, (2) two stacked oversized parallel connectors and (3) a buttress used to tension the springs. In neuromuscular EOS, the SDS is placed bilaterally. Around the concave rod, a 100 N spring (spring constant (k) = 1.33 N/mm, growing length 83mm) was inserted, the convex rod received a weaker 50 N spring (k = 0.67 N/mm, growing

length 83mm). Both springs were maximally compressed. The rods that house the spring are left with 6-7 cm of residual rod length, which is the growth potential during follow-up. The parallel connectors were then secured to the distal anchor rods and the rod containing the spring was allowed to slide freely in the connectors.

The OWSER (Figure 2) consists of two titanium components: (1) a 5.5 mm titanium long rod with a notched end, and (2) a sliding domino that passively migrates only one way across the notched segment. The sliding domino is fixated with a short rod to the distal anchor. Implant growth potential (i.e. the notched segment of the long rod) can be either 50 mm or 80mm. For the BiPOWR study, we performed bilateral OWSER implantation, using implants with 50 mm reserve length. We did not perform manual axial trunk traction to achieve lengthening in the outpatient clinic. We instead relied only on passive lengthening due to spinal growth, in combination with normal traction and bending generated through daily activities.

All patients in the BiPOWR trial were allowed unrestricted physical activities postoperatively.

Figure 1: Spring Distraction System
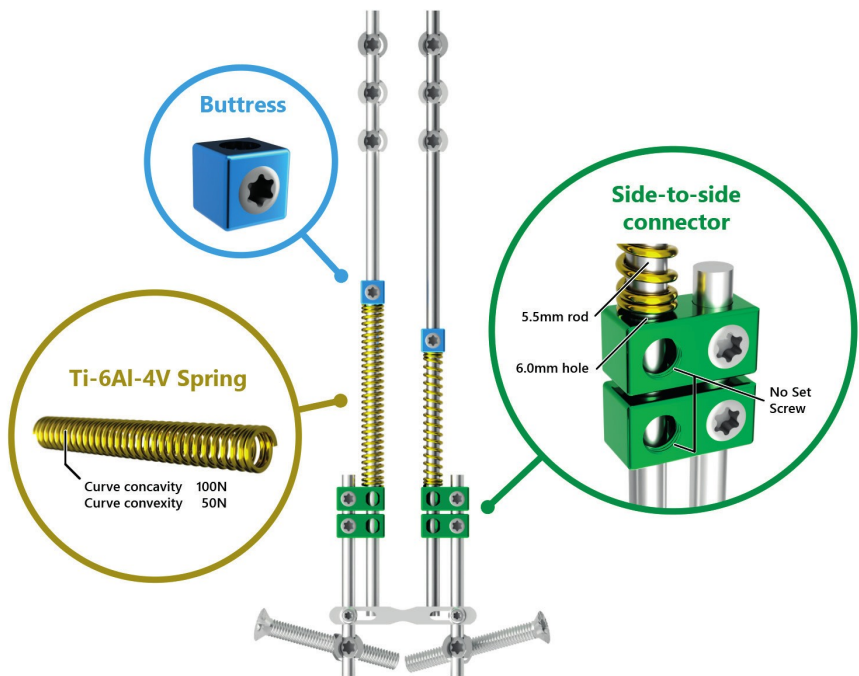
The SDS consists of three components that are added to standard growing rods. It provides a continuous distraction force during follow-up, without the need for repeated lengthenings. In the BiPOWR trial, the distal anchors are iliosacral screws. **Green.** A side-to-side connector with one oversized hole through which a CoCr rod can slide freely. **Gold.** Ti6Al4V springs which can be compressed over the rod. **Blue.** The buttress compresses the spring against the side-to-side connector.

Figure 2: One Way Self-Expanding Rod

The OWSER is a growing rod that passively lengthens one way as the spine grows. In the BiPOWR trial, the distal anchors are iliosacral screws instead of pedicle screws. **Blue.** the proximal fixation consists of hooks positioned in a claw configuration. Two crosslinks are added for torsional stability (green). **Red.** The growing domino, combined with a rod that is serrated across its distal length, allows for lengthening. The reserve length can be 50mm or 80mm long. Movement in the other direction is prevented by a split retaining ring system inside the domino.

Outcomes

Demographic parameters such as age, sex, and etiology were recorded as well as surgical parameters such as surgical time and estimated blood loss. Radiographic measurements included main coronal Cobb angle, pelvic obliquity (measured according to the method described by Maloney et al.[175]), T5-T12 kyphosis and L1-S1 lordosis. In addition, we measured T1-T12 and T1-S1 height and -length. Height was calculated as the shortest distance between horizontal lines that were drawn through the midpoint of the upper and lower endplate. For the length measurements, a spline curve was drawn through each endplate that followed the curvature of the spine. These freehand length measurements are less influenced by changes in coronal and sagittal curve.[59,137] All height and length measurements were drawn on both the coronal and sagittal radiographs and the values were averaged. Initial implant growth in the first days after surgery was assessed as the achieved leng-

thening compared to the maximally loaded spring (SDS) or initial notched rod length (OWSER).

We investigated the occurrence of (serious) adverse events ((S)AEs) in both groups. (S)AEs were classified as disease-related (i.e. related to EOS such as respiratory insufficiency), surgery-related (e.g. surgical site infection) or implant-related (e.g. mechanical failure). For disease- and surgery-related complications we only registered SAEs, i.e. those events which (could) result in permanent disability/damage, or required hospitalization (or lengthening thereof), an unplanned return to the operating room (UPROR), or outpatient medical managing (e.g. antibiotic treatment for SSI). For implant-related complications, all AEs were registered. This includes all complications that were visible on patient radiographs, also if they did not have any apparent clinical consequences (e.g. failure to lengthen), a comprehensive list with criteria for these criteria in "growth-friendly" systems was published previously.[113] To classify severity of (S)AEs, we used the method of Smith et al.[154] In case of (S)AEs, the time of occurrence after initial surgery was also recorded.

All radiographic measurements were performed independently by two researchers (JVCL and CST), using the Surgimap v2.3.2.1 software (Nemaris, New York, USA). Both researchers were blinded to the other's measurements. For all continuous measurements the arithmetic mean of both assessors' measurement was taken. Interrater reliability between both authors, calculated using the intraclass correlation coefficient, was 0.92, indicating excellent reliability. In regard to (S)AEs, the Data Safety and Monitoring Board arbitrated the final decision on presence or absence of (S)AEs in case no consensus was reached.

Statistics

Baseline characteristics are shown in both groups. Changes in outcome parameters over time are shown as mean (SD) or median (IQR). We employed a mixed repeated-measures ANOVA to determine differences between pre- and post-operative values. Age at surgery and sex were added as covariates. The interaction between follow-up and treatment group was calculated to determine whether the post-operative change differed significantly between groups. The changes from post-operatively until 1 year follow-up were investigated with linear mixed models, to account for missing data, changes in treatment group during follow-up, different follow-up times and to identify the independent effects of several variables. A restricted maximum likelihood estimator model was created for each radiographic variable with sex, age at surgery, pre-operative value, follow-up time and treatment group as fixed effects. In addition, the interaction between follow-up time and treatment group was added as a fixed effect, to identify whether changes over time differed between groups. Patient ID was added as a random effect.

(S)AE rates in both groups were shown as (S)AEs/patient/year. The time to complications between groups were plotted in Kaplan-Meier curves, and proportional hazards were compared with the Mantel-Cox method.

The statistical procedures were performed in IBM SPSS Statistics 28.0 (IBM Corp., Armonk, NY, USA) with the exception of the linear mixed models, which were performed in R Statistical software version 4.0.2 (R Foundation for Statistical Computing, Vienna, Austria) and the survival analysis, which was performed in GraphPad Prism v 10.2.3 (Graphpad Software, San Diego, CA, USA). A p<0.05 was chosen as statistical significance.

Results

Patient inclusion and protocol deviations
During the study period (2019-2023), 30 patients were included, 16 in the SDS group and 14 in the OWSER group. This discrepancy occurred because 2 patients in the SDS group passed away before the end of the 12 month follow-up, due to causes not related to the intervention. These patients were replaced, but the data of all patients was ultimately included in the analysis, up until the point where the patients were lost to follow-up. One of the OWSER patients suffered an SAE that necessitated a re-operation and implant change. The caregivers of this patient had the strong desire that their child receive the SDS implant for the remainder of the study period. Given that a linear mixed model was used for the follow-up analysis (which accurately takes into account the outcome differences if a participant changes from their allocated group), we agreed with this request. This patient was left in the analysis and was followed until the end of the study period. A CONSORT flow diagram of study participants can be seen in Figure 3.

7

Figure 3: CONSORT patient flow diagram
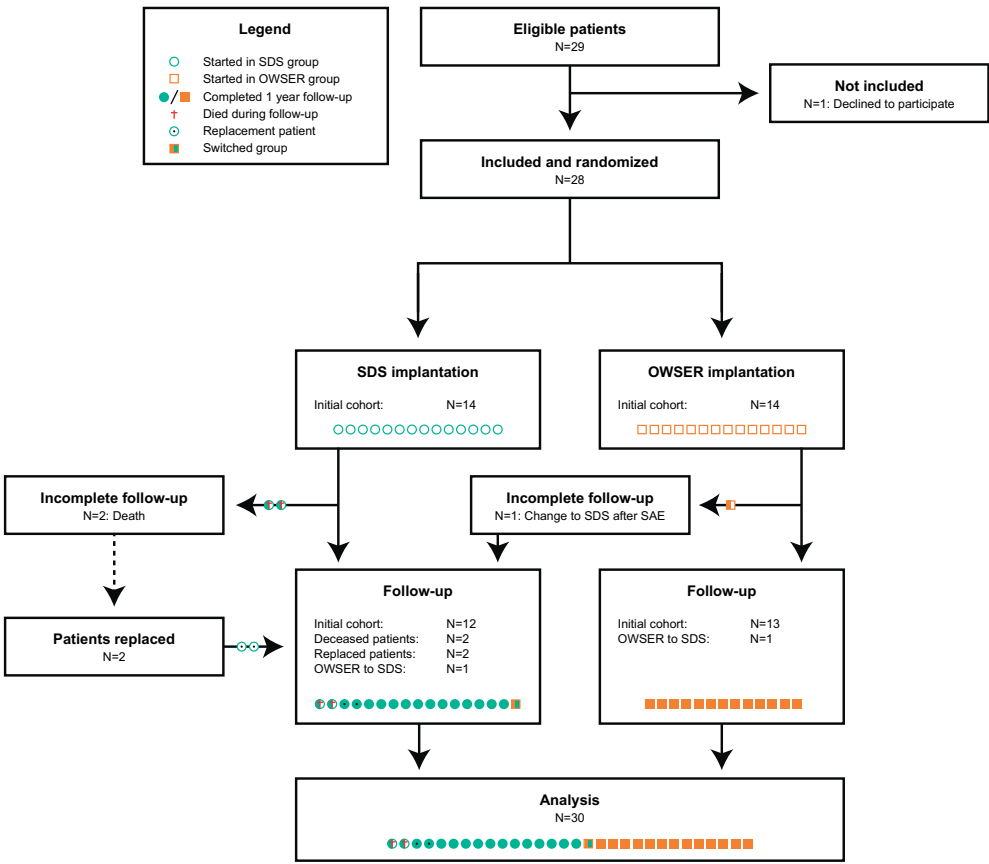
Baseline characteristics

Baseline characteristics are reported in Table 2. Mean age of patients at surgery was 9.0 years, 20/30 patients were male. Many different neuromuscular EOS etiologies were included, spinal muscular atrophy was most prevalent. Median surgical time was 180 minutes, median estimated blood loss was 300 mL and median time to discharge was 6 days.

Table 2. Baseline characteristics

Variable			All patients (N=30)	SDS patients (N=16)	OWSER patients (N=14)
Demographics		Sex (Female)	10/30 (33%)	6/16 (38%)	4/14 (29%)
		Age at surgery (years)	9.0 (SD 1.6)	8.6 (SD 1.5)	9.3 (SD 1.7)
	EOS etiology	SMA type I	3 (10%)	2 (12.5%)	1 (7.1%)
		SMA type II	8 (26.7%)	6 (37.5%)	2 (14.3%)
		Cerebral palsy	2 (6.7%)	1 (6.3%)	1 (7.1%)
		Spina bifida	2 (6.7%)	1 (6.3%)	1 (7.1%)
		Spinal cord injury	2 (6.7%)	1 (6.3%)	1 (7.1%)
		Congenital myopathy	2 (6.7%)	1 (6.3%)	1 (7.1%)
		4q22 syndrome	1 (3.3%)		1 (7.1%)
		KCNQ2 epileptic encephalopathy	1 (3.3%)		1 (7.1%)
		Lennox-Gestaut epileptic encephalopathy	1 (3.3%)	1 (6.3%)	
		Merosin deficient congenital dystrophy 1a	1 (3.3%)	1 (6.3%)	
		Angelman syndrome	1 (3.3%)		1 (7.1%)
		Myelitis transversa	1 (3.3%)		1 (7.1%)
		Noonan syndrome	1 (3.3%)	1 (6.3%)	
		Spastic tetraplegia	1 (3.3%)		1 (7.1%)
		Aicardi-Gourtiers syndrome	1 (3.3%)		1 (7.1%)
		Nemalin myopathy	1 (3.3%)	1 (6.3%)	
		Hydrocephalus	1 (3.3%)		1 (7.1%)
Pre-operative characteristics		Surgical time (minutes)	180 (IQR 64)	170 (IQR 72)	193 (IQR 41)
		Estimated blood loss (mL)	300 (IQR 158)	300 (IQR 150)	320 (IQR 185)
		Time until discharge (days)	6.0 (IQR 2.0)	5.0 (IQR 2.0)	6.5 (IQR 2.0)

7

	Main coronal Cobb (°)	74.9 (SD 14.7)	77.0 (SD 15.0)	72.4 (SD 14.4)
	Pelvic obliquity (°)	35.5 (SD 14.9)	37.4 (SD 17.4)	33.3 (SD 11.8)
	T5-T12 kyphosis (°)	27.0 (SD 20.9)	21.8 (SD 19.1)	33.5 (SD 22.0)
Pre-operative measurements	L1-S1 lordosis (°)	-37.0 (IQR 29.2)	-28.6 (IQR 26.4)	-46.8 (IQR 28.6)
	T1-T12 height (mm)	179 (SD 25)	172 (SD 22)	188 (SD 26)
	T1-S1 height (mm)	292 (SD 37)	282 (SD 39)	303 (SD 32)
	T1-T12 freehand length (mm)	201 (SD 22)	193 (SD 15)	211 (SD 24)
	T1-S1 freehand length (mm)	331 (SD 36)	319 (SD 30)	344 (SD 38)

SDS: spring distraction system; OWSER: one way self-expanding rod; SMA: spinal muscular atrophy; SD: standard deviation; IQR: interquartile range

Curve characteristics

Curve correction results are shown in Table 3, Figure 4 and Supplement 1. The results of the linear mixed models are shown in Supplement 2. Mean coronal curve decreased from 74.9° pre-operatively, to 37.6° post-operatively and remained stable at 37.7° at 1 year follow-up. In SDS patients, the main coronal curve decreased 52% post-operatively, while at 1 year follow-up, coronal curve correction was 48%. For OWSER, the main coronal curve correction was 47% post-operatively, and 50% at 1 year follow-up. The changes over time were not statistically significant between groups, both for the immediate follow-up (p=0.128) and at 1 year follow-up (p=0.180). With respect to pelvic obliquity, both groups showed 60-70% correction post-operatively, which was maintained at 1 year follow-up.

When comparing T5-T12 kyphosis and L1-S1 lordosis between groups, we observed that SDS patients had a somewhat lower T5-T12 kyphosis and L1-S1 lordosis pre-operatively. L1-S1 lordosis increased substantially (from -28.6° to -46.9°) in the SDS group, although most post-operative radiographs were made in a non-weightbearing position in both groups (in contrast to most other radiographs which were performed in a sitting position). When comparing post-operative to 12-month follow-up in the linear mixed model changes over time in T5-T12 kyphosis (p=0.417) and L1-S1 lordosis (p=0.776) were not different between groups.

Table 3. Changes over time

Variable		Pre-operative	Post-operative	Post-operative change		P value between groups[a]	12 months	Follow-up change[b]		P value between groups[c]
				Absolute	%			Absolute	%	
Main coronal Cobb (°)	SDS	77.0	36.9	-40.1	-52%	0.128	39.0	+2.1	+6%	0.180
	OWSER	72.4	38.4	-34.0	-47%		36.2	-2.2	-6%	
Pelvic obliquity (°)	SDS	37.4	11.1	-26.3	-70%	0.253	12.3	+1.2	+11%	0.162
	OWSER	33.3	13.0	-20.3	-61%		12.2	-0.8	-6%	
T5-T12 kyphosis (°)	SDS	21.8	15.2	-6.6	-30%	0.806	12.4	-2.8	-18%	0.417
	OWSER	33.5	23.4	-10.1	-30%		21.2	-2.2	-9%	
L1-S1 lordosis (°)	SDS	-28.6	-46.9	-18.3	+64%	0.844	-30.1	+16.8	-36%	0.776
	OWSER	-46.8	-43.4	+3.4	-7%		-40.8	+2.6	-6%	
T1-T12 freehand length (mm)	SDS	193	207	+14	+7%	0.150	225	+18.0	+9%	0.295
	OWSER	211	222	+11	+5%		231	+9.0	+4%	
T1-S1 freehand length (mm)	SDS	319	345	+26	+8%	0.929	371	+26.0	+8%	0.928
	OWSER	344	365	+21	+6%		383	+18.0	+5%	
Cumulative concave implant growth (mm)	SDS	NA	7.9	NA	NA	NA	30.9	+23.0	+291%	0.808
	OWSER	NA	4.0	NA	NA		23.2	+19.2	+480%	
Cumulative convex implant growth (mm)	SDS	NA	9.3	NA	NA	NA	29.7	+20.4	+219%	0.389
	OWSER	NA	5.8	NA	NA		24.3	+18.5	+319%	

SDS: spring distraction system; OWSER: one way self-expanding rod; NA: not applicable

[a] Interaction between time and group in the mixed ANOVA comparing SDS and OWSER groups. Gender and age at surgery are covariates.

[b] Change between 1 year follow-up and post-operatively

[c] Interaction between time and group in the linear mixed model comparing SDS and OWSER groups. Gender, age at surgery and pre-operative values are covariates.

7

Figure 4: Coronal- and sagittal curve changes over time
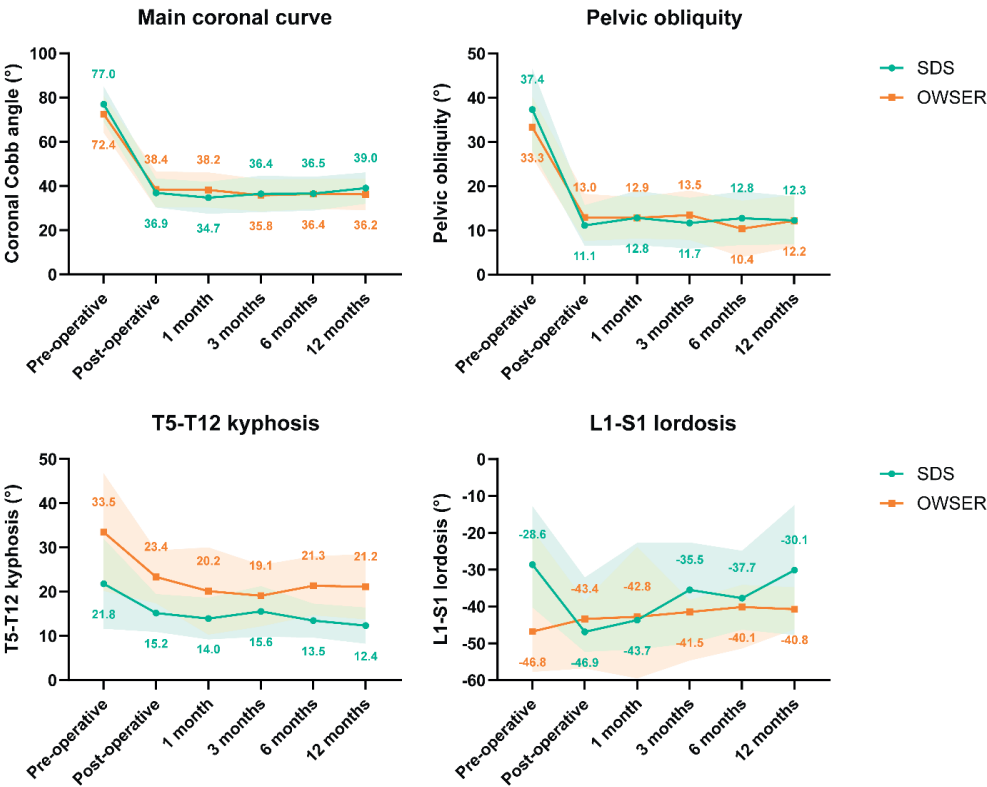
Mean or median and 95% confidence interval of each timepoint are plotted for each group.

Spinal- and implant growth

Spinal height- and length results can be seen in Table 3, Figure 5 and Supplement 1. Since OWSER patients were slightly older (and thus taller) at baseline, we looked mainly at the changes between post-operative and 1 year follow-up. The T1-T12 height during 1 year follow-up increased 18 mm in the SDS group, and 9 mm in the OWSER group. For T1-S1 height, growth was 27 mm/year for SDS and 17 mm/year for OWSER.

The freehand length values, which are less influenced by simultaneous changes in coronal or sagittal deformity, similarly showed substantial growth in both groups. The T1-T12 segment increased 18 mm/year for SDS and 9 mm/year for OWSER. For the T1-S1 segment, this was 26 mm/year (SDS) and 18 mm/year (OWSER). The substantial differences between groups disappeared when comparing both groups in the linear mixed model (Supplement 2) showing that both systems support growth of the spine very similarly when correcting for age, sex and pre-operative length. The one-year growth rate following the post-operative phase (1 year follow-up radio-

graph compared to first post-operative radiograph) was similar for both the concave side of the implant (SDS: 23 mm/year; OWSER: 19 mm/year; p=0.808) as well as the convex side (SDS: 20 mm/year; OWSER: 19 mm/year; p=0.389).

Initial implant growth is the rod expansion due to tissue creep that can be seen at the first post-operative radiograph. The SDS spring had already distracted 7.9 mm on the concave side and 9.3 mm on the convex side, compared to 4.0 mm (p=0.022) and 5.8 mm (p=0.019) in the OWSER group. This length gain was not included in the growth rate over time.

(Serious) Adverse Events

During the study period, 16 (S)AEs were recorded, 5 in the SDS group and 11 in the OWSER group, which corresponded to 0.30 (S)AEs/patient/year in the SDS group, and 0.78 (S)AEs/patient/year in the OWSER group. There was 1 UPROR in the SDS group (0.06/patient/year) and 5 UPRORs in the OWSER group (0.35/patient/year). Especially a higher number of mechanical failures explained this difference (Table 4). In the SDS group, two deaths occurred in the follow-up period between 6 and 12 months post-operatively, when the patient was at home. In both patients, no apparent relation was found between the treatment and the event. One patient aspirated and went into cardiac arrest. The other patient was inadvertently uncoupled from his respiratory equipment, resulting in respiratory insufficiency and cardiac arrest. There were only 2 cases of SSI. One SDS patient suffered a superficial SSI which was treated only with oral antibiotics. One patient in the OWSER group suffered a deep SSI. This patient underwent 2 UPRORs in which irrigation and debridement was performed, followed by vacuum assisted closure of the wound and 12 weeks of antibiotics. Both groups had a patient who showed complete implant expansion within 1 year (Figure 6). In both patients, expected residual growth was high, and both patients were re-operated; the SDS patient underwent retensioning of the springs, while the OWSER patient received new OWSER rods. In one OWSER patient, the set screws fixating the OWSER domino to the anchor rod failed, which caused complete implant lengthening and loss of correction within 3 month follow-up (Figure 7). This patient was re-operated and received a new OWSER device. In two other OWSER patients, a failure in the ratchet mechanism occurred, causing loss of correction in one for which the OWSER was replaced. During UPRORs in both groups, some metallosis was observed at the sliding connections.

7

Figure 5: Spinal height/length changes over time
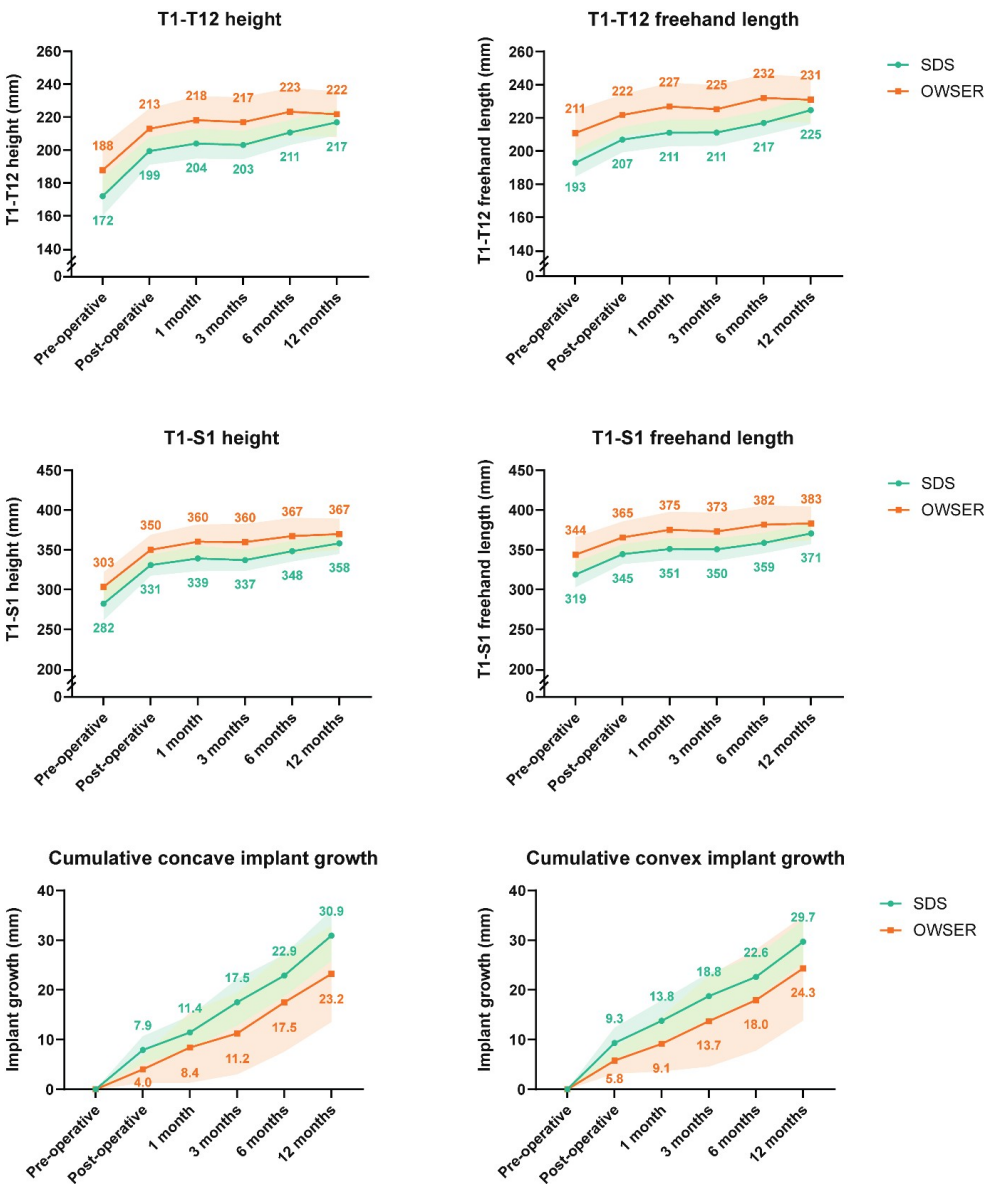
Mean and 95% confidence interval of each timepoint are plotted for each group.

Table 4. (S)AE's and UPRORs

Patient	(S)AE number	(S)AE	(S)AE type	(S)AE severity[a]	UPROR	Treatment
SDS 1	1	Superficial SSI	Surgery	I	No	Oral antibiotics
	2	Complete implant extension	Implant	IIa	Yes	Retensioning of spring and lengthening of the growing rod
SDS 2	3	Respiratory insufficiency due to aspiration	Disease	IV	No	None
SDS 3	4	Respiratory insufficiency	Disease	II	No	Prolonged admission
SDS 4	5	Respiratory insufficiency due to accidental uncoupling from breathing equipment	Disease	IV	No	None
OWSER 1	6	Respiratory insufficiency	Disease	II	No	IC admission
OWSER 2	7	OWSER ratchet mechanism failure with implant shortening	Implant	I	No	Expectative
OWSER 3	8	OWSER set screw failure with loss of correction	Implant	IIa	Yes	New OWSER implantation
	9	Complete implant extension	Implant	IIa	Yes	New OWSER implantation
OWSER 4	10	Failure to lengthen	Implant	I	No	Expectative
OWSER 5	11	OWSER ratchet mechanism failure with implant shortening	Implant	IIa	Yes	Revision to SDS treatment
	12	Pneumonia	Disease	II	No	Prolonged admission + antibiotics
OWSER 6	13	Pneumonia	Disease	II	No	Prolonged admission + antibiotics
OWSER 7	14	Deep SSI	Surgery	IIb	Yes	I&D (2x) + vacuum assisted closure + IV and oral antibiotics
OWSER 8	15	Pneumonia	Disease	II	No	Prolonged admission + antibiotics
	16	OWSER endcap loosening	Implant	I	No	Expectative

UPROR: unplanned return to the operating room; SDS: spring distraction system; OWSER: one way self-expanding rod; SSI: surgical site infection; I&D: Irrigation and debridement

[a]Disease-related complications: Grade I: Outpatient medical management; Grade II: Inpatient medical management; Grade III: Requires abandoning growth-friendly strategy; Grade IV: Death. Surgery- or implant-related complications: Grade I: Does not require unplanned surgery; Grade IIa: Requires 1 unplanned surgery; Grade IIb: Requires multiple unplanned surgeries; Grade III: Requires abandoning growth-friendly strategy; Grade IV: Death

7

Figure 6: SDS complication

Pre-operative   Post-operative   9 month follow-up   4cm growth <1Y   After revision
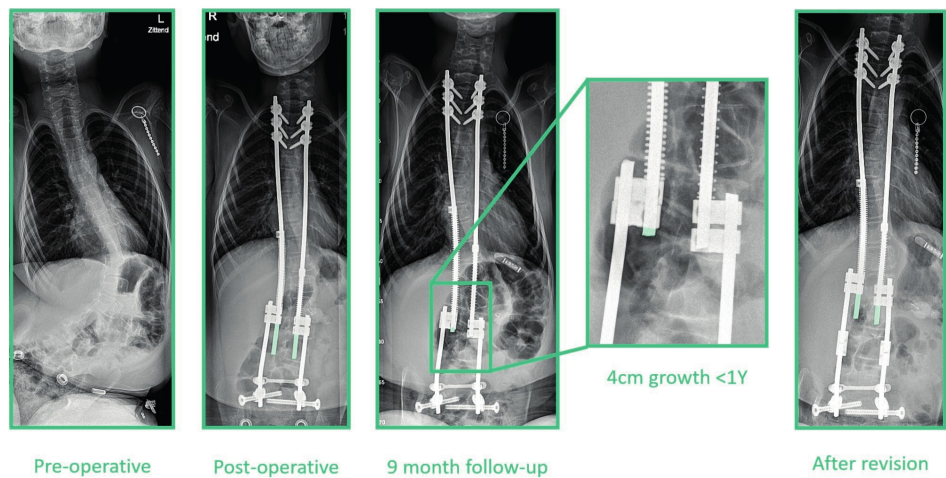
Example of an SDS patient that showed almost complete implant expansion within 1 year. Note the initial lengthening between insertion and the first radiograph of 20 mm. As there was still at least 3 years of expected spinal growth, the choice was made to perform a re-operation in which the springs were re-tensioned and the distal anchor rod construct was lengthened. The colored segment of the sliding rod denotes how much implant growth is left.

Figure 7: OWSER complication

Set screws   Set screw slippage
Pre-operative   Post-operative   Rod serrations   3 month follow-up   Original domino position
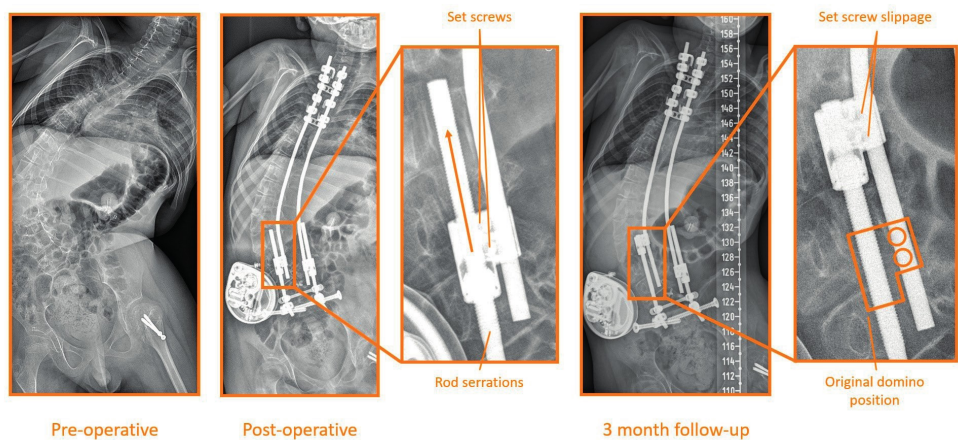
In this patient, the set screws that connect the OWSER domino to the anchor rod failed, causing the domino to erroneously move up on the serrated rod, without achieving any spinal lengthening or additional correction. In this patient, the OWSER rod was replaced during a re-operation.

(S)AE-free survival is graphed in a Kaplan-Meier curve in Figure 8. The Mantel-Cox test showed a hazard ratio (SDS hazard/OWSER hazard) of 0.34 (95% CI 0.11 to 1.09), however, this was not statistically significant (p=0.07).

Figure 8: Kaplan-Meier curves for (S)AE-free survival
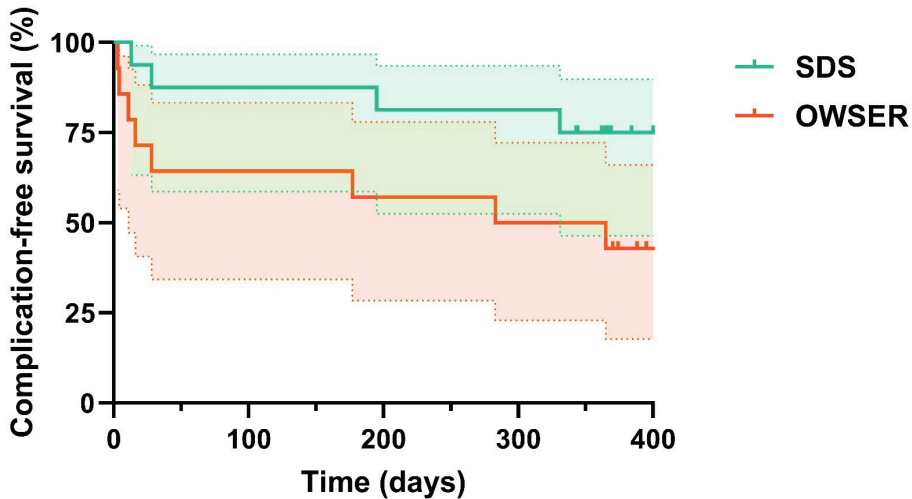
Survival curves for both groups with 95% confidence intervals. Ticks denote censored patients.

Discussion

The current study aimed to describe the one-year efficacy and safety of two novel "growth-friendly" implants to surgically treat neuromuscular EOS. Both implants provided 50% of curve correction, which could be maintained at 1 year follow-up. Height- and length gain was favorable for both techniques and often exceeded physiological T1-S1 growth (1.5-2.0 cm/year) as described by Dimeglio.[5,7] These values are higher than those seen in MCGR cohorts.[36,143,176] This may be explained by the fact that SDS and OWSER exhibit continuous, gradual growth. This contrasts the intermittent, forceful distractions often seen in TGR or MCGR, which may cause stiffening of the spine, requiring higher distraction forces and which result in reduced growth over time, known as the 'law of diminishing returns'.[35,96] Whether this phenomenon is absent in SDS and OWSER patients is not yet known, and will require longer follow-up.

To allow for comparison among "growth-friendly" techniques in terms of growth we calculated length gain during the "true" growing period (i.e. the period between the first post-operative radiograph and the radiograph at one year.[31] Although the most

accurate way to measure spinal length is 3D assessment, this is time consuming and likely not much better than the biplanar method that we used. All measurements indicated that the spinal length gain in the first year was often more than physiological growth, especially in the SDS group. This is likely not accelerated bone growth, but the result of tissue creep and remodelling due to continuous distraction. This opportunity to take advantage of tissue visco-elasticity is a feature of both systems and was clearly demonstrated by the mean initial length gain of 4.9 mm (OWSER) and 8.6 mm (SDS) between surgery and the first post-operative radiograph, due to stretching and spring distraction respectively. The fact that OWSER patients often had a proximal anchor block comprising more levels than SDS patients could have attributed to a relatively small difference in growth over time.

Unfortunately, two patients died during the study. While not ideal in a strict RCT environment, we prospectively decided that in such a situation, the patients could be replaced, as not replacing the patients would have resulted in an underpowered study, which invalidates the results and which would waste the useful study data that was already collected. By replacing these two patients, while also including their results (and the associated SAEs), a fair and balanced analysis between systems could still be performed. These two patient deaths emphasizes the fragility of the neuromuscular EOS population. It confirms that interventions, that can destabilize the fragile balance of these children, especially hospital admission and surgery, should be avoided wherever possible. In that regard, it was encouraging to see that with our bipolar single-surgery approach, only one deep SSI occurred during the study period (3.3%).

A previous meta-analysis in studies including neuromuscular patients showed SSI rates of around 10%.[169] Other studies have shown that the deep infection risk increases with more extensive surgeries and with each subsequent surgery following the initial surgery.[33,177] Depending on the maintenance of correction, it may also be possible to forego definitive spinal fusion, as this "final" surgery carries an additional 40% UPROR risk in neuromuscular patients.[178] Obviously, follow-up until after skeletal maturity is necessary before any conclusions can be drawn on this treatment option.

As expected for this population and procedure, (S)AEs and UPRORs could not be prevented. Especially in the OWSER group, there was a tendency toward implant-related (S)AEs that required UPRORs. Several of these implant failures were related to the ratchet mechanism which apparently is vulnerable and may be improved. Another reason for UPROR was excessive length gain that exceeded the implant capacity within one year. This happened for one patient in both groups and was not related to an anchor- or implant failure, but largely a result of further correction and stretching. As both patients had substantial growth left, we decided to retension/replace the implants. This finding indicates that longer reserve implant lengths are

desirable. The OWSER implant already has a version with a lengthening capacity of 80 mm instead of 50 mm. For SDS, the residual rod length can simply be left longer and springs can be stacked.[179] However, there are technical challenges as the extra length can protrude, especially in small children.

The BiPOWR study is the first comparative trial that utilizes a randomized design to compare different "growth-friendly" implants for EOS. So far, most systems were investigated retrospectively or in single arm prospective cohort studies, which are prone to confounding (by indication) and (selection) bias, although these issues can be mitigated with sound methodological practices.[160,180,181] Another way to compensate for such biases is the use of real world data from (large) registries that are published more and more and probably tell us most accurately what is the value of these implants.

A strength of the current study was the strict randomization and blinding design which enabled unbiased comparison between systems in terms of efficacy and safety. While parents often showed initial apprehension when hearing that their child would be randomized to a surgical intervention, we were able to explain the importance of this practice for the validity of the results. Ultimately, all eligible patients, except for one, chose to be included into the trial. Another strength is that all radiographs were systematically measured by the same two authors, reducing measurement variability. (S)AE's were scored using previously reported grading- and classification criteria, which allows for less ambiguity when deciding whether an (S) AE needed to be included.

Limitations of the study include its relatively small cohort with many different neuromuscular diseases. In addition, the follow-up of only 1 year is short and only allows to focus on initial efficacy and safety. Whether the "law of diminishing returns" remains absent for the SDS and OWSER implants is not yet known. This will require much longer follow-up and will be the subject of future research. Only then can we draw conclusions on long-term efficacy and -safety.

Conclusion

Two self-distracting "growth-friendly" implants were investigated and compared for the treatment of neuromuscular EOS. Both the Spring Distraction System (SDS) and the One Way Self-Expanding Rod (OWSER) achieved coronal curve correction of around 50%, which was maintained at one year follow-up. Spinal length increase was excellent for both systems and partially the result of creep. (Serious) Adverse Events occurred at a relatively low rate in both cohorts, with an unplanned return to the OR rate of 6% for SDS and 35% for OWSER per patient per year.

Supplement 1. Curve characteristics and spinal height and length over time

		Pre-operative	Post-operative	1 month	3 months	6 months	12 months
Main coronal Cobb (°)	All patients	74.9 (SD 14.7)	37.6 (SD 13.0)	36.3 (SD 12.3)	36.1 (SD 12.7)	36.4 (SD 12.3)	37.7 (SD 12.2)
	SDS	77.0 (SD 15.0)	36.9 (SD 12.3)	34.7 (SD 12.5)	36.4 (SD 14.2)	36.5 (SD 13.8)	39.0 (SD 12.8)
	OWSER	72.4 (SD 14.4)	38.4 (SD 14.1)	38.2 (SD 12.4)	35.8 (SD 11.4)	36.4 (SD 10.7)	36.2 (SD 11.8)
Pelvic obliquity (°)	All patients	35.5 (SD 14.9)	12.0 (SD 8.8)	12.9 (SD 9.1)	12.5 (SD 9.3)	11.7 (SD 10.4)	12.2 (SD 9.5)
	SDS	37.4 (SD 17.4)	11.1 (SD 8.6)	12.8 (SD 10.6)	11.7 (SD 9.9)	12.8 (SD 10.9)	12.3 (SD 9.8)
	OWSER	33.3 (SD 11.8)	13.0 (SD 9.2)	12.9 (SD 7.3)	13.5 (SD 8.8)	10.4 (SD 10.0)	12.2 (SD 9.6)
T5-T12 kyphosis (°)	All patients	27.0 (SD 20.9)	19.0 (SD 9.9)	16.2 (SD 9.8)	17.0 (SD 9.8)	16.8 (SD 9.0)	16.6 (SD 10.2)
	SDS	21.8 (SD 19.1)	15.2 (SD 8.0)	14.0 (SD 8.2)	15.6 (SD 9.9)	13.5 (SD 6.9)	12.4 (SD 6.7)
	OWSER	33.5 (SD 22.0)	23.4 (SD 10.4)	20.2 (SD 11.8)	19.1 (SD 9.7)	21.3 (SD 9.9)	21.2 (SD 11.6)
L1-S1 lordosis (°)	All patients	-37.0 (IQR 29.2)	-44.8 (IQR 14.3)	-43.7 (IQR 21.8)	-38.6 (IQR 19.8)	-39.9 (IQR 16.8)	-37.9 (IQR 20.0)
	SDS	-28.6 (IQR 26.4)	-46.9 (IQR 19.7)	-43.7 (IQR 23.8)	-35.5 (IQR 18.8)	-37.7 (IQR 21.4)	-30.1 (IQR 28.5)
	OWSER	-46.8 (IQR 28.6)	-43.4 (IQR 15.2)	-42.8 (IQR 19.3)	-41.5 (IQR 13.0)	-40.1 (IQR 9.1)	-40.8 (IQR 10.8)
T1-T12 height (mm)	All patients	179 (SD 25)	206 (SD 19)	210 (SD 20)	209 (SD 20)	216 (SD 19)	219 (SD 19)
	SDS	172 (SD 22)	199 (SD 16)	204 (SD 16)	203 (SD 15)	211 (SD 14)	217 (SD 14)
	OWSER	188 (SD 26)	213 (SD 21)	218 (SD 23)	217 (SD 24)	223 (SD 23)	222 (SD 23)
T1-T12 freehand length (mm)	All patients	201 (SD 22)	214 (SD 19)	218 (SD 20)	218 (SD 20)	224 (SD 19)	228 (SD 19)
	SDS	193 (SD 15)	207 (SD 14)	211 (SD 14)	211 (SD 14)	217 (SD 13)	225 (SD 15)
	OWSER	211 (SD 24)	222 (SD 21)	227 (SD 22)	225 (SD 23)	232 (SD 22)	231 (SD 23)
T1-S1 height (mm)	All patients	292 (SD 37)	340 (SD 30)	349 (SD 32)	347 (SD 31)	357 (SD 31)	363 (SD 28)
	SDS	282 (SD 39)	331 (SD 25)	339 (SD 28)	337 (SD 24)	348 (SD 23)	358 (SD 23)
	OWSER	303 (SD 32)	350 (SD 33)	360 (SD 34)	360 (SD 36)	367 (SD 36)	367 (SD 36)

		Pre-operative	Post-operative	1 month	3 months	6 months	12 months
T1-S1 freehand length (mm)	All patients	331 (SD 36)	354 (SD 31)	362 (SD 32)	361 (SD 32)	369 (SD 32)	376 (SD 30)
	SDS	319 (SD 30)	345 (SD 23)	351 (SD 24)	350 (SD 24)	359 (SD 23)	371 (SD 24)
	OWSER	344 (SD 38)	365 (SD 35)	375 (SD 35)	373 (SD 37)	382 (SD 38)	383 (SD 35)
Cumulative concave implant growth (mm)	All patients	NA	6.1 (SD 5.3)	10.0 (SD 8.6)	14.6 (SD 10.9)	20.5 (SD 11.9)	27.3 (SD 13.2)
	SDS		7.9 (SD 5.2)	11.4 (SD 5.8)	17.5 (SD 8.1)	22.9 (SD 7.6)	30.9 (SD 9.2)
	OWSER		4.0 (SD 4.7)	8.4 (SD 11.1)	11.2 (SD 12.9)	17.5 (SD 15.6)	23.2 (SD 16.0)
Cumulative convex implant growth (mm)	All patients	NA	7.7 (SD 5.5)	11.6 (SD 8.1)	16.4 (SD 11.5)	20.5 (SD 12.0)	27.2 (SD 13.1)
	SDS		9.3 (SD 5.8)	13.8 (SD 7.1)	18.8 (SD 8.1)	22.6 (SD 7.6)	29.7 (SD 7.8)
	OWSER		5.8 (SD 4.6)	9.1 (SD 8.7)	13.7 (SD 14.4)	18.0 (SD 16.0)	24.3 (SD 17.3)

SDS: spring distraction system; OWSER: one way self-expanding rod; NA: not applicable; SD: standard deviation; IQR: interquartile range

Supplement 2: Results of linear mixed models

Main coronal Cobb angle

Predictors	Estimates	95% CI	p value
Intercept	-0,17	-30,09 to 29,76	0,991
Sex (Female)	-1,38	-9,89 to 7,13	0,742
Age at surgery (years)	0,54	-2,05 to 3,13	0,670
Pre-operative main coronal Cobb (°)	0,43	0,15 to 0,71	0,004
Change over time (days)	+0,01	0,00 to 0,01	0,162
Treatment (OWSER)	-0,62	-6,68 to 5,44	0,840
Change over time per group (OWSER)	-0,01	-0,02 to 0,00	0,180

T1-T12 freehand length

Predictors	Estimates	95% CI	p value
Intercept	54,53	19,46 to 89,59	0,003
Sex (Female)	0,80	-7,35 to 8,95	0,841
Age at surgery (years)	0,21	-2,58 to 3,00	0,878
Pre-operative T1-T12 freehand length (mm)	0,79	0,58 to 1,00	<0,001
Change over time (days)	0,03	0,03 to 0,04	<0,001
Treatment (OWSER)	-1,24	-6,26 to 3,79	0,627
Change over time per group (OWSER)	0,00	-0,01 to 0,00	0,295

Pelvic obliquity

Predictors	Estimates	95% CI	p value
Intercept	-9,66	-28,26 to 8,94	0,305
Sex (Female)	1,22	-4,75 to 7,18	0,679
Age at surgery (years)	0,98	-0,87 to 2,83	0,287
Pre-operative pelvic obliquity (°)	0,37	0,18 to 0,56	0,001
Change over time (days)	0,00	-0,00 to 0,01	0,338
Treatment (OWSER)	-0,92	-5,29 to 3,45	0,676
Change over time per group (OWSER)	0,00	-0,01 to 0,00	0,162

T1-S1 freehand length

Predictors	Estimates	95% CI	p value
Intercept	108,90	52,09 to 165,71	<0,001
Sex (Female)	4,71	-8,99 to 18,41	0,486
Age at surgery (years)	-0,71	-5,51 to 4,10	0,765
Pre-operative T1-S1 freehand length (mm)	0,77	0,55 to 0,98	<0,001
Change over time (days)	0,05	0,04 to 0,06	<0,001
Treatment (OWSER)	-3,06	-11,01 to 4,90	0,448
Change over time per group (OWSER)	0,00	-0,01 to 0,01	0,928

T5-T12 kyphosis

Predictors	Estimates	95% CI	p value
Intercept	5,97	-7,41 to 19,35	0,378
Sex (Female)	-0,92	-5,75 to 3,92	0,698
Age at surgery (years)	0,23	-1,38 to 1,75	0,799
Pre-operative T5-T12 kyphosis (°)	0,35	0,23 to 0,46	<0,001
Change over time (days)	0,00	0,00 to 0,00	0,239
Treatment (OWSER)	2,25	-2,76 to 7,25	0,364
Change over time per group (OWSER)	0,00	-0,01 to 0,01	0,417

Concave implant growth

Predictors	Estimates	95% CI	p value
Intercept	-10,09	-27,01 to 6,83	0,240
Sex (Female)	-1,22	-7,37 to 4,94	0,688
Age at surgery (years)	2,42	0,32 to 4,52	0,014
Change over time (days)	0,05	0,04 to 0,05	<0,001
Treatment (OWSER)	-6,79	-12,57 to -1,01	0,022
Change over time per group (OWSER)	0,00	-0,01 to 0,02	0,808

L1-S1 lordosis

Predictors	Estimates	95% CI	p value
Intercept	-47,82	-77,09 to -18,55	0,002
Sex (Female)	-2,00	-12,70 to 8,80	0,706
Age at surgery (years)	1,08	-2,33 to 4,49	0,520
Pre-operative L1-S1 lordosis (°)	0,05	-0,03 to 0,27	0,265
Change over time (days)	0,02	0,01 to 0,02	<0,001
Treatment (OWSER)	-0,79	-11,48 to 9,90	0,880
Change over time per group (OWSER)	0,00	-0,02 to 0,01	0,776

Convex implant growth

Predictors	Estimates	95% CI	p value
Intercept	-3,81	-21,43 to 13,82	0,669
Sex (Female)	-3,73	-10,14 to 2,67	0,242
Age at surgery (years)	2,01	0,04 to 3,99	0,046
Change over time (days)	0,04	0,03 to 0,05	<0,001
Treatment (OWSER)	-7,09	-12,90 to -1,20	0,019
Change over time per group (OWSER)	0,01	-0,01 to 0,02	0,989

The linear mixed models investigated whether changes during follow-up were different between groups, when correcting for age at surgery, sex, pre-operative value, and follow-up time. The curves shown are example curves of boys with a mean age at surgery and mean pre-operative value. Their slope shows whether the trajectory is different for either of the groups. The difference in starting height is a change that can be attributed to the different treatments and is not influenced by the pre-operative value.

Part III
Optimizing Spring Distraction
System treatment
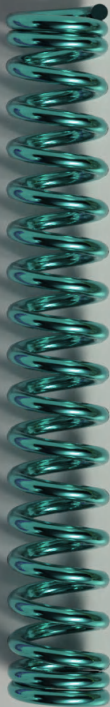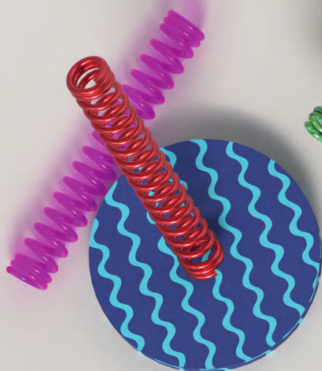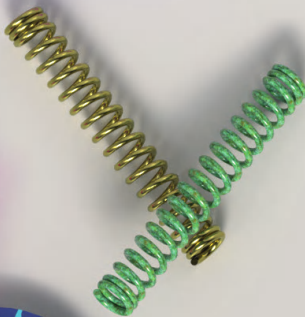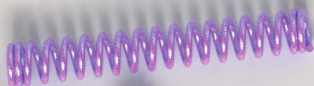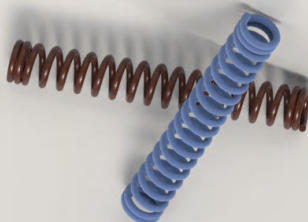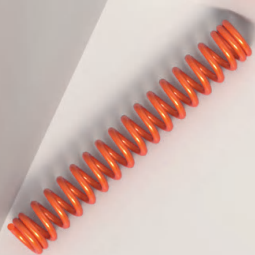
Chapter 8

Identifying Complications and Failure Modes of Innovative Growing Rod Configurations Using the (Hybrid) Magnetically Controlled Growing Rod (MCGR) and the Spring Distraction System (SDS)

J.V.C. Lemans

C.S. Tabeling

R.M. Castelein

M.C. Kruyt

Abstract

Background
Magnetically controlled growing rods (MCGRs) offer non-invasive distractions in Early-Onset Scoliosis (EOS). However, implant-related complications are common, reducing its cost-effectiveness. To improve MCGRs functionality and cost-effectiveness, we often combine a single MCGR with a contralateral sliding rod (hybrid MCGR). Recently, we developed the spring distraction system (SDS) as an alternative, which provides continuous distraction forces through a helical spring. This study aims to identify complication rates and failure modes of EOS patients treated with either of these innovative systems.

Methods
This single-centre retrospective study included EOS patients treated with a (hybrid) MCGR or SDS between 2013 and 2018. Baseline demographics, and data regarding complications and implant growth were measured. Complication rate, complication profile, complication-free survival and implant growth were compared between groups.

Results
Eleven hybrid- and three bilateral MCGR patients (4.1-year follow-up) and one unilateral, eleven hybrid and six bilateral SDS patients (3.0-year follow-up) were included. Groups had similar age, sex, aetiology distribution, and pre-operative Cobb angle. Complication rate was 0.35 complications/patient/year for MCGR patients and 0.33 complications/patient/year for SDS patients. The most common complications were failure to distract (MCGR-group; 8/20 complications) and implant prominence (SDS-group; 5/18 complications). Median complication-free survival was 2.6 years, with no differences between groups (p = 0.673). Implant growth was significantly higher in the SDS-group (10.1 mm/year), compared to the MCGR-group (6.3 mm/year).

Conclusion
(Hybrid) MCGR and SDS patients have similar complication rates and complication-free survival. Complication profile differs between the groups, with frequent failure to distract leading to significantly reduced implant growth in (hybrid) MCGR patients, whereas SDS patients frequently exhibit implant prominence and implant kyphosis.

Introduction

Early onset scoliosis (EOS), if left untreated, is a life-threatening condition.[182] The challenge in surgical EOS treatment is to control the curve while maintaining adequate spinal growth. Traditional Growing Rod (TGR) treatment, wherein rods are periodically surgically distracted, is associated with high rates of wound complications and increased anaesthetic exposure, with potential adverse neurodevelopmental effects.[34] In contrast, the Magnetically Controlled Growing Rod (MCGR) offers non-invasive distractions, thus removing the need for re-operations.[39] However, frequent lengthening procedures are still required. In addition, the MCGR is difficult to contour, and implant-related complications are frequent, with an incidence of almost 50% during the first 2–3 years.[45] Many of these complications are mechanical in nature, like anchor failures, rod fractures and a failure to distract.[183] This last category includes specific failure modes of the internal mechanism (e.g. drive pin or lead screw fractures), and is hypothesised to be caused by high-frictional forces inside the actuator.[41,43] While newer versions of the MCGR have been developed, mechanical complications remain prevalent.[184] The re-operations necessary to correct these complications are a serious burden for the patient and increases treatment cost dramatically, potentially making MCGR treatment less cost-effective than previously described, as calculations were based only on a relatively short follow-up. [185–188] To improve MCGRs cost-effectiveness, and to provide apical control, we often combined one MCGR on the curve concavity with a contralateral rod fixated to the apex which can slide freely proximally and distally. Several studies have shown that this innovative hybrid configuration shows similar results compared to bilateral MCGR use.[142,143] However, even in the hybrid configuration, some MCGR disadvantages remain, such as the difficulty contouring the MCGR rod, and the necessity of repetitive lengthenings.

   Recently, we developed the spring distraction system (SDS), which is based on a continuous distraction aided growth-guidance concept. This system exerts a continuous distractive force with a compressed titanium spring that is positioned around a sliding rod (Figure 1). This implant has important advantages, such as the potential to further reduce the curve after insertion and the fact that it does not have to be periodically lengthened. The design of the SDS and its preliminary and 2-year follow-up clinical performance have recently been reported.[58,59] However, its provisional design is not yet fully optimised, as the connectors are used off-label and do not prevent the release of metal debris. To ultimately improve these innovative growing-rod constructs in terms of complications and failure modes, understanding of the specific strengths and weaknesses of both systems is essential. Therefore, the current study aims to report and compare follow-up adjusted complication rate and

8

complication profile of EOS patients treated with either the (hybrid) MCGR or SDS. Secondary aims are to describe complication-free survival, and implant growth.

Figure 1. Spring distraction system concept
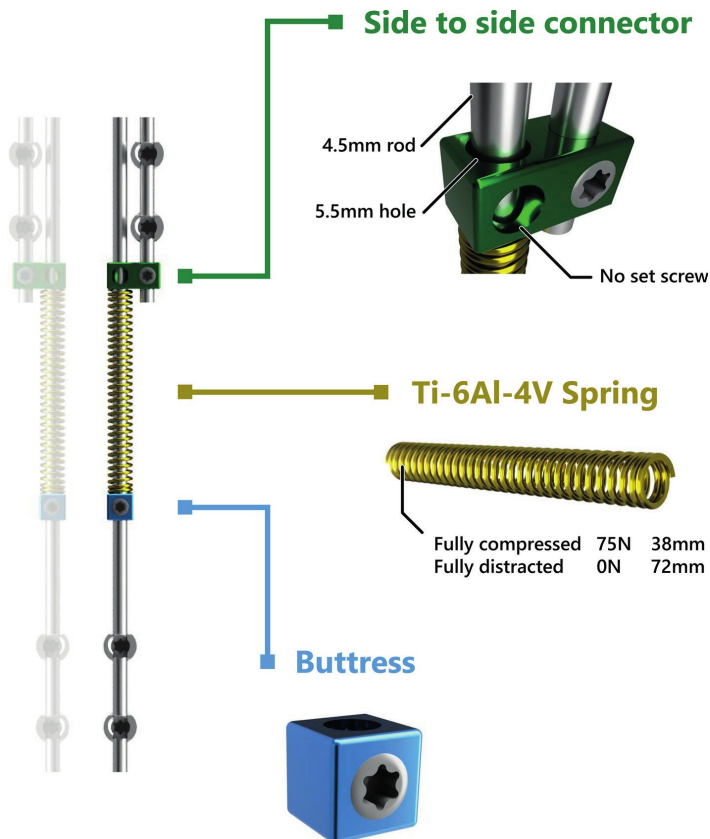
The SDS consists of three parts that are added to a traditional screw-rod construct: (1) The side-to-side connector (green) with one oversized hole through which a rod can slide freely. (2) The spring (gold) can be compressed over the rod by (3) the buttress (blue) during surgery, and then provides a continuous distraction force.

Materials and Methods

Study design and study period

This study was approved by the Institutional Review Board of the UMC Utrecht [METC 18/638 and METC 16/276]. Data were collected from all EOS patients implanted with either a unilateral, bilateral- or hybrid MCGR or SDS between 2013 and 2018. Our institution used MCGR exclusively from the end of 2013 until October 2016. Since then, patients have the option to participate in a prospective clinical study investigating the SDS (Growing Rods with the Addition of a Distraction Spring - GRADS study). Before study approval, an extensive Investigational Medical Device Dossier including risk analysis was created in accordance with the European Medical Device Regulations (MDR). All patients before October 2016 received the MCGR, while most (18/19) eligible patients after this date opted for the SDS. Patients that were revised from another growing-rod system to either MCGR or SDS were excluded.

Surgical techniques

All patients underwent intra-operative neuromonitoring. For both implant systems, anchors on at least two subsequent levels were placed proximally and distally, to which the 4.5 or 5.5 mm growth-friendly constructs were mounted. In neuromuscular patients with a main curve that extended to the pelvis, bilateral iliosacral screws (Tanit, EUROS, La Ciotat, France) were used distally. Three MCGR patients received a bilateral MCGR (MAGEC, NuVasive, San Diego, CA, USA) (Figure 2a), the other 11 MCGR patients received a hybrid construct, with an MCGR on the curve concavity and a sliding rod fixed to the apical level on the curve convexity (Figure 2b), as previously described.[142,143] MCGR patients were lengthened at the outpatient clinic once every 2–3 months, where distraction was performed in a prone position until the Electronic Remote Control showed ≥10 mm or clunking was felt. In case of failure-to-distract, a new lengthening was attempted after 3 months. If that failed, a trial was done under anaesthesia with manual traction. If all these failed and the curve progressed, this was a reason to revise the implant. For the SDS, in idiopathic and syndromic patients, a similar hybrid configuration with a concave SDS and convex sliding rod was used (Figure 2c). In neuromuscular and most congenital patients, a bilateral SDS was implanted (Figure 2d). One congenital SDS patient received only a concave SDS, with no contralateral rod (Figure 2e). At the end of surgery, intrawound vancomycin was left in the deep and superficial wound. Drains were not routinely used. No post-operative braces were used, and there were no restrictions in activities after surgery.

8

Figure 2. Implant configurations
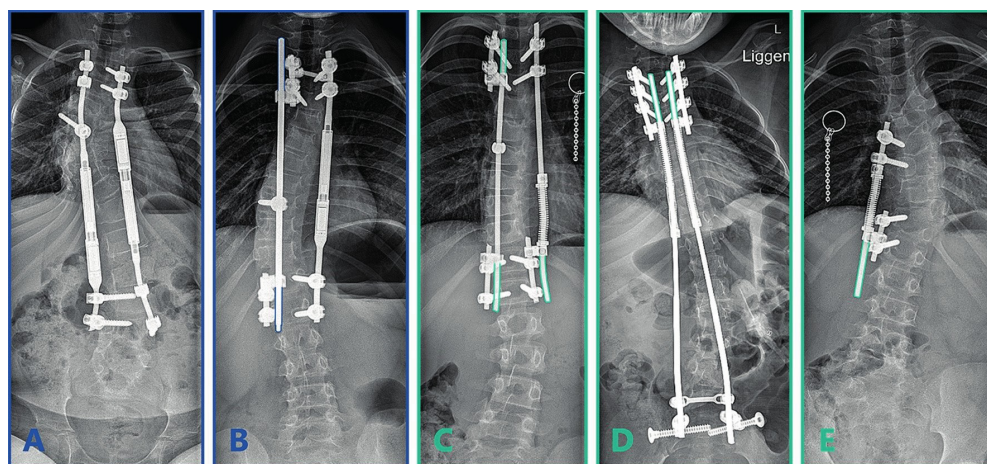
Different MCGR and SDS configurations, coloured rod outlines represent the parts of the rod that can freely slide. **a.** Bilateral (offset) MCGR. **b.** Unilateral concave MCGR combined with a convex sliding rod that is fixated to the apex for apical control (hybrid). The convex rod can freely slide through the proximal and distal side-to-side connectors. **c.** Unilateral concave SDS combined with a convex sliding rod that is fixated to the apex for apical control. The convex rod can freely slide through the proximal and distal side-to-side connectors. **d.** Bilateral SDS fixated to the pelvis with ilio-sacral screws. **e.** Unilateral concave SDS without a convex rod.

Data collection
Demographic-, disease-specific- and surgical parameters as well as data regarding implant-related complications were obtained through review of the electronic patient record and the spinal radiographs. Complication type, interval between initial surgery and onset of complications and the necessity for re-operation was recorded, irrespective of whether the re-operation had already taken place or was postponed to be treated with final fusion surgery. When an implant had reached its maximum distraction length (4–6 cm) and had to be replaced (MCGR) or re-tensioned (SDS), this was not deemed a complication, but the re-operation was counted towards the total number of re-operations. Specific complications that were evaluated and their diagnostic criteria are shown in Table 1.

   In addition, during each outpatient clinic visit in which a spinal radiography was performed (generally every 6 months), cumulative length increase in the MCGR actuator or SDS spring was measured and plotted over time. Measurements were performed on calibrated radiographs and were normalised for coronal and sagittal tilt of the actuator or spring. All chart reviews and radiographic measurements were performed independently by two observers (JVCL and CST). Disagreements were discussed until consensus was reached. Radiographic length measurements were

averaged between both observers. A two-way mixed intraclass correlation coefficient of 0.993 showed that there was excellent correlation between the observers.

Table 1. Evaluated complications

Complication	Definition used
Neurological injury	Neurological deficit that is either permanent or that necessitates a re-operation. This does not include temporary loss of neuromonitoring signals
Anchor complications	Screws or hooks that loosen or exhibit pull-out or cut-out
Rod complications	Rod fractures or rod slippage
Failure to distract	No radiological implant growth during two consecutive MCGR lengthenings (MCGR) or during 6-months follow-up (SDS) May be caused by: 1. MCGR driving rod/actuator failure 2. SDS spring/connector/buttress failure 3. Spontaneous fusion
Proximal junctional kyphosis	Angle between PIV and PIV + 2 ≥ 10°, and increase ≥ 10° compared to pre-operatively[189]
Implant prominence	Prominence of the implant through the soft tissues, causing local pain or skin breakdown
Wound dehiscence	Loss of integrity of the closed surgical wound
Superficial SSI	CDC criteria for superficial SSI[190]
Deep SSI	CDC criteria for deep SSI[190]
Late SSI	Conforming to CDC criteria for SSI except for time of occurrence (30- and 90 days for superficial- and deep SSI's, respectively)[190]
Other	Any complication necessitating a re-operation not mentioned above

MCGR: magnetically controlled growing rod, SDS: spring distraction system, SSI: surgical site infection, CDC: Centres for Disease Control and Prevention, PIV: proximal instrumented vertebra

8

Statistical analysis

Summaries of demographic and radiographic data were reported as mean with standard deviation (SD). Baseline characteristics were compared between groups with a Chi-squared test (categorical data) or independent t-test (continuous data). The number of complications per patient was calculated and normalised for the mean follow-up length to find the number of complications/patient/year.

The complication data were also used to perform a Kaplan–Meier survival analysis comparing both groups. The outcome was the occurrence of a complication and survival time was thus the time until the first complication occurred. Patients who did not suffer a complication were censored at their latest follow-up date. The survival curves of both groups were statistically compared with the Log-Rank test. Depending on whether the proportional hazard assumption was met, the hazard ratio was used to compare the instantaneous risk of complications between both groups.

To compare implant growth between groups, implant length at latest follow-up was used to calculate the linear annual growth rate with a linear regression analysis. Implant length at the first post-operative erect radiograph (t = 0) was set at 0. As the cumulative implant length increase was compared to this value, an intercept-free regression was performed. The slope of both groups was then compared with an independent t-test. Statistical analyses were performed with IBM SPSS Statistics 25.0.0.2 (IBM Corp., Armonk, NY, USA). The Kaplan–Meier survival analyses and regression analyses were performed with GraphPad Prism 9.0.0 (GraphPad Software, San Diego, CA, USA). Two-tailed statistical significance was set at p<0.05.

Results

Population characteristics

In total, 14 MCGR (11 hybrid and 3 bilateral constructs) and 18 SDS patients (one unilateral, 11 hybrid and six bilateral constructs) were consecutively included. Patient characteristics are summarised in Table 2. Mean age at surgery was 7.9±1.6 and 8.4±1.9 years for the MCGR and SDS group, respectively. Mean follow-up was 4.1 ± 1.6 years for the MCGR group and 3.0±0.4 years for the SDS group (p=0.025). Surgery time and time to discharge were similar between both groups. Pre- and post-operative Cobb angles were similar in both groups, the MCGR group showed a post-operative correction of 44%, for SDS this was 48%. Cobb angle at latest follow-up was higher in the MCGR group, 53.5° vs. 39.8° (p=0.029). A higher proportion of SDS patients received fixation to the pelvis, compared to the MCGR group (SDS: 7/18, MCGR: 1/14; p=0.040), and all SDS patients received a 4.5 mm system while most patients in the MCGR group (10/14) received a 5.5 mm system (p<0.001).

Table 2. Patient demographics

	MCGR (N=14)	SDS (N=18)	P value
Male	5/14	10/18	0.266
Age at surgery (years)	7.9 ± 1.6	8.4 ± 1.9	0.436
EOS aetiology			0.585
Idiopathic	4	3	
Congenital	3	4	
Syndromic	3	2	
Neuromuscular	4	9	
BMI (kg/m^2)[a]	16.8 ± 3.1	15.9 ± 2.6	0.380
Surgery time (minutes)[a]	203 ± 73	221 ± 51	0.418
Time to discharge (days)[a]	7.8 ± 3.4	8.3 ± 10.0	0.845
Follow-up (years)	4.1 ± 1.6	3.0 ± 0.4	0.025
Cobb angle (°)			
Pre-operatively	70.3 ± 20.9	66.2 ± 13.6	0.507
Post-operatively	39.6 ± 19.5	34.3 ± 13.0	0.364
Latest follow-up	53.5 ± 18.6	39.8 ± 15.1	0.029
Pelvic fixation[a]	1/14	7/18	0.040
Implant configuration[a]			0.467
Unilateral concave distraction only	0	1	
Unilateral concave distraction + convex sliding rod	11	11	
Bilateral distraction	3	6	
Rod diameter[a]			<0.001
4.5 mm	4	18	
5.5 mm	10	0	

EOS: Early Onset Scoliosis, BMI: Body Mass Index

[a]Measurements associated with the initial surgery

8

Complication rate

Overall, implant- and procedure-related complications were common in both groups (Table 3). In the (hybrid) MCGR group, there were 20 (1.4/patient), which corresponded to 0.35 complications/patient/year. Ten MCGR patients (71%) suffered from at least one such complication. In the SDS group, 18 (1.0/patient) complications were observed, corresponding to a similar rate of 0.33 complications/patient/year. Eleven SDS patients (61%) showed at least one complication.

Table 3. Incidence of implant- or procedure-related complications

	MCGR	SDS	
Neurological injury	1	0	
Anchor complications	4	3	
Proximal anchor		2	0
Apical anchor		1	0
Distal anchor		1	3
Rod complications	2	4	
Rod fracture		2	3
Rod slippage		0	1
Failure to distract	8	2	
MCGR actuator failure		8	0
Side-to-side connector failure		0	2
Rod growing out of connector due to fast growth	0	1	
Proximal junctional kyphosis	3	0	
Implant prominence	0	5	
Wound dehiscence	0	1	
Superficial SSI	1	0	
Deep SSI	0	1	
Late superficial SSI	1	1	
Total number of complications	**20**	**18**	
Complications per patient	**1.4**	**1.0**	
Complications per patient per year	**0.35**	**0.33**	

SSI: surgical site infection

Complication profile

Complication profile for both groups can be seen in Table 3, a timeline of all complications is reported in Supplement 1. Radiographs of representative complications for both groups can be seen in Figure 3 (MCGR) and Figure 4 (SDS). In the (hybrid) MCGR group, the most common complication was failure to distract (8/20 complications), which was diagnosed in these eight patients after a mean of 3.3±1.4 years (range 1.2–6.3). In seven cases of failure to distract, a re-operation was performed. In these cases, the dysfunction of the rods was confirmed during surgery and the MCGRs were explanted and returned to the manufacturer for further analysis. Radiographs taken before re-operation showed a clear failure mode of the MCGR actuator in two patients. Both rods displayed the previously described "crooked-rod sign", which was followed by a driving pin fracture in one patient (Figure 3a) and a fracture of the radial bearing (and the driving pin) in the other (Figure 3b).[191] The other implant-related complications included four anchor failures, two rod fractures, three cases of PJK, two wound complications and one post-operative neurologic injury, which recovered completely after surgical re-exploration.

In the SDS group, the most frequent complication was implant prominence (5/18 complications), due to increased kyphosis of the rods in the side-to-side connector (Figure 4b, c). Since the sliding hole in the connector is 1 mm oversized, it is possible for the sliding distraction rod to angulate with the fixed rod due to the off-axial distraction forces. The other complications included three distal iliosacral screw failures, four rod complications, two cases of side-to-side connector failure, three wound complications and one case where the rod grew out of the side-to-side connector. This last patient showed exceptionally fast growth that quickly outpaced the free length of the rod.

8

Figure 3. Magnetically controlled growing rod complications
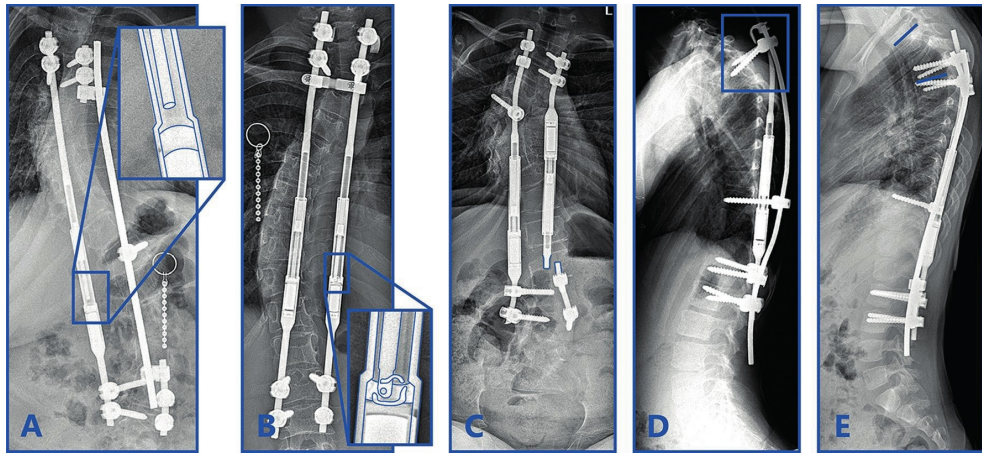
Examples of Magnetically Controlled Growing Rod complications. **a.** Actuator rod that is broken and that is disengaged from the rest of the implant. **b.** The actuator rod is disengaged from the actuator pin and radial bearing debris is present in the actuator portion of the MCGR. **c.** Rod fracture close to the distal foundation after 1.5 years. **d.** Anchor failure of the proximal hook and pedicle screws. **e.** Proximal junctional kyphosis.

Figure 4. Spring distraction system complications
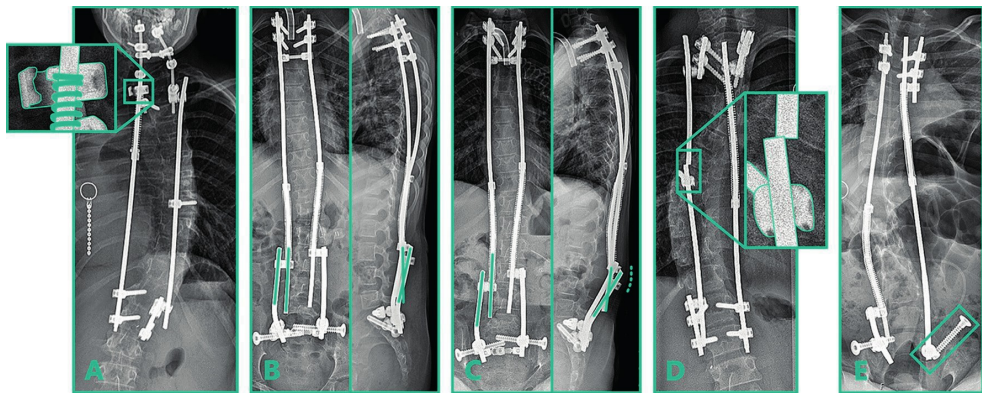
Examples of spring distraction system complications. **a.** Fatigue failure of sliding side-to-side connector. **b.** Post-operative radiograph showing the angle that the rods make in the coronal and sagittal plane. **c.** After several years of follow-up, distraction caused kyphosis between the sliding and the static rod that resulted in prominence (dashed line). **d.** Rod fracture near the apical screw. **e.** Distal anchor failure. The iliosacral screw backed out of its original iliosacral trajectory.

Re-operation rate

Of the 20 complications in the (hybrid) MCGR group, 14 (70%) necessitated a single re-operation. Combining some complications into a single re-operation, and including one re-operation due to reaching the maximum length of the MCGR, 13 re-operations were required in total, corresponding to 0.9 re-operations/patient. Three patients exhibiting PJK and one patient with failure to distract did not require a re-operation. This latter patient did not have much remaining growth left and did not receive a definitive fusion due to increased surgical risk. Of the 18 complications in the SDS group, 16 (89%) necessitated one or more re-operations. Fifteen complications necessitated a single re-operation, one complication necessitated two re-operations. Combining several re-operations, and including two spring re-tensioning re-operations, 17 were required in total, or 0.9 re-operations/patient. One superficial wound dehiscence and one late superficial infection did not require a re-operation. In both groups, no complication required abandoning growth-friendly treatment.

Survival analysis

Figure 5 shows the Kaplan–Meier survival analysis of all patients combined and of the (hybrid) MCGR and SDS groups separately. Median survival time for all patients was 2.6 years with no significant differences between groups (MCGR 2.8 years; SDS 2.5 years; p=0.673). This indicates that after 2.6 years, half of the patients included in the study had suffered from at least one complication. As the proportional hazard assumption was violated (Figure 5 shows that the survival functions of the groups cross several times), the hazard ratio between groups was not calculated.

Figure 5. Kaplan–Meier analysis of complication-free survival
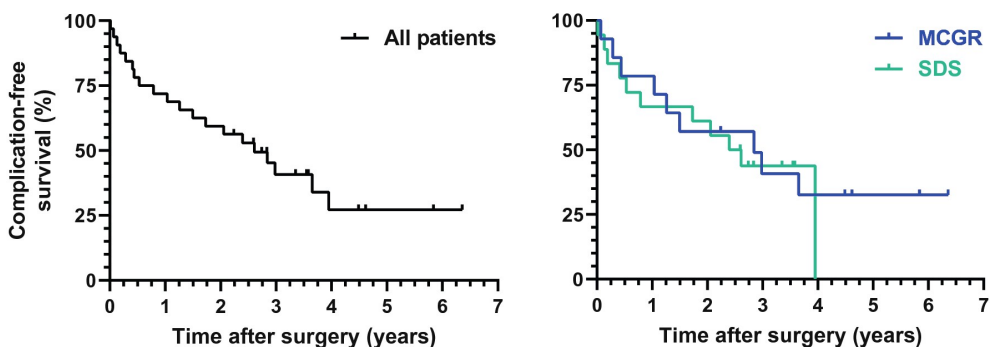
Survival time to the occurrence of a complication was evaluated for all patients (left) and for the MCGR and SDS groups separately (right).

Figure 6. Cumulative implant lengthening over time
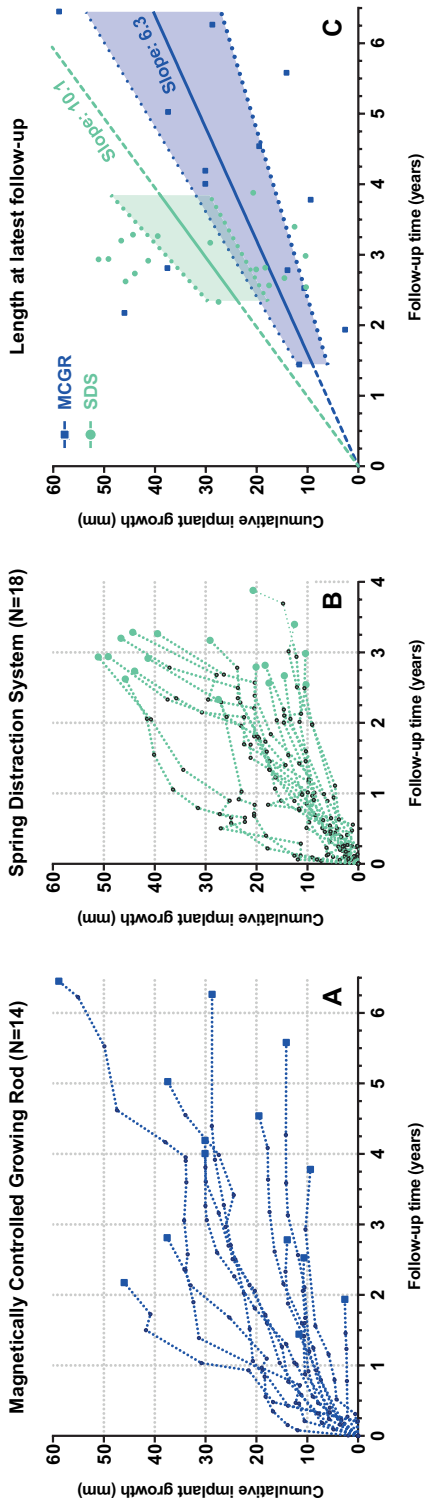
Cumulative implant length over time is plotted for the MCGR (**a**) and the SDS (**b**) group. The measured values (dashed) of each patient are shown. With the cumulative implant length at latest-follow-up, a linear regression was performed for each group **c.** The intercept-free slopes and their 95% confidence intervals are shown.

Implant growth

Cumulative implant growth in the (hybrid) MCGR and SDS patients is shown in Figure 6a, b. At latest follow-up, 9/18 (50%) of SDS patients showed a cumulative implant growth that exceeded 10 mm/year. For the (hybrid) MCGR group, this occurred in only 2/14 (14%) patients. The cumulative implant growth in both groups was compared in a linear regression analysis shown in Figure 6c. The linear regression slope of the SDS group equaled 10.1 mm/year (95% CI 7.6–12.7), which was significantly higher (p=0.017) than the MCGR slope of 6.3 mm/year (95% CI 4.2–8.3).

Discussion

This study investigated complication and implant data from 2 different cohorts. Although this is not the optimal study design, we believe the current single-centre comparison of both implant systems is relevant as it highlights the strengths and weaknesses of both technologies. As also reported by other studies, the implant- or procedure-related complication rate of growth-friendly systems is high, between 0.11 and 0.38/patient/year.[38,42,139,147,183,192] Normalised for follow-up, complication rate for the (hybrid) MCGR and SDS groups in our study was 0.35 and 0.33 complications/patient/year, respectively.

Failure to distract was the most common (hybrid) MCGR complication, with rods failing to distract in 8/14 patients after a mean of 3.3 years. This obviously impacted the mean implant growth rate (6.3 mm/year), which was significantly lower than the growth observed in the SDS group (10.1 mm/year). The growth provided by the SDS is more in line with what can be expected from physiological spinal growth.[5,6] Failure to distract is frequently reported in MCGR literature.[44,45,183] Mechanical explantation studies attribute this to the extreme frictional forces that the drive mechanism has to withstand.[43,44] The fact that the actuator portion of the rod cannot be contoured and thus more contouring must take place proximally or distally results in significant off-axis loading, which exacerbates this issue, and which may also be the reason for the high rates of anchor pull-out and proximal junctional kyphosis.[147] These vulnerabilities are inherent to the MCGR design, which is why these complications remain prevalent in the literature, despite several implant iterations.[44,45] Smaller actuator dimensions could mitigate some of these issues and lower complication rate, although at the expense of a reduced lengthening potential and/or distraction force. In addition, a more dynamic coupling could further decrease internal friction and implant stresses.

In contrast to most other studies investigating the MCGR, we routinely used a hybrid MCGR construct, where a single MCGR is combined with a contralateral sliding rod. Adding the contralateral sliding rod provides apical control and reduces the risk of rod fracture compared to single rod constructs. We have shown previously that

8

hybrid MCGRs provide similar curve correction and spinal growth compared to bilateral constructs.[142,143] The current study shows that, especially for longer follow-up times, the mechanical failure rate of this hybrid MCGRs is comparable to that of bilateral MCGRs, where mechanical failure is seen in 50–88% of patients during treatment.[38,139,183,192,193] However, as our hybrid strategy differs in several ways from the recommended bilateral MCGR configuration, our results with respect to complication profile and implant growth cannot be extended to bilateral MCGR configurations.

The most frequent complication in the SDS cohort was implant prominence, caused by increased implant kyphosis. This is a direct result of posterior distraction forces combined with a single side-to-side connector that allows for residual bending in the sagittal plane. Currently, we use two stacked side-to-side connectors, which makes this increase of implant kyphosis impossible. However, this has the disadvantage of causing more friction and wear with potential effects on growth, which emphasises that the sliding connection with off-label use of these connectors is suboptimal. In addition, the use of the iliosacral screw initially caused distal anchor complications, these are now prevented with routine use of distal cross-connectors. We believe that with an improved low-friction axial stable bearing and improved iliosacral fixation, the complication rate of the SDS could be reduced further. The effect of such implant changes on curve correction, spinal growth, and incidence of complications will be subject of further investigation.

The SDS provides dynamic loading of the spine, i.e. it allows the implant to transmit load forces to the spine, harnessing the dampening potential of the intervertebral disc. This is in contrast to static implants like TGR and MCGR, where forces are transmitted mostly through the implant. This dynamic loading of the SDS theoretically decreases mechanical stress on the anchors and rods.[126] It may also attenuate stress-shielding that takes place in the segments between the anchors, preventing vertebral osteopenia, which may prove advantageous for final fusion surgery. [100,194,195] In the current study, the expected reduction in rod stresses did not lead to a decrease in rod fractures in the SDS group (SDS 3/18 patients; MCGR 2/14 patients), although this rate is likely biased due to the application of thinner 4.5 mm rods in the SDS group. Currently, we mainly implant 5.5 mm rods; whether this will prevent rod fractures is subject of investigation as part of a continuous design improvement cycle. Other differences between both groups in the current study include a relatively larger proportion of neuromuscular patients in the SDS group (50% vs 29%), which explains the increased incidence of complications with iliosacral fixation in this group. Fortunately, deep SSIs were uncommon in both groups, likely due to routine usage of intrawound vancomycin powder.

Strengths of the current study includes the fact that the data is obtained from 2 comparable, prospective cohorts, both treated in a single tertiary spine center. The assessment of procedure-related complications with pre-specified criteria and the

use of two observers, make our results repeatable and robust. However, there were several important limitations. First, this study is a retrospective analysis of prospectively collected data, and therefore there is the risk of confounding, selection bias and experience bias. Despite extensive experience with TGR before the (hybrid) MCGR cohort, the team (composed of the same staff during both cohorts) had another 2–3 years more experience with growth-friendly implants at the time of the SDS cohort. In addition, the follow-up for the SDS group is therefore generally shorter. While using follow-up adjusted complications rates mitigates this issue in part, it is possible that certain complications commonly occur within a certain time frame. Depending on whether this window presents early or late following surgery, the complication rate for the SDS group may have been over- or underestimated in this study. Third, patient characteristics and implant configurations were varied and sample size was limited. Finally, these are only intermediate follow-up results. To definitively assess complication rate, patients should be followed at least until final fusion and probably longer.[178,196,197]

Conclusion

In the (hybrid) MCGR and SDS cohorts, 71% and 61% of patients suffered from at least 1 complication, with a follow-up adjusted complication rate of 0.35 and 0.33 complications/patient/year, respectively. Median complication-free survival across all patients was 2.6 years. There were differences in complication profile between both groups, such as the high rate of failure to distract leading to significantly lower implant growth in (hybrid) MCGR patients, compared to SDS patients (6.3 mm/year vs. 10.1 mm/year). The typical failure mode for the SDS was implant prominence following implant kyphosis. These data may guide future implant improvements of both innovative systems.

Supplement 1. Complication timeline

Post-operative follow-up (years)
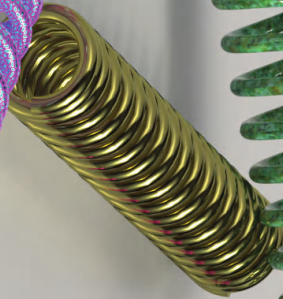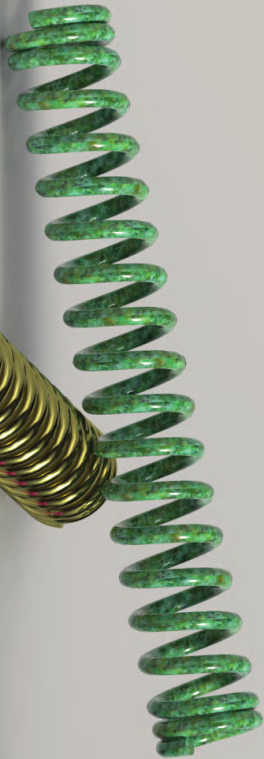
Chapter 9

The Spring Distraction System for Growth-Friendly Surgical Treatment of Early Onset Scoliosis: A Preliminary Report on Clinical Results and Safety after Design Iterations in a Prospective Clinical Trial

C.S. Tabeling

J.V.C. Lemans

A. Top

E.P. Scholten

H.W. Stempels

T.P.C. Schlösser

K. Ito

R.M. Castelein

M.C. Kruyt

Abstract

Background
The Spring Distraction System (SDS) is a dynamic growth-friendly implant to treat early onset scoliosis (EOS). Previous SDS studies showed promising results in terms of curve correction and complication profile. Nevertheless, complications did occur, which led to modifications in the implant design. The main iterations were a larger rod diameter and a more sagittal stable sliding mechanism. The purpose of this study was to investigate the performance of these iterations.

Methods
All patients treated with the modified SDS and >1 year follow-up were included. Radiographic outcomes, severe adverse events (SAEs), unplanned returns to the operating room (UPRORs) and health-related quality of life (HRQoL) were investigated.

Results
Seventeen EOS patients (three congenital, four idiopathic, nine neuromuscular, one syndromic) were included. Mean age at surgery was 9.5 ± 2.5 years. Similar to the first generation SDS, about 50% initial correction was achieved and maintained, and spinal growth was near physiological. Most importantly, SAEs and UPRORs were diminished and favorable with 0.10/patient/year. In addition, HRQoL increased during the first year postoperatively, indicating the implant was well accepted.

Conclusion
These preliminary results indicate that the iterations of the SDS are effective in terms of reducing SAEs and UPRORs and increasing HRQoL in patients with EOS.

Introduction

Early onset scoliosis (EOS) is a three-dimensional (3D) curvature of the spine and trunk with mixed etiology, that occurs in children nine years of age or younger.[198] It is an uncommon condition with a complex group of underlying diagnoses, which, if left untreated, can cause progressive thoracic insufficiency and respiratory failure, ultimately leading to death.[144,199]

The early onset nature of this disease puts children at a high risk of progression; therefore, early intervention is important.[182] The main goals in treating EOS are to control the 3D deformity of the thorax, allow for thoracic and pulmonary development, to minimize complications, procedures, hospitalizations and burden for the family, and to improve overall development of the child. The initial treatment of EOS can be conservative, such as casting or bracing.[200] However, operative treatment is frequently required to allow adequate growth of the thorax.[19,201,202] This is important, because a T1–T12 height below 18 cm at skeletal maturity has been related to poor pulmonary function.[6,203] In order to facilitate spinal growth, growth-friendly strategies were developed. The traditional growing rods and vertical expandable prosthetic titanium rib devices require regular surgical distraction, leading to a burden on the patient, the family and the healthcare system, as well as concerns about mental development due to repeated anesthesia.[34,204,205] To overcome this huge disadvantage, magnetically controlled growing rods (MCGRs) were introduced, which allow distraction with an external magnet.[206] However, the MCGR has a high implant-related complication rate, which requires revision surgery in about 30–50% of patients after 2 years.[33,39,45,130,139,207] In addition, metal debris issues led to a temporary suspension of the CE certification and an international advice to limit MCGR implantations.[43,48] Although MCGR does not require surgical lengthening, the repeated out-patient clinic visits still pose a burden on patients and families. [33,208] Moreover, due to its rigid nature, the device is difficult to contour to the spine, especially in the sagittal plane, and because the spine is immobilized and unloaded, this may lead to implant failure, stress shielding and stiffening of the spine.[96] Finally, in repeated lengthenings, the "law of diminishing returns" is encountered, meaning that with every lengthening procedure, the yield of subsequent procedures tends to decrease.[35]

To counter these limitations, we developed a self-distracting dynamic implant, the Spring Distraction System (SDS).[58] Its concept consists of compressed springs, mounted around conventional rods, which continuously distract the scoliotic spine. The first generation of SDS consisted of three main components that were added to the standard 4.5 mm growing rods: a side-to-side connector with one oversized hole, a compressed spring that provides a maximum 75 N distraction force at full compression and a locking buttress to pretension the spring over the rod (Figure 1).

9

Figure 1. The Spring Distraction System
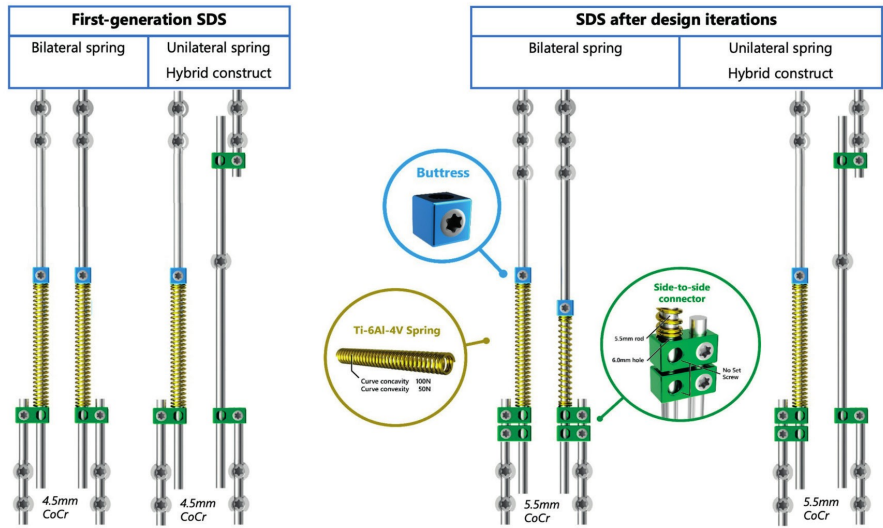
Left: First-generation SDS with three components added to the 4.5 mm rods: a side-to-side connector (green) with one oversized hole that was kept unlocked, a compressed spring (gold) that provides a 75 N distraction force and a locking buttress (blue). **Right:** Current SDS with 5.5 mm rods and an extra parallel connector. Moreover, an increased portfolio of springs with a 50 N and a 100 N version.

Since the SDS is not yet registered as a medical device, all patients treated with the SDS are part of a prospective clinical trial. The results of the first 18 primary SDS patients at more than two years of follow-up were previously reported.[59] The main goals, to control the curve and maintain growth, were achieved. However, rod breakage and implant prominence due to increased kyphosis were a concern, leading to about 0.3 unplanned reoperations per patient per year.[113] To address these issues the design was improved by converting to 5.5 mm instead of 4.5 mm rods and adding one sliding connector to prevent kyphosis (Figure 1). Moreover, a 50 N and 100 N spring were added to the portfolio. This allowed more strategic positioning of the springs unilaterally as a concave spring, or bilaterally with symmetrical or asymmetrical springs.

The aim of this preliminary study was to assess the performance of the modified SDS with respect to curve maintenance, growth, severe adverse events (SAEs), rod breakage and increased kyphosis in particular, unplanned returns to the operating room (UPRORs) and patient reported outcomes, after a minimum follow-up of one year.

Materials and Methods

Study Design and Study Period

Data were collected from two prospective cohorts in which the SDS was implanted - the GRADS study and the BiPOWR study (ClinicalTrials.gov Identifier: NCT04021784) - between April 2019 and December 2020. The GRADS study is a single-center prospective cohort study investigating the SDS in all EOS patients. The BiPOWR study is a multicenter, randomized controlled clinical trial, comparing two growth-friendly distraction devices in non-ambulant neuromuscular EOS patients indicated for bipolar fixation extended to the pelvis. Both studies were approved by the Institutional Review Board of the UMC Utrecht (METC 16/276; METC 18/179) and patients were included after informed consent. Inclusion criteria were all EOS patients that failed conservative treatment and were treated >1 year with an SDS that consisted of a 5.5 mm rod and double parallel connector. Exclusion criteria for SDS treatment were patients with connective tissue diseases that may not allow continuous distraction such as Marfan and Ehlers–Danlos syndrome, osteogenesis imperfecta and neurofibromatosis. This study followed the STROBE guideline for reporting observational studies.[136]

Surgical Techniques and Implant Configurations

The surgical technique for placement of earlier versions of the SDS were described by Wijdicks et al. and Lemans et al.[58,59] In short, small posterior incisions were used to create the proximal and distal anchors. Proximally, two or three consecutive pedicle screws were used per side and distally two pedicle screws or an iliosacral screw (Tanit®; Euros, SAS, La Ciotat, France) was placed. If the distraction device was applied unilaterally, usually a hybrid construct was made with a contralateral sliding rod fixed to the apex.[143] Somatosensory and motor-evoked potential monitoring were used intraoperatively. Skin-to-skin surgical time and blood loss were recorded.

For this study, we used standard 5.5 mm cobalt-chromium rods (CoCr) with 50 N, 75 N or 100 N medical-grade titanium (Ti6Al4V) spring(s). The spring was positioned on the sliding rod between a locking buttress (Stryker, Leesburg, VI, USA) and two oversized parallel connectors (NuVasive, San Diego, CA, USA) that allowed axial sliding without angulation (i.e., kyphosing within the connector). The spring behaved according to Hooke's Law, therefore there was a decline in force with expansion. We mostly used the 100 N springs, which have a decline in force of 1.33 N/mm.

We applied four different SDS configurations, depending on the curve magnitude and EOS etiology (Figure 2). Most idiopathic, congenital and syndromic patients received a hybrid configuration with an SDS on the concavity and a sliding rod with apical control on the convexity. Neuromuscular patients usually had a bilateral SDS configuration extending to the pelvis with a 100 N spring on the concavity and 50

9

N on the convexity. Postoperatively, all patients were allowed unrestricted physical activities.

Figure 2. Different SDS configurations
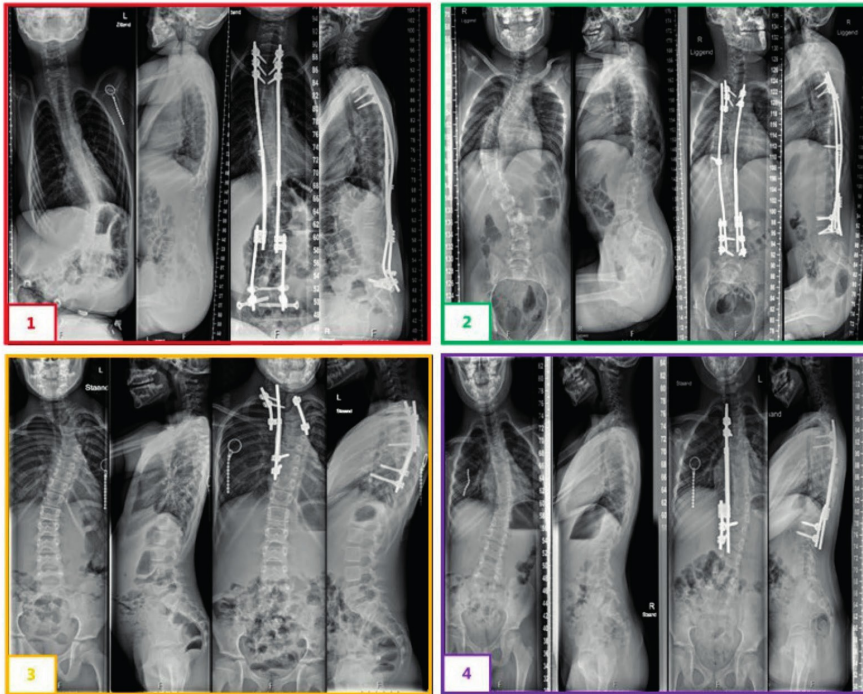
(1) A 10-year-old male with neuromuscular scoliosis with a bilateral system with concave and convex springs fixated to S1, note the fully distracted spring after two years. **(2)** A 10-year-old male with an idiopathic-like scoliosis treated with a hybrid system with a concave spring and a convex sliding rod fixated with an apical screw. **(3)** A 7-year-old female with a congenital scoliosis treated with a unilateral system with a concave spring and convex hemi-epiphysiodesis. **(4)** A 9-year-old female with syndromic scoliosis treated with a unilateral system with a concave spring only.

Outcomes

Clinical data included sex, age at initial surgery and etiology of the scoliosis. Surgery time, blood loss and SAEs, categorized as implant-related (e.g., failure to distract) or procedure-related (e.g., surgical site infection), were scored. The number of UPRORs was separately scored. Health-related quality of life (HRQoL) was measured preoperatively, postoperatively and after one year with the validated Dutch EOSQ-24 questionnaire.[138,155]

Radiographic Outcomes

All patients underwent full-spine erect coronal and sagittal radiographs preoperatively, postoperatively - as soon as the patient was fit for the radiograph - after one year and at the latest follow-up. Radiographic outcomes included Cobb angle magnitude of the primary measured within the instrumented area) and secondary scoliotic curves, T1–T12 and T1–S1 height, and the T5–T12 kyphosis and L1–S1 lordosis were measured by two observers (CT, AT) in Surgimap Software v.2.3.2.1 (Nemaris Inc., New York, NY, USA). When the difference between observers was <5°, the mean of the two measurements was taken. Larger differences were discussed until a consensus was reached.

Statistical Analysis

Descriptive analyses were conducted in Microsoft Excel (Microsoft, Washington, IL, USA). Patient characteristics and outcome measures were reported as means with standard deviation or range. Graphs were created using GraphPad Prism Version 9.3.0 (GraphPad Software, San Diego, CA, USA).

9

Results

Patient Characteristics

In total, we included 17 patients (three congenital, four idiopathic, nine neuromuscular, one syndromic) with a mean age of 9.5±2.5 years at surgery and a mean follow-up of 1.9±0.5 years. One patient was lost to follow up at 11 months due to death, unrelated to the implant or surgical procedure. This patient suffered from spinal muscular dystrophy type 1 and died by sudden cardiac arrest due to hypoxia, caused by aspiration. All other patients were followed according to protocol. Mean surgery time was 169 min (range: 100–240) and mean blood loss was 395mL (range: 100–700). Patients were discharged after a mean of 5 days (range: 4–9). Patient characteristics are summarized in Table 1.

Table 1. Demographics

	Mean ± SD or Median (range) or N (%)
Patients	17
Female	7/17 (41%)
Male	10/17 (59%)
Age at surgery (years)	9.5 ± 2.5
EOS etiology	
Congenital	3/17 (18%)
Idiopathic	4/17 (24%)
Neuromuscular	9/17 (53%)
Syndromic	1/17 (6%)
Surgery time skin-to-skin (minutes)	169 (range: 100-240)[a]
Blood loss (mL)	395 (range: 100-700)[b]
Time to discharge (days)	5 (range: 4-7)
Follow-up (years)	1.9 ± 0.5
Implant configuration	
Concave + convex springs	9/17 (53%)
Concave spring + convex apical screw	6/17 (35%)
Concave spring + convex epiphysiodesis	1/17 (6%)
Concave spring only	1/17 (6%)

[a.] For one patient, surgery time was unavailable.

[b.] For one patient, blood loss was unavailable.

Radiographic Outcomes

The mean preoperative main Cobb angle was 78±20°, which was reduced to 38±12° (51% reduction) postoperatively. After one year of follow-up, the mean Cobb angle was 40±12° and at latest follow-up 41±13° (Figure 3). The secondary curve also reduced with surgery, from 43° to 21° and remained at 29° and 28° after one year and at latest follow-up, respectively (Figure 3). The mean preoperative T5–T12 kyphosis was 33±19° and 22±12° postoperatively, which was maintained at one year follow-up (Figure 4). Mean preoperative L1–S1 lordosis was 54±16° and was 50±18° at latest follow-up (Figure 4). Mean T1–T12 and T1–S1 height preoperatively to postoperatively was 167.8±20.0 mm to 185.7±24.1 mm and 293.8±35.8 mm to 337.2±35.8 mm, respectively (Figure 5). Mean T1–T12 and T1–S1 height gain due to surgery was 17.9 mm and 43.3 mm overall and growth in year one was 5.1 mm and 8.6 mm, respectively. All radiographic outcomes are summarized in Table 2.

Table 2. Curve correction, sagittal profile and spinal growth

	Preoperative	Postoperative	After 1 Year	Latest Follow-Up
Primary Cobb angle (°)	78 ± 20	38 ± 12	40 ± 12	41 ± 13
Secondary Cobb angle (°)	43 ± 21	28 ± 15	29 ± 16	28 ± 15
T5-T12 kyphosis (°)	33 ± 19	22 ± 12	23 ± 14	22 ± 17
L1-S1 lordosis (°)	54 ± 16	47 ± 15	44 ± 20	51 ± 17
T1-T12 height (mm)	167.8 ± 20.0	185.7 ± 24.1	190.8 ± 22.9	192.5 ± 21.5
T1-S1 height (mm)	293.8 ± 35.8	337.2 ± 35.8	345.8 ± 33.9	350.5 ± 35.6

Figure 3. Coronal Cobb changes
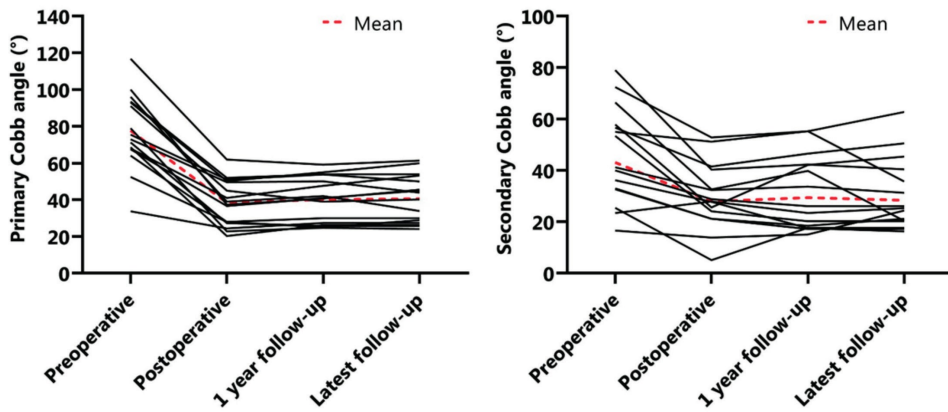
Left: Primary Cobb angle (°) changes over time. **Right:** Secondary Cobb (°) angle over time.

9

Figure 4. Sagittal Profiles
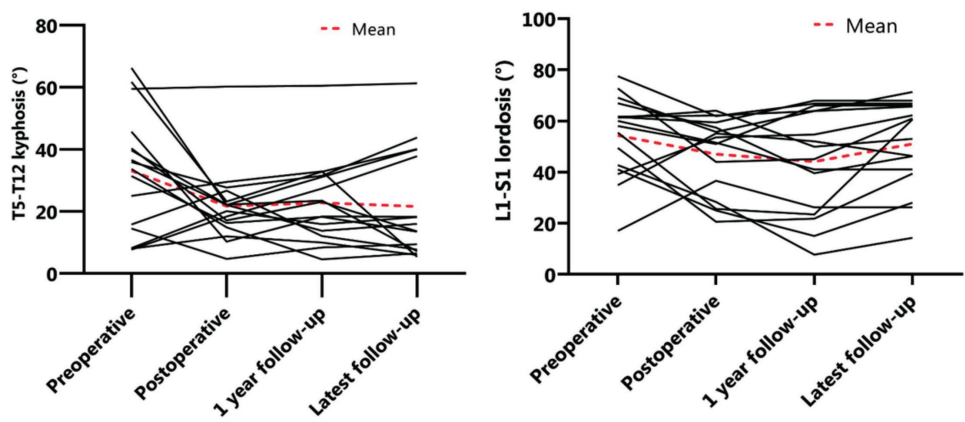
Left: T5–T12 kyphosis (°) over time.. **Right:** L1–S1 lordosis (°) over time.

Figure 5. Spinal height changes
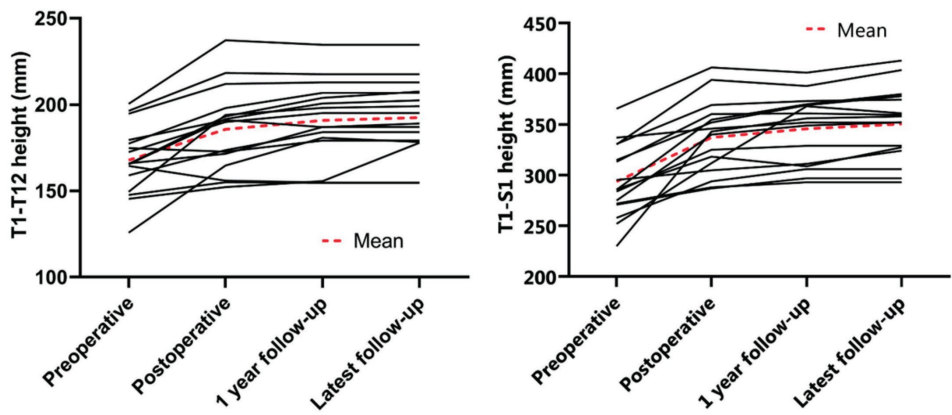
Left: T1–T12 height (mm) over time. **Right:** T1–S1 height (mm) over time.

Severe Adverse Events and Unplanned Returns to the Operating Room
An overview of SAEs and UPRORs is shown in Table 3. In two patients, progressive curves adjacent to the instrumented section were a reason for reoperation at 10 and 12 months. A third patient showed an unexpected high growth rate, which caused the spring to fully expand already after 11 months. This was not considered as an SAE, as it is a positive outcome of distraction, but it did require a reoperation 14 months after the initial surgery for a small spring retensioning. After initial surgery,

this patient had a superficial surgical site infection, which was treated with oral antibiotics. Based on these three SAEs and three UPRORS during a follow-up of 1.9 years, we calculated 0.1 SAE and UPROR per patient per year. Most importantly, there were no implant related SAEs such as rod breakage or implant protrusion, as observed with the first-generation SDS.

Table 3. Overview of severe adverse events (SAEs) and unplanned returns to the operating room (UPRORs)

Patient	Sex	Age at SAE	Underlying Disease	Initial Surgery	SAEs	UPRORs and Treatment
P03	F	9.1 years	VACTERL association	SDS T2-L1 + bilateral hemivertebra resection +unilateral hemi-epiphysiodesis T7-L1	Adding on above proximal anchor	Extension to C4
P06	F	11.2 years	Microcephalus	SDS T2-L4	Adding on below distal anchor	Extension to L5
P12	M	10.2 years	Myelomeningocele; Chiari II malformation	SDS T2-Ilium	Superficial Surgical Site Infection	Spring retension

Health-Related Quality of Life

Twelve out of sixteen patients completed the EOSQ-24 questionnaires at all analyzed follow-up moments (Table 4). Mean overall scores initially decreased from 61.6±18.5 preoperatively to 57.3±17.7 postoperatively and thereafter improved to 68.9 ± 14.1 after one year of follow-up (Figure 6).

9

Table 4. Health-related quality of life

EOSQ-24 domain	Pre-operative	Post-operative	After 1 Year
General health	67.7 ± 27.4	66.7 ± 17.9	70.8 ± 18.7
Pain/discomfort	60.4 ± 21.2	53.6 ± 19.7	61.5 ± 19.6
Pulmonary function	80.2 ± 25.8	78.1 ± 28.8	89.6 ± 13.9
Transfer	66.7 ± 30.8	57.3 ± 25.3	79.2 ± 23.4
Physical function	55.6 ± 31.8	46.5 ± 29.0	57.6 ± 31.5
Daily living	30.2 ± 24.1	30.2 ± 27.9	36.5 ± 25.3
Fatigue/energy level	67.7 ± 30.4	51.0 ± 27.4	66.7 ± 24.6
Emotion	62.5 ± 18.5	56.3 ± 18.8	74.0 ± 24.1
Parental burden	60.8 ± 26.2	60.0 ± 20.8	73.3 ± 19.0
Financial burden	83.3 ± 24.6	83.3 ± 30.8	93.8 ± 15.5
Overall satisfaction	62.5 ± 26.7	61.5 ± 17.2	70.8 ± 15.4
Overall mean score	61.6 ± 18.5	57.3 ± 17.7	68.9 ± 14.1

Raw scores from 1–5 were transformed into scaled scores ranging between 0 and 100. Higher scores indicate better patient outcomes. Higher parental and financial burden scores indicate less negative impact in the past 4 weeks. The domain overall satisfaction is the mean of the child satisfaction and parental satisfaction domains. 12/17 patients/parents completed the questionnaire at each follow-up.

Figure 6. Overall mean scores of the Early-Onset Scoliosis Questionnaire plotted over time
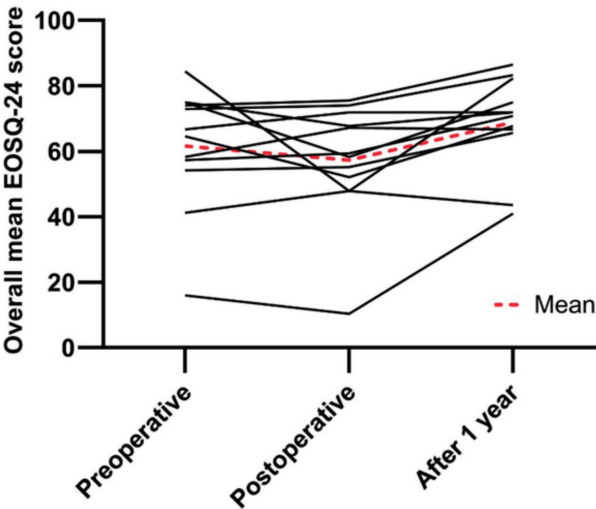
Discussion

In the current study we investigated an iteration of the SDS design, to mitigate material-related complications. In addition to good curve control and maintenance of growth, it appeared that the number of SAEs and especially UPRORs diminished compared to the first generation.[59,113] Obviously, as this is a preliminary study, the numbers were low, and a statistical analysis on an underpowered study was not worthwhile. However, the rate of SAEs and UPRORs decreased from about 0.3/patient/year, to <0.10/patient/year, which compared favorably to other growth-friendly systems.[31,33,39,42,45,205] Moreover, and maybe as a consequence, HRQoL improved, with even better scores one year after implantation compared to pre-implantation. This finding indicates that the implant may be better accepted than the first generation.[113] However, in the current study, fewer patients completed the EOSQ-24 at each follow-up, which could have caused a bias.

To prevent (excessive) kyphosis and subsequent material protrusion, we added an extra parallel connector in the current SDS design. This was effective, as the sagittal curves were well maintained after postoperative reduction. This differed from the previous SDS versions, where a substantial increase was observed that was intentional in selected cases, but a reason for revision in others. Since scoliosis in general can be considered as the result of a relative posterior shortening, we consider some increase of kyphosis beneficial, and future generations of SDS will be designed to accommodate that with rod contouring. Additionally, it should be mentioned that more rigidity in the sagittal plane may be a reason for rod failure over time, and although we have not seen this yet, it may appear in the coming years.

This preliminary study has obvious limitations, including the small patient cohort that was followed for a relatively short follow-up period. Furthermore, some patients were at the end of their growth spurt, which may explain less spinal growth after SDS treatment compared to the previous studies.[58,113] It is not possible to compare results of different SDS configurations, as the indication for uni- or bilateral springs is largely dependent on the etiology. Neuromuscular curves typically receive a bilateral SDS, in contrast to idiopathic curves. We will continue to further optimize the design, as metal wear between the sliding rod and connectors is still a concern, but also fundamental questions, such as which forces and configurations are optimal for specific conditions (e.g., etiology and curve type), demand for further investigations.

9

Conclusions

After a design iteration of the SDS, similar curve maintenance was observed compared to the previous system, with less implant-related complications and unplanned reoperations. These findings suggested that the earlier identified "room for improvement" indeed existed and allowed us to make an effective implant which may have less failures than the alternatively available systems.
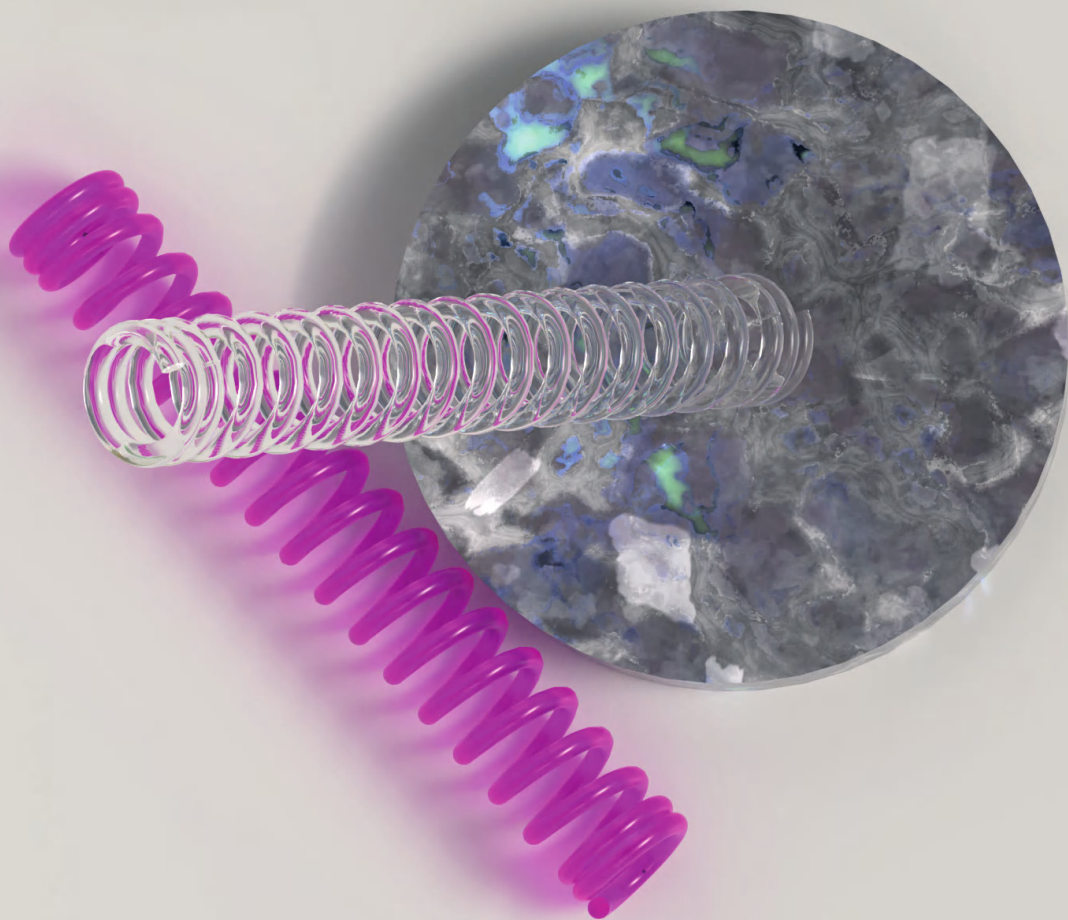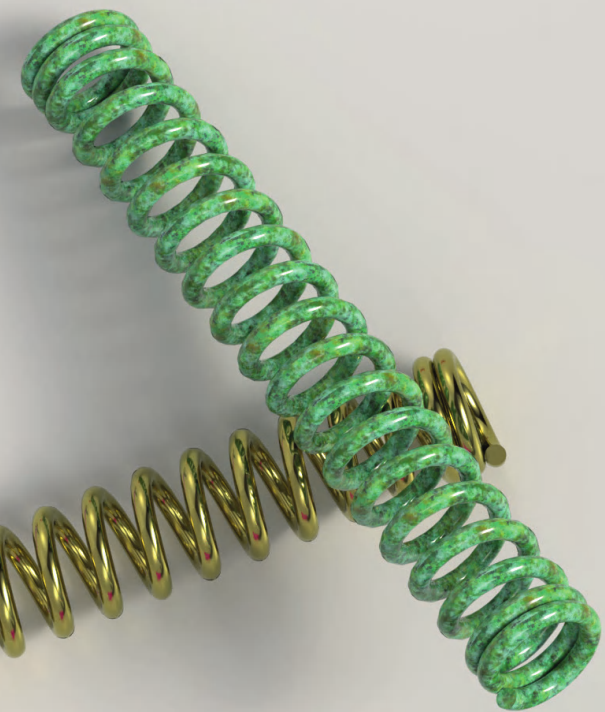
Chapter 10

Health-Related Quality of Life in Early Onset Scoliosis Patients Treated With the Spring Distraction System: What to Expect in the First 2 Years After Surgery

J.V.C. Lemans
A. Top
C.S. Tabeling
E.P. Scholten
H.W. Stempels
T.P.C. Schlösser
R.M. Castelein
M.C. Kruyt

Abstract

Purpose
The Spring Distraction System (SDS) is a novel "growth-friendly" implant for the treatment of Early-Onset Scoliosis (EOS). This prospective study aims to determine the evolution of the "24-Item Early-Onset Scoliosis Questionnaire" (EOSQ-24) scores during 2-year follow-up after SDS surgery. Secondary aims include investigating the relation between EOSQ-24 scores and EOS etiology, and evaluating the impact of an unplanned return to the operating room (UPROR) on HRQoL.

Methods
All SDS patients with at least 2-year follow-up were included. Caregivers completed the EOSQ-24 pre-operatively, post-operatively, and at 6, 12, and 24 month follow-up. Mean total and -domain scores were graphed over time. Repeated-measures ANOVA analyzed the influence of etiology on EOSQ-24 scores. Multiple regression analyzed associations between UPRORs and EOSQ-24 scores.

Results
Forty-nine patients were included. Mean total EOSQ-24 scores decreased from 70 pre-operatively to 66 post-operatively, then gradually increased to 75 (24 months). Most domains exhibited changes over time, with initial declines, but eventually surpassing pre-operative levels after 2-year follow-up. Neuromuscular/Syndromic patients had lower scores, but showed similar improvements over time compared with other etiologies. Multiple regression showed lower Parental Burden domain score (−14 points) in patients with UPRORs, although no significant reductions were found in total score, or in other domains.

Conclusion
HRQoL decreases immediately following SDS surgery but quickly recovers and exceeds pre-operative levels at 2-year follow-up in all domains. Neuromuscular/Syndromic patients have lower initial scores, but progress similarly over time. UPRORs do not influence EOSQ-24 scores, except for a negative impact on the Parental Burden domain in the short term.

Introduction

Early-onset scoliosis (EOS) is a deformity of the spine and trunk that occurs before the age of ten and can lead to substantial morbidity if left untreated.[144] For severe progressive curves, several surgical treatment options are available, including the traditional growing rod (TGR) and magnetically controlled growing rod (MCGR). While both systems offer adequate curve correction and growth, complication rates are high, and the repeated lengthenings are a burden for the patient, their caregivers, and the healthcare system.[33,45] At our institution, the spring distraction system was developed out of an unmet patient need (Figure 1). It provides continuous and dynamic distraction forces and achieves stable curve correction and near-normal growth without the need for repetitive surgical or outpatient lengthenings.[58,59,113,179] However, the effect of SDS treatment on health-related quality of life (HRQoL) has not yet been characterized.

Figure 1. Spring distraction system concept
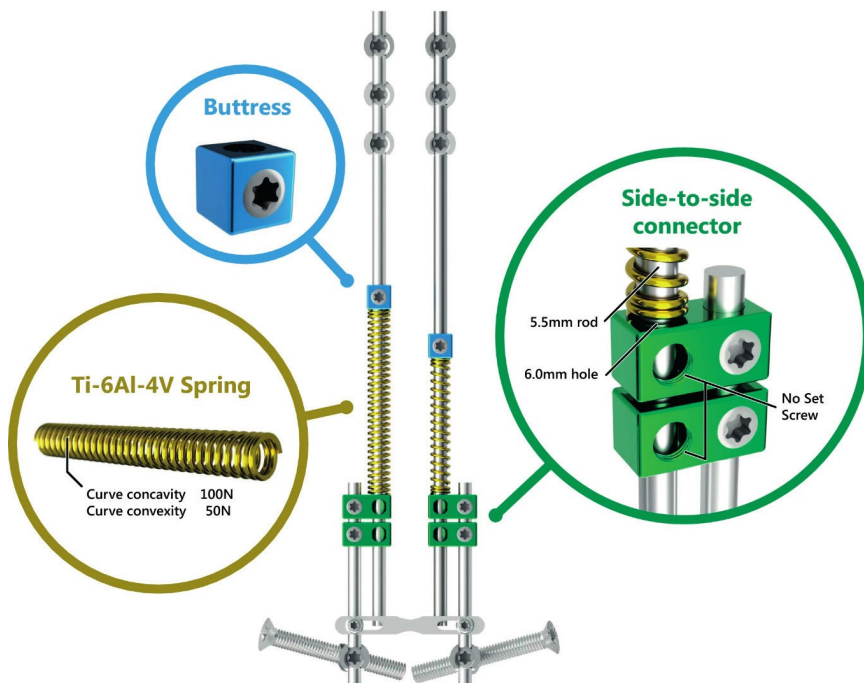
The SDS is a "growth-friendly" system that provides a continuous distraction force during follow-up, without the need for repeated lengthenings. Different configurations are used for different curve morphologies. The SDS consists of standard instrumentation to which several components are added. **Green:** Two side-to-side connectors that have an oversized hole that can accommodate a sliding CoCr rod. **Gold:** Uni- or bilateral Ti6Al4V springs that are mounted on the rod and which can be compressed. **Blue:** A buttress block that compresses the spring against the side-to-side connector.

To study HRQoL in EOS, the "24-Item Early-Onset Scoliosis Questionnaire" (EOSQ-24) was developed.[155] The EOSQ-24 is a questionnaire filled out by parents or caregivers and has been cross-culturally validated in several languages.[138,209,210] It consists of 24 questions that correspond to 12 domains: General Health, Pain/Discomfort, Pulmonary Function, Transfer, Physical Function, Daily Living, Fatigue/Energy Level, Emotion, Parental Burden, Financial Burden, Child Satisfaction, and Parental Satisfaction. The total score and the scores of subdomains range from 0 to 100 points, with a higher score denoting better outcomes.

Several clinical studies using the EOSQ-24 have been performed, which have shown that differences between patients are correlated with EOS etiology.[155,211,212] Other studies have compared HRQoL between MCGR and TGR treatment.[149,213] While the EOSQ-24 has the ability to discriminate between subgroups of patients with different curve severities or treatment status, very little is known on the over-time changes in HRQoL in EOS patients after surgery, as longitudinal data is sparse. [212] The natural course of HRQoL for untreated EOS is even more unclear, although one study found severely decreased HRQoL in adult, untreated EOS patients with large curves.[214]

The main aim of the current study was to determine EOSQ-24 score evolution over time in EOS patients treated with the SDS. Secondary aims were to show differences in EOSQ-24 scores between different etiologic groups, and to determine whether unplanned return to the operating room (UPROR) leads to reduced HRQoL scores.

Methods

Study design and ethical review
The current study uses the data of the ongoing prospective clinical trial that was initiated in 2016 after ethical approval by the institutional review board of UMC Utrecht (METC 16/276). All EOS patients who received the SDS are prospectively followed as part of the GRADS (Growing Rods with the Addition of a Distraction Spring) cohort. Caregivers were asked to complete the validated, Dutch version of the EOSQ-24 pre-operatively, immediately post-operatively and at each follow-up visit. [138] Patients with a pre-operative EOSQ-24, at least two post-operative EOSQ-24's and at least 2-year follow-up were included in the current analysis.

Surgical treatment
At UMC Utrecht, SDS treatment is offered to EOS patients with an indication for "growth-friendly" treatment, except in patients with diseases that compromise soft tissue- or bone strength such as osteogenesis imperfecta or Marfan syndrome. The surgical technique for SDS has been described previously.[58,59,179] Anchors and rods are implanted comparable to TGR, but the rods are not fixated in side-to-side con-

nectors, but are allowed to slide freely in the connector. In addition, helical springs of 50N, 75N, or 100N are mounted on the rods unilaterally or bilaterally. Following surgery, braces are not applied and there are no restrictions in load-bearing and (sport) activities.

Data collection

EOSQ-24 data of each patient was collected at 5 time points: pre-operatively, immediately post-operatively, and at 6-, 12-, and 24-month follow-up. In addition, patient- and curve-related baseline characteristics were obtained. These included age at surgery, sex, curve magnitude, etiology, and pre-operative coronal Cobb angle. For each patient, the presence or the absence of UPRORs within 2-year follow-up was determined.[113]

Multiple imputation for missing data

We used multiple imputation with parcel summary scores (PSS) as an advanced statistical method to address individual missing items and entire missing questionnaires.[157] This method provides reliable results, outperforming complete case analysis and mean imputation if >10% of subjects have missing data.[157,215] The method comprises several steps:

1: Missing items are identified at each time point.
2: PSS are created; these are the average of the available questions which are used as surrogate for the missing question itself. This information is used as a predictor to impute questions at other time points. The temporary score is only used in the imputation process.
3: Through the PSS, missing items are imputed based on a combination of other filled-out values in the same questionnaire, values of past and future completed questionnaires of the same patient, and patient etiology.
4: All imputed datasets are merged into one multiple imputation dataset. From the single question scores, category and total scores are calculated and analyzed.

Statistical analyses

Following multiple imputation, mean EOSQ-24 scores were calculated and graphed over time. To test whether the total EOSQ-24 score or any of its domains changed over time, a mixed repeated-measures ANOVA was performed for each category, with time as the within-subjects factor and etiology as the between-subjects factor. Several post hoc analyses were performed: Pre-operative vs. post-operative, post-operative vs. 6 months, 6 months vs. 1 year, 1 vs. 2 years, pre-operative vs. 2 years, and post-operative vs. 2 years.

10

The effect of etiology was analyzed in the mixed repeated-measures ANOVA. Due to the small number of syndromic EOS patients, these patients were added to the neuromuscular group, as it has been previously shown that both groups have similar EOSQ-24 scores.[211] Similar to the time effect, we first determined whether there were significant differences in the F statistic followed by post hoc analyses: Idiopathic vs. Congenital, Idiopathic vs. Neuromuscular and Congenital vs. Neuro-muscular. In addition, the interaction effect between time and etiology was evaluated to determine whether EOSQ-24 score evolution was different between etiologies.

To investigate the effect of UPRORs on EOSQ-24 score, we first investigated the difference in EOSQ-24 scores before and after UPRORs in all patients who suffered an UPROR with a paired t-test. As the trend over time in patients without UPRORs is unknown and could be subject to confounding, we also performed a multiple regression analysis in all patients with EOSQ-24 (domain) score as the dependent variable and the onset of an UPROR within the study period as the independent variable. For patients with UPRORs, the first EOSQ-24 after the UPROR was used as the dependent variable. For patients without UPRORs, we used the EOSQ-24 at 2-year follow-up. These different points were chosen to maximize potential differences and provide a worst-case scenario analysis. As we expected pre-operative EOSQ-24 values and etiology to be potential confounders, these were added in the model so that the effect of UPRORs on EOSQ-24 score could be independently investigated. We also repeated the analysis using the EOSQ-24 score at 2-year follow-up in all patients, to evaluate the effects of UPRORs on long-term HRQoL.

Statistical significance was set at $p < 0.05$. The false discovery rate (i.e., the rate of Type I errors due to multiple testing) for the post hoc analyses after analyzing the main effects was controlled at 5% through the Benjamini–Hochberg method, and the adjusted *P* values were calculated.[216] All statistical procedures were performed with IBM SPSS Statistics for Windows, Version 27.0. (IBM Corp., Armonk, NY, USA). Figures were created with GraphPad Prism version 9.3.0 (GraphPad Software, San Diego, CA, USA).

Results

Baseline demographics
Out of 59 SDS patients with 2-year follow-up, 49 were included for analysis. Ten patients did not have a filled-out pre-operative EOSQ-24 and were excluded. Mean age at surgery was 8.7 years, 49% of patients were girls (Table 1). Almost all neuromuscular patients (22/23; 96%) were non-ambulatory. All patients with other etiologies were ambulatory. The mean pre-operative coronal Cobb angle was 70°, which was corrected to 39° and which was mostly maintained at 2-year follow-up at

45°. Sixteen patients (33%) required UPRORs for surgical site infections, or implant-related complications.

Table 1. Baseline characteristics

Variable	Mean (SD) or N (%)
Age at surgery	8.7 years (2.0)
Gender	
Female	24/49 (49%)
Male	25/49 (51%)
First growth implant vs. conversion	
Primary	42/49 (86%)
Conversion	7/49 (14%)
Etiology	
Congenital	12/49 (25%)
Idiopathic	11/49 (22%)
Neuromuscular	23/49 (47%)
Syndromic	3/49 (6%)
Ambulatory	27/49 (55%)
Pre-operative Cobb angle	70.3° (23.1)
Patients with UPROR <2 years	16/49 (33%)

Missing data

During data collection, we observed that 25 patients (51%) had no missing data, while 7 patients (14%) filled out all questionnaires but had at least one missing answer. In 17 patients (35%), an entire questionnaire was missing during follow-up. In total, 8.0% of items (i.e., individual EOSQ-24 questions) were missing and had to be imputed (if a complete questionnaire had not been filled out, this amounted to 24 missing items). Missingness of data was observed to be related to etiology (i.e., missing at random), but was not related to the magnitude of EOSQ-24 score itself.

EOSQ-24 scores over time

EOSQ-24 scores over time are shown in Table 2 and graphed in Figure 2. Mean total EOSQ-24 score decreased from 70 ± 15 pre-operatively to 66 ± 15 post-operatively. Scores normalized at 6-month follow-up at 72 ± 17 and increased further to 74 ± 16 at 1-year and 75 ± 16 at 2-year follow-ups. Several domains did not show significant changes over time (General Health, Pulmonary Function, Financial Burden, Child Satisfaction and Parental Satisfaction). The results of post hoc analyses are shown

10

in Table 3. In all domains, EOSQ-24 scores decreased immediately post-operatively, but recovered completely within 6 months and were higher at 2-year follow-up compared to pre-operatively. These changes were statistically significant for the Total Score (+5.6), Pain/Discomfort- (+11), Daily Living- (+8.9), and Parental Burden domains (+8.4).

Table 2. Results of mixed repeated-measures ANOVA: effect of time

EOSQ-24 domain	Pre-operative	Post-operative	6 months	12 months	24 months	P value[a]
Total	70 (SD 15)	66 (SD 15)	72 (SD 17)	74 (SD 16)	75 (SD 16)	<0.001[b]
General Health	62 (SD 19)	64 (SD 18)	62 (SD 19)	69 (SD 18)	66 (SD 21)	0.135
Pain/Discomfort	59 (SD 27)	49 (SD 24)	64 (SD 19)	69 (SD 21)	70 (SD 23)	<0.001
Pulmonary Function	76 (SD 25)	78 (SD 22)	76 (SD 23)	77 (SD 25)	81 (SD 21)	0.564[b]
Transfer	65 (SD 50)	47 (SD 32)	68 (SD 31)	71 (SD 30)	71 (SD 29)	<0.001[b]
Physical Function	57 (SD 37)	49 (SD 33)	60 (SD 36)	57 (SD 38)	63 (SD 37)	0.006[b]
Daily Living	47 (SD 33)	44 (SD 34)	50 (SD 34)	50 (SD 36)	56 (SD 36)	0.022
Fatigue/Energy level	59 (SD 28)	50 (SD 24)	60 (SD 27)	68 (SD 24)	65 (SD 24)	<0.001
Emotion	66 (SD 25)	57 (SD 26)	70 (SD 24)	71 (SD 25)	71 (SD 24)	0.007[b]
Parental Burden	62 (SD 23)	60 (SD 24)	68 (SD 25)	72 (SD 25)	71 (SD 24)	<0.001[b]
Financial Burden	81 (SD 25)	82 (SD 26)	81 (SD 27)	84 (SD 27)	92 (SD 16)	0.097[b]
Child Satisfaction	62 (SD 28)	62 (SD 27)	65 (SD 27)	70 (SD 20)	68 (SD 25)	0.106[b]
Parental Satisfaction	63 (SD 30)	64 (SD 27)	67 (SD 25)	68 (SD 23)	66 (SD 27)	0.478[b]

[a]Based on time effect in mixed repeated-measures ANOVA

[b]Greenhouse–Geisser correction was used due to non-sphericity of data

Table 3. Post hoc analyses of different time points in the mixed repeated-measures ANOVA

EOSQ-24 domain	Pre-operative vs. Post-operative		Post-operative vs. 6 months		6 months vs. 1 year		1 year vs. 2 years		Pre-operative vs. 2 years		Post-operative vs. 2 years	
	Change[a]	P value[b]	Change[a]	P value[b]	Change[a]	P value[b]	Change[a]	P value[b]	Change[a]	P value[b]	Change[a]	P value[b]
Total	− 3.3	0.131	5.8	0.002	2.1	0.277	1.0	0.578	5.6	0.008	8.9	<0.001
General Health	Main effect not statistically significant											
Pain/Discomfort	− 9.5	0.058	15	0.005	5.2	0.170	0.5	0.942	11	0.023	20	<0.001
Pulmonary Function	Main effect not statistically significant											
Transfer	− 18	0.002	21	0.002	2.8	0.614	0.4	0.964	6.2	0.373	24	<0.001
Physical Function	− 7.4	0.120	11	0.037	− 3.5	0.442	6.6	0.120	6.5	0.105	14	0.002
Daily Living	− 2.7	0.613	5.6	0.270	0.2	0.976	5.8	0.166	8.9	0.038	12	0.006
Fatigue/Energy level	− 9.1	0.079	9.7	0.037	8.1	0.105	− 2.4	0.578	6.3	0.166	15	<0.001
Emotion	− 8.4	0.131	13	0.002	0.5	0.942	0.1	0.976	5.4	0.284	14	0.005
Parental Burden	− 2.1	0.607	7.9	0.033	3.7	0.225	− 1.1	0.745	8.4	0.037	11	0.002
Financial Burden	Main effect not statistically significant											
Child Satisfaction	Main effect not statistically significant											
Parental Satisfaction	Main effect not statistically significant											

[a]Positive value denotes an increase in HRQoL over time

[b]Benjamini–Hochberg adjusted p value with false discovery rate set at 0.05

Figure 2. Health-related quality of life over time
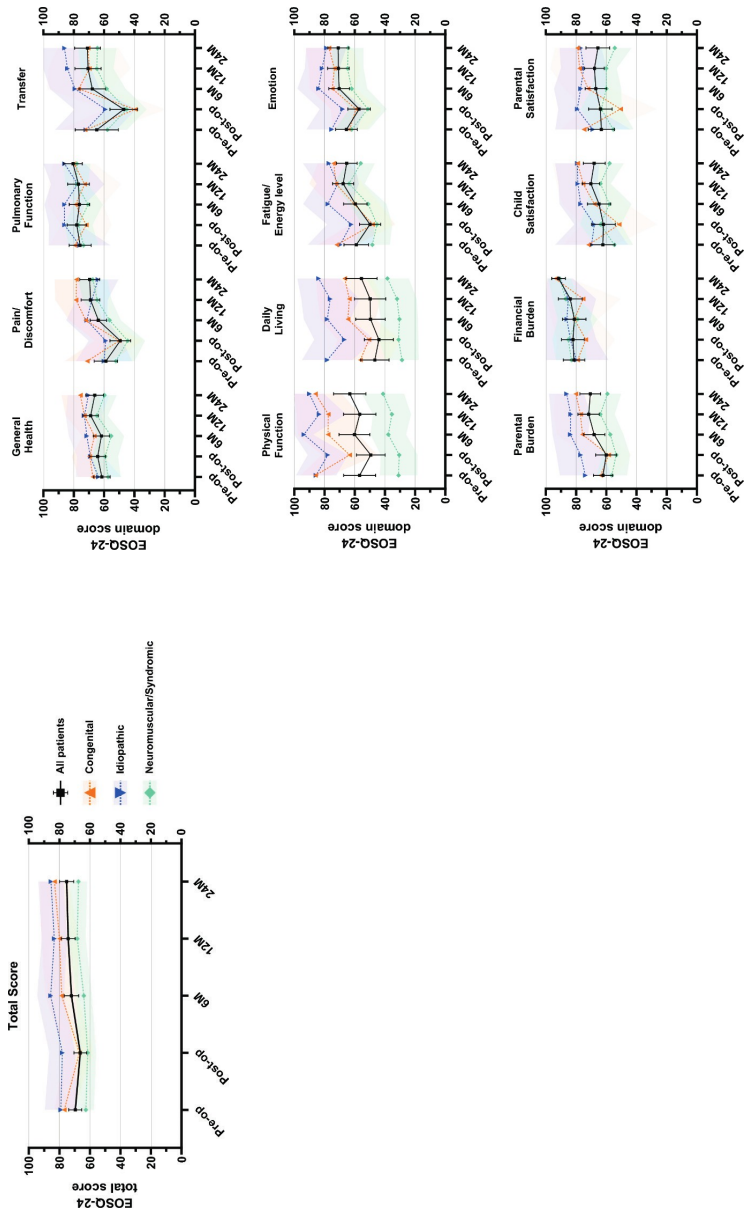
Black line and whiskers indicate the mean and 95% confidence interval of the entire patient cohort. Colored dashed lines and shaded area indicate the mean and 95% confidence interval for each etiologic group.

Table 4. Results of mixed repeated-measures ANOVA: effect of etiology

EOSQ-24 domain	Effect of etiology	Pairwise comparison of etiology[a]						Interaction of time x etiology
		I-C		I-NM		C-NM		
	P value	Mean	P value[b]	Mean	P value[b]	Mean	P value[b]	P value
Total	<0.001	5.3	0.344	18	0.001	12	0.016	0.229[c]
General Health	0.023	−1.0	0.856	10	0.070	11	0.041	0.837
Pain/Discomfort	0.064	Main effect not statistically significant						0.224
Pulmonary Function	0.556	Main effect not statistically significant						0.409[c]
Transfer	0.051	Main effect not statistically significant						0.615[c]
Physical Function	<0.001	8.1	0.452	51	<0.001	43	<0.001	0.418[c]
Daily Living	<0.001	17	0.167	45	<0.001	28	0.009	0.711
Fatigue/Energy level	0.019	6.5	0.462	19	0.027	12	0.116	0.109
Emotion	0.030	8.0	0.344	17	0.028	8.6	0.229	0.883[c]
Parental Burden	0.003	10	0.261	23	0.005	13	0.081	0.340[c]
Financial Burden	0.719	Main effect not statistically significant						0.691[c]
Child Satisfaction	0.033	5.5	0.462	15	0.036	9.6	0.163	0.110[c]
Parental Satisfaction	0.015	4.6	0.542	17	0.027	12	0.081	0.075[c]

[a] A positive value denotes that the first group has higher scores compared to the second group and vice versa

[b] Benjamini–Hochberg adjusted P value with false discovery rate set at 0.05

[c] Greenhouse–Geisser correction was used due to non-sphericity of data

10

Influence of etiology on EOSQ-24 scores

The effect of etiology is seen in Table 4. EOSQ-24 scores across etiologies are shown in Figure 2. There were significant differences in all domains except the Pain/ Discomfort, Pulmonary Function, and Transfer and Financial Burden domains, with the lowest scores for neuromuscular patients, followed by congenital patients and the highest scores for idiopathic patients. The differences between idiopathic and neuromuscular patients ranged between 10 and 51 points, depending on domain. The differences between congenital and neuromuscular patients ranged between 8.6 and 43 points. The largest differences between etiologies were seen in Physical Function domain (mean score across time points; idiopathic: 86, congenital: 78, neuromuscular: 35) and the Daily Living domain (mean score across time points; idiopathic: 77, congenital: 60, neuromuscular: 32). Differences between idiopathic and congenital patients were relatively small (−1.0 to 17) and not significant in any domain.

Interactions between time and etiology were not seen in any domain, suggesting that the improvement in EOSQ-24 scores over time was similar in all etiological groups

Influence of etiology on EOSQ-24 scores

The pre- and post-UPROR EOSQ-24 scores in the 16 patients with UPRORs can be seen in Table 5. In patients with UPRORs, the mean time between the UPROR and the next EOSQ-24 was 94 ± 50 days. In many domains, an improvement was seen in the post-UPROR EOSQ-24 scores. Although not statistically significant, this coincides with the trend of improvement of HRQoL over time seen in all patients. The results of multiple regression investigating the effect of UPRORs in all patients are shown in Table 6. A significant decrease in EOSQ-24 score was seen in the Parental Burden domain (−14 points, 95% CI −26; −1.6) in patients with an UPROR. In addition, the presence of UPRORs was correlated with sizable decreases that approached significance in the Transfer (−11 points, 95% CI −30; 8.0), Child Satisfaction (-7.6 points, 95% CI −25; 9.3), and Parental Satisfaction (−11 points, 95% CI −25; 3.9) domains. The results of multiple regression with 2-year EOSQ-24 values in all patients are shown in Supplement 1. When looking at the long-term follow-up, the (modest) negative effect of UPRORs on HRQoL disappears, except for the Satisfaction domains, where a trend toward further decrease is seen in the long term.

Table 5. Comparison of EOSQ-24 scores before and after an UPROR

EOSQ-24 domain	Score before UPROR	Score after UPROR	Paired difference (95% CI)[a]	P value
Total	66	70	4.0 (−0.82; 8.8)	0.103
General Health	63	62	−0.94 (−14; 12)	0.884
Pain/Discomfort	53	63	10 (−5.0; 25)	0.193
Pulmonary Function	75	79	3.8 (−8.0; 16)	0.532
Transfer	60	58	−1.7 (−29; 25)	0.893
Physical Function	45	55	9.4 (−7.1; 26)	0.264
Daily Living	42	55	13 (−5.3; 32)	0.159
Fatigue/Energy level	54	61	7.0 (−7.4; 21)	0.338
Emotion	59	69	10 (−5.3; 25)	0.194
Parental Burden	57	59	2.7 (−5.4; 11)	0.517
Financial Burden	83	87	3.9 (−16; 23)	0.692
Child Satisfaction	68	61	− 6.6 (−23; 10)	0.437
Parental Satisfaction	59	57	− 2.3 (−17; 13)	0.753

Analyzed in all patients with an UPROR within 2 years (N = 16)

[a]A positive number denotes higher EOSQ-24 score after the UPROR compared to before the UPROR

10

Table 6. Multiple regression analysis investigating the effect of UPRORs on HRQoL

EOSQ-24 domain	Proportion of explained variation	Constant	Pre-operative domain score	Presence of UPROR	Etiology	
					Congenital	Neuromuscular
	R^2 value	B (95% CI)	B (95% CI)	B (95% CI)	B (95% CI)	B (95% CI)
Total	0.52	41 (18; 63)	0.56 (0.28; 0.84)	−3.7 (−11; 3.6)	0.31 (−8.9; 9.5)	−8.9 (−18; 0.53)
General Health	0.37	38 (12; 64)	0.54 (0.20; 0.88)	−4.1 (−16; 8.2)	2.8 (−11; 16)	−7.5 (−20; 5.4)
Pain/Discomfort	0.26	47 (28; 65)	0.33 (0.08; 0.57)	−4.3 (−17; 8.1)	9.7 (−6.3; 26)	−1.6 (−16; 13)
Pulmonary Function	0.25	59 (37; 81)	0.35 (0.11; 0.59)	0.55 (−13; 14)	−7.3 (−23; 8.2)	−12 (−26; 1.9)
Transfer	0.15	67 (42; 92)	0.19 (−0.09; 0.48)	−11 (−30; 8.0)	−7.4 (−28; 14)	−13 (−32; 6.7)
Physical Function	0.68	32 (5.3; 59)	0.70 (0.40; 1.0)	−1.2 (−15; 12)	−6.1 (−24; 12)	−15 (−37; 7.9)
Daily Living	0.55	35 (7.8; 62)	0.63 (0.29; 1.0)	9.2 (−6.8; 25)	−6.1 (−26; 14)	−21 (−44; 1.1)
Fatigue/Energy level	0.41	42 (22; 62)	0.48 (0.24; 0.71)	1.4 (−12; 15)	−2.8 (−19; 14)	−14 (−30; 2.6)
Emotion	0.17	56 (29; 83)	0.27 (−0.05; 0.59)	0.7 (−14; 16)	3.9 (−14; 22)	−11 (−27; 5.7)
Parental Burden	0.47	46 (22; 69)	0.51 (0.21; 0.81)	−14 (−26; −1.6)	5.6 (−9.1; 20.4)	−11 (−25; 2.6)
Financial Burden	0.08	76 (54; 99)	0.18 (−0.07; 0.43)	−3.5 (−16; 8.9)	4.3 (−11; 19)	−3.1 (−17; 11)
Child Satisfaction	0.18	73 (51; 94)	0.09 (−0.18; 0.34)	−7.6 (−25; 9.3)	2.2 (−16; 20)	−15 (−32; 1.6)
Parental Satisfaction	0.27	63 (43; 83)	0.22 (−0.01; 0.45)	−11 (−25; 3.9)	2.9 (−15; 21)	−15 (−31; 1.6)

Analyzed with data from all patients (N = 49). For patients with an UPROR, the EOSQ-24 result at the first time point after the UPROR was used as the dependent variable. For patients without an UPROR, the 2-year follow-up EOSQ-24 was used as the dependent variable

Discussion

The present study investigated changes in HRQoL over time in a diverse EOS population that underwent SDS treatment. We observed a general trend where EOSQ-24 scores declined immediately following surgery, but recovered to baseline or higher within 6 months. At 2-year follow-up, the mean score in each domain was higher than pre-operative levels, with a statistically significant relation for the total score, and the Pain/Discomfort, Daily Living, and Parental Burden domains. These changes are considered clinically relevant as they surpass the minimal clinically important difference (MCID) when using distribution-based approaches (e.g., a change of >1 SEM or >0.2 SD).[217] However, formal MCIDs for the EOSQ-24 have not yet been established, which makes conclusions regarding clinical relevance preliminary. However, not all EOSQ-24 domain scores improved over time, such as the Parental Satisfaction domain.

The findings from this study can be utilized to counsel patients and their caregivers about the expected subjective health changes during the initial two years after surgery. It is promising to note that HRQoL continued to improve with longer follow-up in all patient groups, possibly due to the SDS allowing patients to resume normal activities without restrictions and periodic lengthenings. However, it remains to be seen if this positive trend continues until after SDS graduation.

Neuromuscular/Syndromic patients showed lower initial scores in several domains as expected, but the improvement over time was similar to their peers with other etiologies. Interestingly, no correlation was seen between etiology and the Pulmonary Function domain, while one would expect lower scores in neuromuscular patients. This observation aligns with a previous study indicating that the Pulmonary Function domain of the EOSQ-24 demonstrates high variability and limited association with pulmonary function test (PFT) results, particularly in patients with a forced vital capacity <40%.[218] We do not routinely perform PFTs, as these are burdensome and oftentimes cannot be reliably obtained in young patients, especially if there is developmental delay.[170]

Previous studies have investigated EOSQ-24 scores in different settings. Ramo et al. showed in a large cross-sectional study of over 600 EOS patients that neuromuscular and syndromic patients have significantly lower EOSQ-24 scores compared to idiopathic and congenital patients, and that the latter two groups have very similar scores. [211] In a follow-up study, Shaw et al. showed that "growth-friendly" treatment mainly stabilizes HRQoL after 2 years, and that the evolution is similar in different etiologies, which is in line with our own data.[219] However, in contrast to our study, they identified no domains where patients improved at 2-year follow-up compared to baseline. However, the MCID used in that study (>20% increase) could be considered conservative. In patients with UPRORS, no decline in HRQoL was observed over time. Instead, a trend of improvement was seen, aligning with the general trend in the entire patient

10

group. After adjusting for curve etiology and pre-operative score in the linear regression, we found significantly lower scores in the Parental Burden domain (−14 points, 95% CI −26; −1.6). There was also a trend towards worse scores in the Transfer (−11 points, 95% CI −30; 8.0) and Parental Satisfaction (−11 points, 95% CI −25; 3.9) domains, but no decrease in the total score. This contrasts with a previous study, which saw a decrease in total EOSQ-24 score.[220] This could be due to several reasons. First, the mean time between UPRORs and the next questionnaire was >90 days. In that timeframe, EOSQ-24 scores could have decreased, but normalized to baseline again. Second, it is possible that the current analysis was underpowered to detect the relatively small differences between groups. Third, UPRORs are generally less extensive surgeries compared to the primary surgery. This may result in a smaller decrease in scores compared to the primary surgery, which the EOSQ-24 may not be able to detect. When looking at the long-term follow-up in all patients, no relation was seen between UPRORs and HRQoL, suggesting that UPRORs do not negatively affect HRQoL in the long-term. We chose UPRORs instead of complications as they could more objectively be defined as being present compared to complications.

A major strength of the current study is its longitudinal design. The current study is the first to investigate the change in HRQoL across many fixed post-operative time points in a prospective EOS patient cohort, where other studies often opt for a cross-sectional design.[149,213] Additionally, we utilized multiple imputation with PSS to account for missing EOSQ-24 item values, enabling advanced statistical analysis and increasing study power compared to a complete case analysis, which would exclude nearly 50% of participants. Limitations of the study include the relatively low sample size per condition and the short follow-up of 2 years. However, the included SDS patients will be followed up with the EOSQ-24 until after skeletal maturity, which may provide information for the long-term follow-up of HRQoL. Another limitation is the absence of a comparison group, making it challenging to determine whether patients undergoing SDS treatment have different HRQoL compared to those treated with another implant, or those who have not been treated surgically at all.

Conclusion

Following SDS surgery, EOSQ-24 scores decrease post-operatively in several domains. However, all scores recover to pre-operative levels within 6 months, and in several domains, scores exceed pre-operative levels at 2-year follow-up. Patients with neuromuscular/syndromic EOS etiology initially score lower in several domains, but their progression following surgery is similar to the other etiologies. The total EOSQ-24 score and the score in most EOSQ-24 domains are unaffected by the presence of UPRORs although they lead to worse scores in the Parental Burden domain in the short term.

Supplement 1. Multiple regression analysis investigating the effect of UPRORs on HRQoL

EOSQ-24 domain	Proportion of explained variation	Constant	Pre-operative domain score	Presence of UPROR	Etiology	
					Congenital	Neuromuscular
	R² value	B (95% CI)	B (95% CI)	B (95% CI)	B (95% CI)	B (95% CI)
Total	0.50	39 (15; 62)	0.59 (0.32; 0.87)	-1.4 (-8.8; 6.0)	-0.89 (-11; 9.0)	-7.9 (-18; 2.1)
General Health	0.40	35 (12; 59)	0.56 (0.28; 0.85)	-6.3 (-17; 4.0)	4.0 (-10; 18)	-5.3 (-18; 7.1)
Pain/Discomfort	0.25	40 (20; 61)	0.38 (0.14; 0.63)	4.5 (-8.4; 17)	9.9 (-7.8; 28)	5.3 (-11; 21)
Pulmonary Function	0.29	53 (32; 75)	0.42 (0.19; 0.66)	4.5 (-7.2; 16)	-7.8 (-23; 7.7)	-8.2 (-22; 5.7)
Transfer	0.11	77 (49; 105)	0.13 (-0.16; 0.43)	-1.5 (-20; 17)	-16 (-39; 8.2)	-20 (-41; 2.2)
Physical Function	0.68	21 (-6.5; 48)	0.81 (0.53; 1.1)	-2.0 (-16; 12)	-4.2 (-23; 14)	-3.9 (-26; 18)
Daily Living	0.58	24 (-5.8; 55)	0.74 (0.42; 1.1)	7.2 (-8.4; 23)	-1.4 (-23; 21)	-10 (-36; 16)
Fatigue/Energy level	0.38	48 (28; 68)	0.41 (0.19; 0.63)	5.9 (-6.3; 18)	-4.6 (-21; 12)	-14 (-30; 2.1)
Emotion	0.16	59 (32; 86)	0.26 (-0.05; 0.56)	4.4 (-10; 19)	0.87 (-19; 20)	-12 (-29; 5.3)
Parental Burden	0.46	50 (27; 74)	0.51 (0.23; 0.79)	-8.0 (-20; 3.9)	-0.42 (-16; 15)	-16 (-31; -1.6)
Financial Burden	0.12	75 (59; 93)	0.19 (0.00; 0.38)	3.3 (-6.7; 13)	2.8 (-10; 16)	-1.3 (-13; 11)
Child Satisfaction	0.23	76 (53; 99)	0.08 (-0.17; 0.33)	-10 (-25; 4.3)	0.27 (-19; 19)	-18 (-35; -0.40)
Parental Satisfaction	0.31	64 (43; 86)	0.23 (-0.01; 0.46)	-14 (-29; 0.9)	1.5 (-18; 21)	-16 (-34; 1.1)

Analyzed with data from all patients (N=49). For all patients, the 2-year follow-up EOSQ-24 was used as the dependent variable.

10

217
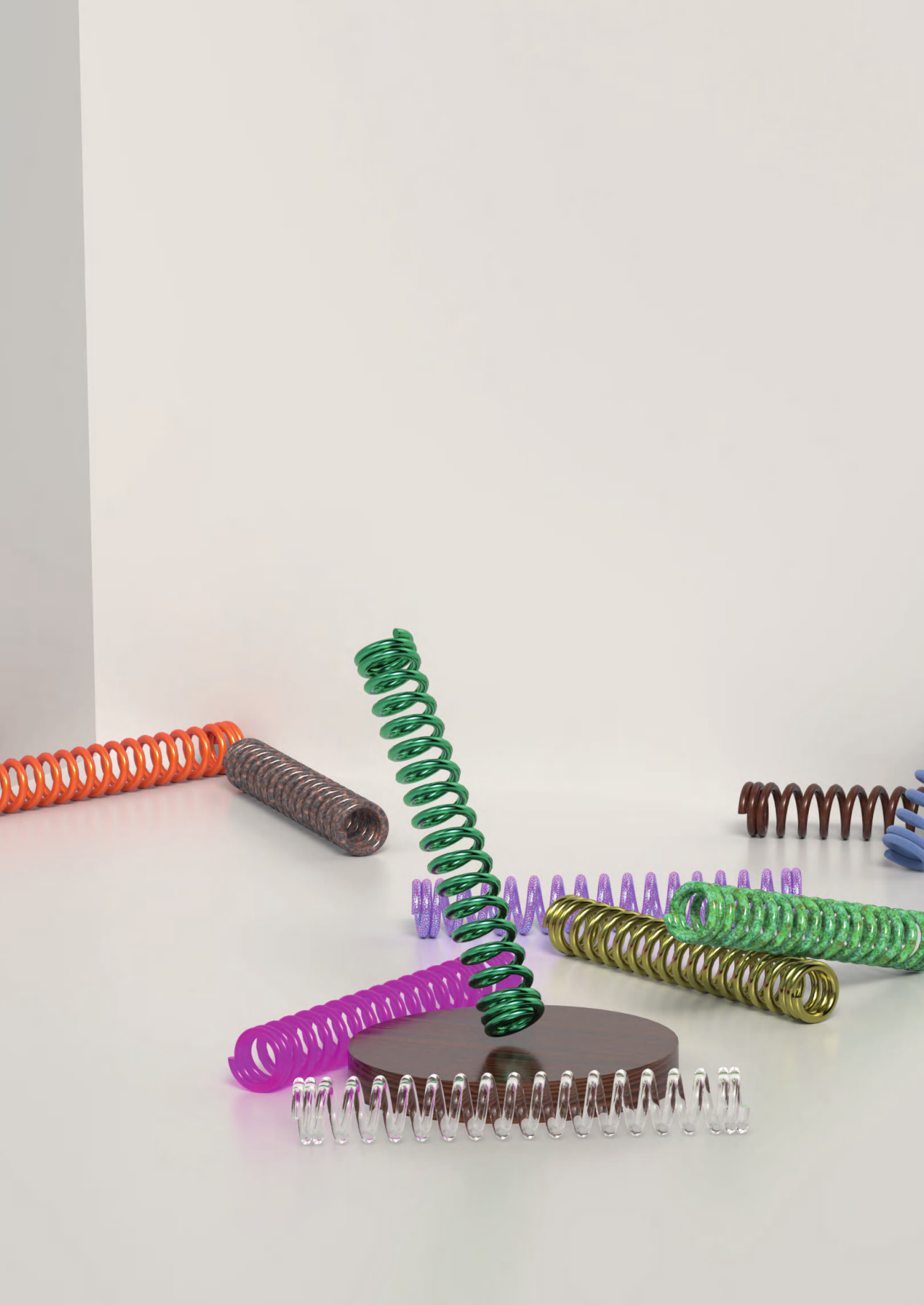
Efficacy of the Spring Distraction System for Different Etiologies of Early Onset Scoliosis: Evaluating an Evolving Treatment Concept

C.S. Tabeling
I.E. Blaauw
H.W. Stempels
T.P.C. Schlösser
K. Ito
R.M. Castelein
M.C. Kruyt
J.V.C. Lemans

Abstract

Background Context
Early onset scoliosis (EOS) is a challenging condition that requires "growth-friendly" implants for severe cases. The spring distraction system (SDS) was developed to correct and support growth without the need for repeated lengthenings (surgical or outpatient). The overall efficacy of this dynamic system was shown in prospective studies involving heterogeneous patient populations where different strategies were applied for different etiologies.

Purpose
To determine and compare the performance of the SDS between patients with different etiologies of EOS.

Study Design/Setting
Cohort study

Patient sample
Skeletally immature EOS patients of varying etiology

Outcome Measures
Major coronal Cobb angle, T5-T12 kyphosis, L1-S1 lordosis, T1-T12 height, T1-S1 height, serious adverse events (SAEs) and unplanned returns to the operating room (UPRORs)

Methods
Retrospective analysis of two prospective study cohorts involving SDS patients with a minimum of two-year follow-up. Outcomes were compared between different etiological groups. Differences between pre- and post-operatively were compared with a mixed repeated-measure ANOVA. Differences between post-operatively and later follow-up were compared using linear mixed models. SAE- and UPROR rates were compared and a Kaplan-Meier survival analysis was performed.

Results
In total, 64 patients with EOS were included (14 congenital, 41 neuromuscular, and 9 idiopathic). The mean age at surgery was 8.4±1.7 years, with idiopathic patients significantly older than congenital patients (p=0.017). The mean follow-up length was 3.7±1.4 years, with congenital patients having significantly longer follow-up than neuromuscular or idiopathic patients. Cobb angle increase after the correction during follow-up was minimal for congenital and neuromuscular patients (0.4°/year

and 0.9%/year, respectively), in idiopathic patients this was significantly more (3.6%/year). T1-T12 height increased at an average rate of 5.3 mm/year, with no significant differences between etiologies. T1-S1 growth was 7.5 mm/year in the idiopathic patients, 8.9 mm/year in congenital patients, and 10.0 mm/year in neuromuscular patients, with no significant differences between etiologies. A total of 52 SAEs (mostly implant-related) and 10 implant-related AEs occurred after a mean follow-up of 3.7 years, corresponding to an SAE rate of 0.20/patient/year in the congenital group, 0.22/patient/year in the neuromuscular group, and 0.24/patient/year in the idiopathic group. A total of 44 UPRORs were recorded, corresponding to an UPROR rate of 0.18/patient/year in the congenital group, 0.22/patient/year in the neuromuscular group and 0.09/patient/year in the idiopathic group.

Conclusions
The SDS performs well across EOS etiologies in in terms of curve correction, spinal growth, and SAE/UPROR rates. Neuromuscular and idiopathic patients showed the best initial correction, while idiopathic patients had less sustained correction. Spinal growth was near physiological and similar across etiologies. SAE rates were comparable and neuromuscular patients had the highest UPROR rate.

Introduction

Early onset scoliosis (EOS) presents in children before the age of 10 years and, when progressive, results in cardiopulmonary compromise and a loss of health-related quality of life (HRQoL).[182] Various etiologies are considered relevant to the heterogenous population of EOS patients, as demonstrated in the C-EOS classification: congenital/structural, neuromuscular, syndromic and idiopathic.[198] Currently, treatment for EOS patients is mostly guided by age and curve size, although each etiology has typical spinal characteristics that likely require tailored treatment strategies.[221] The aim of treatment is to control the spinal deformity while allowing the spine and trunk to grow for optimal pulmonary function.[13] When conservative management is insufficient, surgical intervention is indicated.[17,112,222–224] Several "growth-friendly" implants have been developed, including SHILLA growth-guidance, the traditional growing rod (TGR), and the magnetically controlled growing rod (MCGR). While these techniques are effective, they have several disadvantages that burden the patient and limit their efficacy.[38,45,130,192,207]

The most important issue with rigid distraction based instrumentation is the need for periodic surgical or outpatient lengthenings using relatively high and abrupt forces (>250 N). This not only poses a burden to the patient, but also risks damage and subsequent stiffening of the spine, which may result in diminishing returns.[33,35,43,225] Additionally, high complication and failure rates are associated with the complex distraction mechanism (e.g., MCGR) and repetitive surgeries and anaesthesia.

To address these limitations, the spring distraction system (SDS) was developed as a continuous and dynamic distraction system.[58,59] This system exerts a continuous, dynamic distraction force via a compressed helical spring around standard growing rods that slide through a side-to-side connector. The device was developed in 2015, in response to an unmet need in several exceptional EOS patients, but its indications were subsequently broadened to include any EOS patient with a progressive curve and significant remaining spinal growth, thus requiring "growth-friendly" surgery.[58] Due to the versatility of the system, different strategies are used for different types of scoliosis, for example long bipolar fixation with bilateral springs for neuromuscular cases, and short hybrid fixation with unilateral spring distraction combined with a contralateral sliding rod for idiopathic cases. Currently, the implant is not yet registered; therefore, all patients are meticulously followed up in two prospective clinical trials. Two-year follow-up data have shown promising results, including adequate curve correction and -control, physiological levels of spinal growth, and improved HRQoL.[59,179,225] However, whether SDS treatment demonstrates similar efficacy and safety across different EOS etiologies remains unknown. The current study aims to investigate the performance of SDS as used for different etiologies in terms of curve

control and spinal growth. A secondary aim is to compare the complication profile and unplanned return to the operating room (UPROR) profile of these groups.

Materials and Methods

Study design and inclusions
This study is a retrospective analysis of EOS patients included in two prospective clinical trials investigating the SDS: the GRADS study (Research Portal number NL55705.041.16) and the multicenter BiPOWR study (Clincaltrials.gov ID: NCT04021784, Research Portal number NL64018.041.17). All SDS patients, except those who were converted from another "growth-friendly" system, with at least two-year follow-up were included in the current analysis (N=68). Exclusion criteria for SDS treatment were the presence of connective tissue diseases (e.g., Marfan Syndrome) or severe bone pathology (e.g., osteogenesis imperfecta). When a patient graduated from SDS treatment (defined as either undergoing final fusion or reaching sufficient skeletal maturity with SDS in situ, whichever comes first), the measurements were performed on the radiograph before graduation (thus always with the SDS in situ).

Spring Distraction System
The SDS consists of one or more titanium (Ti-6AI-4V) helical coil springs positioned around a standard cobalt-chrome (CoCr) sliding rod (Figure 1). The spring exerts pressure against a side-to-side connector that is left unlocked on the CoCr sliding rod, allowing continuous distraction, overcoming the need for repetitive lengthening events. The spring is pre-tensioned using a standard buttress (Stryker, Leesburg, VI, USA) to provide a continuous distractive force along the rods, which linearly declines with lengthening according to Hooke's law ($Fs = k \cdot x$). The springs can be positioned strategically either uni- or bilaterally and with different forces, as shown in Figure 2. When used unilaterally, the spring is often combined with a contralateral sliding rod that aims to provide apical control (i.e., a hybrid construct).[143,226] When a spring fully expands but the patient has not yet reached end of growth, it can be re-tensioned during a minor surgery. Different strategies were employed for different types of scoliosis: congenital deformities were typically treated with unilateral convex hemi-epiphysiodesis combined with a concave distraction, idiopathic types with hybrid systems consisting of concave distraction and a convex sliding rod and neuromuscular patients were treated with bilateral spring distraction. During the study, design optimizations resulted in a change of the preferred rod diameter from 4.5 mm to 5.5 mm, along with increasing spring lengths and more spring force options (ranging from 50 N to 150 N).[179]

11

Figure 1. The Spring Distraction System (SDS)
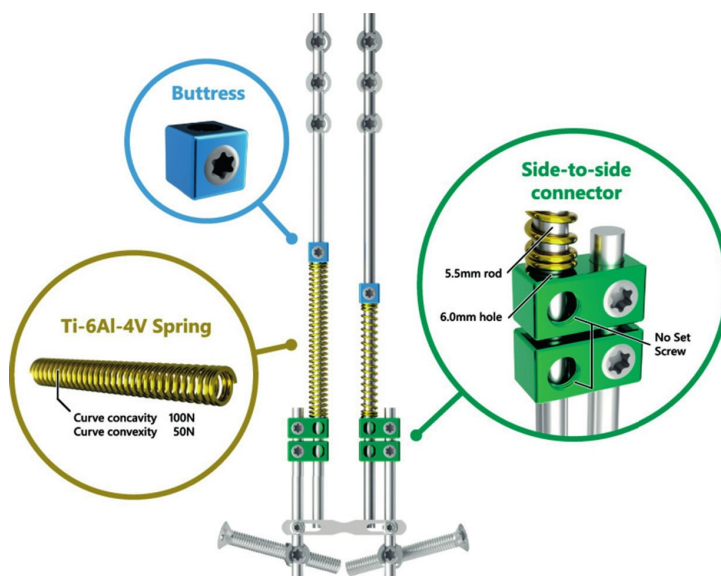
The SDS has three components added to standard CoCr growing rods (4.5 or 5.5mm) to offer a continuous distraction force. The configuration generally used in neuromuscular EOS patients is shown, with ilio-sacral screws as the distal anchor instead of pedicle screws. **Green:** Two stacked side-to-side connectors with an oversized hole for the sliding rod. **Gold:** Ti6Al4V springs ranging from 50 N to 150 N. **Blue:** Buttress to tension the spring against the connector.

Figure 2. SDS configurations
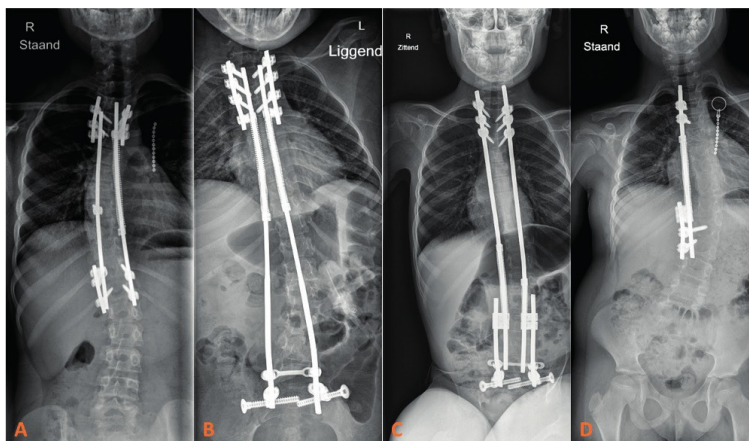
(A) Hybrid construct with a unilateral SDS and a contralateral passive sliding rod fixed to the apex, typically used for idiopathic EOS. **(B)** Bilateral construct with two similar springs (bilateral 75N springs) and **(C)** Bilateral construct with two different spring forces (concavity: 100N, convexity: 50N). **(D)** Unilateral construct typically only used for congenital deformities.

The spine is typically approached through two separate skin incisions – cranial and caudal –through which pedicle screws are bilaterally inserted in two or three levels using a freehand technique. For cases involving the pelvis (mostly in neuromuscular EOS), ilio-sacral screws (Tanit, Euros, Le Ciotat, France) are often used. In the case of a hybrid construct (Figure 2a), an additional small incision is made for the insertion of (the) apical screw(s). The rod is carefully contoured in both the coronal and sagittal plane. Then, the side-to-side connectors with an oversized hole for sliding are temporarily fixed to the sliding rod, leaving a residual rod length of 4–6 cm to accommodate lengthening. The spring is pre-tensioned against the side-to-side connectors with a buttress, using standard distraction instruments. The sliding rod is then inserted sub-fascially and mounted to the anchors. Prophylactic intra-wound vancomycin powder is used routinely in all EOS patients.[227] An explanation of a typical surgery in an idiopathic EOS patient can be seen in the video linked to in the introduction of this thesis. Postoperatively, patients are not restricted in mobilization and do not need to wear a brace.

Outcome parameters

Baseline demographics and surgical characteristics (skin-to-skin surgery time, estimated blood loss and days until discharge) were prospectively recorded. Radiographic measurements included coronal Cobb angles, T5-T12 kyphosis, L1-S1 lordosis and the T1-T12 and T1-S1 heights. Measurements were assessed by three authors (CST, IB and JVCL). Heights were determined by drawing a perpendicular line between two horizontal lines through the midpoints of the vertebral endplates. Coronal and sagittal heights were averaged. All radiographs were calibrated using rod diameters (4.5 mm or 5.5 mm). All radiographic measurements were performed using Surgimap v.2.3.2.1 (Nemaris Inc, New York, NY, USA).

(Serious) adverse events (SAEs) and unplanned returns to the operating room (UPRORs)

SAEs and UPRORs were recorded prospectively and retrospectively reviewed by two observers (CST, IB). Consensus on the type of event was reached through panel discussion using a flow chart (Figure 3). Adverse events were defined as serious when they (could have) resulted in permanent or significant disability/damage, or required (lengthening of) hospitalization, such as an UPROR. We distinguished events that were disease-related (e.g., respiratory insufficiency in neuromuscular patients), surgery-related (e.g., deep surgical site infection) or implant-related (e.g., rod fracture). Implant re-tensioning due to excessive spinal growth was not considered as an adverse event, as growth is desirable, but was recorded as an UPROR. Adverse events (undesirable effects but without clinical implications) like a screw failure visible on radiograph were recorded only when implant-related. Any additional

11

surgery related to SDS treatment until final fusion or end of growth was considered an UPROR. During one UPROR multiple SAEs could be addressed. Final fusion after the arbitrary age of 12 years was not considered an UPROR. The rate of SAEs and UPRORs was determined per patient per year.

Figure 3. SAE and UPROR flowchart
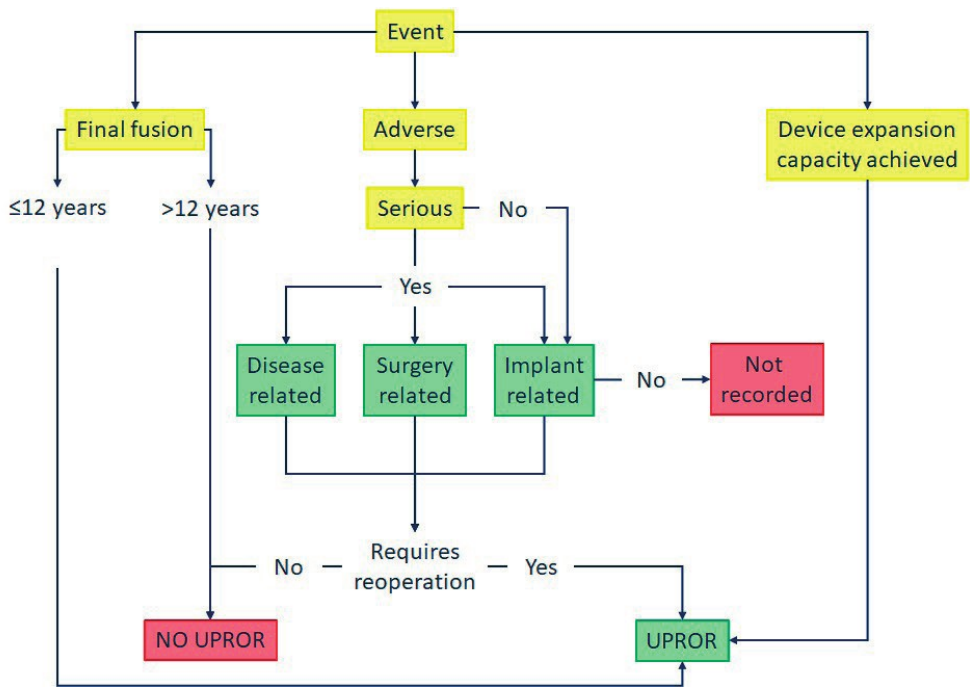
Statistical analysis

Normally distributed data are presented as mean and standard deviation (SD). A one-way ANOVA was used to compare baseline characteristics and SAEs and UPRORs across etiologies. Post-hoc testing with correction for multiple testing was performed using the Holm-Bonferroni procedure. Changes over time were compared in two steps. First, the difference between preoperative and directly postoperative (as soon as patients were fit for the radiograph) measurements was compared using a mixed repeated-measures ANOVA. The interaction between follow-up and etiology was added to identify differences over time between etiologies. Second, changes from postoperative measurements until latest follow-up (before EOS graduation) were analyzed using linear mixed models (LMMs). This method allows for integration of data from different patients, even when patients had missing data points or had much longer or shorter follow-up than others. To determine specific effects, a restricted maximum likelihood estimator model was created for each outcome with gender,

preoperative value, follow-up time, and etiology as fixed effects. Patient ID was added as a random effect. In addition, the interaction between follow-up time and etiology was added as a fixed effect to identify whether changes over time differed between etiologies. For each model, we evaluated whether the model had increased predictive performance when using a non-linear association compared to a linear association, using the Akaike Information Criterion. If no differences were found, a standard linear relationship model was used.

Event-free survival of UPRORs was visualized using a Kaplan-Meier curve. Statistical analysis was performed in SPSS version 29.0.1.0 (IBM SPSS Statistics, Armonk, NY, USA). The LMMs were conducted in R Statistical software version 4.0.2 (R Foundation for Statistical Computing, Vienna, Austria). Data visualization was performed using GraphPad Prism version 10.1.2 (GraphPad Software, LLC, Boston, MA, USA). Statistical significance was defined as $p<0.05$.

Results

Patient demographics

A total of 68 patients were reviewed: 14 congenital/structural (hereafter referred to as "congenital"), 41 neuromuscular, 4 syndromic, and 9 idiopathic. Due to the small number of syndromic patients, this group was excluded from further analysis. An overview of all etiologies and underlying pathologies is shown in Supplement 1. A total of 25 patients graduated from SDS treatment after a mean follow-up of 3.2 years, with 23 patients undergoing a final fusion, and two patients where the SDS was left in situ. Baseline characteristics as well as the SDS strategy are summarized in Table 1. The mean age at surgery was 8.4±1.7 years, with idiopathic patients being older at surgery compared to congenital patients (p=0.017). The mean follow-up length was 3.7±1.4 years, with congenital patients having longer follow-up than neuromuscular or idiopathic patients. The mean preoperative major curve for all patients combined was 73±18°, with no significant differences between groups. Similarly, the mean preoperative T5-T12 kyphosis was 25° and mean L1-S1 lordosis was 49°, both comparable across etiologies. Surgical duration (i.e, skin-to-skin time), estimated blood loss and time to discharge were also similar across all etiologies. As expected, neuromuscular patients had significantly longer constructs (16 levels) compared to congenital (13 levels) or idiopathic (12 levels) patients. There were four unilateral constructs (all congenital patients), 25 hybrid constructs (in 9 congenital, 7 neuromuscular, and 9 idiopathic patients), and 35 bilateral constructs (in one congenital and 34 neuromuscular patients). Thirty-three patients were instrumented to the pelvis, all were neuromuscular. A more detailed overview of instrumentation strategies is shown in Table 1 and Supplement 1.

11

Table 1. Baseline characteristics

	All (N=64)	Congenital (N=14)	Neuromuscular (N=41)	Idiopathic (N=9)	P value
Age at surgery (years)	8.4±1.7	7.6±2.0	8.4±1.5	9.7±1.7[1]	0.017
Girls (%)	29 (45%)	8 (57%)[2]	14 (34%)	7 (78%)[2]	0.035
Preoperative primary curve (°)	73±18	75±26	73±13	67±16	0.566
Preoperative secondary curve (°)	37±16	45±15	33±16	42±8	0.156
Preoperative T5-T12 kyphosis (°)	25±20	28±29	24±23	29±14	0.761
Preoperative L1-S1 lordosis (°)	49±19	55±15	46±21	53±12	0.257
Preoperative T1-T12 height (mm)	168±29	142±23	173±23[1]	191±21[1]	<0.001
Preoperative T1-S1 height (mm)	284±41	264±33	282±40	325±31[1,2]	0.001
Surgical duration (min)	189±45	187±58	190±44	182±30	0.880
Estimated blood loss (mL)	385±191	409±203*	382±181	367±238	0.880
Instrumented levels	15±3	13±4	16±2[1,3]	12±2	<0.001
Instrumented to pelvis	33 (52%)	0	33 (80%)[1,3]	0	<0.001
Free endplates within construct	10±3	7±3	12±2[1,3]	7±2	<0.001
Time to discharge (days)	7±6	7±4	7±7	5±1	0.654
Follow-up length (years)	3.7±1.4	4.5±1.6[2,3]	3.5±1.4	3.3±0.7	0.012

	All (N=64)	Congenital (N=14)	Neuromuscular (N=41)	Idiopathic (N=9)	P value
Implant configuration	8.4±1.7	7.6±2.0	8.4±1.5	9.7±1.7[1]	<0.001
Unilateral construct	4	4	0	0	
Concave 75 N	3	3	0	0	
Concave 100 N	1	1	0	0	
Bilateral construct	35	1	34	0	
Concave 75 N, Convex 75 N	16	1	15[a]	0	
Concave 100 N, Convex 50 N	19	0	19	0	
Hybrid construct	25	9	7	9	
Concave 75 N, Convex 0 N	17	7	4	6	
Concave 100 N, Convex 0 N	8	2	3	3	

Post-hoc testing with correction for multiple testing through the Holm-Bonferroni procedure.

*Estimated blood loss data was missing in three congenital patients

[a] In two neuromuscular patients the springs were partially compressed perioperatively (60 N remaining)

[1] Significantly greater compared to the congenital group

[2] Significantly greater compared to the neuromuscular group

[3] Significantly greater compared to the idiopathic group

11

Curve outcomes

Curve changes over time for each group are shown in Figure 4. The overall posto-perative main curve correction was 47% (Table 2). For congenital patients, this correction was 33%, while neuromuscular and idiopathic patients achieved an average correction of 51%. The LMM investigating the interaction between etiology and follow-up (Figure 5, Table 3) showed that idiopathic EOS patients had more increase in Cobb angle after the correction during follow-up of 3.6%/year, whereas congenital (0.4%/year) and neuromuscular patients (0.9%/year) showed a significantly lower increase.

Immediately following surgery, T5-T12 kyphosis was reduced in neuromuscular patients (-8°, -33%), increased somewhat in congenital patients (+5°, + 18%), while kyphosis remained stable in idiopathic patients (+1°, +3%). L1-S1 lordosis was mildly reduced postoperatively in all groups, with no differences between groups. In the LMMs of T5-T12 kyphosis (Supplement 2), the relationships over time were best described by polynomial equations (i.e., non-linearly). During follow-up, T5-T12 kyphosis remained stable in congenital and neuromuscular patients. In idiopathic patients, kyphosis increased during the first years, especially when compared to neuromuscular patients (p=0.030). After that time, kyphosis normalized again. For L1-S1 lordosis (Supplement 3), all patients showed a tendency towards increasing lordosis over time, with no differences between groups.

Table 2. Curve characteristics and spinal height per etiology over time

	Etiology	Pre-operative	Post-operative	Change (%)	P value between groups
Primary curve (°)	Congenital	75±27	50±19	-25 (-33%)	0.023
	Neuromuscular[1]	73±15	36±13	-37 (-51%)	
	Idiopathic[1]	67±15	33±14	-34 (-51%)	
Secondary curve (°)	Congenital	41±19	28±16	-13 (-32%)	0.896
	Neuromuscular	33±17	21±10	-12 (-36%)	
	Idiopathic	42±8	28±13	-14 (-33%)	
T5-T12 kyphosis (°)	Congenital[2]	28±30	33±18	+5 (+18%)	0.042
	Neuromuscular	24±23	16±14	-8 (-33%)	
	Idiopathic	29±14	30±9	+1 (+3%)	
L1-S1 lordosis (°)	Congenital	55±15	51±14	-4 (-7%)	0.938
	Neuromuscular	46±21	40±13	-6 (-13%)	
	Idiopathic	53±12	46±13	-7 (-13%)	
T1-T12 height (mm)	Congenital	142±23	153±19	+11 (+8%)	0.055
	Neuromuscular	173±24	196±20	+23 (+13%)	
	Idiopathic	191±21	211±20	+20 (+10%)	
T1-S1 height (mm)	Congenital	264±33	282±29	+18 (+7%)	<0.001
	Neuromuscular[1,3]	280±36	327±32	+45 (+16%)	
	Idiopathic[1]	325±31	354±30	+29 (+9%)	

Post-hoc testing with correction for multiple testing through the Holm-Bonferroni procedure.

[1]Change is significantly greater compared to the congenital group

[2]Change is significantly greater compared to the neuromuscular group

[3]Change is significantly greater compared to the idiopathic group

11

Table 3. Linear mixed model results of main coronal Cobb angle over time

Predictors	Estimates	95% CI	P value
Female	1.9	-5.5 to 9.3	0.607
Preoperative Cobb angle (°)	0.4	0.2 to 0.6	<0.001
Postoperative Cobb angle (°)[1]	5.5	-11.1 to 22.0	0.516
Postoperative Cobb angle across etiology (°)[1]			
Idiopathic	Reference	Reference	Reference
Congenital	11.6	-1.0 to 24.2	0.070
Neuromuscular	0.7	-10.6 to 11.9	0.908
Cobb angle change per year (°)[1]	3.6	1.9 to 5.2	<0.001
Cobb angle change per year across etiology (°)[1]			
Idiopathic	Reference	Reference	Reference
Congenital	-3.2	-5.1 to -1.4	<0.001
Neuromuscular	-2.7	-4.5 to -0.9	0.003

The graph shows the mean line per etiology (based on a male with the median preoperative Cobb angle) and the individual patient lines. For clarity, the individual lines are shown as straight lines between only the first and last postoperative follow-up. For the statistical analysis, all follow-up points in between were also considered. Using the above predictors (gender, preoperative Cobb angle and etiology), the follow-up Cobb angle can be predicted for patients undergoing SDS treatment. The marginal R^2 value of the above model was 0.67, outlining that the above predictors could predict 67% of the variation between data points.

[1]The initial change is added for all groups, but for the congenital and neuromuscular group, additional changes are later added. Since the idiopathic group is the reference group, and no changes are added for the idiopathic group, the initial changes are identical to changes in the idiopathic group.

Example: What is the expected main coronal Cobb angle after 3 years for a female congenital EOS patient with a preoperative main coronal Cobb angle of 70°?

- Female: Add 1.9° if female.
- Preoperative Cobb angle: Start with 0.4° for every preoperative 1.0°.
- Postoperative Cobb angle: Add 5.5°.
- Postoperative Cobb angle across etiology: Add 11.6° if congenital.
- Cobb angle change per year: Add 3.6° for every year.
- Cobb angle change per year across etiology: Subtract 3.2° for every year if congenital.

The total expected main coronal Cobb angle becomes: 1.9 + 28 + 5.5 + 11.6 + 10.8 – 9.6 = 48.2°

Figure 4. Coronal curves, sagittal curves, T1-T12 and T1-S1 height over time
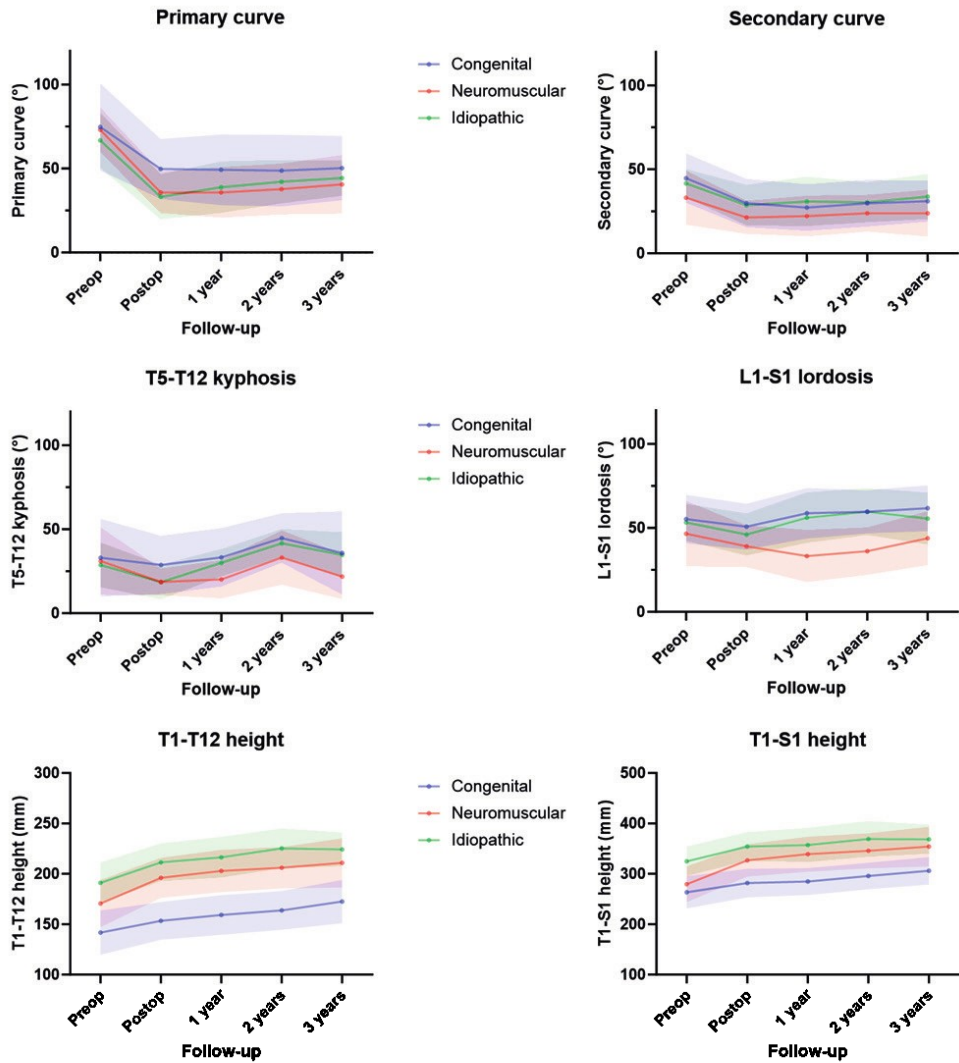
Measurements (mean ± SD) at group level up to three years of follow-up.

Figure 5. Linear mixed model results of main coronal Cobb angle over time
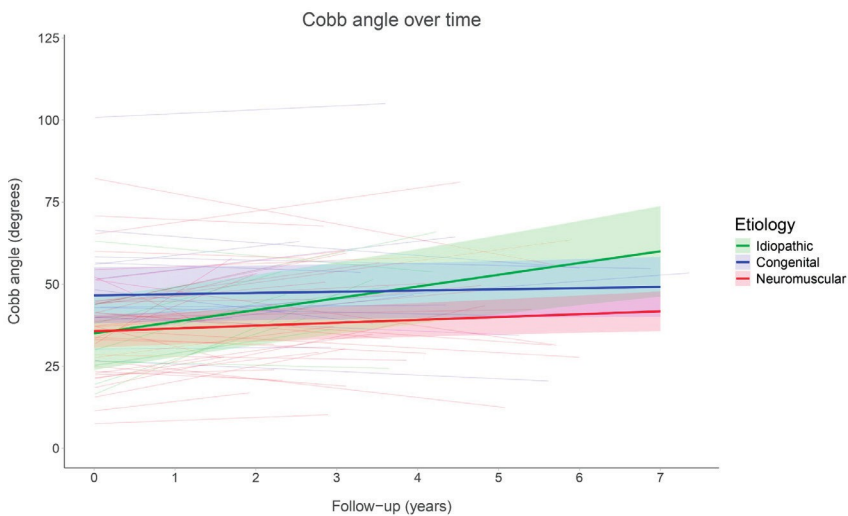
Spinal growth

Spinal growth data are presented in Table 2, Table 4, and Figure 6. Immediately following SDS implantation, increases in T1-T12 height were observed (due to curve reduction and soft-tissue lengthening), which were largest in neuromuscular patients (+23 mm, 13%), followed by idiopathic patients (+20 mm, 10%) and congenital patients (+11 mm, 8%). For T1-S1 height, the immediate change in the neuromuscular group (+45 mm, 16%) was significantly greater than the increase in both the idiopathic group (+29 mm, 9%) and the congenital group (+18 mm, 7%).

During follow-up, both T1-T12 height and T1-S1 height were excellently predicted using LMMs, after correcting for gender, etiology and preoperative height with R^2 values of 0.93 for both lengths. T1-T12 height increased at an average rate of 5.6 mm/year, with no significant differences between etiologies. In the LMM, T1-S1 growth was 7.4 mm/year in the idiopathic patients. In congenital and neuromuscular patients, growth was slightly larger although the differences were not statistically significant (8.9 mm/year and 9.8 mm/year, respectively). As the trends over time were best described by linear rather than exponential relationships, no evidence of time-dependent diminishing growth was found across the entire follow-up period in any of the groups.

Table 4a. Linear mixed model results of T1-T12 height over time

Predictors	Estimates	95% CI	P value
Female	0.7	-6.3 to 7.7	0.839
Preoperative T1-T12 height (mm)	0.7	0.6 to 0.8	<0.001
Postoperative T1-T12 height (mm)[1]	79.4	51.3 to 107.4	<0.001
Postoperative T1-T12 height across etiology (mm)[1]			
Idiopathic	Reference	Reference	Reference
Congenital	-22.3	-36.1 to -8.6	0.002
Neuromuscular	-1.6	-12.5 to 9.4	0.779
T1-T12 height change per year (mm)[1]	5.6	3.8 to 7.5	<0.001
T1-T12 height change per year across etiology (mm)[1]			
Idiopathic	Reference	Reference	Reference
Congenital	-0.4	-2.5 to 1.6	0.689
Neuromuscular	0.0	-1.9 to 2.0	0.969

The graph shows the mean line per etiology (based on a male with the median preoperative T1-T12 height) and the individual patient lines. For clarity, the individual lines are shown as straight lines between only the first and last postoperative follow-up. For the statistical analysis, all follow-up points in between were also considered. Using the above predictors (gender, preoperative T1-T12 height and etiology), the follow-up T1-T12 height can be predicted for patients undergoing SDS treatment. The marginal R2 value of the above model was 0.93, outlining that the above predictors could predict 93% of the variation between data points.

[1]The initial change is added for all groups, but for the congenital and neuromuscular group, additional changes are later added. Since the idiopathic group is the reference group, and no changes are added for the idiopathic group, the initial changes are identical to changes in the idiopathic group.

Example: What is the expected T1-T12 height after 5 years for a male neuromuscular EOS patient with a preoperative T1-T12 height of 180mm?

- Male: Add nothing if male.
- Preoperative T1-T12 height: Start with 0.7mm for every preoperative 1.0mm.
- Postoperative T1-T12 height: Add 79.4mm.
- Postoperative T1-T12 height across etiology: Subtract 1.6mm if neuromuscular.
- T1-T12 height change per year: Add 5.6mm for every year.
- T1-T12 height change per year across etiology: Add 0mm for every year if neuromuscular.

The total expected T1-T12 height becomes: 126 + 79.4 - 1.6 + 28 + 0 = 231.8mm

Table 4b. Linear mixed model results of T1-S1 height over time

Predictors	Estimates	95% CI	P value
Female	1.4	-9.0 to 11.9	0.785
Preoperative T1-S1 height (mm)	0.7	0.6 to 0.9	<0.001
Postoperative T1-S1 height (mm)[1]	115.5	69.4 to 161.5	<0.001
Postoperative T1-S1 height across etiology (mm)[1]			
Idiopathic	Reference	Reference	Reference
Congenital	-28.3	-48.0 to -8.7	0.005
Neuromuscular	7.6	-9.4 to 24.5	0.376
T1-S1 height change per year (mm)[1]	7.4	4.8 to 10.0	<0.001
T1-S1 height change per year across etiology (mm)[1]			
Idiopathic	Reference	Reference	Reference
Congenital	1.5	-1.4 to 4.4	0.321
Neuromuscular	2.4	-0.4 to 5.2	0.093

The graph shows the mean line per etiology (based on a male with the median preoperative T1-S1 height) and the individual patient lines. For clarity, the individual lines are shown as straight lines between only the first and last postoperative follow-up. For the statistical analysis, all follow-up points in between were also considered. Using the above predictors (gender, preoperative T1-S1 height and etiology), the follow-up T1-S1 height can be predicted for patients undergoing SDS treatment. The marginal R2 value of the above model was 0.93, outlining that the above predictors could predict 93% of the variation between data points.

[1]The initial change is added for all groups, but for the congenital and neuromuscular group, additional changes are later added. Since the idiopathic group is the reference group, and no changes are added for the idiopathic group, the initial changes are identical to changes in the idiopathic group.

Figure 6a. Linear mixed model results of T1-T12 height over time
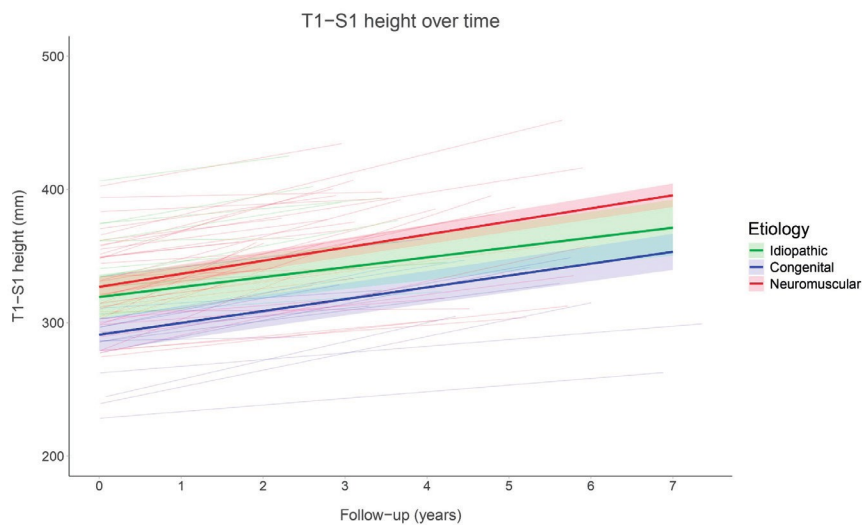
Figure 6b. Linear mixed model results of T1-S1 height over time

11
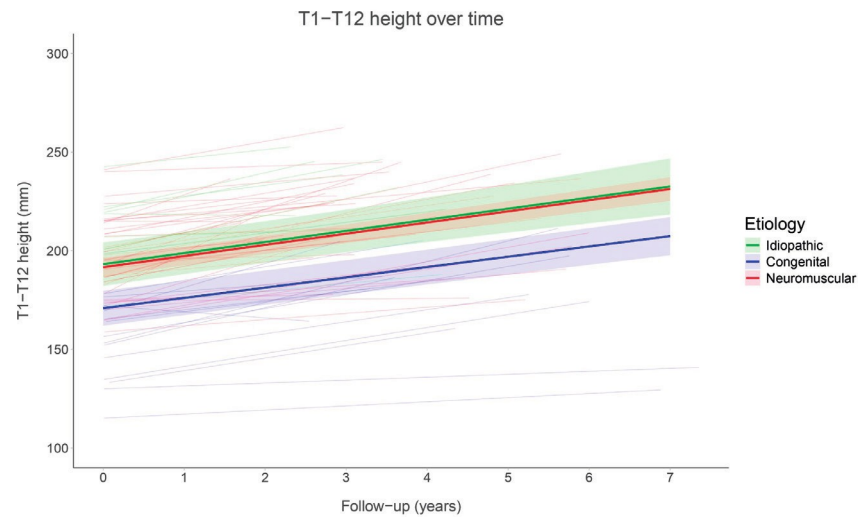
Severe adverse events (SAEs) and unplanned returns to the operating room (UPRORs)

A comprehensive overview of all (S)AEs and UPRORs is provided in Supplement 4. A total of 52 SAEs occurred after a mean follow-up of 3.7 years corresponding to 0.22 SAEs/patient/year. The congenital group experienced 13 SAEs (0.21/patient/year), the neuromuscular group 32 (0.22/patient/year), and the idiopathic group 7 (0.24/patient/year). Within the first two years of follow-up, a first SAE occurred in 10% of congenital patients, 51% of neuromuscular patients and 25% of idiopathic patients. In addition to the SAEs, 10 implant-related AEs occurred during follow-up. The most frequent SAEs were implant-related (33 SAEs), primarily caused by rod fractures of the initially used 4.5 mm rods and excessive kyphosis of the system (Figure 7). Surgery-related SAEs (21%) were heterogenous, with the most common being deep surgical site infections (N=4). Disease-related SAEs (15%) included three patients with pulmonary insufficiency requiring hospitalization and antibiotic treatment. Additionally, a third patient was admitted to the intensive care unit one month postoperatively due to a resuscitation scenario caused by a breath-holding spell. Two neuromuscular patients died of respiratory failure due to pulmonary infections unrelated to the implant.

A total of 44 UPRORs were recorded, corresponding to 0.19 UPRORS/patient/year (Table 5). Congenital and idiopathic patients had the lowest rates of UPRORs, with 0.18 and 0.09 UPRORs/patient/year, respectively. Neuromuscular patients experienced the highest rate of 0.22 UPRORs/patient/year. The most common UPROR was spring re-tensioning surgery (n=11), which was performed in 3 congenital and 8 neuromuscular patients after an average interval of 1.9 years post-index surgery. In nine cases, spring re-tensioning was combined with surgeries to address other complications (e.g., connector slip). Kaplan-Meier analysis revealed UPROR-free survival rates after four years of 50% for congenital patients, 34% for neuromuscular patients, and 61% for idiopathic patients (Figure 8).

Table 5. Overview of (S)AEs and UPRORs per etiology

	Congenital	Neuromuscular	Idiopathic	Total
SAE total	**13**	**32**	**7**	**52**
Disease related	0	8	0	8
Surgery related	6	5	0	11
Implant related	7	19	7	33
SAE/patient/year	0.20	0.22	0.24	0.22
AE total	**1**	**6**	**3**	**10**
AE/patient/year	0.02	0.05	0.10	0.04
UPROR total	**12**	**29**	**3**	**44**
UPROR/patient/year	0.18	0.22	0.09	0.19

Figure 7. Excessive kyphosis of SDS
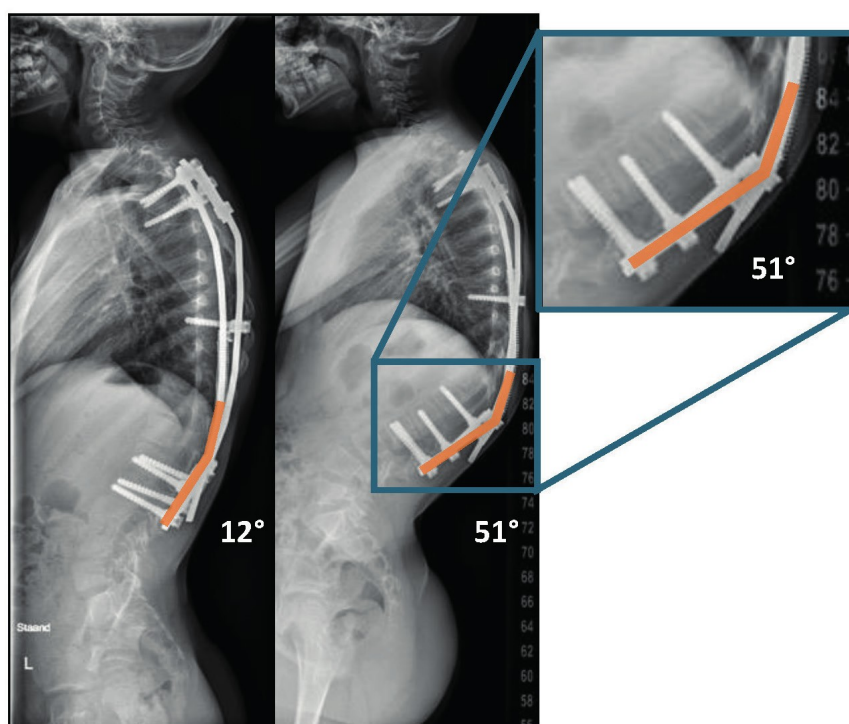
Typical complication of kyphosis with material prominence in patients with the old SDS configuration using only one side-to-side connector.

11

Figure 8. Kaplan-Meier analysis of UPROR-free survival
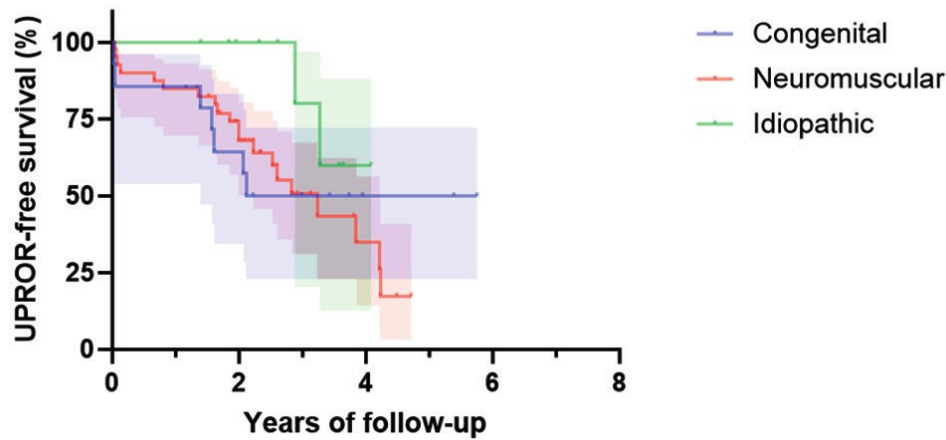
Survival time to the occurrence of an UPROR for all. Ticks denote censored patients.

Discussion

This study broadens the understanding of the efficacy of SDS treatment across various EOS etiologies. Although different strategies were used, we consider the SDS (irrespective of the configuration) as a concept and made an attempt to compare performance of this concept for the different etiologies. In general, the results align with previous reports demonstrating the efficacy of the technique and relatively low complication rates.[38,45] Notably, neuromuscular patients, a vulnerable subgroup, appeared to benefit most from SDS treatment. The ability to control the curve in idiopathic EOS patients on the other hand is not yet optimal. It could be hypothesized that the underlying mechanism, along with increased activity levels and muscle tone in idiopathic patients, are more powerful and less susceptible to the corrective distraction forces that were used. These forces were perhaps too low for these patients, due to the older age at surgery and the hybrid configuration with only one 75 N spring, instead of a bilateral SDS that typically involves a total of 150 N of distraction force. Based on our systematic review and meta-analysis, the use of stronger springs in older (idiopathic) patients is feasible and safe, which is why we changed the treatment strategy and currently use 100 N or even 150 N springs.[125]

   A recent study by Grabala et al. presented the long-term outcomes of an international cohort of patients treated with the MCGR, performing similar subgroup analyses for different etiologies. They reported an improvement in the main coronal curves across all subgroups of approximately 47%, however, this included the results

after final fusion. Their analysis of spinal height increase also included the patients who had undergone final fusion, which affects results and complicates comparisons between techniques or etiologies.[228] Fortunately, the authors provided relevant data suitable for comparison with this current study.[229] They observed true (i.e., after insertion and before final fusion) T1-T12 growth of 6.2 mm/year in idiopathic patients, 5.5 mm/year in congenital patients, and 5.2 mm/year in neuromuscular patients, which is comparable to our observations. Literature on T1-T12 and T1-S1 growth rates in patients treated with TGR or MCGR varies widely, ranging from 2–23 mm/year.[31] Due to the heterogeneity of datapoints in this study, spinal growth was best described using LMMs. Interestingly, this method revealed that T1-T12 and T1-S1 growth did not diminish over time, suggesting that the SDS does not suffer from the "law of diminishing returns".[35]

In this study, the most frequent (S)AEs were implant-related (63%), mainly due to rod fractures (45%), highlighting room for improvement. Indeed, transitioning to 5.5 mm rods reduced these events drastically, with only one rod fracture observed in 19 patients with an average follow-up of 2.5 years. Spring re-tensioning was the most common reason for UPRORs (25%). This was a reason to change to longer springs when possible which, due to the lower spring constant, maintain distraction force for a longer period. Future studies will have to confirm this effect. Re-tensioning was not classified as an SAE in this study, as it is a consequence of extensive growth, which is considered as a favorable effect of the SDS. This extra length gain – of up to 1.6 cm – above physiological growth results partly from viscoelastic changes (i.e., tissue creep) between insertion and the first erect radiograph, and was not included in measured height gain.

The overall UPROR rate was 0.19/patient/year, lowest in idiopathic patients (0.09/patient/year), and highest in neuromuscular patients (0.22/patient/year). A recent study by McIntosh et al. reported a similar UPROR rate of 0.20/patient/year in patients treated with the MCGR.[230] As expected and seen in previous literature, the neuromuscular patients had a high UPROR rate, which occurred after a mean of 1.8 years. This is partially the result of a more vulnerable patient population with a higher risk of infection and a higher susceptibility to implant kyphosis and subsequent implant prominence as they generally have less soft tissue coverage. This tendency for kyphosis has been addressed by using two stacked parallel connectors instead of one and was shown to be effective in a previous study.[179] It should be mentioned that the definition of UPROR (and SAE) influences these numbers; definitive spinal fusion at age ≥12 years for example was arbitrarily not considered an UPROR, if we set this threshold at 13 years there would be four additional final fusions included, increasing the UPROR rate to 0.21/patient/year.

Although this current study was not designed for comparison to other "growth-friendly" systems, regarding curve correction, spinal growth, SAE and UPROR rates,

the performance of the SDS seems comparable and satisfactory. An appealing opportunity with the SDS is that this technique is just the beginning of dynamic growth guidance, offering tremendous room for improvement. For example, many strategic configurations may be used, and identifying optimal spring forces may improve outcomes. Furthermore, the SDS design supports personalized treatment strategies, allowing adjustments in spring length and force, tailored to specific EOS etiologies and curve types.

Limitations of this study include the small number of patients per etiology and the strategic differences in SDS configurations per etiology, which makes it impossible to address only one variable. Also the changes of rod size, spring length and spring forces during the study precludes identification of one optimal strategy. Nevertheless, we regard the SDS as an evolving concept that is constantly improved while used for different etiologies of EOS. Unfortunately, syndromic scoliosis was hardly represented, which is due to the safety policy of excluding patients with compromised tissue integrity and bone strength. Moreover, the case mix in this study may not fully represent the broader population of EOS patients, as our academic hospital is a specialized center for specific neuromuscular patients, like spinal muscular atrophy. Finally, although this is a multicenter study, the results mostly come from the academic hospital where the technique was invented.

Conclusion

The current study shows that the SDS performs relatively well in terms of curve correction, spinal growth and adverse events for different EOS etiologies. Initial curve correction is highest in neuromuscular and idiopathic patients, and lowest in congenital patients. During follow-up, the SDS appeared less capable to maintain correction for idiopathic patients as compared to the other etiologies. Spinal growth over time was similar between etiologies. The SAE rate was comparable between etiologies, neuromuscular patients had the highest UPROR rate.

Supplement 1. Underlying pathology and implant configuration

Patient	Etiology	Underlying pathology	SDS configuration	Spring force	
				Concave	Convex
P1	C	Unilateral hemivertebra	Unilateral	75 N	
P2	C	Spondylocarpotarsal synostosis syndrome	Bilateral	75 N	75 N
P3	C	Klippel-Feil syndrome	Hybrid	75 N	
P4	I		Hybrid	75 N	
P5	NM	Spina bifida	Hybrid	75 N	
P6	C	Thoracolumbar hemivertebrae	Unilateral	75 N	
P7	NM	Spina bifida	Bilateral	75 N	75 N
P8	I		Hybrid	75 N	
P9	NM	Ullrich congenital muscular dystrophy	Hybrid	75 N	
P10	NM	Spina bifida	Bilateral	75 N	75 N
P11	NM	Congenital myopathy	Bilateral	75 N	75 N
P12	NM	SMA type ll	Bilateral	60 N	60 N
P13	NM	Congenital myopathy	Bilateral	75 N	75 N
P14	C	Klippel-Feil syndrome	Hybrid	75 N	
P15	C	Hemivertebrae, block vertebrae	Hybrid	75 N	
P16	NM	Myasthenia Gravis	Bilateral	75 N	60 N
P17	NM	SMA type ll	Bilateral	75 N	75 N
P18	I		Hybrid	75 N	
P19	NM	Brain-lung-thyroid syndrome	Hybrid	75 N	
P20	NM	Bohring-Opitz syndrome	Bilateral	75 N	75 N
P21	C	Hemivertebrae	Unilateral	75 N	
P22	NM	SMA type ll	Bilateral	75 N	75 N
P23	NM	Cerebral palsy	Bilateral	75 N	75 N
P24	NM	SMA type ll	Bilateral	75 N	75 N
P25	NM	SMA type ll	Bilateral	75 N	75 N
P26	NM	Spina bifida	Bilateral	75 N	75 N
P27	NM	Chondrodysplasia punctata	Hybrid	75 N	
P28	I		Hybrid	75 N	
P29	C	VACTERL	Hybrid	75 N	
P30	I		Hybrid	75 N	
P31	C	Hemivertebrae	Hybrid	75 N	
P32	NM	SMA type ll	Bilateral	75 N	75 N

11

P33	NM	Emery-Dreifuss muscular dystrophy	Bilateral	75 N	75 N
P34	NM	SMA type ll	Bilateral	100 N	50 N
P35	I		Hybrid	100 N	
P36	I		Hybrid	75 N	
P37	NM	15q syndrome	Hybrid	100 N	
P38	I		Hybrid	100 N	
P39	NM	SMA type ll	Bilateral	100 N	50 N
P40	NM	SMA type ll	Bilateral	100 N	50 N
P41	C	VACTERL	Hybrid	75 N	
P42	I		Hybrid	100 N	
P43	NM	Spinal cord glioma	Bilateral	100 N	50 N
P44	C	Arthrogryposis multiplex congenita	Hybrid	100 N	
P45	C	Chromosomal anomaly	Hybrid	75 N	
P46	NM	Williams syndrome	Hybrid	100 N	
P47	C	Spondylocostal dysostosis	Unilateral	100 N	
P48	NM	SMA type ll	Bilateral	100 N	50 N
P49	C	Arthrogryposis multiplex congenita	Hybrid	100 N	
P50	NM	Spina bifida	Hybrid	100 N	
P51	NM	Spina bifida	Bilateral	100 N	50 N
P52	NM	SMA type ll	Bilateral	100 N	50 N
P53	NM	SMA type lc	Bilateral	100 N	50 N
P54	NM	22q11 deletion syndrome	Bilateral	100 N	50 N
P55	NM	Chomosomal translocation	Bilateral	100 N	50 N
P56	NM	SMA type ll	Bilateral	100 N	50 N
P57	NM	SMA type ll	Bilateral	100 N	50 N
P58	NM	SMA type ll	Bilateral	100 N	50 N
P59	NM	SMA type lc	Bilateral	100 N	50 N
P60	NM	West syndrome	Bilateral	100 N	50 N
P61	NM	SMA type ll	Bilateral	100 N	50 N
P62	NM	Cerebral palsy	Bilateral	100 N	50 N
P63	NM	Congenital myopathy	Bilateral	100 N	50 N
P64	NM	SMA type ll	Bilateral	100 N	50 N

C: congenital; NM: neuromuscular; I: idiopathic; SMA: spinal muscular atrophy; VACTERL vertebral defects, anal atresia, cardiac defects, trachea-esophageal fistula, renal anomalies, limb abnormalities

Supplement 2. Linear mixed model results of T5-T12 kyphosis over time

Predictors	Estimates	95% CI	P value
Female	-2.4	-6.3 to 1.4	0.213
Preoperative T5-T12 kyphosis (°)	1.0	0.8 to 1.1	<0.001
Postoperative T5-T12 kyphosis (°)[1]	3.5	-3.9 to 10.9	0.355
Postoperative T5-T12 kyphosis across etiology (°)[1]			
Idiopathic	Reference	Reference	Reference
Congenital	0.3	-7.7 to 8.4	0.932
Neuromuscular	-2.5	-9.6 to 4.6	0.487
T5-T12 kyphosis change during slope 1 (°)[1,2]	22.2	7.1 to 37.4	0.004
T5-T12 kyphosis change during slope 2 (°)[1,2]	-12.4	-51.1 to 26.3	0.529
T5-T12 kyphosis change during slope 1 across etiology (°)[1,2]			
Idiopathic	Reference	Reference	Reference
Congenital	-8.9	-26.1 to 8.4	0.312
Neuromuscular	-17.9	-34.0 to -1.8	0.030
T5-T12 kyphosis change during slope 2 across etiology (°)[1,2]			
Idiopathic	Reference	Reference	Reference
Congenital	11.1	-28.5 to 50.7	0.581
Neuromuscular	11.9	-27.8 to 51.6	0.556

The graph shows the mean line per etiology (based on a male with the median preoperative T5-T12 kyphosis) and the individual patient lines. For clarity, the individual lines are shown as straight lines between only the first and last postoperative follow-up. For the statistical analysis, all follow-up points in between were also considered. Using the above predictors (gender, preoperative T5-T12 kyphosis and etiology), the follow-up T5-T12 kyphosis can be predicted for patients undergoing SDS treatment. The marginal R2 value of the above model was 0.81, outlining that the above predictors could predict 81% of the variation between data points.

[1]The initial change is added for all groups, but for the congenital and neuromuscular group, additional changes are later added. Since the idiopathic group is the reference group, and no changes are added for the idiopathic group, the initial changes are identical to changes in the idiopathic group.

[2]Since the changes over time were best described with a non-linear spline curve (with the inflection point after 3.5 years), differences in slopes are shown separately for the first (slope 1) and second (slope 2) part of the spline curve.

11

T5–T12 kyphosis over time
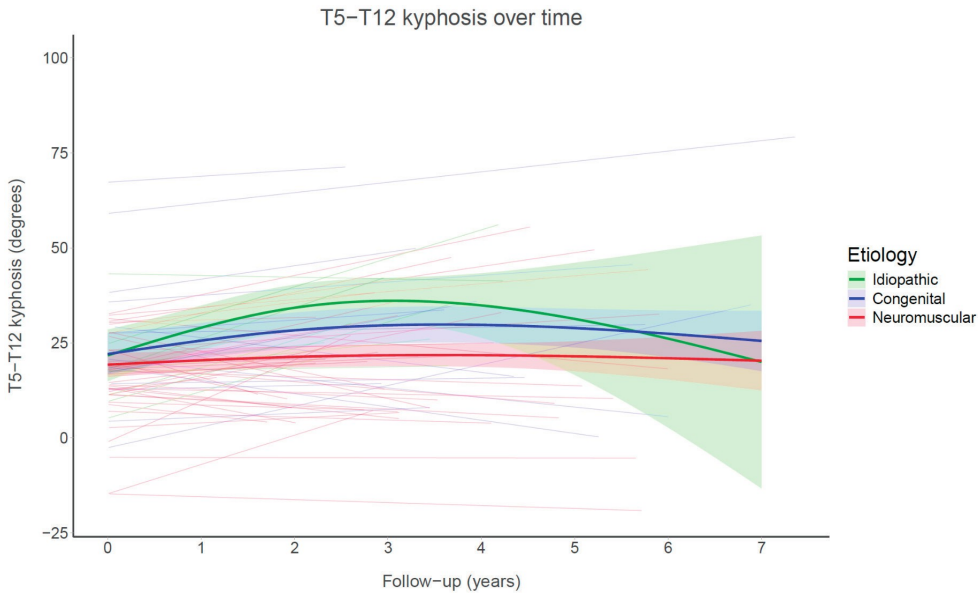
Supplement 3. Linear mixed model results of L1-S1 lordosis over time

Predictors	Estimates	95% CI	P value
Female	-4.1	-10.9 to 2.7	0.230
Preoperative L1-S1 lordosis (°)	0.6	0.3 to 0.8	<0.001
Postoperative L1-S1 lordosis (°)[1]	27.0	13.3 to 40.7	<0.001
Postoperative L1-S1 lordosis across etiology (°)[1]			
Idiopathic	Reference	Reference	Reference
Congenital	0.9	-11.1 to 12.9	0.882
Neuromuscular	-12.7	-23.4 to -2.0	0.021
L1-S1 lordosis change per year (°)[1]	2.5	-0.3 to 5.3	0.084
L1-S1 lordosis change per year across etiology (°)[1]			
Idiopathic	Reference	Reference	Reference
Congenital	0.0	-3.1 to 3.2	0.980
Neuromuscular	-1.0	-4.1 to 2.0	0.505

The graph shows the mean line per etiology (based on a male with the median preoperative L1-S1 lordosis) and the individual patient lines. For clarity, the individual lines are shown as straight lines between only the first and last postoperative follow-up. For the statistical analysis, all follow-up points in between were also considered. Using the above predictors (gender, preoperative L1-S1 lordosis and etiology), the follow-up L1-S1 lordosis can be predicted for patients undergoing SDS treatment. The marginal R2 value of the above model was 0.55, outlining that the above predictors could predict 55% of the variation between data points.

[1]The initial change is added for all groups, but for the congenital and neuromuscular group, additional changes are later added. Since the idiopathic group is the reference group, and no changes are added for the idiopathic group, the initial changes are identical to changes in the idiopathic group.

L1–S1 lordosis over time
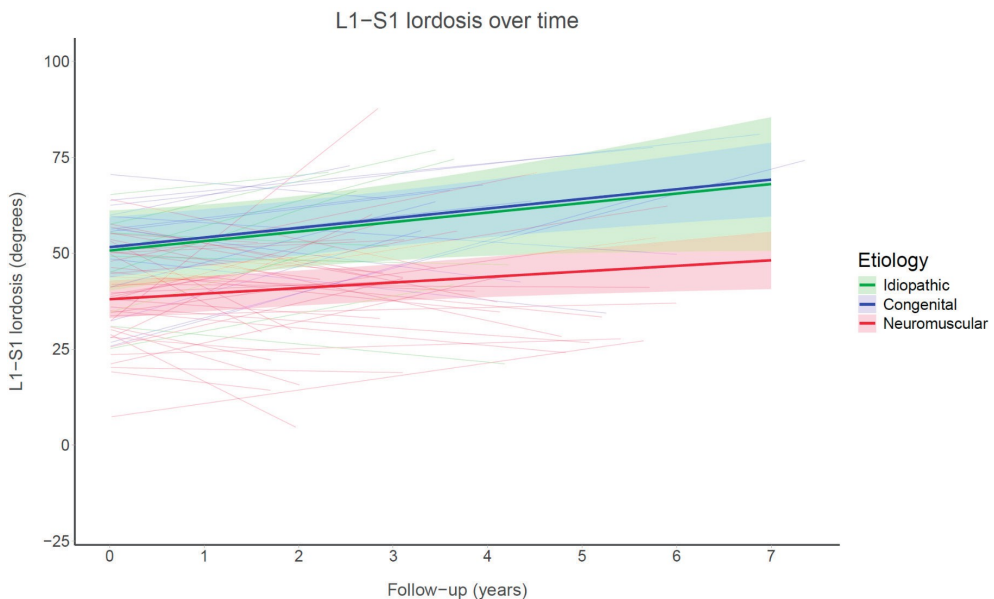
Supplement 4. Patient (S)AE and UPROR data

Patient	Etiology	Event	(S)AE			Treatment	UPROR
			Disease	Surgery	Implant		
P1	C	Rod fracture			X		
		End of spring				Re-tension surgery	X
P2	C	Dura tear		X			
		End of spring				Re-tension surgery	X
P3	C	Failure connector			X	Conversion to PSF ≥12 years	
P4	I						
P5	NM	Adding on		X		Conversion to PSF ≥12 years	
P6	C						
P7	NM	Excessive kyphosis			X	Revision surgery	X
		Failure anchor			X	Revision surgery	X
		End of spring				Conversion to PSF <12 years	X
P8	I	Excessive kyphosis			X	Conversion to PSF ≥12 years	
P9	NM	End of spring				Re-tension surgery	X
P10	NM	Pressure ulcer		X		I&D	X
		Rod protrusion			X	Revision surgery	X
		Failure anchor			X	Revision surgery	X
P11	NM	Rod fracture			X	Conversion to 5.5 mm rods	X
		Failure connector			X	Conversion to PSF <12 years	X
P12	NM	Pulmonary insufficiency	X				
		End of spring				Re-tension surgery	X
P13	NM	Excessive kyphosis			X	Re-tension surgery	X

Patient	Etiology	Complication				Treatment	
P14	C	End of spring				Re-tension surgery	X
		Excessive kyphosis	X			Conversion to 5.5 mm rods	X
P15	C						
P16	NM	Excessive kyphosis	X			Revision surgery	X
P17	NM	Pulmonary insufficiency			X		
		End of spring				Re-tension surgery	X
P18	I	Rod fracture	X				
		Rod fracture	X			Conversion to PSF ≥12 years	
P19	NM	Rod fracture	X				
		Rod protrusion	X			Revision surgery	X
		Failure connector	X			Conversion to PSF <12 years	X
P20	NM	Excessive kyphosis	X				
		Failure anchor	X				
		Buttress slip	X			Revision surgery	X
P21	C	dSSI		X		I&D and revision surgery	X
		Adding on		X		Conversion to PSF ≥12 years	
P22	NM	End of spring				Re-tension surgery	X
P23	NM	Death			X		
P24	NM	End of spring				Re-tension surgery	X
		Disconnection rod	X			Conversion to PSF ≥12 years	
P25	NM						

11

Patient	Type	Complication			Intervention	
P26	NM	dSSI	X		I&D	X
		Failure connector	X		Revision surgery	X
		Failure anchor	X			
		Rod fracture	X			
		Rod fracture	X		Conversion to PSF ≥12 years	X
P27	NM	dSSI	X		I&D	X
		Pulmonary insufficiency		X		
		Adding on	X		Conversion to 5.5 mm rods	X
P28	I	Rod fracture	X			
P29	C	Temporary NM loss	X		Staged procedure	X
		Rod fracture	X		Conversion to 5.5 mm rods	X
		Rod fracture	X		Conversion to PSF ≥12 years	X
P30	I	Failure to distract	X			
P31	C					
P32	NM					
P33	NM	End of spring	X		Re-tension surgery	X
		Death		X		
P34	NM					
P35	I	Rod fracture	X		Conversion to 5.5 mm rods	X
		Rod slip	X		Revision surgery	X
P36	I					
P37	NM	Excessive kyphosis	X		Conversion to 5.5 mm rods	X
P38	I	Failure connector	X			

P39	NM	Excessive kyphosis	X		Revision surgery	X
P40	NM				Conversion to PSF ≥12 years	
P41	C	Malposition rod	X			
		Adding on		X	Revision surgery	X
P42	I	Rod fracture	X			
		Disconnection rod	X		Conversion to 5.5 mm rods	X
P43	NM	Failure anchor	X			
P44	C					
P45	C	dSSI	X	X	I&D	X
		Failure anchor	X		Revision surgery	X
					Buttress release	X
		Rod fracture	X		Conversion to 5.5 mm rods	X
P46	NM					
P47	C					
P48	NM					
P49	C					
P50	NM					
P51	NM	Failure anchor	X		Revision surgery	X
		Rod fracture	X		Conversion to PSF <12 years	X
P52	NM	End of spring			Re-tension surgery	X
P53	NM					
P54	NM	End of spring			Conversion to PSF ≥12 years	X

		End of spring	Conversion to PSF ≥12 years
P55	NM		
P56	NM		
P57	NM		
P58	NM		
P59	NM		
P60	NM		
P61	NM		
P62	NM	Pulmonary insufficiency	X
		Pulmonary insufficiency	X
P63	NM		
P64	NM		

PSF: posterior spinal fusion, I&D: irrigation and debridement, dSSI: deep surgical site infection, NM loss: neuromonitoring loss.

Most implant related (S)AEs were treated during an UPROR. Anchor failure was treated with replacement of the anchor; Excessive kyphosis was often treated with converting to two connectors, replacement of rods and springs. Connector failure was treated with replacement and sometimes replacement of rods.

Part IV
Double Spring Reduction:
The move towards two springs
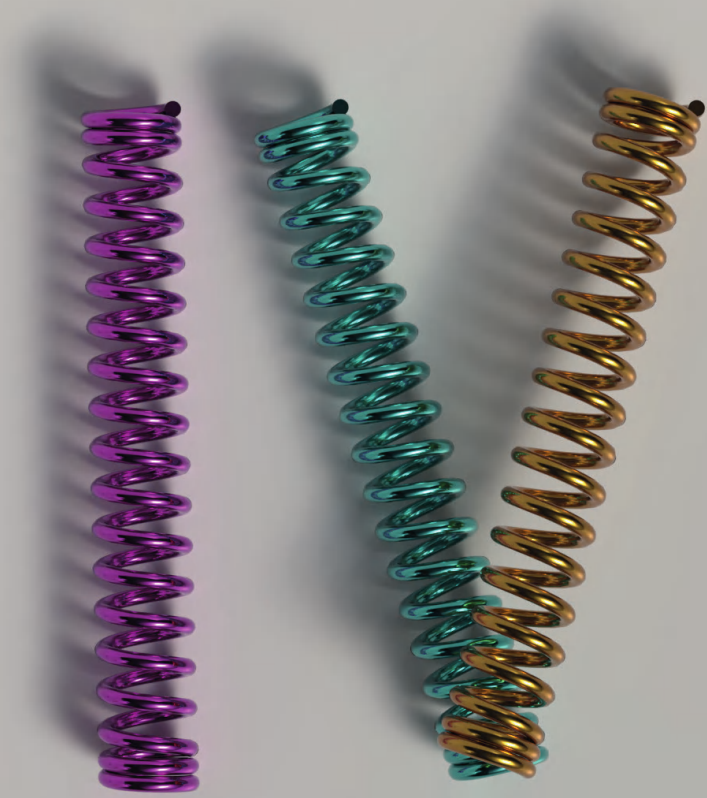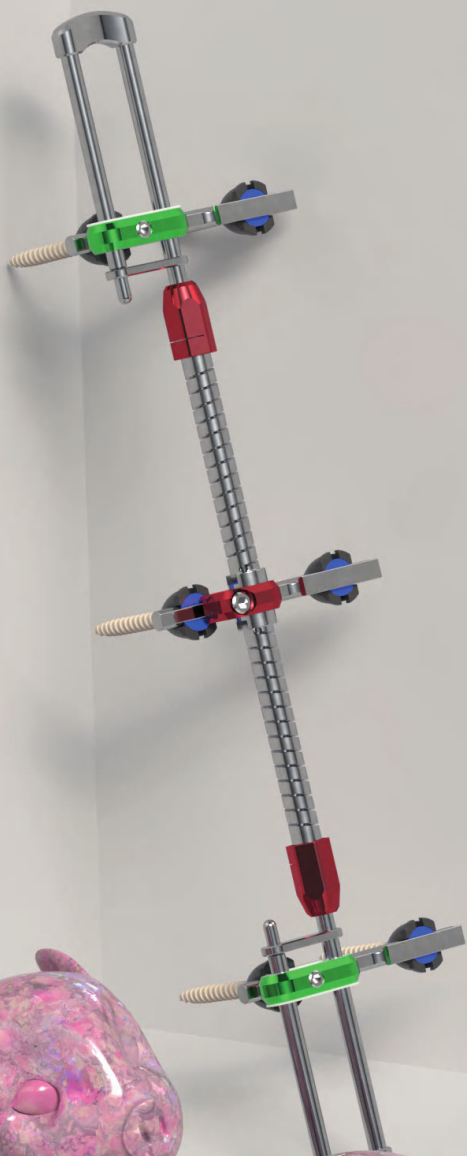
Chapter 12

Induction of a Representative Idiopathic-Like Scoliosis in a Porcine Model Using a Multidirectional Dynamic Spring-Based System

S.P.J. Wijdicks
J.V.C. Lemans
G. Overweg
E.E.G. Hekman
R.M. Castelein
G.J. Verkerke
M.C. Kruyt

Abstract

Background Context
Scoliosis is a 3D deformity of the spine in which vertebral rotation plays an important role. However, no treatment strategy currently exists that primarily applies a continuous rotational moment over a long period of time to the spine, while preserving its mobility. We developed a dynamic, torsional device that can be inserted with standard posterior instrumentation. The feasibility of this implant to rotate the spine and preserve motion was tested in growing mini-pigs.

Purpose
To test the quality and feasibility of the torsional device to induce the typical axial rotation of scoliosis while maintaining growth and mobility of the spine.

Study Design
Preclinical animal study with 14 male, 7 month old Gottingen mini-pigs. Comparison of two scoliosis induction methods, with and without the torsional device, with respect to 3D deformity and maintenance of the scoliosis after removal of the implants.

Methods
Fourteen mini-pigs received either a unilateral tether-only (n=6) or a tether combined with a contralateral torsional device (n=8). X-rays and CT-scans were made postoperative, at 8 weeks and at 12 weeks. Flexibility of the spine was assessed at 12 weeks. In 3 mini-pigs per condition, the implants were removed and the animals were followed until no further correction was expected.

Results
At 12 weeks the tether-only group yielded a coronal Cobb angle of 16.8±3.3°For the tether combined with the torsional device this was 22.0±4.0°. The most prominent difference at 12 weeks was the axial rotation with 3.6±2.8° for the tether-only group compared to 18.1±4.6° for the tether-torsion group. Spinal growth and flexibility remained normal and comparable for both groups. After removal of the devices, the induced scoliosis reduced by 41% in both groups. There were no adverse tissue reactions, implant complications or infections.

Conclusion
The present study indicates the ability of the torsional device combined with a tether to induce a flexible idiopathic-like scoliosis in mini-pigs. The torsional device was necessary to induce the typical axial rotation found in human scoliosis.

Clinical Significance
The investigated torsional device could induce apical rotation in a flexible and growing spine. Whether this may be used to reduce a scoliotic deformity remains to be investigated.

Introduction

Adolescent idiopathic scoliosis (AIS) is a complex three-dimensional (3D) deformity of the spine. This deformation develops in 2-3% of the growing population and progresses into a deformation that needs medical attention in about 10% of the patients. The deformity is characterized by axial rotation, apical lordosis and lateral deviation of the spine, with most of the deformity occurring in the discs.[231] This has led to the concept that vertebral rotation and subsequent disc response plays an important role in the initiation and further development of the deformity.[3,232,233] Currently, children with smaller curves with a proven tendency to progress are treated in a brace in an attempt to halt progression during the vulnerable growth period until the spine has matured. This treatment has shown some efficacy; however, this strongly relies on patient compliance. Unfortunately, achieving complete patient compliance is difficult since the brace should be worn for a considerable period of time during, in a crucial phase of both emotional and physical pubertal development.[19] The end result is often disappointing with a significant residual curve up to 50 degrees and in 25% of braced patients, surgery is still required despite adequate brace treatment.[19]

A potentially more effective treatment strategy could be an internal brace that transmits the corrective forces directly to the spine and enforces 100% compliance. Because of the prominent rotational component in scoliosis, such an internal brace device should exert an axial, derotational torque to the spine. In order to allow derotation, posterior lengthening should be applied to facilitate the longer anterior column in scoliosis to derotate back to the midline. Furthermore, the implant should be flexible to keep the spine mobile and allow for growth. Based on our previously developed torsional device[234] and our experience with posterior spring distraction in early onset scoliosis treatment,[58,59] we developed a combination of these devices to generate both posterior distraction and axial plane rotational force. This double spring reduction (DSR) concept could revolutionize scoliosis treatment as it has the potential to reduce the curve and even return the spine to a great extent into its normal alignment and biomechanical function.

Ideally, this concept should be investigated in a true scoliosis model. However, due to the unique biomechanical features of the human spine, accurate preclinical animal models do not exist.[235] A numerical, finite element model could offer an alternative, and even make personalized treatment possible, but deriving accurate (personal) mechanical data of the spine is not yet possible.[236–239] A surrogate method is to investigate the ability of the individual or combined components to induce and subsequently reduce scoliosis-like deformities in a growing animal model. Rigorous induction methods like rib fusions or unilateral rods that fuse the spine are less optimal from that perspective, as the deformity is often very rigid, uniplanar, unpredictable, and thus behaves more like a congenital scoliosis.[235,240,241] A more relevant induction

method is through unilateral flexible posterior tethering.[241,242] However, the fixations often fail especially due to the large forces generated during the growth spurt in domestic large animals. Mini-pigs have been proposed as an animal model because of a more moderate growth during a period of 2 years. This diminishes the tension on the bone-implant interface.[40,243] While unilateral flexible posterior tethering has been able to induce a flexible scoliosis, not much rotation is achieved.[241,242]

The aim of this study was to test the feasibility and quality of the torsional device in combination with a contralateral tether to induce the typical axial rotation of scoliosis while maintaining growth and mobility of the spine.

Materials and Methods

Ethical review and study design
This study was approved by the Animal Experiments Committee of Utrecht University. Six mini-pigs received a left-sided posterior tether only and eight pigs concurrently received the torsional device on the contralateral side. As we expected more variance in the results of the torsional device due to the additional force and higher chance of failure, we included two more animals in this group. Development of scoliosis was monitored with 3D radiological imaging for 3 months. Fluoroscopy movies were made directly after removing the implants to assess flexibility of the spine. Three mini-pigs per condition were followed after removal of the implants to determine the consistency of the deformity.

Animals
We used 14 male Göttingen mini-pigs (Ellegaard Göttingen mini-pigs, Denmark), aged 7.6 months (range 7.5-7.8) at index surgery.

Devices
The tether consisted of an ultra-high molecular weight polyethylene (Dyneema, The Netherlands) rope with a thickness of 2 mm and an ultimate strength of 2500 N/mm2. The tether can be loosely tensioned by guiding the rope through a custom-made buckle of 2 stainless steel rings (EN 1.4404 / AISI 316L) (Figure 1a). The torsional device is a further development of a previously used version.[234] The device consists of two medical grade titanium (Ti6Al4V) U-loops with sliding connectors that contain type PA2200 nylon bearings and two torsion springs in series, made of a nickel-cobalt alloy (MP35N) with a lockable connector in between (Figure 1b). The torsion springs generate a torque of 2.03±0.043 Nm by a 45° rotation in each direction (clockwise or counter clockwise) (Figure 2). All connectors can be mounted to a customized 4.5 mm rail-type transverse rod that is fixed with bilateral pedicle screws (MESA, Stryker Spine, USA). These cranial and caudal anchors can slide

12

longitudinally over the U-loops to transfer the torque while still allowing growth and spinal motion. The U-loops have been designed such that with spinal growth, the anchors slide from the flexible arms of the U-loop to the stiffer semi-circular part at the end. This counteracts the decrease in torsion in the springs that occurs with apical rotation during follow-up, resulting in torque that remains relatively constant over time.[244] The torsional device allows 5.0 cm of growth, 2.5 cm on both the cranial and caudal side. Pre-implantation fatigue experiments were done according to ASTM F2624 standards. The implants successfully completed 1.500.000±100.000 fatigue cycles, simulating a life span of 12 years. The wear on the bearings after 1.500.000 cycles was 38±1.2 mm3 per bearing, without metal-to-metal contact. The entire implant was made for human implantation and the size used in this study is appropriate for clinical application.

Figure 1. Induction implants
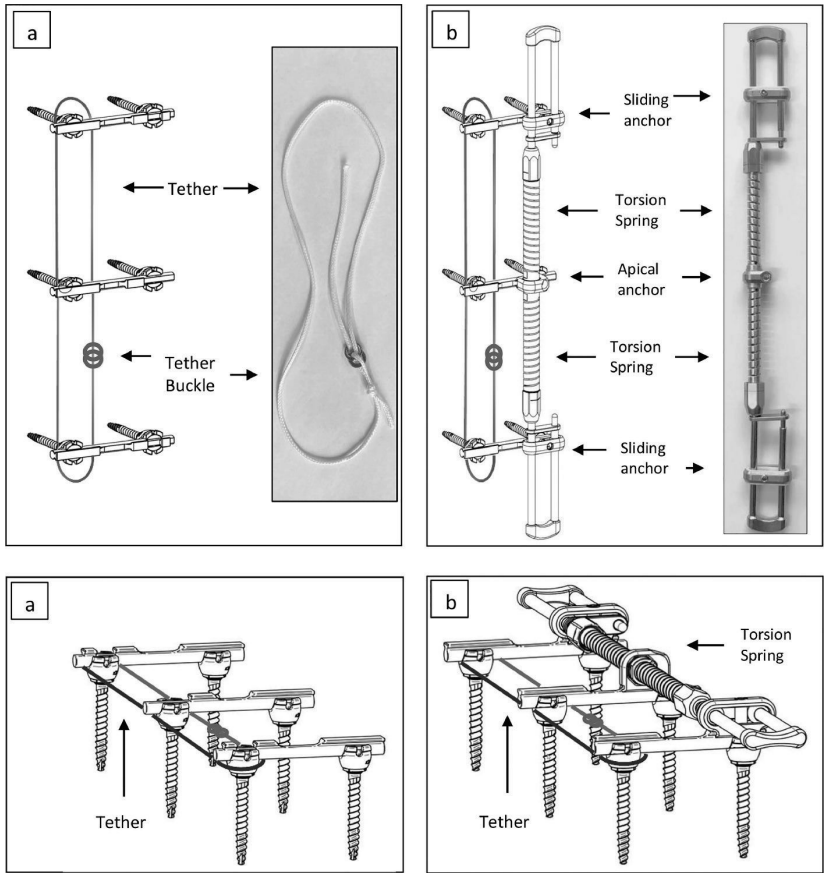
(a) Tether-only and **(b)** Tether-torsion.

Figure 2. Induction method
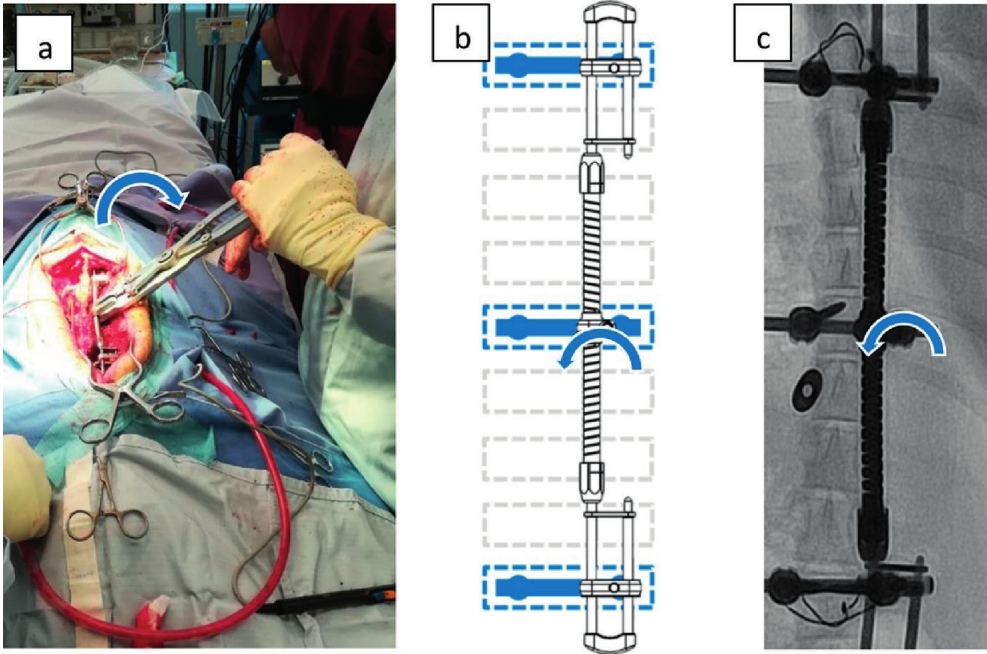
(a) The connector in between the springs was rotated 45° counter-clockwise (when looking from cranial to caudal) and locked into the apical anchor. **(b and c)** The spring then applies a torque of approximately 2 Nm in the clockwise direction.

Surgery

Perioperative antibiotic prophylaxis was given with Amoxicillin/clavulanic acid (10 mg/kg). After anesthesia with propofol (4.5 mg/kg/h), remifentanyl (0.007 mg/kg/h) and cisatracurium (0.7 mg/kg/h), the back was shaved and decontaminated with Chlorhexidine and Iodine. After radiological identification of the spinal levels, a midline skin incision was made to expose the spinal musculature. Pedicle screw insertion was done by a spine surgeon (MK) via a Wiltse type approach to minimize disturbance of the periosteum. Bilateral bicortical pedicle screws for a 4.5mm rod system were placed in each of the vertebrae T10, T14 (Göttingen mini-pigs have 15 thoracic vertebrae) and L3 under fluoroscopic guidance, with three free vertebrae between each instrumented vertebra. For each vertebra the screws were connected with a customized transverse bridge resembling a rail rod. Cerclage wires were used to protect the proximal and distal anchors from pulling out due to the tether force. The tether was always placed on the left side and looped around the proximal and distal screws. It was minimally tensioned such that there was no play in the cord, but without enforcing scoliosis and locked by four flat knots.

The torsional device was placed on the right side intramuscularly. The sliding and apical connectors were placed on the rail and locked. Then the connector in between the springs was rotated 45° counter-clockwise (when looking in a cranio-caudal direction) and locked into the apical anchor. The spring will then apply a continuous torque of approximately 2 Nm in the clockwise direction (as commonly seen in idiopathic scoliosis) during follow-up. Before closure, the surgical site was thoroughly irrigated with sterile saline and 5cc of depomycine (200mg/ml) was dripped into the wound. After closure in three layers, sterile gauzes soaked in povidone-iodine (10%) were placed over the wound with transparent foil (3M Tegaderm Transparent Film Roll, 3M, USA) and fastened with brown tape. Immediately after surgery, AP and lateral X-rays and CT's of the anaesthetized pigs were taken with a motorized C-arm (Allura FD20, Philips, Netherlands). The positioning of the mini-pigs for imaging was standardized, with front and back feet pointing forward under the body.

Follow-up

After recovery, the pigs were returned to the other members of the herd and checked daily. After 8 and 12 weeks, AP and lateral radiograph and a CT scan were made under sedation with ketamin (13 mg/kg), midozolam (0,7 mg/kg) and atropine (0,05 mg/kg) without the need for intubation. Fluoroscopy movies were made during application of 3-point manual bending forces (at apex and contralaterally at the distal and proximal foundations) to assess spinal flexibility after removal of the implants at 12 weeks. To study the behavior of the scoliosis without instrumentation, 3 animals in each condition were followed after removal of the devices until the scoliosis reached a plateau phase and we expected no more correction.

Sagittal and coronal angulations were measured of the instrumented segments in the anatomical plane (using plain radiographs without correction for 3-dimensional deviations) with the Cobb method. Growth of the implant was determined from CT scans by measuring the distance between the superior pedicle screw heads of (T10, T14 and L3) on both the convex and concave side. These same CT scans were used to assess apical rotation using a semiautomatic image processing technique and software (ScoliosisAnalysis 4.1, Imaging Sciences Institute, Utrecht, The Netherlands). By manually angulating a plane in the 3 orthogonal directions the endplates were visualized in the true transverse plane. The software drew a straight line between the geometric centers of the vertebral body and spinal canal. The angle of these lines was calculated to determine the apical vertebral rotation relative to the distal and proximal vertebrae. An x-y-z coordinate model was created of each vertebra based on the bony contours from the "true" transverse sections of the endplates. Based on this model, anterior and posterior length of the disks and vertebrae were calculated. A relative measure was used for comparisons: AP%=(The anterior length-posterior length)/posterior length*100%.

Implant inspection
After explantation the torsional devices were sent to the biomechanical laboratory for inspection. Spring function and wear of the bearings were compared with the condition before implantation.

Statistical analysis
For comparison between post-operative and end of follow-up, t-test or paired sample t-test were used. For data appearing non-normally distributed, Mann-Whitney u-test or Wilcoxon test were used. A p-value <0.05 was considered significant. Descriptive statistics and statistical analysis were performed with IBM SPSS Statistics 24.0 (IBM Corp. Armonk, New York, NY, USA).

Results

General
At the time of surgery, the mean age of the mini-pigs was 7.6±0.1 months and the mean weight was 20.1±1.4 kg. Three months after surgery, the weight had increased to 30.2±2.5 kg. The growth was according to their normal growth charts. All surgeries were uneventful and there were no complications in terms of wound infection or implant failure. Postoperative radiographs confirmed correct positioning and minimal tension on the tether. After 3-months, all animals had developed a coronal Cobb angle varying between 10° and 30° (mean 19.3°). All the curves were as intended including sagittal lordosis. CT analysis did not show spontaneous fusions or

12

ectopic ossifications. Upon retrieval of the implants there were no signs of excessive wear or metal debris. The springs were encapsulated with scar tissue but this did not hamper their torsional function (Figure 3).

Figure 3. Rotational implant
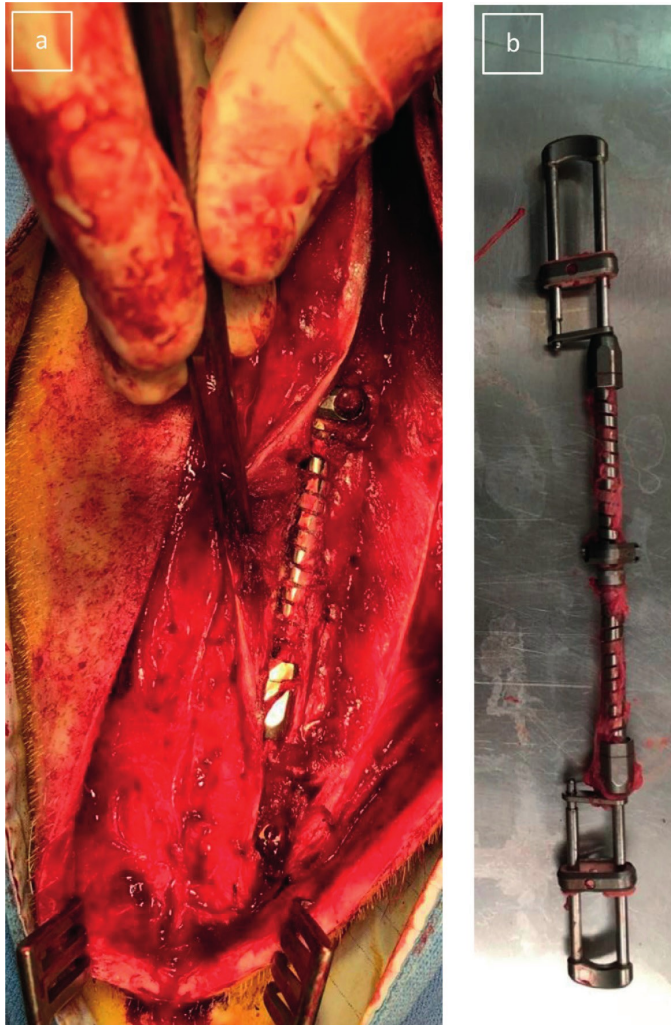
(a) Intra-operative view of the rotational implant after 3 months. **(b)** Rotational implant after explantation.

Radiological measurements

Standard deviations and significance of all measurements are provided in Table 1, Table 2 and 3. For the tether-only group, the mean coronal Cobb angle increased from a mean of 0.6° immediately after surgery to 16.8° at 12 weeks. For the tether-torsion group this was from 3.8° to 22.0°. In the plain X-ray sagittal plane, the instrumented lordosis increased from a natural 3.8° after surgery to 12.0° for the tether-only group and from -3.7° (kyphosis) to 11.5° (lordosis) for the tether-torsion group. As expected, the most prominent differences were observed for apical rotation, measured on the 3D reconstructions. For the tether-only group, this hardly increased from 2.3° to 3.6°. The tether-torsion group showed an obvious increase from 6.5° to 18.1° (Figure 4, Figure 5 and 6). The mean anterior to posterior length difference for the whole spine, measured in the "true" sagittal reconstructed plane, was 1.5% for the tether-only group and 1.6% for the tether-torsion group. For the bony vertebrae this was minimal, whereas this AP% obviously increased in the discus: 13.4% for the tether-only group and 21.3% for the tether-torsion group (Figure 7). Instrumented growth was 1.1 cm on the concave and 2.0 cm on the convex side for the tether-only group and 1.2 cm on the concave and 1.9 cm on the convex side for the tether-torsion group.

   After removal of the implants (3 tether-only and 3 tether-torsion minipigs), mobility was assessed with 3 point bending on video fluoroscopy. The coronal angles before and after bending changed 5.1±1.2° for the tether-only group and 4.9±1.6° for the tether-torsion group, there was no indication of fused segments. The animals that were followed after removal of the implants showed some reduction of the scoliosis during the first 4 weeks, which remained stable up to 8 weeks. For the tether-only group, the coronal deformity decreased from 17.7±2.6° to 10.5±4.9° = -41% and the axial rotation remained minimal, from 4.2±3.0° to 4.4±2.2° = +4%. In the tether-torsion group, the coronal deformity decreased from 24.8±1.6° to 14.5±3.5° = -41% and the axial rotation from 18.9±0.7° to 15.8±3.2° = -16%.

Table 1. Coronal and Sagittal angles measured on X-rays and axial rotation on CT-scans (°)

		Tether only (N=6)	Tether-torsion (N=8)	P value
Coronal Cobb angle	Post-operative	0.6±0.4	3.8±3.1	
	12 week follow-up	16.8±3.3	22.0±4.0	
	Increase	15.2±3.8	18.2±4.2	0.19
Instrumented lordosis	Post-operative	3.8±4.5	-3.7±6.5	
	12 week follow-up	12.0±5.0	11.5±3.7	
	Increase	8.1±7.0	15.1±8.3	0.12
Axial Rotation	Post-operative	2.3±1.9	6.5±2.7	
	12 week follow-up	3.6±2.8	18.1±4.6	
	Increase	1.3±4.3	11.6±5.2	<0.01[a]

[a]Significant difference

Table 2. Concave and convex instrumented length measured on CT-scans (mm)

		Tether only (N=6)	Tether-torsion (N=8)	P value
Concave height	Post-operative	159.1±2.8	161.6±5.2	
	12 week follow-up	170.3±7.0	173.4±4.2	
	Increase	11.3±4.3	11.8±5.8	0.86
Convex height	Post-operative	160.6±1.8	164.5±5.8	
	12 week follow-up	180.2±3.8	183.7±6.5	
	Increase	19.6±3.7	19.3±3.7	0.83

Table 3. Anterior-posterior percentage (AP%) over time measured on CT-scans

Ant-Post length discrepancy (%)[a]		Tether only (N=6)	Tether-torsion (N=8)	P value
Total Spine	Post-operative	+0.6±1.0	+0.5±1.2	
	12 week follow-up	+2.2±1.0	+2.1±0.9	
	Increase	+1.5±0.9	+1.6±1.4	0.88
Vertebral bodies	Post-operative	-1.3±0.6	-1.8±1.1	
	12 week follow-up	-1.5±0.9	-1.8±1.2	
	Increase	+0.1±0.9	+0.0±1.2	0.97
Intervertebral discs	Post-operative	+15.8±8.0	+18.3±10.3	
	12 week follow-up	+29.2±4.4	+39.2±9.9	
	Increase	+13.4±6.9	+21.3±6.6	0.04[b]

[a]A positive percentage indicates a larger anterior length compared to posterior length. For instance, +5% indicates that anterior length is 5% greater than posterior length.
[b]Significant difference

Figure 4. Radiographs of tether-only condition normalized for size
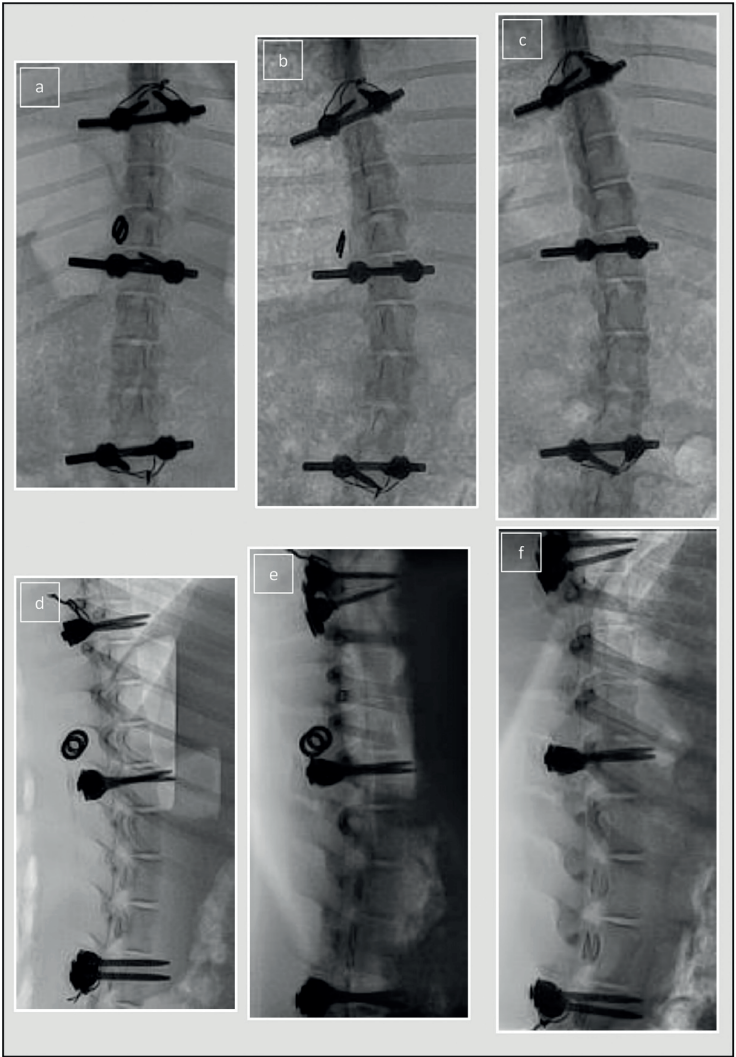
(**a**) Anterior-posterior directly post-operative (**b**) at 12 weeks and (**c**) 8 weeks after tether release (**d**) Lateral directly post-operative (**e**) at 12 weeks and (**f**) 8 weeks after tether release.
Note the increase in length.

Figure 5. Radiographs of tether-torsion condition normalized for size
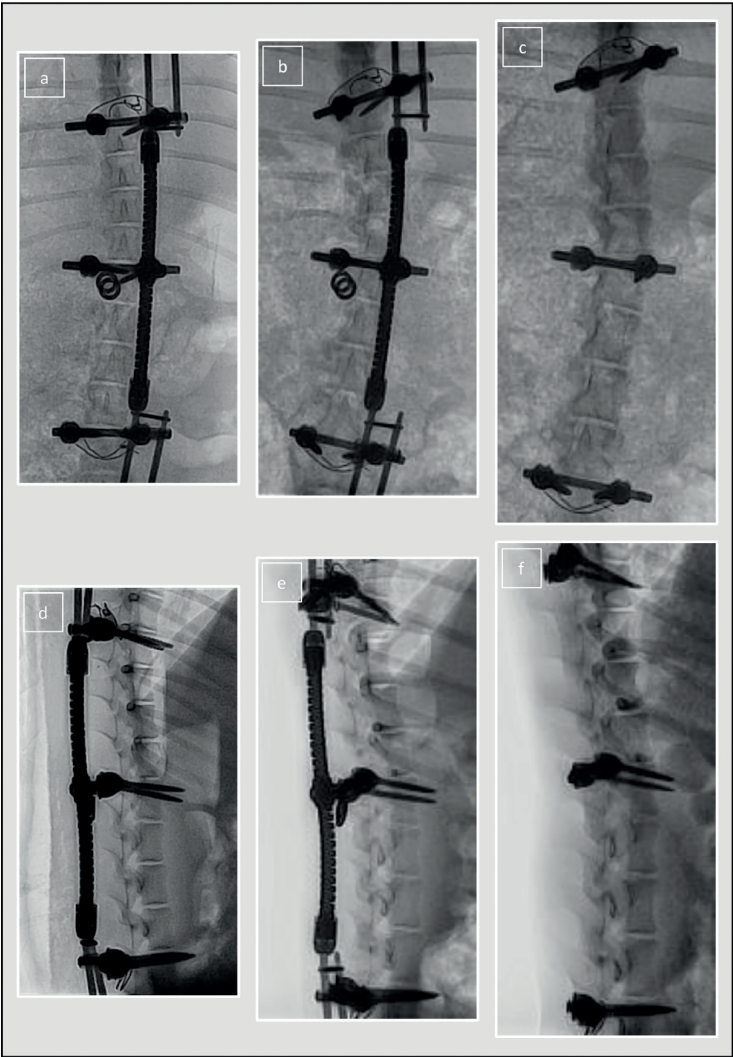
(a) Anterior-posterior directly post-operative **(b)** at 12 weeks and **(c)** 8 weeks after tether release and implant removal **(d)** Lateral directly post-operative **(e)** at 12 weeks and **(f)** 8 weeks after tether release and implant removal. Note the increase in length.

Figure 6. Deformation in time per sample of the tether-only (n=6) and tether-torsion (n=8) condition in degrees (°)
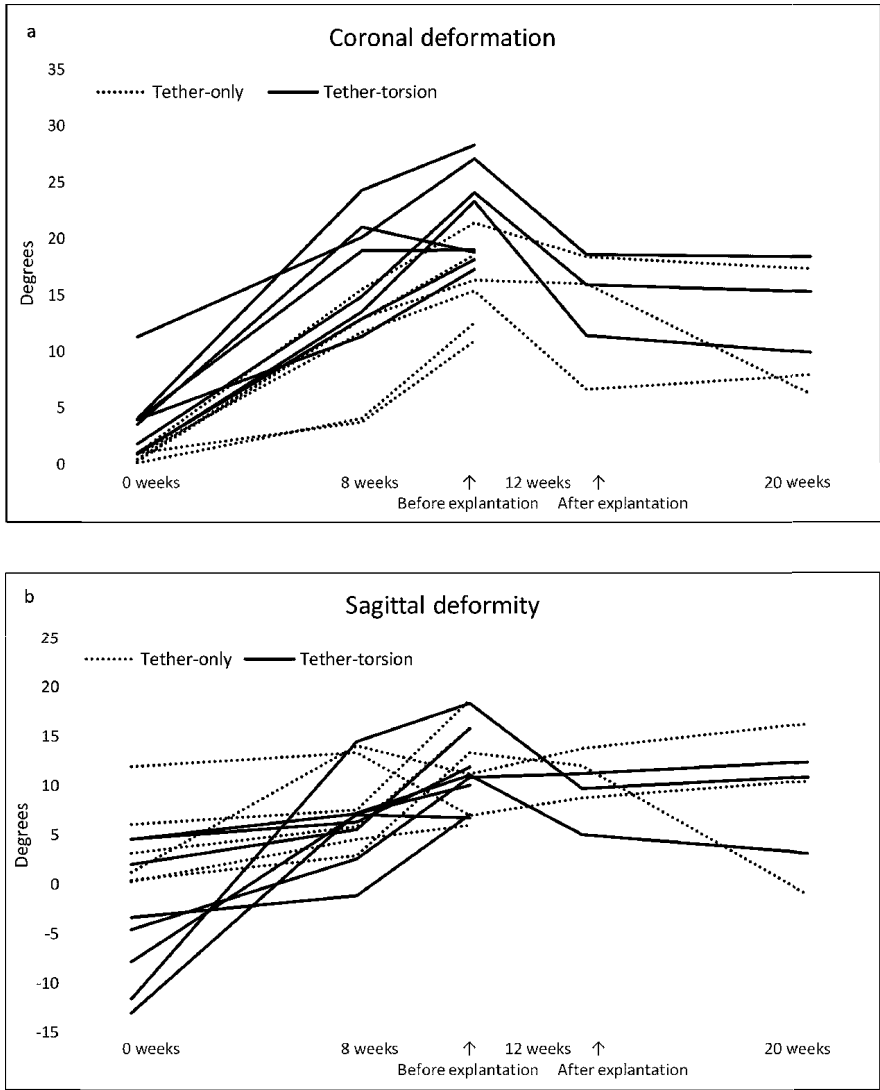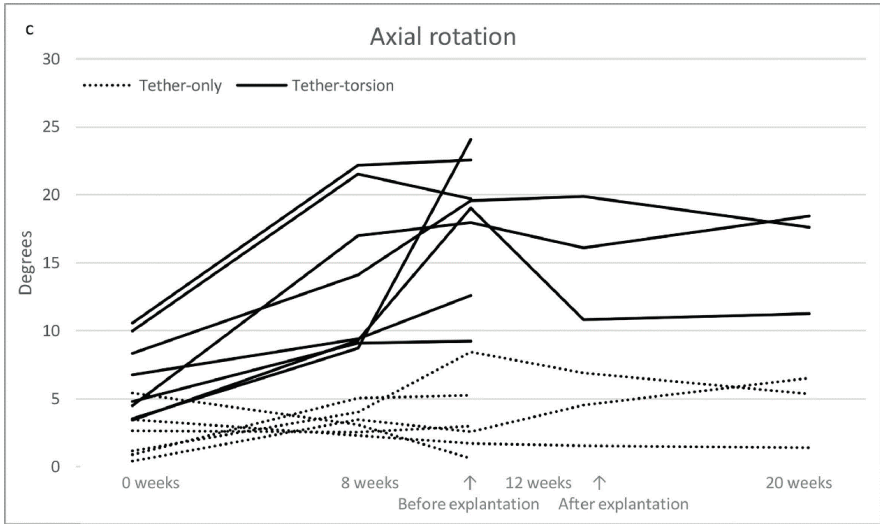
(a) Coronal angles after implantation, at 8 weeks, at 12 weeks, after explantation and pre-termination (b) Instrumented Lordosis in the anatomical plane after implantation, at 8 weeks, at 12 weeks, after explantation and pre-termination (c) Axial rotation after implantation, at 8 weeks, at 12 weeks, after explantation and pre-termination.

Figure 7. Anterior-posterior % (AP%) over time for total instrumented spine, the bony vertebrae and the discs in the true lateral plane
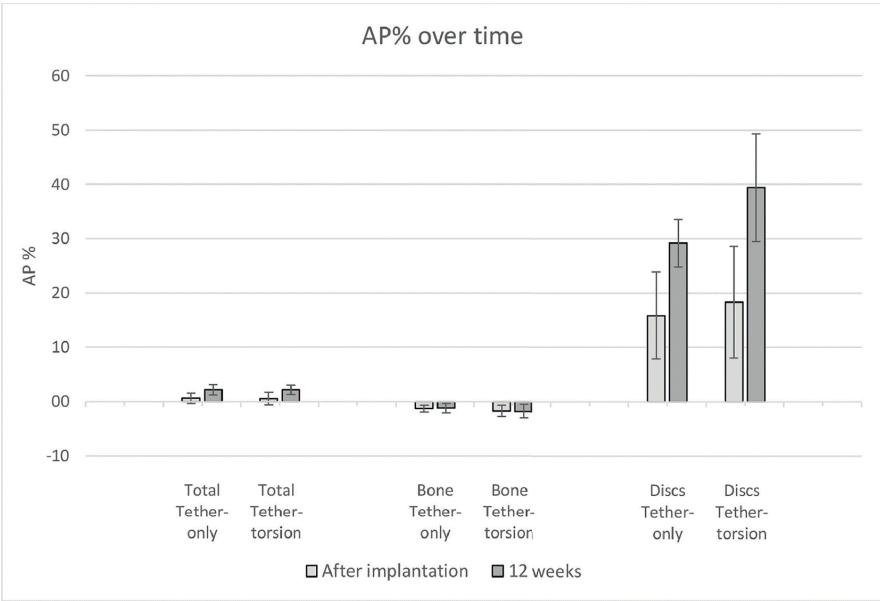
A positive percentage indicates a larger anterior length compared to posterior length.

Error bars indicate SD, * = Significant.

12

273

Inspection of the retrieved implants
The nylon bearings showed some wear consistent with movement. Wear was not enough to cause metal-to-metal contact. The springs and U-loops maintained their integrity. The rotational torque of the springs remained unchanged with 2.08±0.051 Nm at 45° rotation. The wear of the bearings was in line with the fatigue experiments, 1.2±0.13 mm3 per bearing.

Discussion

The ultimate purpose of the implant we developed is to reduce the rotation component of a scoliotic spine, because we consider this the most important aspect of idiopathic scoliosis. Since no animal model exists that develops a scoliosis spontaneously, that is similar to human idiopathic scoliosis, we decided to test the implant on vertebrae that will not normally develop a rotational deformity. For that purpose, scoliosis was induced in mini-pigs using a unilateral tether with or without the addition of the torsional device. Although similar coronal curves were induced with both treatments, only the torsional device achieved significant intervertebral rotation similar to human idiopathic scoliosis. This characteristic apical rotation remained most prominent after removal of the torsional device, indicating a permanent change of especially the intervertebral disks without ankylosis of the facets. Furthermore, one of the main advantages in the predictability of the coronal curve in combination with the significant rotation at the end of induction. These findings are promising for the ability of the torsional device to reduce the rotational component of scoliosis in the clinical setting.

To address the coronal and sagittal components of a real scoliosis, a distraction force should be added to the torsional device, in order to provide room for the longer anterior column, that is an integral part of the deformity, to swing back to the midline. Spring distraction techniques that we currently use, investigate and have reported on for early onset scoliosis treatment offer a reliable possibility to reach that goal. [58,59] Based on these results we can begin implementing derotation and distraction Double Spring Reduction (DSR) concept in pre-clinical studies. We do realize that there are no true (animal) models for idiopathic scoliosis and testing the DSR or its components in an animal spine, that would normally not develop this deformity, is the second best experimental set up.[235] Therefore, we believe that the subsequently obtained scoliotic animal model in this study may be the most appropriate model to investigate the entire DSR reduction strategy.

Previously different animal models have been investigated in sheep, goats, pigs and mini-pigs. We preferred the porcine model because of similarities of the vertebrae to the human spine.[245–251] Mini-pigs were chosen because of a more steady growth over 2 years, which is an advantage compared to the steep and short growth

spurts of domestic cattle.[242,252] This gives us a sufficiently remaining growth period after induction to investigate a scoliosis reduction device. Moreover, the steady moderate growth diminishes the tension on the bone-implant interface and allows gradual induction of scoliosis.[40,243] We did investigate a previous version of the torsional device in domestic pigs, where it was used stand alone. In that study we similarly found rotation, but limited to 9 degrees and only minimal coronal deformation of 6 degrees, which cannot be regarded as a suitable model for scoliosis.[234] In the current mini-pig model, including a contralateral tether, the mean coronal curves were 19 degrees, which we consider as relevant although smaller than other studies where more aggressive techniques were used in faster growing animals.[240,241,253–255] However, more important than coronal curve size is that the curves are consistent, the spine remains mobile and includes all 3D characteristics, including axial rotation and anterior lengthening in the disk, of idiopathic scoliosis.[234]

To our knowledge, the scoliosis obtained with the torsional device resembles idiopathic curvatures more closely than any other current animal model. This is mainly due to the apical rotation with imposed anterior length increase, as is typical for human scoliosis. This anterior length increase was subtle and only in the relatively small disks, therefore it was only apparent in 3D reconstructed images and not evident with plane X-rays. Other important aspects of the implant are enabling growth and maintaining spinal mobility. Both appeared favorably, as there was no difference in growth of the convex side with or without the torsional device. Flexibility was confirmed after 12 weeks, however this could not be compared to untouched spines.

Clinical relevance

In this study we only investigated the feasibility of the torsional device. To determine its potential for clinical use, preclinical efficacy studies will be a next step. Fortunately, the induced scoliosis appears to be a very suitable model for that, including the fact that the coronal curve remained at about 60% after the instrumentation was removed. This reduction is also seen in other studies without fusion.[239,250] In our opinion the observed reduction confirms the idiopathic-like nature of the curve as the spine remains mobile and returns to a stable state. Interestingly, the rotational component appears to be persistent in the tether-torsion group after instrumentation was removed. This strengthens our believe that, in scoliosis, the disc is the first and most important structure to address.

Limitations

Currently it is unknown if the induced curvature is progressive due to the short time span of intervention and explantation. Furthermore, while we compared a torsional device with a tether to a tether only, we did not compare with a third group; torsional only. Before starting this trial we already had data on the torsional only implant in

12

domestic pigs, but further research will be done on implanting a torsional only device in mini-pigs. Because some corrections in the mobile spine is lost after explantation, the reduction effect of implants in a second stage should still be compared to a control group. We realize that while these results are promising, we will not proceed to human clinical trials before further pre-clinical testing.

Conclusion

The present study indicates the feasibility of a torsional device to induce intervertebral rotation as part of an idiopathic-like scoliosis in mini-pigs. During the induction period, the spine retained growth capacity and mobility. After removal of the implant, rotational and coronal deformity remained. Further studies are currently in development to determine efficacy of this device for the treatment of scoliosis.
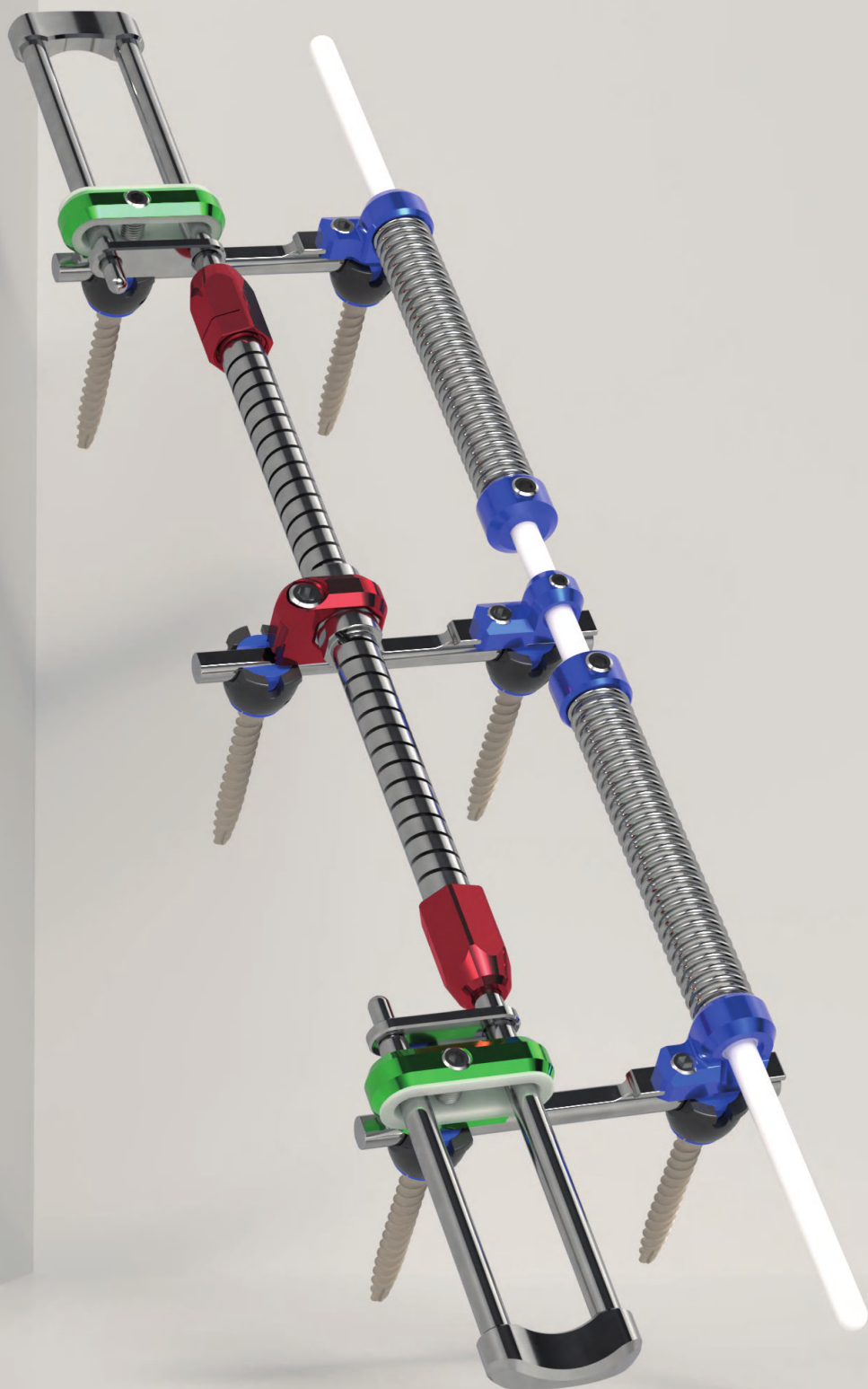
Chapter 13

Three-Dimensional Correction of Scoliosis by a Double Spring Reduction System as a Dynamic Internal Brace: A Pre-Clinical Study in Göttingen Minipigs

J.V.C. Lemans

S.P.J. Wijdicks

G. Overweg

E.E.G. Hekman

T.P.C. Schlösser

R.M. Castelein

G.J. Verkerke

M.C. Kruyt

Abstract

Background Context
Adolescent idiopathic scoliosis (AIS) is a major skeletal deformity that is characterized by a combination of apical rotation, lateral bending and apical lordosis. To provide full 3D correction, all these deformations should be addressed. We developed the Double Spring Reduction (DSR) system, a (growth-friendly) concept that continuously corrects the deformity through two different elements: A posterior convex Torsional Spring Implant (TSI) that provides a derotational torque at the apex, and a concave Spring Distraction System (SDS), which provides posterior, concave distraction to restore thoracic kyphosis.

Purpose
To determine whether the DSR components are able to correct an induced idiopathic-like scoliosis and to compare correction realized by the TSI alone to correction enforced by the complete DSR implant.

Study Design/Setting
Preclinical randomized animal cohort study.

Patient Sample
Twelve growing Göttingen minipigs.

Outcome Measures
Coronal Cobb angle, T10-L3 lordosis/kyphosis, apical axial rotation, relative anterior lengthening.

Methods
All mini-pigs received the TSI with a contralateral tether to induce an idiopathic-like scoliosis with apical rotation (mean Cobb: 20.4°; mean axial apical rotation: 13.1°, mean lordosis: 4.9°). After induction, the animals were divided into two groups: One group (N=6) was corrected by TSI only (TSI only-group), another group (N=6) was corrected by a combination of TSI and SDS (DSR-group). 3D spinal morphology on CT was compared between groups over time. After 2 months of correction, animals were euthanized.

Results
Both intervention groups showed excellent apical derotation (TSI only-group: 15.0° to 5.4°; DSR-group: 11.2° to 3.5°). The TSI only-group showed coronal Cobb improvement from 22.5° to 6.0°, while the DSR-group overcorrected the 18.3° Cobb

to -9.2°. Lordosis was converted to kyphosis in both groups (TSI only-group: -4.6° to 4.3°; DSR-group: -5.2° to 25.0°) which was significantly larger in the DSR-group (p<.001).

Conclusions
The TSI alone realized strong apical derotation and moderate correction in the coronal and sagittal plane. The addition of distraction on the posterior concavity resulted in more coronal correction and reversal of induced lordosis into physiological kyphosis.

Clinical Significance
This study shows that dynamic spring forces could be a viable method to guide the spine towards healthy alignment, without fusing it or inhibiting its growth.

Introduction

Adolescent idiopathic scoliosis (AIS) is a major skeletal deformity with pulmonary and cardiac consequences,[10,256] that is characterized by a combination of apical rotation, lateral bending and apical lordosis. These deformities are largely due to anterior lengthening that is mainly located in the intervertebral disc (IVD).[3,4,53,257] To achieve correction in all planes, all these deformations should be addressed, with specific attention to sufficient posterior concave distraction to accommodate the longer anterior column, so that it may rotate back into the midline.

Current treatments for adolescent idiopathic scoliosis (AIS) either stabilize the curve with bracing or surgically fuse the spine. Bracing can be effective in preventing curve progression, but only with strict patient compliance to wear the brace >16 hours per day.[18,19] Even then, residual curves can be considerable.[19] Spinal fusion is more effective in correcting the 3D morphology of the spine, however at the cost of spinal mobility, which adversely affects long-term quality of life of these patients.[258] Only at very young age, serial (Mehta) casting is known to be able to "cure" the spine; that is to resolve the deformity while retaining a flexible spine.[17] However, such permanent rigid casts, which apply large corrective forces, are not tolerated by older children.

To achieve similar results for these patients, an internal brace could possibly overcome many of the disadvantages of serial casts. Most importantly, strategic forces can be exerted on the spine with 100% compliance. By using dynamic and flexible implants, such application of prespecified forces and torques is possible. For this purpose, we developed the Double Spring Reduction (DSR) implant (Figure 1), which consists of two different spring implants, the torsional spring implant (TSI) and the spring distraction system (SDS). Together, these temporary flexible implants provide continuous apical axial torque (TSI) and posterior distraction forces (SDS) to the spine during the years that it has a chance to mature into a reduced and stable configuration. The implant can accommodate growth, and can therefore be used when the child has not yet reached skeletal maturity. This "growth-friendly" feature not only allows for early correction of AIS curves of older children, it also allows for treatment of "tweeners" aged 9–11, where current "growth-friendly" implant results are often disappointing when compared to results of spinal fusion.

Figure 1. Double Spring Reduction implant
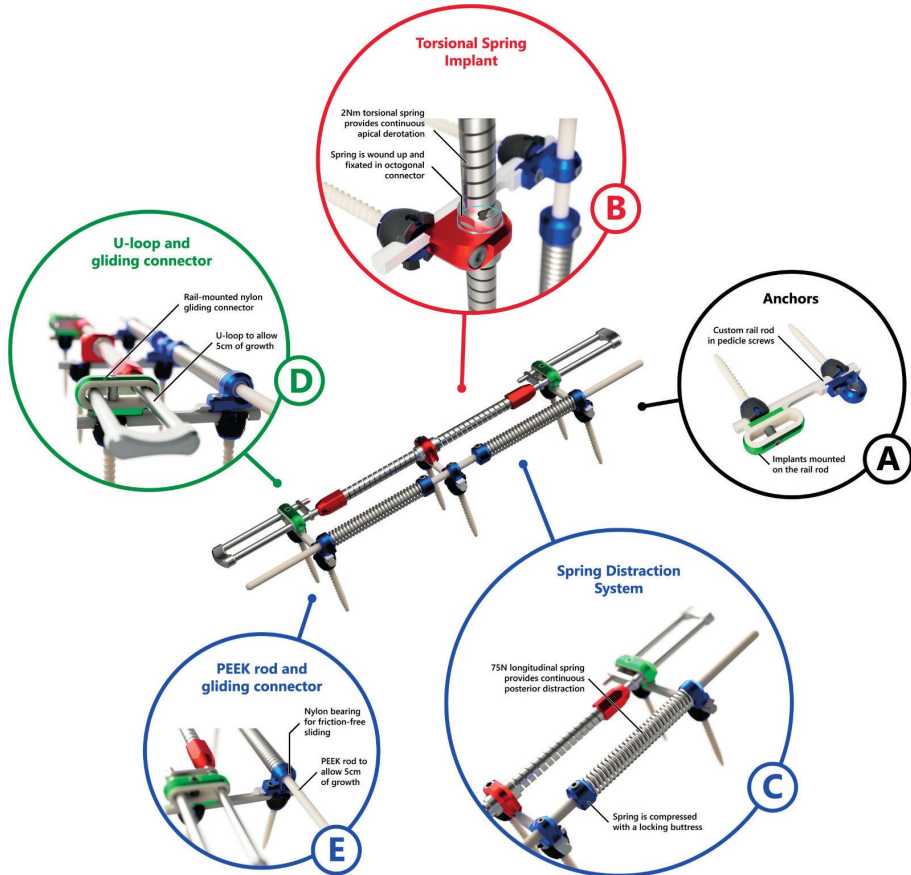
The Double Spring Reduction implant consists of two different springs that are mounted on top of custom rail rods **(A)**. The torsional spring implant (TSI) is fixated to the curve convexity **(B)** and exerts a continuous axial torque to the apical level. The spring distraction system **(C)** is fixated to the curve concavity. Both the torsional spring implant **(D)** and spring distraction system **(E)** have sliding connectors that allow for spinal growth.

13

Previous studies have investigated the concept of the TSI, concluding that it has the potential to provide strong apical (de-)rotation with only a very small increase in spinal stiffness.[234,244] A recent preclinical study by our group in growing Göttingen minipigs has shown that the TSI, combined with a flexible tether, was able to induce a morphologically idiopathic-like scoliosis whilst retaining mobility and growth.[259] After implant removal, the deformity remained and was shown to reside mainly in the IVD, indicating permanent spinal changes similar to those seen in human AIS.

We performed the current study to determine whether the internal brace concept (DSR) is able to correct the established idiopathic-like scoliosis. In addition, we investigated whether correction with torsion alone is equally effective when compared to a combination of both torsion and posterior distraction.

Materials and Methods

Ethical Approval
This study was performed in the AAALAC certified experimental surgery animal laboratory of Utrecht University. Ethical approval was granted by the Animal Experiment Committee of Utrecht University before the start of this study (AVD 115002016804).

Study Design
The current study consisted of 2 phases (Figure 2). Phase 1 was the induction phase, wherein a scoliosis was induced in 12 growing Göttingen minipigs through implantation of a left-sided unilateral, posterior tether combined with a contralateral TSI, tensioned to provide 2 Nm of axial torque.[259] After 3 months of induction, the curves were confirmed with CT scans and phase 2, the reduction phase, was initiated. All 12 minipigs were operated again, the induction forces were released and animals were randomized into two groups, each undergoing a different method of scoliosis reduction: (1) Reduction by only de-rotating the curve apex with the torsional TSI (TSI only-group, N=6), or (2) Reduction by combining the TSI with the concave distraction implant SDS (DSR-group, N=6). After the reduction surgery, 2 months of follow-up was allowed for spinal remodeling. Then, the animals were euthanized. Spinal morphology between groups was compared with 3D imaging at several timepoints.

Animal Model
The Ellegaard Göttingen minipig is bred specifically for research purposes, and has a predictable linear growth curve from birth to 2 years of age, which can be translated very well to pediatric spinal growth.[5,260] In addition, spinal anatomy is similar in size and shape to human pediatric anatomy. The animals can be housed in groups, and

Figure 2. Experiment timeline
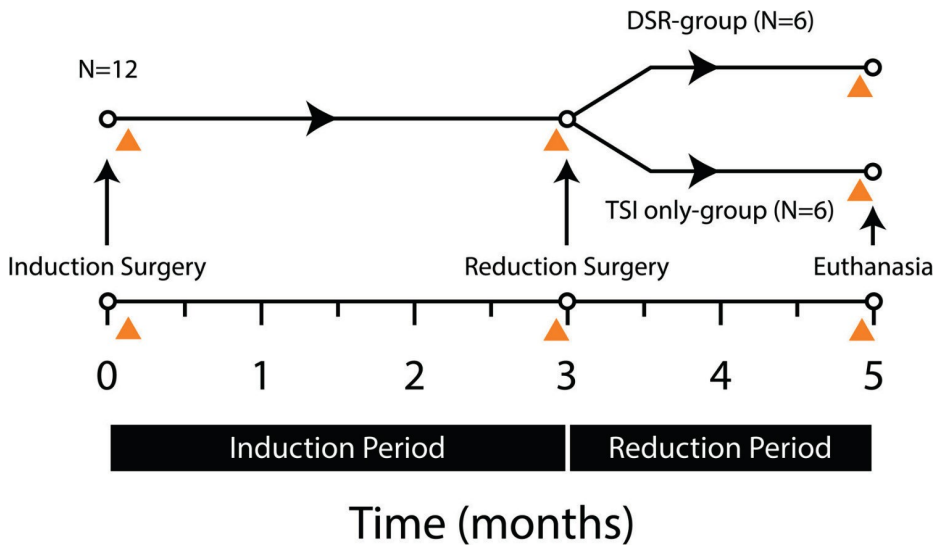
In 12 animals, scoliosis induction is performed with a left-sided tether and 2 Nm of apical torque to the right. After 3 months, animals are divided into two groups for a reduction period of 2 months: Six animals received only the TSI-implant, while six were treated with the complete DSR-implant (ie, derotation and distraction). The orange triangles denote moments where spinal morphology was analyzed with imaging.

their small stature makes animal husbandry less cumbersome as compared to larger cattle. Whilst the minipig spine is positioned horizontally and not upright like the human spine, it serves as a representative scoliosis model, since it has been shown that muscle forces in quadrupeds ensure similar axial compressive force vectors comparable to vertical human spinal loading.[248]

Double Spring Reduction Implant
The complete internal brace, the DSR implant (Figure 1), consists of two different flexible components: (1) the TSI, and (2) the SDS. These are positioned on either side of the posterior spine and mounted on posterior pedicle screw anchors. Both components deliver continuous forces and torques in all planes, while allowing mobility and growth of the spine.

The TSI (Figure 1B) consists of two in-line nickel-cobalt alloy (MP35N) torsion springs with titanium U-loops at the upper- and lower ends that can slide through the upper and lower anchor bearings that are mounted to T10 cranially and L3 caudally. At the apex (T14), the connector between both springs can be pre-tensioned with 2 Nm by 45° of rotation and then be mounted to the apical anchor to deliver the axial torque. The U-shaped loops (Figure 1D) are designed so that with spinal growth, the combined torsional stiffness of the springs and the loops increase, causing the cor-

13

rective torque to remain essentially the same in spite of the decreasing pre-tension angle. This counteracts the decrease in torque that would otherwise take place due to apical derotation over time. The TSI has a growth potential of 100 mm, 50 mm on both the cranial- and caudal side and adds <20% additional spinal stiffness, which is far less than what is found with contemporary correction implants.[244]

The SDS (Figure 1C) consists of two titanium (ASTM Grade 19) coil springs around a flexible 4mm polyether ether ketone (PEEK) rod. The rod slides through nylon bearings (Figure 1E) on the upper and lower anchor, and has a growth potential of 50mm on each side. The central part is mounted to the apical anchor to prevent buckling. The springs are tensioned to deliver 75 N with a simple buttress that is fixated to the rod. Distraction force linearly decreases with length gain based on the spring constant (k) and Hooke's law ($Fd = k \cdot x$). The SDS principle has been used in our clinic for treatment of early-onset scoliosis patients, with satisfactory curve correction and remaining spinal growth.[58,59,113]

Surgical Technique

The surgical induction technique has been described previously, it is summarized here for completeness (Figure 3).[259] After standard surgical preparation of the minipigs, exposure through a dorsal midline approach was performed spanning levels T10, T14 (Göttingen minipigs have 15 thoracic vertebrae) and L3. At these three levels, bilateral pedicle screws were implanted under fluoroscopic guidance (Mesa Small Stature, Stryker, Kalamazoo, MI, USA). Custom rail rods were then mounted to connect the left and right pedicle screws (Figure 1A) and create a cranial, apical, and caudal anchor. Between each anchor, three vertebral bodies, four IVDs and four pairs of apophyseal joints were left untouched.

For scoliosis induction, an UHMWPE tether (Dyneema, DSM, Geleen, The Netherlands) was looped around the cranial and caudal anchors on the left side and closed tight but without tension. The TSI was mounted on the right side, with bearings that fit on the rails cranially and caudally, leaving the apical connector unlocked. The apical part of the torsional spring (Figure 1B) was then rotated 45° in the axial plane with a custom wrench (to induce a right-sided scoliosis) and was subsequently locked to the apical rail (Figure 3A/B). Immediately following surgery, radiographic,- and CT imaging was obtained. The animals were returned to their housing units where they were kept in groups and fed ad libitum.

Figure 3. Induction- and reduction surgery
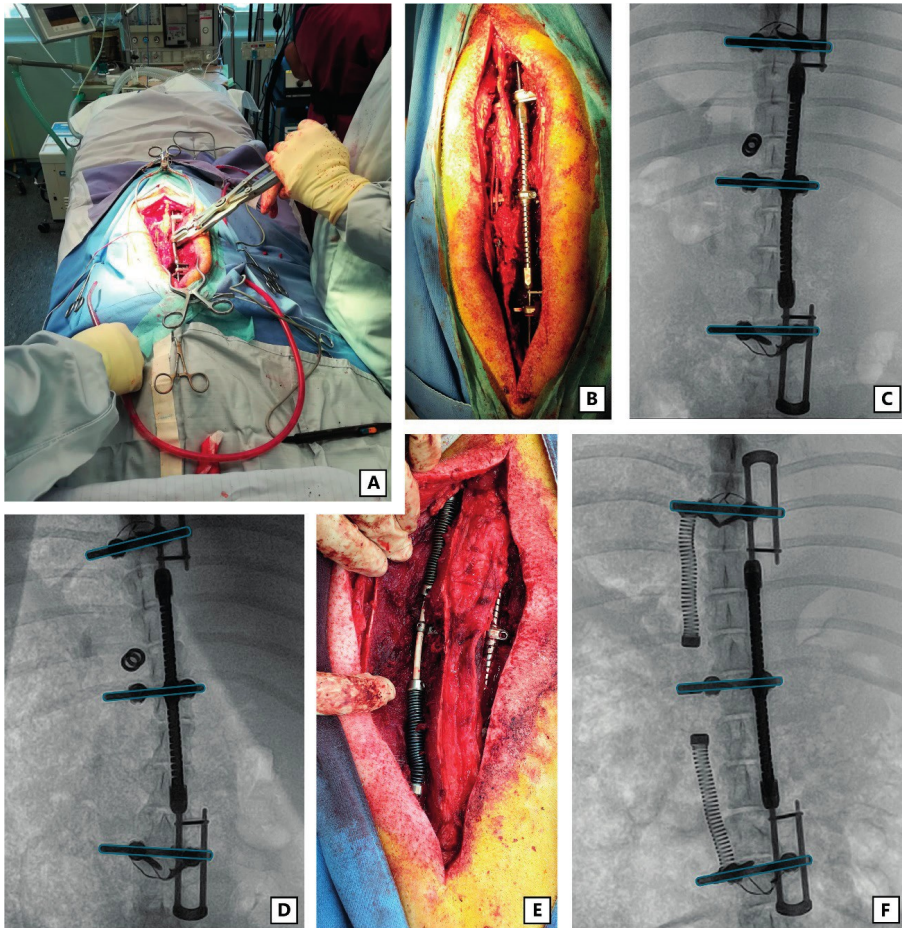
(A) During induction, the TSI is wound up by rotating it 45° in the clockwise direction (looking in the cau-do-cranial direction), to deliver 2Nm torque. **(B)** Close-up of the TSI (right) and the implanted tether (left). **(C)** Radiograph immediately following induction surgery. The rails are outlined in blue to highlight the change in coronal deformity over time. The buckles with which the tethers are fixated can be seen on the left, the tether itself is radiolucent. **(D)** After 3 months, the scoliosis can be seen, including axial rotation. Also note the spinal growth seen as translation of the U-loops relative to the cranial and caudal anchors. **(E)** During the reduction surgery, the torsional spring force is reversed and two distraction springs on a (radiolucent) flexible PEEK rod are fixated to the left-side. **(F)** After 2 months, the scoliosis was reduced in the axial and sagittal plane, and was even overcorrected in the coronal plane.

Three months following the induction surgery, the animals were anaesthetized and CT scans were made to visualize scoliosis morphology and signs of implant failure. After exposure, the integrity of the tether was checked before it was released and subsequently removed. On the right side, the apical connector of the TSI was unloc-

13

ked and returned back to neutral. Mobility of the spine was assessed manually under dynamic fluoroscopic imaging. The TSI was then rotated 45° in the other direction, to reduce the rotational deformity and was then locked again. After randomization, the wound was then either closed immediately (TSI only-group) or an SDS was first implanted on the concave side (DSR-group). The SDS rod was fixated to the apical anchor and could slide through two sliding bearings that were mounted on the cranial and caudal anchor. Then the springs were tensioned to 70±5 N with the buttress.

After 2 months of follow-up, CT and radiography were performed. Following this, the minipigs were euthanized by intracardiac injection of pentobarbital, compliant with the 2020 American Veterinary Medical Association guidelines for the euthanasia of animals.[261] The implants were removed and checked for damage and the spines were manually tested for flexibility.

Radiographic Analysis

Coronal Cobb angle and instrumented kyphosis were measured on the coronal and sagittal CT reconstructions, More detailed analysis of axial rotation and relative anterior-posterior and convex-concave lengthening of both the intervertebral discs and vertebral bodies was performed using the ScoliosisAnalysis 4.1 software (Imaging Sciences Institute, Utrecht University). This validated method has been used previously and is detailed in Figure 4.[3,4,53] First, the superior- and inferior vertebral endplates and spinal canals were segmented in the true transverse plane (ie, accounting for coronal and sagittal tilt). Then, the centroid (ie area center) of the vertebral endplate and spinal canal was calculated and the anterior-posterior (AP) axis, which intersects both centroids, was drawn. The two points where the AP axis intersects the segmented endplate were defined to be the anterior and posterior midline points of the endplate. A line perpendicular to the AP axis, intersecting the centroid of the endplate, defined the left-right axis, and the left and right borders of the vertebra. The x- y- and z-coordinates of each point were determined and the anterior, posterior, concave, and convex lengths of each vertebra and intervertebral disc could then be calculated geometrically using the formula:

$$d(P1, P2) = \sqrt{(x1 - x2)^2 + (y1 - y2)^2 + (z1 - z2)^2}$$

Where P1 and P2 are two similar points on two different endplates (eg, anterior, posterior, left, right) that are to be compared, d is the shortest distance between these points, and $x1,2$, $y1,2$ and $z1,2$ are the respective 3D coordinates. By comparing the upper- and lower endplate of the same vertebra, lengths corresponding to that vertebra can be calculated, while comparing the lower endplate of one vertebra with the upper endplate of the vertebra below yields values corresponding to the IVD

space. Axial rotation of an endplate was defined as the angular difference between its AP axis relative to the AP axis of L3. The axial rotation of a vertebral body was determined by averaging the AP axis of the upper- and lower endplate. This yields a difference in rotation between the apical level (T14) and the most cranial (T10) and most caudal (L3) instrumented level. The apical rotation was then obtained by taking the mean of both rotation differences.

Figure 4. Radiographic measurements
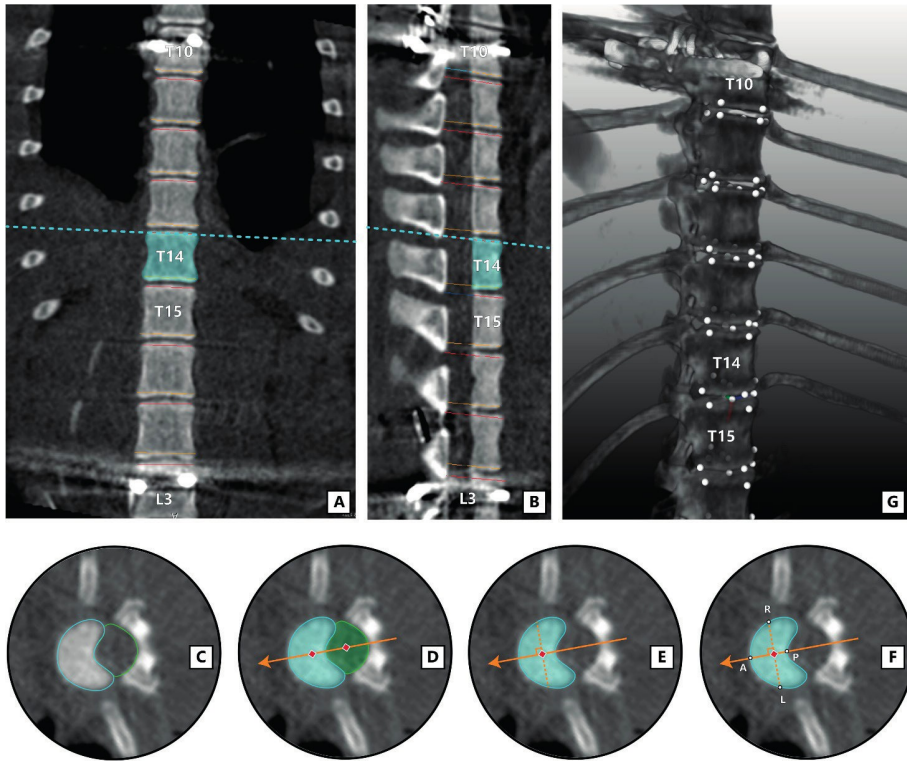
The endplates of each investigated vertebra (T14 in example above) are segmented. **(A–B)** First, lines are drawn that correct for coronal **(A)** and sagittal **(B)** tilt of each endplate, so that the corresponding axial view corresponds to the true axial plane. **(C)** In this plane, the endplate (blue) and spinal canal (green) are manually segmented. **(D)** The ScoliosisAnalysis v4.1 software computes the centroid of both the vertebral body and the spinal canal (red diamonds). The line through these centers defines the vertebral anterior-posterior axis (orange arrow). **(E)** A line perpendicular to this axis, intersecting the centroid of the vertebral body is then constructed (dashed orange line). **(F)** Where these two lines intersect the segmentation of the vertebral body, the following points are drawn: anterior (A), posterior (P), left (L) and right (R). **(G)** The x-, y- and z-coordinates of each point of each endplate are extracted, and relevant lengths and angles between endplates are calculated.

13

Statistical Analysis

Prospectively, a power calculation was performed based on our earlier induction animal study.[259] The study was powered to show a difference in correction capabilities between the DSR-group and the TSI only-group after the introduction of the reduction implants. To detect a difference in coronal Cobb angle between groups of 5° (SD 3.0), with a power of 80% and an alpha of 0.05, six animals per group were needed. Differences in curve morphology between start of the induction period (immediately following induction surgery) and the end of the induction period (after 3 months, just before reduction surgery) were calculated for all 12 animals and shown as mean ± SD. Following this, paired t-tests comparing both timepoints were performed. If the residuals of differences were non-parametric, the Wilcoxon-signed rank test was performed. For the analysis of the reduction period, 2 way repeated measurement ANOVA was performed comparing both the DSR- and TSI-groups over time. Two-tailed significance for all analyses was set at p=.05. Statistical analyses and data visualization were performed with GraphPad Prism 9.2.0. (Graphpad Software, San Diego, CA, USA).

Results

General Outcomes and Complications

Mean age of the animals during the induction surgery was 7.4 months and mean weight was 20.3 kg, with no significant difference between groups. Weight increased in 5 months to 34.3 kg according to their normal growth charts.[260] During both the induction- and reduction phase, there were no major complications or malpositions of pedicle screws. All tethers functioned as expected and were intact and removed during the reduction surgery. The spines remained flexible in the instrumented segment and the axial torque was successfully inverted in all minipigs. One of the minipigs suffered a deep surgical site infection following reduction surgery. Subfascial pus collections were seen on the CT scan obtained pre-euthanasia, although no clinical symptoms of infection were observed in the months before. Tissue and pus cultures obtained post-euthanasia showed infection with Trueperella pyogenes. All TSI implants were intact upon removal with no signs of substantial wear of the bearings. In one animal in the DSR-group, the SDS PEEK sliding rod buckled out which negatively influenced the distraction force. Curve morphology results of this minipig were included in all analyses.

Radiographic Outcomes

Significant changes were induced in all evaluated radiological parameters during the induction period (Table 1). Cobb angle increased from 6.2° immediately postoperatively, to 20.4° after 3 months. Instrumented kyphosis changed from 6.2° to -4.9°. Axial rotation of the apical level increased from 6.5° to 13.1° at the end of induction. The anterior spine lengthened during induction, with modest but significant changes in the vertebral bodies (A–P ratio from 0.98 – 0.99), and larger changes in the IVD (A-P ratio from 1.12–1.19).

13

Table 1. 3D curve morphology during induction period

	Immediately after induction surgery (N=12)	End of induction period (N=12)	P value
Coronal Cobb angle (°)	6.2±3.2	20.4±4.3	<0.001
Instrumented kyphosis (°)[a]	6.2±5.4	-4.9±5.3	<0.001
Apical axial rotation (°)	6.5±2.9	13.1±5.6	<0.001
Relative anterior lengthening[b]			
Total A-P ratio	1.01±0.01	1.02±0.01	<0.001
Vertebral body A-P ratio	0.98±0.01	0.99±0.01	0.049
Intervertebral disc A-P ratio	1.12±0.08	1.19±0.04	<0.001

[a]Negative value represents a lordosis in the instrumented segment.
[b]A-P ratio >1 denotes longer anterior length compared to posterior length.

Changes after the 2 month reduction period for both groups are shown in Table 2. For the TSI only-group, Cobb angle reduced from 22.5° to 6.0°. For the DSR-group, the curve was overcorrected from 18.3° to -9.2°. The change in coronal curve was significantly larger in the DSR-group. For the sagittal plane, the instrumented kyphosis in the TSI only-group changed from -4.6° (ie, lordosis) at the end of induction to 4.3° (ie, kyphosis) at the end of reduction. In the DSR-group, a change from lordosis to kyphosis was seen as well, from -5.2° to 25.0°. The induced kyphosis was significantly greater in the DSR-group. In the axial plane, the mean apical axial rotation (ie, the relative rotation of level T14 compared to the mean rotation of the most cranial and caudal instrumented level) for the TSI only-group decreased from 15.0° to 5.4°. For the DSR-group, this rotation similarly decreased from 11.2° to 3.5°. Figure 5 shows the mean rotation per level for each of the groups. In both groups, axial rotation can be observed immediately following induction surgery. In terms of distribution of rotation at the end of induction, a gradual increase is observed from the non-apical areas towards the apical area. In both groups, the rotation appears to be symmetrically distributed between the cranial and caudal part of the spine.

Table 2. 3D curve morphology during reduction period

	TSI only-group (N=6)			DSR-group (N=6)			P value between groups[d]
	End of induction period	End of reduction period	P value (TSI only-group)[c]	End of induction period	End of reduction period	P value (DSR-group)[c]	
Coronal Cobb angle (°)	22.5±3.9	6.0±2.3	<0.0001	18.3±3.1	-9.2±7.3	<0.0001	0.0123
Instrumented kyphosis (°)[a]	-4.6±4.4	4.3±3.9	0.0015	-5.2±5.6	25.0±6.8	<0.0001	<0.0001
Apical axial rotation (°)	15.0±3.7	5.4±3.4	0.0130	11.2±4.6	3.5±5.1	0.0202	0.6494
Relative anterior lengthening[b]							
Total A-P ratio	1.02±0.001	1.01±0.01	0.0109	1.03±0.01	0.98±0.01	<0.0001	0.0004
Vertebral body A-P ratio	0.99±0.01	0.98±0.01	0.4055	0.99±0.01	0.97±0.01	<0.0001	0.0017
Intervertebral disc A-P ratio	1.19±0.03	1.12±0.04	0.0239	1.19±0.04	1.05±0.07	0.0004	0.0622

[a]Negative value represents a lordosis in the instrumented segment.
[b]A-P ratio >1 denotes longer anterior length compared to posterior length.
[c]P **value** related to the change over time within one group (paired t-test).
[d]P value related to the change over time between groups (2-way repeated measure ANOVA).

13

Figure 5. Vertebral axial rotation over time
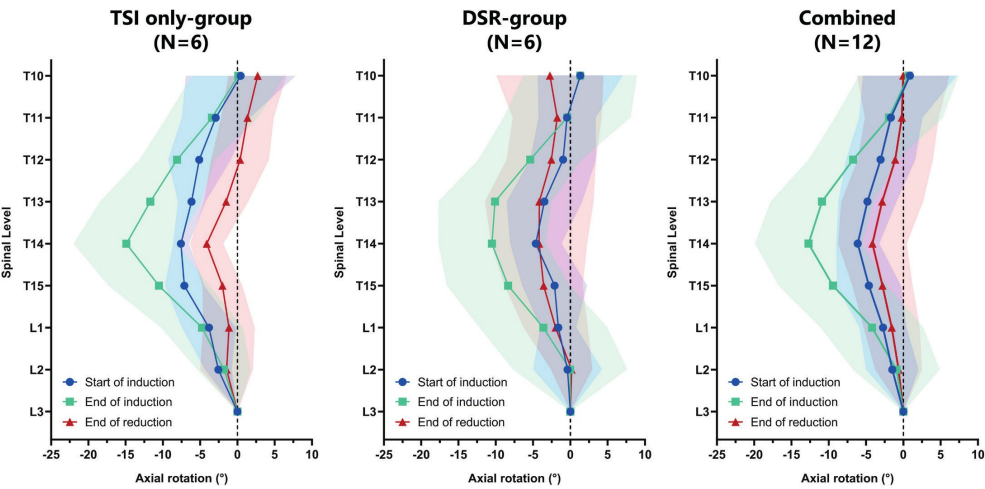
Cumulative rotation of each vertebra relative to the most distal instrumented level (L3). Mean values and standard deviations (shaded area) are shown. Negative values represent a right-sided rotation.

Both the TSI only-group and DSR-group were able to (partly) reduce the anterior lengthening of the IVD during the reduction period (Figure 6). However, only in the DSR treatment, did we also find a significant posterior lengthening of the vertebral body, indicating asymmetrical growth (A–P ratio 0.99–0.97).

Figure 6. Relative anterior spinal lengthening over time
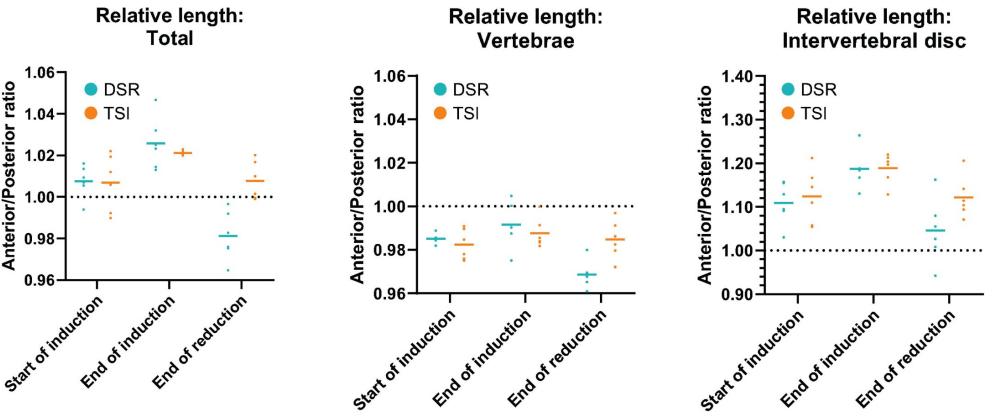
The relative lengths (anterior length/posterior length) of both groups are shown, for the total spine (ie, vertebral bodies + intervertebral discs, left), for the vertebral bodies alone (middle) and for the intervertebral discs alone (right). A value > 1 indicates a segment that is longer anteriorly than posteriorly, as is common in human scoliosis.

Discussion

The current study investigated the potential of reducing scoliosis with instrumented apical derotation alone (TSI only-group) or in combination with posterior distraction (DSR-group). We used the same TSI implant to first induce scoliosis, a method that we previously showed to generate a very predictable idiopathic-like spinal deformity that remained for months, even after removal of the implants.[259]

By applying torque only (with the TSI), almost complete reduction of axial rotation could be achieved within 2 months. This resulted in correction of the coronal and sagittal plane as well, likely as a consequence of coupled motions in the spine,[262,263] but complete reduction could not be achieved. By adding a distraction force (SDS) to the TSI (thus utilizing the DSR concept), considerably more correction and even over-correction was obtained. This correction could be related directly to reduction in the typical relative anterior lengthening that is mainly present in the IVD, a pheno-menon that we described extensively for human scoliosis.[3,4,53] This finding shows that by combining axial torque and concave distraction (DSR) we have a powerful tool to correct scoliosis simultaneously in all planes. However, it also indicates that the forces should be tailored to the specific condition as overcorrection is a risk. One way to mitigate this is to selectively release one of the forces when full correction in that plane has been achieved. Due to the position of the implant and the familiarity with this approach, this would be a minimally invasive procedure. Besides full cor-rection, we observed that normal growth and mobility of the instrumented segment was maintained.

In our opinion, this brings us one step closer to our goal of curing scoliotic spines in adolescents. This would require a paradigm shift in scoliosis care, namely that patients be treated surgically at an earlier age, perhaps already in the range of curves which are currently braced (30°–50°). We propose that DSR may replace those brace treatments that are likely to fail or those that will likely end with considerable remai-ning curves. Compared to bracing, DSR has the obvious drawback of requiring a surgical intervention. However, the implant can be inserted less invasively and after insertion, the burden for both patients and caregivers will be much lower as there are no mobilization restrictions and no compliance issues. Furthermore, the transmis-sion of forces through DSR's internal brace concept is superior to that of an external brace, especially for correction of the axial rotation.

DSR is not the first surgical technique to attempt gradual correction of AIS curves in the growing spine. In recent years, an increasing body of evidence has been ge-nerated wherein growth modulation has been achieved through anterior vertebral body tethering (AVBT). However, we believe AVBT has several disadvantages when compared to DSR. It halts growth on the convex side, and is limited in the amount of correction that can be achieved, in particular in the axial plane.[264] In contrast, DSR is

13

able to continuously correct all planes simultaneously, whilst stimulating (not halting) the shorter concavity of the curve.

In addition to its use in AIS patients, DSR could also be used in growing EOS patients, as DSR has considerable advantages over current "growth-friendly" implants. Especially in older EOS patients (ie, "tweeners"), curve correction is often poor and complication rates are high, which has led to several studies concluding that spinal fusion in these patients may be more effective than "growth-friendly" treatment. [265,266] DSR allows for increased apical derotation, while its flexibility decreases stress- shielding of the spine, which may ultimately lead to reduced implant stresses and implant complications.[244,267] However, since the time interval until skeletal maturation is longer than for AIS, DSR treatment of EOS patients may be somewhat unpredictable, an issue that is currently also observed in younger patients (Sanders 1–2) treated with AVBT.[264,268]

Limitations of the current study are mainly related to the use of an animal model. Although the scoliosis morphologically resembles human scoliosis more than any other animal model, we do not know exactly how a human scoliotic spine will react to these dynamic forces. Based on our clinical experience using only spring distraction forces, especially idiopathic curves can be very difficult to correct or even control, suggesting that the etiological mechanism remains to be overcome.[59,113] Future fundamental and clinical studies will teach us more on this important aspect of the technology.

Conclusion

In our representative idiopathic-like, scoliotic animal model, correction with only axial torque was able to correct rotation of the apex, in addition to partially correcting the coronal curve, apical lordosis and anterior lengthening of the IVD. However, adding posterior distraction to the axial torque (DSR), resulted in stronger correction in the coronal and sagittal planes, in addition to posterior vertebral growth modulation.
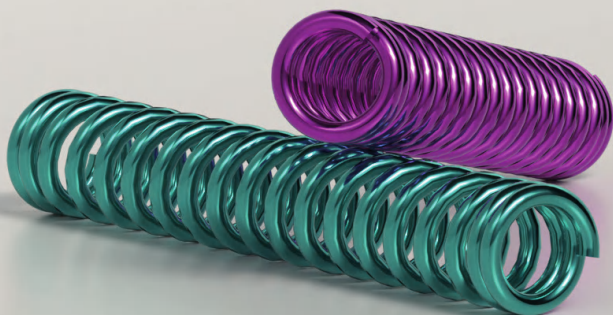
Chapter 14
General Summary and Discussion

J.V.C. Lemans

Scoliosis remains one of the most fascinating diseases in the field of orthopaedics. The contrast between the obvious phenotype and its somewhat enigmatic etiology is striking and has been the subject of intense study for several centuries. The disease, and the treatment thereof, have even given the field of orthopaedics its name (orthos=straight; paidion=child), a term constructed by the French physician Nicolas Andry, who first mentioned it in his 1741 book titled: "Orthopædia: Or the Art of Correcting and Preventing Deformities in Children".[269] The face of this book has become the global icon of orthopaedics, a crooked tree, which is being guided to be straight (Figure 1).

Figure 1: The cover of "Orthopædia: Or the Art of Correcting and Preventing Deformities in Children"
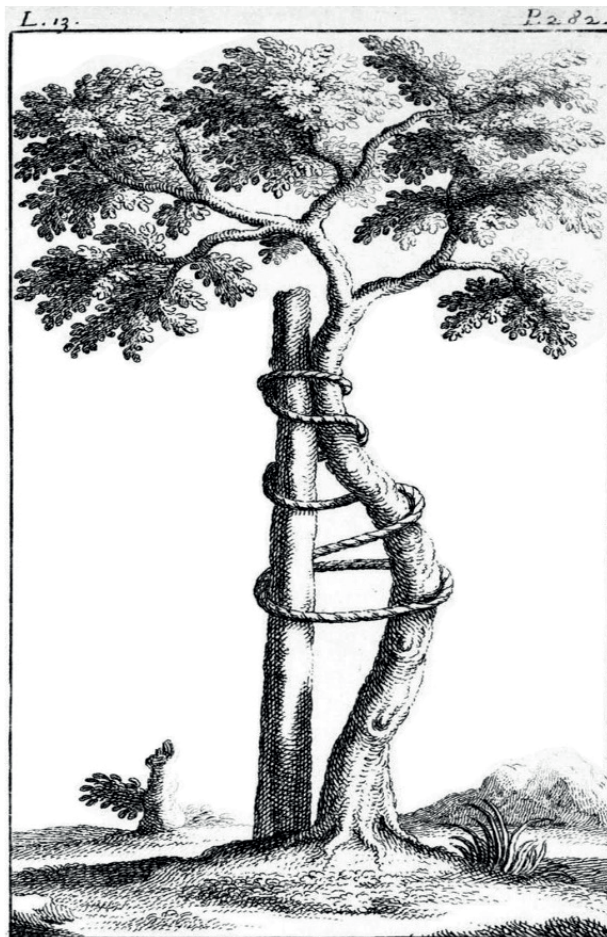
However, realigning the spine during growth has proven to be extremely difficult. While bracing in AIS can certainly be effective (if compliance is adequate), the results

for EOS remain disappointing. Before "growth-friendly" techniques were available, EOS was therefore a disease with a poor prognosis due to pulmonary insufficiency. [144,270] Although pedicle screw instrumentation revolutionized surgical treatment of AIS, but for EOS, an early spinal fusion resulted in truncal shortening and suboptimal respiratory function.[14]

However, in the last two decades, new techniques have been developed that enabled correction of the curve while maintaining growth. From non-operative Mehta casting to surgical innovations like TGR, Shilla, VEPTR, MCGR and VBT, these techniques resulted in a surge in EOS research, in particular the pulmonary effects of EOS, its classification and in HRQoL outcomes in EOS.[15,149,170,198,199,214,218,219,271]

Despite the recent innovations, treatment of EOS is still highly heterogenous, many surgical treatments are often unpredictable, have specific disadvantages and sometimes yield disappointing results. When we were faced with a patient for which all contemporary EOS strategies were not an option, we had to go to the drawing board to envision an implant that could do the job; that implant is what we now call the SDS. We started with one tiny piece of a complex puzzle. A puzzle which, when completed, shows us what an ideal "growth-friendly" implant looks like. In **Chapter 1**, we identified many questions, i.e. missing pieces of the puzzle. In this thesis, we have gathered many of these important pieces. Some were easy to find (the corners, so to say), others were excruciatingly difficult and are still missing. Hopefully, at the end of this chapter, when you squint through your eyes and look at the puzzle in its current state, you will see what the completed picture is supposed to look like.

Part I: A new philosophy laid the groundwork for the clinical investigations of SDS. In **Chapter 2**, we have tried to provide estimations for the limits of distraction forces of the pediatric spine. Through extensive review of clinical and biomechanical lite-rature we estimate that maximum forces of 200N (age 5-6), 250N (age 7-8) and 300N (age 9 and above) could be applied safely. These values were the maximum limits that were used in the subsequent clinical studies. It is likely that higher forces can be tolerated, as forces in TGR distractions and HGT are often higher than 300N. However, the current force limits includes a conservative safety factor, to account for the fact that the spring force is continuous, not subject to stress relaxation and cannot be easily released. The importance of employing such a safety factor was shown by one of the early SDS patients, who had neurofibromatosis type 1 (NF-1) and presented with EOS with a major curve of 58°. She was initially treated with a TGR when she was 7 years old and underwent two successful TGR lengthenings. At age 9, she was converted to a bilateral SDS configuration (75N on each side). She had no peri-operative complications and an uneventful admission. However, after two weeks, she presented with a complete epiphysiolysis of the lower endplate of

14

T4, just below the proximal instrumented levels (Figure 2), the structure shown in **Chapter 2** to be at risk when distraction forces are too high.

Figure 2: Epiphysiolysis of endplate in NF-1 patient following SDS
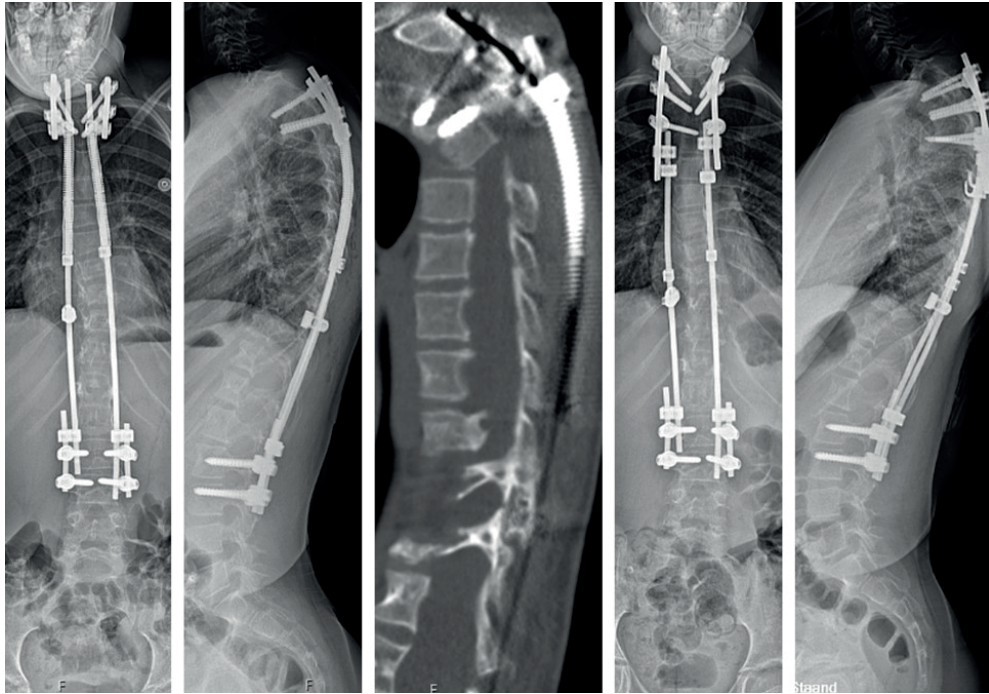
The two left pictures show the post-operative situation after SDS implantation of the NF type 1 patient. The radiographs show excellent coronal and sagittal alignment. The middle picture shows the situation after 2 weeks, with a rupture of the lower epiphysis of T4. A remnant of the endplate can still be seen in the original position. The two pictures on the right show the configuration after re-operation, back to a TGR configuration.

She was re-operated to realign and fuse levels T2-T4. She made a complete recovery. According to the algorithm in **Chapter 2**, a force of 150N should have been safe to use. However, these calculations were based on normal bone- and soft tissue strength. It is known that children with NF-1 have bony dysplasias with reduced strength.[272] Due to this, we made the choice to exclude patients with bone- or soft tissue weakness (e.g. Marfan disease, Ehlers-Danlos disease, osteogenesis imperfecta) during studies with SDS. Obviously, the fact that the force generated by SDS cannot be controlled except through surgery (unlike MCGR, where the force can be completely removed in the outpatient clinic), makes it all the more important that the correct force is chosen at the initial operation. It is likely that in high-risk patients, smaller forces should be applied. However, which fraction should be investigated

further. This would be possible with FEA, where alterations can be made to the material properties of bone and tissues. These alterations could be based on retrieved tissues of patients with bone- or soft tissue weakness.

In **Chapter 3**, we determined differences between TGR and SDS EOS treatment in a representative finite element model. We demonstrated that additional lengthenings in TGR resulted in higher peak von Mises stresses in the rods compared to SDS treatment. The distribution of stresses was also different between strategies; SDS rod stresses were highest near the distal rod-screw interface. The effect of different spinal motions on implant stresses was not explored, this remains an interesting avenue of investigation in the future. What we did see was that SDS resulted in less stress-shielding of the intervertebral disc. If this is true, this has important implications. Several studies in EOS populations have suggested that treatment with either TGR or MCGR cause the IVD to lose height, which negates potential beneficial effects on vertebral modulation. The study by Rong et al. showed in 2D radiographs, that for the levels that are under distraction, the IVD height decreases 3.9%/year, compared to levels outside of the distraction, where IVD height increases 2.7%/year. [101] These results were confirmed separately in a 3D MRI study of SMA patients undergoing MCGR treatment.[102] After 5 years, a stagnation of IVD height, reduction of IVD volume, and degenerative IVD changes on MRI were seen. However, whether these changes were due to stress-shielding of the IVD, or due to fixation of the segment is unknown. We are currently investigating this effect in 2D and in 3D in our SDS patients, to determine whether this effect can be prevented using SDS.

Part II: From bench to bedside investigated whether SDS treatment is safe and effective. **Chapter 4** tested the SDS in four young patients with severe congenital anomalies. Two patients had severe scoliosis in the cervicothoracic region. The other two had a very rare thoracic lordosis caused by spondylocarpotarsal synostosis syndrome, that would lead to pulmonary complications or even death. These four patients showed correction of the curve and adequate spinal growth after SDS insertion. Some patients even showed continued curve correction over time. Most impressively, kyphosis was stimulated in all patients, coming from a mean of -6° (i.e. thoracic lordosis) pre-operatively, to 13° post-operatively, to 36° after 2 years follow-up.

Based on the efficacy seen in **Chapter 4**, we looked at a broader EOS population in **Chapter 5**. In total, 24 patients with a mixed etiology were chosen and treated with SDS and followed for at least 2 years. Overall, a 50% curve correction was seen that was maintained and more than 10mm of T1-S1 growth per year could be gained.

In **Chapter 6**, we address an issue that has plagued the EOS literature for some time, namely that all studies are based on retrospective cohorts. These studies are prone to selection bias and confounding.[181] In addition to this, the fact that there are

14

many differences between different centers, make it difficult to compare results from one center to the other. In theory, randomization can circumvent these biases and the RCT is often regarded as the highest Level of Evidence. This is why, in **Chapter 6**, we designed the world's first RCT of EOS patients (BiPOWR), which compared two novel treatments, the SDS and the OWSER in a neuromuscular patient population. **Chapter 6** not only provided us with a clear protocol, it offers researchers and surgeons around the world a framework that they can use for any randomized trial in the field of EOS, and which economic, psychological, organizational and statistical factors should be considered. In **Chapter 7**, the results of the BiPOWR RCT are presented. The study showed that the neuromuscular EOS population is extremely fragile, as 2 of the 30 patients passed away during their 1 year follow-up. However, the SDS and the OWSER provided around 50% initial curve correction, that could be maintained at 1 year follow-up. Both systems also provided adequate spinal growth. However, there were more SAEs and UPRORs in the OWSER group compared to the SDS group. The BiPOWR study also shows the weaknesses of the RCT design.[159] First, the selected RCT populations are very restricted, to allow for a homogenous patient group that can be compared fairly.[159,180] This makes generalizability difficult, and in a (relatively) small research field such as EOS, this leads to long inclusion periods, even when utilizing a multicenter approach. It took us around 2-3 years to include 30 patients. In addition, for studies that follow patients for a long period of time (ideally until several years after the end of growth), gathering all data in an RCT takes a huge amount of time and money. This is why the choice was made in BiPOWR to set the initial sub-analysis endpoint at 1 year. Obviously, all patients will be prospectively followed outside the protocol until after end of growth, so that we can report efficacy- and complication results across the entire period of growth of these children.

In **Part III: Optimizing Spring Distraction System treatment**, we try to optimize SDS treatment with iterations based on findings from the ongoing study. First, we evaluated growth and complications in an initial SDS cohort and compared them to a MCGR cohort in **Chapter 8**. We saw similar complication rates in both groups, but interestingly, there were several complications that were group-specific. Of course, it needs to be said that not all complications are always preventable. However, for SDS, three important complications were identified that could be addressed relatively easy. These were:

1. Rod fractures
There is a clear relation in rod diameter used and the propensity for rod fractures. [118] Because the first patients for whom the SDS was designed were very young, we chose 4.5mm rods as a standard to house the springs. However, in older patients

that were included in the study later on, this resulted in rod fractures in 3/18 (17%) patients.

2. Implant hyperkyphosis

Since the side-to-side connectors need to be slightly oversized to allow for easy sliding of the rod (and prevent high frictional forces), the rod tends to angulate in the sagittal plane due to the distraction forces. This can cause problematic posterior protrusion of the implant, which in turn can lead to skin issues.

3. Ilio-sacral anchor failure

In neuromuscular EOS patients, the distal anchor was often created with ilio-sacral screws. We observed mechanical complications of this fixation like screws backing out or loosening of the connectors.

Following **Chapter 8**, we tested whether the measures below were effective in preventing these complications.

1. Increase rod diameter

We increased the diameter of the CoCr rods from 4.5mm to 5.5mm. This extra 1mm is not an issue when low profile screws are used.

2. Use two stacked side-to-side connectors

This lowers the potential for angulation of the rod, thus also lowering the risk of implant protrusion. However, it will add rigidity to the system which may cause more fatigue issues.

3. Adding a cross-connector to the distal anchor site

Adding a cross-connector between the two distal anchor rods, increases the rigidity of the ilio-sacral screw construct, which theoretically reduces their risk of failure.

In **Chapter 9**, these design improvements were compared to the initial SDS cohort. In addition to the above changes, new spring types were also introduced. Instead of a one-size-fits-all 75N spring, we designed 100N and 50N springs. These could be used in a differential configuration (e.g. 100N on the concave side and 50N on the convex side). With the implemented changes, the number of complications and UP-RORS were reduced by about 70%. Interestingly, no cases of rod fracture, implant protrusion and distal anchor failure were seen in the second-generation cohort at the short follow-up evaluation, which underscores the value of the continuous cycle of optimizations.

14

In **Chapter 10**, we looked beyond the standard radiographic parameters that are often a main outcome in scoliosis research, and investigate the effect of SDS surgery on HRQoL of patients (and parents/caregivers). We saw that immediately following surgery, scores in many domains decline (e.g. pain, transfers, energy level). This feels intuitive, as the surgery and post-operative admission period are moments that children and parents look towards with some amount of apprehension. Fortunately, the scores increase again to their initial level at 6 month follow-up and even continued improving in many domains after that. In addition, we observed that the changes over time were similar for all etiological groups, and also that UPRORs did not negatively impacted HRQoL scores. These results allow us to adequately counsel patients and parents, as to the subjective changes they can expect between surgery and 2 years of follow-up.

In **Chapter 11**, we compared different etiological EOS groups to see whether outcomes other than HRQoL (which was investigated in **Chapter 10**) differ between idiopathic, neuromuscular and congenital/structural EOS patients. We saw that initial post-operative curve correction was similar between all etiologies. However, during follow-up, the coronal curve in idiopathic patients could not be fully controlled and increased more than those in congenital and neuromuscular patients. This could be due to the idiopathic patients being older at surgery, and potentially require higher spring forces, or it could be due to the difference in configuration that is used in idiopathic patients (who mostly receive a hybrid construct with a convex apical control rod) compared to neuromuscular and congenital patients (who most often receive bilateral spring construct without an apical control rod). There is evidence however that apical control constructs are effective in maintaining curve correction and spinal growth in TGR constructs.[226] It is possible that in systems that allow for continuous growth, the continuous propensity of the apex to move to its original offset position leads to laterally directed forces on the apical rod (which wants to move with the apex). These lateral forces (that increase under the influence of gravity) are then passed on to the proximal and distal sliding anchors, increasing friction and counteracting some of the longitudinal forces that want to lengthen the spine and further correct the curve. This might also be why patients with Shilla growth-guidance, which always have several levels of apical control, generally show a tendency towards curve progression.[273] However, recent studies investigating apical control in TGR do show that patients who undergo this technique, ultimately have better pulmonary function at follow-up, even if corrected for T1-T12 height. This means that we should not blindly stare at how the coronal curve changes over time, but also direct our attention to functional outcomes. At the same time, future efforts investigating SDS should be directed to minimize frictional forces between connector and rod, to have optimal force transfer and minimal metal wear. Currently such an axial sliding bearing (ASB) is part of the new IMDD for the study.

Finally, in **Part IV: Double Spring Reduction: The move towards two springs** we add a sophisticated torsional spring to the distraction concept shown in the previous chapters. In **Chapter 12**, we first induced scoliosis in 14 minipigs. Six received induction with only a unilateral flexible tether, and 8 were induced with both a tether and the torsional spring giving an axial torque. After 3 months, the torsional spring induced significant axial rotation while preserving spine mobility and growth potential. This coincided with significant anterior lengthening, mainly in the discs, which is also what is seen in all types of scoliosis.[53] After removal of the implants, a large part of the scoliosis remained in all 3 planes, confirming the structural nature of the changes. Interestingly, in a previous animal study in large domestic pigs with a previous version of the torsional spring without a tether, we saw only axial rotation being created, and only a minor coronal and sagittal deformity.

Following this chapter, the important question that remained is whether distraction in combination with axial torque, is also able to revert the scoliotic changes. In **Chapter 13**, we investigate whether the induced scoliosis created in **Chapter 12** can be corrected. While derotation alone could correct apical rotation and some of the coronal deformity, when distraction was added (DSR), much stronger coronal and sagittal correction could be obtained. Interestingly, when adding posterior, concave distraction, overcorrection in the coronal plane was even observed after several months. This means that for each patient, there exists a torque and distraction force that will completely correct a 3D scoliosis. However, to prevent overcorrection, we will either need to choose the initial torques and forces carefully, or release them (e.g. by explanting the DSR device) if the curve has been completely resolved. The latter option seems most feasible, since curve characteristics are difficult to predict but can be monitored easily.

Which pieces of the puzzle do we still have to find?

One area that is as of yet unexplored is the long-term effects of SDS treatment. The previous studies show efficacy and safety in the short- to medium-term follow-up. However, whether these effects persist until after the end of growth is not yet known. Currently, since the start of SDS treatment, a cohort of about 30 patients now have finished SDS treatment and have undergone definitive fusion of the spine. These 'graduates' (defined as either having undergone spinal fusion, or who have reached skeletal maturity) will be systematically analyzed to find out whether spinal modulation has occurred and whether this modulation is different compared to contemporary treatments. Analyzing the post-graduate outcomes of these patients is currently underway.

14

We also do not yet know whether SDS treatment is able to modulate the vertebrae and intervertebral discs during growth and if it can guide these structures towards a healthy shape and alignment. When investigating modulation of the vertebral bodies, an avenue of investigation is to analyze the 3D shape. This means reverting the 3 key components that have been shown to be a part of every scoliosis:

1. Coronal plane: By distracting mainly the concave side, can we induce the concave side of each vertebra to become larger, thus reducing the coronal deformity?
2. Sagittal plane: By distracting the posterior side, can we induce posterior lengthening, thus reducing the relative longer anterior length and increasing kyphosis?
3. Axial plane: By unwinding the spine and using apical control, can we reduce the axial rotation of the apical levels?

We also need to know whether distraction induces any changes of the IVD, namely whether the shape can be permanently modulated as well as whether the nucleus pulposus can be reduced. Also, imaging of the IVD can show whether distraction has detrimental effects on IVD height and -health. To investigate this, we require 3D imaging of the spine, which has historically been performed with CT. While this produces excellent bony visualization, CT imaging uses harmful ionizing radiation, which might cause potential malignancies in the future. It has been shown that AIS patients have a 5 fold increased risk for developing cancer during their life, owing to the use of radiographs and CTs.[274] Interestingly, a recent Dutch study found no clear difference in cancer prevalence between AIS patients and controls.[275] However, for EOS patients, the additional risks are likely larger, as they are subjected to radiation from an earlier age and generally require more imaging studies. With the advent of MRI and the recent innovation of synthetic CT (which are created from MRI images), we can answer the above questions without the aforementioned harmful radiation. [276,277] Using MRI for this has the added benefit that more information is gained of the soft tissues such as the IVD, which cannot be seen in detail when using CT.

Looking into the future of SDS

Since the first SDS patient in 2015, we have now worked almost a decade on investigating this technique and trying to improve it. During that time, many improvements have already been made. One major improvement is the use of low-friction connections in the SDS version that is currently valorized (Figure 3). It uses two UHMWP bearings per connector that are housed in the SDS connector. This has several advantages. First, the longer length of the connector prevents kyphosis of the rods. Second, the connector ensures optimal transfer of forces to the sliding rods

as it prevents friction between the rods and the connector. This in turn reduces the amount of metal debris that is of concern when using "growth-friendly" implants. It is known that the MCGR actuator generates large amounts of metal debris, which stains tissues black and increases serum metal ion levels.[166] Several studies have shown increased serum titanium levels in MCGR patients compared to controls. One study found mean titanium serum levels of 10.2 mcg/L in MCGR patients vs. 2.8mcg/L in unoperated EOS patients.[278] Another recent study found that at the end of MCGR treatment titanium levels were increased in 87% of patients, with a median titanium serum level of 6.6mcg/L.[167] The clinical implications of these high serum metal ions have not completely been elucidated. Unlike cobalt and chromium levels, no obvious detrimental health effects have been identified when regarding titanium, although it has been shown that titanium particles can migrate and accumulate into liver, spleen and lymph node tissue.[279] However, since "growth-friendly" implants are used in young, often vulnerable children, the amount of wear debris should be as low as possible.

Bench testing has shown that the ASB indeed greatly reduces metallosis compared to side-to-side connectors. However, it has yet to be tested in patients, which takes years of preparation, especially with the current (very strict) Medical Device Regulation (MDR). When the new version of SDS is ultimately implanted, blood samples of patients will have to be analyzed to measure serum metal ion levels, and compare these to the previous versions of SDS and other "growth-friendly" implant systems.

Figure 3: SDS with new low-friction connector

The most recent version of SDS uses a connector that uses two UHMWP low-friction bearings, that minimize friction forces between the connector and the sliding rod.

When the implant design has been finalized, there is still the question on how to optimally use it. Based on the studies in this thesis, we believe an ideal configuration and treatment regimen exists for each EOS patient, based on age, etiology, curve size- and type. Younger patients have more growth and thus need longer rod- and spring length, while patients with larger or stiffer curves likely need stronger springs to be corrected. Solving these equations will not be easy and will likely require larger cohorts of patients. In silico studies could be of use again to predict the patient-specific optimal configuration. Already, individualized FEMs are used to predict the efficacy of vertebral tethering.[91,280,281] Multiple models could be compared and the spring with the highest predicted efficacy could be selected. Simultaneously, areas of high implant stresses could be pre-operatively identified, and accounted for. However, this would be a time-consuming endeavor, although much of this work can likely be automated in the future.[282]

Looking into the future of DSR

And what can we expect from DSR? If we apply the right forces and torques in just the right places, can we revert a scoliotic spine to a 'healthy' alignment and end up with a spine that is indistinguishable from the spine of a child without scoliosis? This means that we are able to cure the scoliotic spine! We know that this is possible with Mehta casting in the very young, but such a result has never been seen in AIS patients. For that to happen, several things need to occur. We know that distractive forces acting on the vertebral growth plates, can modulate their morphology if given enough time, this is known as the Hueter-Volkmann law.[283] Other groups have shown that employing the Hueter-Volkmann law, for example in vertebral body tethering, can (partly) correct scoliotic changes in the vertebral bodies.[284] However, as is also known from the tethering literature, it is very difficult to predict how quickly these changes take place, and many patients show under- or overcorrection of the bony changes.[268] We also know, partly from work in our own department, that during the change from a healthy alignment into scoliosis, the nucleus pulposus moves towards the convexity. There is evidence that the nucleus pulposus can move back into the midline, but we do not know if we can make it stay in the midline position if we remove corrective forces.[277] Finally, it is currently unclear whether the other soft tissue changes which are part of scoliosis can be reverted.[285,286]

It is possible that complete resolution of AIS can be achieved if we start treatment early and aggressively. This would involve DSR implantation during the period of growth, and explanting the device again at the end of growth. This means treating patients that would now undergo bracing (e.g. with coronal curves of around 25°), which is much earlier than we are doing currently. To make this possible, we must show that DSR can generate predictable and superior results in the growing spine,

something that is the subject of animal- and computational studies that are already being performed. These studies will need to show how certain forces and torques affect the spine over time, so that we can know when to start treatment, which forces and torques to use in different ages and curve sizes and when it is safe to remove the DSR. Obviously, this should be followed with clinical studies, first conducted in EOS patients that are now treated with SDS, that aim to translate these results to human patients.

Optimal DSR treatment also requires AIS curves to be detected at an early age, ideally before the 20-25° range. For that, we need to detect which spines are at risk of becoming scoliotic. A potential candidate parameter for this use is the posteriorly inclined triangle (PIT) area, which has recently shown to predict which spines will progress into scoliosis and which will not in patients who initially did not suffer from scoliosis.[287] Finding these children without the need to radiograph everyone is the next challenge. Perhaps screening with radiation-free spinal ultrasound imaging could be the key for detecting eligible children from an early age, potentially even before they develop scoliosis.[288]

If we can detect scoliosis early and treat patients early with DSR, the following case could be a glimpse into the future of DSR treatment:

> *"A 9 year old girl visits the school physician, where scoliosis screening with a spinal ultrasound shows a 5° coronal curve and a large PIT area. She is referred to an orthopedic surgeon, who follows her to see whether the curve progresses over time. When she is 11 years old (pre-menarche), the curve is 20°. The choice is made to apply DSR. Based on bone age, weight and curve parameters, and pre-operative FE modelling, she receives 2Nm of torque and 100N of distraction. The curve gradually diminishes during the next years. When she is 15 years old (Risser 5), DSR is explanted. She grows into adulthood with a straight, flexible and healthy spine."*

This could be the future of scoliosis treatment.

Let's work to make it happen.

14
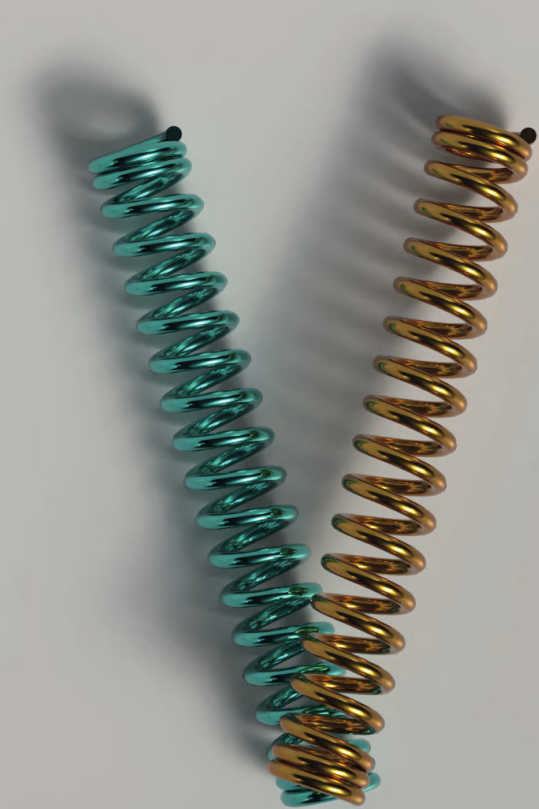
Appendix I: Nederlandse Samenvatting

Scoliose is één van de meest fascinerende aandoeningen in het veld van de orthopedie. Het contrast tussen het duidelijke fenotype en de enigszins raadselachtige oorzaak is opvallend en is al eeuwenlang het onderwerp van onderzoek. De ziekte en de behandeling ervan hebben zelfs de orthopedie zijn naam gegeven (orthos=recht; paidion=kind), een term die is bedacht door de Franse arts Nicolas Andry, die de term orthopedie voor het eerst noemde in zijn boek uit 1741 getiteld: "L'Orthopédie, ou l'Art de prévenir et de corriger dans les enfants les difformités du corps".[269] De omslag van dit boek is uitgegroeid tot het wereldwijde icoon van de orthopedie, een kromgroeiende boom, welke langzaam wordt geleid om recht te groeien (Figuur 1).

Figuur 1: De omslag van "L'Orthopédie, ou l'Art de prévenir et de corriger dans les enfants les difformités du corps"
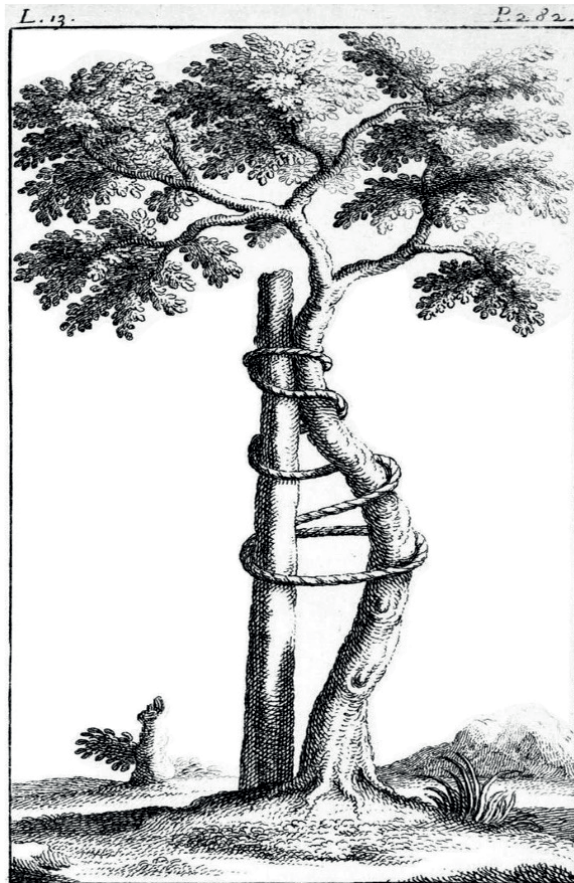
Echter, het recht maken van de rug gedurende de groei is ontzettend moeilijk gebleken. Hoewel het gebruik van een brace bij adolescente idiopathische scoliose (AIS) zeker effectief kan zijn, blijven de resultaten voor early onset scoliose (EOS) teleurstellend. Voordat groeisystemen beschikbaar waren, was EOS daarom een ziekte met een slechte prognose, vooral vanwege longfalen.[144,270] Met de opkomst voor pedikelschroeven kon AIS steeds vaker behandeld worden door middel van het vastzetten van de wervelkolom. In EOS leidt een vroege fusie echter tot verkorting van de borstkas en daarmee ook stagnatie of zelfs verslechtering van de longfunctie.[14]

In de afgelopen twee decennia zijn nieuwe technieken ontwikkeld waarmee scoliose kan worden gecorrigeerd terwijl de rug door kan groeien. Van Mehta-gips tot chirurgische innovaties zoals traditionele groeistaven (TGR), magneetstaven (MCGR) en werveltethering (VBT); al deze technieken hebben geleid tot een exponentiele toename van onderzoek naar EOS.[15,149,170,198,199,214,218,219,271] Ondanks de recente innovaties is de behandeling van EOS nog steeds niet goed gestandaardiseerd. Daarnaast zijn veel chirurgische behandelingen vaak teleurstellend of onvoorspelbaar en hebben ze elk specifieke nadelen. Toen wij werden geconfronteerd met een patiënt voor wie de huidige operatieve technieken geen optie waren, moesten we naar de tekentafel om een implantaat te bedenken die de klus kon klaren; dat implantaat is het veerdistractiesysteem (SDS). We zijn begonnen met een klein stukje van een complexe puzzel. Een puzzel die ons, als hij klaar is, laat zien hoe een ideaal groeisysteem voor EOS eruitziet. In **Hoofdstuk 1** hebben we opgeschreven welke stukjes van de puzzel nog missen. In dit proefschrift hebben we veel belangrijke stukjes verzameld. Sommigen waren makkelijk te vinden (de hoekjes van de puzzel), anderen hebben veel tijd en moeite gekost. Er zijn zeker ook nog stukjes die nog niet gevonden zijn. Als u aan het einde van het hoofdstuk naar de puzzel kijkt in zijn huidige staat, krijgt u, met wat voorstellingsvermogen, toch een mooi overzicht van het uiteindelijke plaatje.

In **Deel I: Een nieuwe filosofie** legden we de basis voor de klinische onderzoeken naar SDS. In **Hoofdstuk 2** hebben we schattingen gemaakt voor de krachtlimieten die gegeven kunnen worden op de rug van kinderen. Door een uitgebreid literatuuronderzoek waarin we keken naar klinische en biomechanische studies zagen we dat krachten van 200N (leeftijd 5-6), 250N (leeftijd 7-8) en 300N (leeftijd 9 en ouder) waarschijnlijk veilig gebruikt konden worden. Deze limieten werden ook gebruikt in de latere klinische studies. Het is goed mogelijk dat er misschien zelfs hogere krachten gebruikt kunnen worden, aangezien bij huidige behandelingen vaak een hogere kracht wordt gebruikt dan 300N. Echter, we hebben een veiligheidsmarge ingebouwd, omdat bij SDS de kracht continu wordt gegeven, en niet eenvoudig kan

A

worden gestopt als deze te groot blijkt te zijn. Eén van de eerste SDS-patiënten, een neurofibromatose type 1 (NF-1) patiënt bezocht de polikliniek met een bocht van 58°. Ze was initieel behandeld middels TGR toen ze 7 jaar oud was en was al enkele keren succesvol chirurgisch verlengd. Op de leeftijd van 9 jaar werd zij geconverteerd naar een bilaterale SDS configuratie (75N aan elke kant). Er waren geen complicaties rondom de operatie en ze kon snel worden ontslagen naar huis. Echter, na 2 weken had ze een complete epifysiolyse van de sluitplaat van T4, net onder de proximale geïnstrumenteerde niveaus (Figuur 2). Dit is ook de structuur die **Hoofdstuk 2** identificeerde als zwakke plek wanneer krachten te groot worden.

Figuur 2: Epifysiolyse van sluitplaat in NF-1 patiënt na SDS
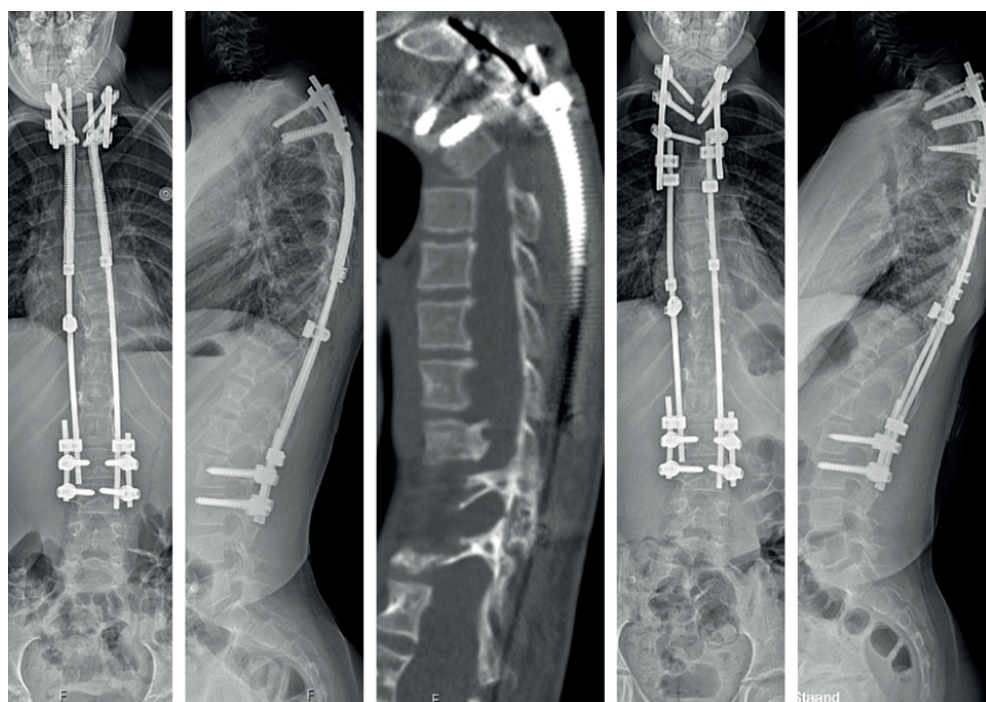
De twee linkerafbeeldingen laten de post-operatieve situatie zien na SDS implantatie bij de NF-1 patiënt. Er is een uitstekend coronaal en sagittaal alignement. Op de middelste afbeelding is de situatie na 2 weken te zien, met een ruptuur van de sluitplaat van T4. De twee afbeeldingen rechts laten de situatie zien na de heroperatie, terug naar een TGR configuratie.

Ze onderging een heroperatie om niveau T2 tot en met T4 vast te zetten, en herstelde volledig. Volgens het algoritme van **Hoofdstuk 2** had 150N veilig gebruikt moeten kunnen worden bij deze patiënt. Echter, deze berekeningen zijn gebaseerd op normaal ontwikkelde botten en weke delen. Het is bekend dat kinderen met NF-1

botdysplasieën kunnen hebben waardoor de botten minder sterk zijn.[272] Daarom hebben we besloten om patiënten met aandoeningen die het bot of de weke delen kunnen verzwakken (bijv. M. Marfan, M. Ehlers-Danlos of osteogenesis imperfecta) te excluderen in de studies naar SDS. Omdat na implantatie van SDS de kracht niet zonder heroperatie kan worden aangepast (in tegenstelling tot bijvoorbeeld MCGR, waar de kracht poliklinisch kan worden stopgezet), is het essentieel dat de juiste kracht wordt gekozen aan het begin van de behandeling. Waarschijnlijk moet bij de eerder genoemde risicopatiënten een lagere kracht gebruikt worden. Welke kracht dit moet zijn zal verder onderzocht moeten worden. Met eindige element analyse (FEA) is het mogelijk om materiaaleigenschappen aan te passen en hierop computeranalyses uit te voeren, waardoor de aangepaste limieten voor deze patiënten gevonden kunnen worden.

In **Hoofdstuk 3** onderzochten we verschillen tussen TGR en SDS behandeling in een representatief FEA computermodel. We demonstreerden dat TGR verlengingen leiden tot hogere von Mises spanningen in de staven vergeleken met SDS. De locatie van hoge spanning was ook verschillend tussen beide technieken; SDS spanning in de staaf was het hoogst nabij de distale schroef-staaf connectie. Tevens werd gezien dat in het SDS model, er minder stress-shielding van de tussenwervelschijf (IVD) was. Als dit in de praktijk waar is, heeft dat belangrijke consequenties. Meerdere studies in EOS groepen hebben laten zien dat met TGR of MCGR behandeling, de IVD hoogte vermindert over de tijd. De studie van Rong et al. Liet zien dat niveaus die onder distractie staan, de IVD hoogte met 3.9% per jaar afneemt, vergeleken met niveaus buiten de distractie, die nemen 2.7% per jaar in hoogte toe.[101] Deze resultaten werden bevestigd in een 3D MRI studie van SMA patiënten die MCGR behandeling ondergingen.[102] Na 5 jaar MCGR behandeling, werd er stagnatie van IVD hoogte gezien, alsmede een reductie van IVD volume en degeneratieve veranderingen van de IVD. Echter, of deze veranderingen ook werden veroorzaakt door stress-shielding is in deze studies niet onderzocht. We onderzoeken momenteel zelf dit effect in onze SDS populatie in 2D en 3D, om te kijken of dit fenomeen bij SDS patiënten ook optreedt.

Deel II: Van tekentafel tot aan het bed onderzocht of SDS behandeling veilig en effectief is. **Hoofdstuk 4** onderzocht SDS in vier jonge patiënten met congenitale wervelafwijkingen. Twee patiënten hadden een ernstige scoliose in de cervicothoracale wervelkolom. De andere twee patiënten hadden een zeldzame thoracale lordose die werd veroorzaakt door het spondylocarpaletarsale synostose syndroom. De thoracale lordose zou onbehandeld leiden tot longfalen of zelfs tot overlijden van de patiënten. In alle vier patiënten werd correctie van de bocht en voldoende groei van de wervelkolom gezien na SDS implantatie. Enkele patiënten lieten zelfs extra correctie zien naarmate de tijd vorderde. In alle patiënten werd kyfose gestimuleerd,

A

komende van gemiddeld -6° (thoracale lordose) pre-operatief, naar 13° post-operatief, tot zelfs 36° na 2 jaar follow-up.

Naar aanleiding van de positieve resultaten in **Hoofdstuk 4**, bekeken we de resultaten in een meer algemene EOS populatie in **Hoofdstuk 5**. In totaal werden 24 patiënten met verschillende EOS etiologie behandeld met SDS en gevolgd voor ten minste 2 jaar. Gemiddeld werd een 50% correctie van de bocht gezien die niet verslechterde. Tevens groeide het T1-S1 segment gemiddeld 10mm per jaar.

In **Hoofdstuk 6** richtten we ons op een probleem dat al lang speelt in de EOS literatuur, namelijk dat alle studies gebaseerd zijn op retrospectieve cohorten. Deze studies zijn vatbaar voor selectiebias en confounding.[181] Tevens zijn er vaak grote verschillen tussen verschillende centra, deze heterogeniteit zorgt ervoor dat resultaten van studies vaak moeilijk te vergelijken zijn. In theorie kan randomisatie deze vormen van bias omzeilen en de RCT staat daarom bovenaan in de hiërarchie van wetenschappelijk bewijs. In **Hoofdstuk 6** hebben we daarom 's werelds eerste RCT ontworpen die twee behandelingen voor EOS vergelijkt. Deze BiPOWR studie vergelijkt SDS en OWSER in een neuromusculaire EOS populatie. **Hoofdstuk 6** brengt ons niet alleen een duidelijk onderzoeksprotocol, het kan ook gebruikt worden als richtlijn voor andere onderzoekers. Zo kunnen ze zelf een EOS RCT opzetten en weten ze met welke factoren ze rekening moeten houden.

In **Hoofdstuk 7** presenteren we de resultaten van de BiPOWR RCT. De studie laat ten eerste zien dat de neuromusculaire EOS populatie erg kwetsbaar is, tijdens de studie overleden 2 van de 30 patiënten gedurende 1 jaar follow-up. SDS en OWSER gaven ongeveer 50% initiele correctie van de bocht, en deze correctie kon worden vastgehouden bij de 1 jaar follow-up. Beide systemen stimuleerden ook groei van de rug. Wel waren er meer SAEs en heroperaties in de OWSER groep. De BiPOWR studie laat ons ook de kwetsbaarheden van een RCT design zien.[159] Ten eerste zijn de RCT populaties erg restrictief, zodat een homogene groep overblijft die goed te vergelijken is.[159,180] Hierdoor zijn RCTs echter vaak slecht generaliseerbaar en zijn er vaak lange inclusieperiodes nodig. In de BiPOWR studie duurde het 2-3 jaar voordat we de benodigde 30 patiënten konden includeren. Ten tweede, als patiënten voor langere tijd gevolgd moeten worden (in de BiPOWR studie idealiter tot na het einde van de groei), kost een RCT design een enorme hoeveelheid tijd en geld. Hierom is gekozen om het eindpunt van de initiële analyse op 1 jaar te zetten. Uiteraard worden alle patiënten daarna prospectief gevolgd tot na het einde van de groei, zodat we de effectiviteits- en veiligheidsresultaten over de gehele groeiperiode kunnen rapporteren.

In **Deel III: Optimaliseren van SDS behandeling** proberen we SDS behandeling te optimaliseren door middel van initiële bevindingen uit de lopende studies. In **Hoofdstuk 8** vergeleken we groei en complicaties tussen het initiële SDS cohort en een

historisch MCGR cohort. We zagen vergelijkbare complicatiecijfers in beide groepen, maar het type complicaties was anders in de beide groepen. Uiteraard zijn niet alle complicaties te voorkomen, maar voor SDS werden drie belangrijke complicaties gezien die relatief eenvoudig voorkomen kunnen worden. Dit waren:

1. Staafbreuken

Er is een duidelijke relatie tussen diameter van de staaf en het risico op het ontstaan van staafbreuken.[118] Omdat de eerste SDS patiënten erg jong waren, is destijds gekozen voor 4.5mm staven. In oudere (en dus zwaardere) patiënten, leidde dit tot staafbreuken in 3/18 (17%) patiënten.

2. Implantaat hyperkyfose

Omdat de connectoren waar de staven in schuiven iets groter moeten zijn dan de staven zelf (zodat ze makkelijk kunnen glijden), hebben de staven de neiging om in de connector te kantelen in het sagittale vlak. Dit kan leiden tot protrusie van het implantaat naar dorsaal, wat op zijn beurt kan leiden tot druk op de huid.

3. Falen van ilio-sacrale schroef

In neuromusculaire EOS patiënten gebruiken we vaak een ilio-sacrale schroef als distale anker. We zagen mechanische complicaties van deze fixatiemethode, zoals schroeven die uit hun originele traject draaiden of loslating van de connectoren.

Na **Hoofdstuk 8** hebben we enkele maatregelen ingevoerd die bovenstaande complicaties mogelijk kunnen voorkomen.

1. Vergroten van de staafdiameter

We hebben de diameter van de CoCr staven vergroot van 4.5mm naar 5.5.mm. Deze extra 1mm leidt niet tot meer protrusie als low-profile schroeven worden gebruikt.

2. Het gebruik van twee gestapelde staafconnectoren

Dit vermindert het risico op kantelen van de staven in de connectoren. Hierdoor wordt ook het risico op implantaatprotrusie kleiner. Als neveneffect leidt het wel tot een meer rigide systeem.

3. Toevoegen van een cross-connector aan het distale anker

Door het toevoegen van een cross-connector tussen de twee distale ankerstaven, vergroten we de rigiditeit, waardoor het risico op implantaatfalen kleiner wordt.

In **Hoofdstuk 9** werden deze ontwerpverbeteringen toegepast in een nieuw cohort van SDS patiënten en werd deze nieuwe groep vergeleken met het initiële SDS co-

hort. Naast bovenstaande veranderingen, werden ook nieuwe veertypes geïntroduceerd. Naast de al bestaande 75N veer, werden een 100N veer en 50N veer ontworpen. Deze kunnen differentieel gebruikt worden (bijv. 100N op de concaviteit en 50N op de convexiteit). Met al deze aanpassingen konden we het aantal complicaties en heroperaties met 70% terugbrengen. Er waren geen patiënten met staafbreuken, implantaat protrusie en distaal ankerfalen in het tweede-generatie SDS cohort, wat het belang laat zien van het doorlopen van een continue verbeteringscyclus.

In **Hoofdstuk 10** kijken we verder dan de standaard radiologische parameters die vaak de uitkomstmaat zijn in scolioseonderzoek, en onderzoeken we het effect van een SDS operatie op kwaliteit van leven (HRQoL) van patiënten en ouders. We zagen dat direct na de operatie, scores in verschillende domeinen (bijv. pijn, bewegen, energie) verslechteren. Dit is logisch, aangezien de operatie en de daaropvolgende opname spannend zijn voor patiënten en ouders en vaak gepaard gaan met ongemak en pijn. Gelukkig stijgen de scores weer naar het baselineniveau bij 6 maanden follow-up en blijven de scores in veel domeinen ook daarna nog verbeteren. Ook zagen we dat de veranderingen over de tijd vergelijkbaar waren voor verschillende etiologische groepen en dat heroperaties geen negatief effect hadden op HRQoL. Deze resultaten geven ons de kans om patiënten goed voor te lichten over het te verwachten beloop rondom de operatie en de periode daarna.

In **Hoofdstuk 11** vergelijken we verschillende etiologische EOS groepen om te zien of uitkomsten anders dan HRQoL (welke het onderwerp waren van **Hoofdstuk 10**) verschilden tussen idiopathische, neuromusculaire en congenitale EOS patiënten. We zagen dat initiële correctie vergelijkbaar was tussen groepen. Echter, gedurende de follow-up verslechterde de coronale bocht meer in idiopathische patiënten dan in andere groepen. Een mogelijke oorzaak hiervoor kan zijn dat de idiopathische patiënten ouder zijn als ze geopereerd worden en mogelijk sterkere veren moeten krijgen. Het kan ook een gevolg zijn van de verschillen in configuratie tussen idiopathische EOS patiënten (die vaker een hybride constructie krijgen met een convexe apicale glijstaaf) en neuromusculaire of congenitale EOS patiënten. Er is echter literatuur die laat zien dat apicale controlestaven effectief zijn in het behouden van de correctie in TGR patiënten.[226] Het is goed mogelijk dat in dynamische implantaten, de continue neiging van de apex om terug te gaan naar de originele positie leidt tot laterale krachten, die zorgen voor meer wrijving tussen connector en staaf, welke de longitudinale corrigerende veerkrachten tegenwerken. Dit is waarom we momenteel werken aan een verbeterd SDS ontwerp, waarin deze wrijvingskrachten worden geminimaliseerd en ook metallose wordt voorkomen. Het component dat dit mogelijk moet maken heet de axial sliding bearing (ASB), welke onderdeel wordt van het nieuwe IMDD van de studie naar SDS.

Ten slotte wordt in **Deel IV: Double Spring Reduction: De beweging naar twee veren** gekeken naar het toevoegen van een geavanceerde torsieveer aan het eerder beschreven distractieconcept van de vorige hoofdstukken. In **Hoofdstuk 12** induceren we eerst scoliose in 14 Göttingen minivarkens. Zes ondergaan inductie met alleen een unilaterale flexibele tether en 8 ondergaan inductie met een tether in combinatie met een torsieveer die een continu axiaal moment geeft op de apex. Na 3 maanden induceert de torsieveer significant meer axiale rotatie terwijl de mobiliteit en groei van de rug niet gehinderd wordt. Tegelijk werd significante anterieure verlenging gezien, voornamelijk in de IVD, wat ook wordt gezien in alle vormen van scoliose. [53] Na het verwijderen van de implantaten bleef een groot deel van de deformiteit bestaan in alle 3 vlakken, wat laat zien dat de veranderingen structureel zijn.

In **Hoofdstuk 13** onderzochten we of de geïnduceerde veranderingen in **Hoofdstuk 12** weer teruggedraaid kunnen worden met het DSR concept. Hoewel derotatie op zichzelf de apicale rotatie en een deel van de coronale bocht kon corrigeren, leidde het toevoegen van distractie aan derotatie (DSR) tot veel grotere coronale en sagittale correctie. Er werd bij de combinatie van derotatie en distractie zelfs een overcorrectie in het coronale vlak gezien na enkele maanden. Dit betekent dat voor elke patiënt er een combinatie van axiaal moment en distractiekracht bestaat die de 3D scoliose volledig kan corrigeren. Om overcorrectie te voorkomen zullen we de initiële momenten en krachten precies goed moeten kiezen, of de momenten en krachten stopzetten (bijv. door DSR te explanteren) als de bocht volledig gecorrigeerd is. De laatste optie lijkt het meest realistisch, aangezien correctie erg moeilijk te voorspellen is, maar eenvoudig gemonitord kan worden met beeldvorming.

Welke stukjes van de puzzel missen nog?

Eén onderzoeksgebied dat nog verder geëxploreerd moet worden is de langetermijn effecten van SDS behandeling. De eerdere studies keken naar veiligheid en effectiviteit in de korte- tot middellange termijn. Echter, of de effecten blijven tot na de groei is nog niet bekend. Sinds het start van SDS als behandeling, zijn er nu 30 patiënten die klaar zijn met de SDS behandeling, zij hebben een definitieve fusie gehad (in het Engels aangeduid met de term "graduates"). Dit cohort van "graduates" zal systematisch onderzocht worden om te kijken of er modulatie van de bocht is opgetreden en om goed te kunnen vergelijken met andere systemen. Het analyseren van de "graduate" data is een lopend project.

We weten ook niet of SDS in staat is om de morfologie en opmaak van de wervels en IVDs permanent kan veranderen (en dus de rug weer in een gezonde vorm kan sturen). Deze modulatie kan het beste onderzocht worden in 3D. Zo kunnen de 3 componenten van iedere scoliose apart bekeken worden:

A

1. Coronale vlak: Als we hoofdzakelijk de concave zijde van de wervelkolom uit elkaar trekken, kunnen we dan de concave zijde van de wervels verlengen, zodat de coronale bocht kleiner wordt?
2. Sagittale vlak: Als we vooral de achterkant van de wervelkolom uit elkaar duwen, kunnen we dan posterieure verlenging induceren en kyfose creëren?
3. Axiale vlak: Als we een axiaal moment op de apex te geven, kunnen we dan de axiale rotatie van de apicale niveaus verminderen?

We willen ook graag weten of we met veren veranderingen in de IVD kunnen induceren. Dit betekent onderzoeken of de naar convex bewogen nucleus pulposus weer naar zijn oude positie kan worden verplaatst en of we tevens de configuratie van de annulus fibrosus vezels permanent kunnen veranderen. Beeldvorming van de IVD kan ons ook laten zien of distractie negatieve effecten heeft op IVD hoogte en -gezondheid. Om dit te onderzoeken hebben we 3D beeldvorming van de rug nodig, welke historisch altijd verricht werd met CT. Hoewel dit uitstekende visualisatie van de wervels geeft, gebruikt CT schadelijke ioniserende straling, die mogelijk leiden tot kanker in de toekomst.[275] Met de opkomst van MRI en recente innovaties zoals synthetische CT (welke wordt gemaakt van MRI beelden) kunnen bovenstaande vragen beantwoord worden zonder gebruik te maken van schadelijke straling.[276,277] Het gebruik van MRI heeft als bijkomend voordeel dat spieren, pezen en bijvoorbeeld de IVD in meer detail zichtbaar zijn dan met CT.

De toekomst van SDS

Sinds de eerste SDS patiënt in 2015 zijn nu bijna 10 jaar verstreken, waarin we hard hebben gewerkt aan het ontwikkelen en verbeteren van veerdistractie als behandeling van EOS. Gedurende die jaren zijn er vele verbeteringen aangebracht. Een nieuwe verbetering die nu wordt ontwikkeld is het gebruik van speciale connectoren die nauwelijks wrijving ondervinden (Figuur 3). Deze connector is gemaakt van twee UHMWP lagers die in een langere SDS connector zitten. Dit heeft meerdere voordelen. Ten eerste voorkomt de langere connectorlengte dat de staven gaan kyfoseren. Ten tweede zorgt de connector voor een meer optimale krachtoverdracht naar de glijdende staven omdat er veel minder wrijving optreedt. Als bijeffect komt ook minder metaaldebris (ook wel metallose genoemd) vrij. We weten uit de MCGR literatuur dat gedurende het gebruik van MCGR grote hoeveelheden debris vrijkomen. Dit debris kleurt de weefsels zwart en verhoogt de concentraties metalen in het bloed.[166] Meerdere studies hebben laten zien dat de hoeveelheid titanium in het bloed van geopereerde patiënten veel hoger is dan bij controles.[167,278] Of deze verhoogde

concentraties metalen gevaarlijk zijn is nog niet opgehelderd, al is de consensus dat in kwetsbare EOS patiënten, idealiter de concentratie zo laag mogelijk moet zijn. Biomechanische testen laten zien dat de ASB sterk de hoeveelheid metallose verminderd vergeleken met normale connectoren. Dit moet echter nog getest worden in patiënten, een proces wat jaren in beslag neemt, zeker met de huidige Europese Medical Device Regulation (MDR).

Zodra het definitieve SDS implantaat is ontworpen is er nog de vraag hoe we deze het beste kunnen gebruiken. Op basis van de data uit dit proefschrift, geloven we dat er voor iedere EOS patiënt een ideale configuratie en behandeling bestaat, gebaseerd op leeftijd, etiologie en karakteristieken van de bocht. Jongere patiënten moeten nog langer groeien en hebben dus langere staven en veren nodig, terwijl patiënten met grotere of stijvere bochten waarschijnlijk sterkere veren nodig hebben om voldoende correctie te bewerkstelligen. Het oplossen van patiëntspecifieke puzzels is niet eenvoudig, en om dergelijke algoritmes te kunnen maken zijn waarschijnlijk grote cohorten nodig. Computerstudies kunnen opnieuw van waarde zijn om te voorspellen welke configuratie voor een bepaalde patiënt het meest effectief is. Individuele FEMs worden al gebruikt om de effectiviteit van tethering te voorspellen.[91,280,281] Meerdere modellen met verschillende veren kunnen worden vergeleken en de veer met de hoogst verwachte effectiviteit kan worden gekozen. Dit is momenteel nog arbeidsintensief, maar kan waarschijnlijk in de toekomst geautomatiseerd worden.[282]

Figuur 3: SDS met nieuwe connector

De meest recente versie van SDS gebruikt een connector met twee UHMWP lagers, die wrijving tussen staaf en connector minimaliseren.

De toekomst van DSR

En wat kunnen we verwachten van DSR? Als we de juiste krachten en momenten op exact de juiste plekken toepassen, kunnen we een scoliotische rug dan terug begeleiden naar de 'gezonde' configuratie? En op zo'n manier dat de rug aan het einde van de behandeling niet te onderscheiden is van de rug van iemand zonder scoliose? Dat zou betekenen dat we scoliose kunnen genezen! We weten dat dit kan met Mehta gips in hele jonge patiënten, maar een dergelijk resultaat is nog niet gezien in AIS patiënten. Als we daar naartoe willen, moeten er een aantal dingen gebeuren. We weten dat distractiekracht op de groeiplaat van de wervels, de vorm van de wervels kan veranderen. Dit is de wet van Hueter-Volkmann.[283] Andere onderzoekers hebben laten zien dat de wet van Hueter-Volkmann, bijvoorbeeld in tethering, scoliotische afwijkingen in wervels kan corrigeren.[284] Uit dezelfde literatuur is echter ook bekend dat het erg moeilijk is om te voorspellen hoe snel die veranderingen plaatsvinden. Hierdoor vindt vaak onder- of overcorrectie plaats.[268] We weten ook, uit literatuur van onze eigen groep, dat in het proces van scoliose, de nucleus pulposus naar de convexiteit beweegt. We weten dat de nucleus pulposus weer terug kan bewegen naar de midline, maar niet of we de positie daar kunnen houden als we de correctiekrachten weer weghalen.[277] Ten slotte is het onduidelijk of de andere weke delen veranderingen die onderdeel zijn van scoliose weer teruggedraaid kunnen worden.[285,286]

Wellicht kunnen we AIS volledig terugdraaien als we vroeg en agressief behandelen. Dit betekent dat we DSR implanteren gedurende de groei en het implantaat weer verwijderen als de groei is afgelopen. Dit betekent dat we patiënten moeten opereren die momenteel nog behandeld worden middels een brace (met een bocht van ongeveer 25°). Om dit mogelijk te maken, moeten we eerst laten zien dat DSR voorspelbare resultaten kan laten zien die ook beter zijn dan de resultaten van huidige technieken. Deze dier- en computerstudies zijn reeds gestart. Deze studies moeten ook laten zien hoe bepaalde krachten en momenten de rug over de tijd beïnvloeden, zodat we erachter kunnen komen wanneer we moeten starten met DSR behandeling en zodat we weten welke krachten en momenten we nodig hebben. Na dierstudies zullen klinische studies volgen, waarschijnlijk eerst in EOS patiënten (die nu SDS behandeling krijgen), en later ook in AIS patiënten.

Optimale DSR behandeling eist ook een vroege detectie van AIS, voordat de bocht bijvoorbeeld 20° is. Hiervoor is het belangrijk om te weten wie at risk is voor het krijgen van scoliose en wie niet. Een parameter die hiervoor gebruikt kan worden is het "posterior inclined triangle" (PIT) oppervlak. Deze parameter kon in een recente studie in initieel rechte ruggen goed voorspellen wie scoliose gaat ontwikkelen en wie niet.[287] Om deze kinderen te vinden zonder bij iedereen potentieel schadelijke

röntgenfoto's te maken is de volgende horde. Mogelijk is screening met stralingsloze rugechografie de sleutel om kinderen met risico op scoliose vroeg te identificeren.[288] Als we scoliose vroeg kunnen ontdekken en behandelen met DSR, zou de volgende casus in de toekomst zomaar werkelijkheid kunnen zijn:

> *"Een 9-jarig meisje komt bij de schoolarts, waar met echoscreening een coronale bocht van 5° wordt gevonden met een groot PIT oppervlakte. Ze wordt verwezen naar de orthopedisch chirurg, die haar vervolgt om te zien of de bocht groter wordt met de leeftijd. Als ze 11 jaar is (pre-menarche) is de bocht 20°. De keuze wordt gemaakt om DSR toe te passen. Op basis van haar botleeftijd, gewicht en karakteristieken van de scoliose, en pre-operatieve FEA modellen, krijgt ze met DSR een axiaal moment van 2Nm en 100N distractie. De bocht wordt over de jaren steeds kleiner. Als ze 15 jaar oud is (Risser 5), wordt DSR verwijderd. Ze wordt volwassen met een rechte, flexibele en gezonde rug."*

Dit kan de toekomst van de behandeling van scoliose zijn.

Aan de slag.

A

Appendix II: References

[1] Cheng JC, Castelein RM, Chu WC, Danielsson AJ, Dobbs MB, Grivas TB, et al. Adolescent idiopathic scoliosis. Nat Rev Dis Primers 2015. https://doi.org/10.1038/nrdp.2015.30.

[2] Kouwenhoven JWM, Vincken KL, Bartels LW, Castelein RM. Analysis of preexistent vertebral rotation in the normal spine. Spine (Phila Pa 1976) 2006;31:1467–72. https://doi.org/10.1097/01.brs.0000219938.14686.b3.

[3] Schlösser TPC, van Stralen M, Brink RC, Chu WCW, Lam T-P, Vincken KL, et al. Three-Dimensional Characterization of Torsion and Asymmetry of the Intervertebral Discs Versus Vertebral Bodies in Adolescent Idiopathic Scoliosis. Spine (Phila Pa 1976) 2014;39:E1159–66. https://doi.org/10.1097/BRS.0000000000000467.

[4] Brink RC, Schlösser TPC, Colo D, Vavruch L, van Stralen M, Vincken KL, et al. Anterior Spinal Overgrowth Is the Result of the Scoliotic Mechanism and Is Located in the Disc. Spine (Phila Pa 1976) 2017;42:818–22. https://doi.org/10.1097/BRS.0000000000001919.

[5] Dimeglio A. Growth in Pediatric Orthopaedics. Journal of Pediatric Orthopaedics 2001;21:549–55. https://doi.org/10.1097/01241398-200107000-00026.

[6] Dimeglio A, Canavese F. The growing spine: How spinal deformities influence normal spine and thoracic cage growth. European Spine Journal 2012;21:64–70. https://doi.org/10.1007/s00586-011-1983-3.

[7] Dimeglio A. Growth of the spine before age 5 years. Journal of Pediatric Orthopaedics Part B 1992;1. https://doi.org/10.1097/01202412-199201020-00003.

[8] Herring MJ, Putney LF, Wyatt G, Finkbeiner WE, Hyde DM. Growth of alveoli during postnatal development in humans based on stereological estimation. Am J Physiol Lung Cell Mol Physiol 2014;307. https://doi.org/10.1152/ajplung.00094.2014.

[9] Redding G, Song K, Inscore S, Effmann E, Campbell R. Lung function asymmetry in children with congenital and infantile scoliosis. Spine Journal 2008;8. https://doi.org/10.1016/j.spinee.2007.04.020.

[10] Farrell J, Garrido E, Vavruch L, Schlösser TPC. Thoracic Morphology and Bronchial Narrowing Are Related to Pulmonary Function in Adolescent Idiopathic Scoliosis. J Bone Joint Surg Am 2021. https://doi.org/10.2106/JBJS.20.01714.

[11] Redding GJ. Effects of Postnatal Lung Development and Thoracic Insufficiency Syndrome on Lung Function in Children. In: Akbarnia BA, Thompson GH, Yazici M, El-Hawary R, editors. The Growing Spine: Management of Spinal Disorders in Young Children. 3rd ed., Springer; 2022, p. 91–9. https://doi.org/https://doi.org/10.1007/978-3-030-84393-9_6.

[12] Campbell RM, Smith MD. Thoracic Insufficiency Syndrome and Exotic Scoliosis. Journal of Bone and Joint Surgery 2007;89:108–22. https://doi.org/10.2106/jbjs.f.00270.

[13] Campbell RM, Smith MD, Mayes TC, Mangos JA, Willey-Courand DB, Kose N, et al. The characteristics of thoracic insufficiency syndrome associated with fused ribs and congenital scoliosis. Journal of Bone and Joint Surgery - Series A 2003;85:399–408. https://doi.org/10.2106/00004623-200303000-00001.

[14] Karol LA, Johnston C, Mladenov K, Schochet P, Walters P, Browne RH. Pulmonary function following early thoracic fusion in non-neuromuscular scoliosis. Journal of Bone and Joint Surgery - Series A 2008;90:1272–81. https://doi.org/10.2106/JBJS.G.00184.

[15] Vitale MG, Matsumoto H, Bye MR, Gomez JA, Booker WA, Hyman JE, et al. A retrospective cohort study of pulmonary function, radiographic measures, and quality of life in children with congenital scoliosis: An evaluation of patient outcomes after early spinal fusion. Spine (Phila Pa 1976) 2008;33. https://doi.org/10.1097/BRS.0b013e3181714536.

[16] Dubousset J, Herring JA, Shufflebarger H. The crankshaft phenomenon. J Pediatr Orthop 1989;9:541–50. https://doi.org/10.1097/01241398-198909010-00008.

[17] Mehta MH. Growth as a corrective force in the early treatment of progressive infantile scoliosis. Journal of Bone and Joint Surgery - Series B 2005;87-B:1237–47. https://doi.org/10.1302/0301-620X.87B9.16124.

[18] Katz DE, Herring JA, Browne RH, Kelly DM, Birch JG. Brace Wear Control of Curve Progression in Adolescent Idiopathic Scoliosis. The Journal of Bone and Joint Surgery-American Volume 2010;92:1343–52. https://doi.org/10.2106/JBJS.I.01142.

[19] Weinstein SL, Dolan LA, Wright JG, Dobbs MB. Effects of Bracing in Adolescents with Idiopathic Scoliosis. New England Journal of Medicine 2013;369:1512–21. https://doi.org/10.1056/nejmoa1307337.

[20] Albee FH. Transplantation of a portion of the tibia into the spine for pott's disease: A preliminary report. J Am Med Assoc 1911;LVII. https://doi.org/10.1001/jama.1911.04260090107012.

[21] Hibbs RA. Treatment of vertebral tuberculosis by fusion operation: Report of two hundred and ten cases. J Am Med Assoc 1918;71. https://doi.org/10.1001/jama.1918.02600430018006.

[22] HARRINGTON PR. Treatment of scoliosis. Correction and internal fixation by spine instrumentation. J Bone Joint Surg Am 1962;44 A. https://doi.org/10.2106/00004623-196244040-00001.

[23] Desai SK, Brayton A, Chua VB, En TGL, Jea A. The lasting legacy of paul randall harrington to pediatric spine surgery historical vignette. J Neurosurg Spine 2013;18. https://doi.org/10.3171/2012.11.SPINE12979.

[24] Luque ER. Introduction to symposium: The anatomic basis and development of segmental spinal instrumentation. Spine (Phila Pa 1976) 1982;7. https://doi.org/10.1097/00007632-198205000-00010.

[25] Luque ER. Segmental spinal instrumentation for correction of scoliosis. Clin Orthop Relat Res 1982;163. https://doi.org/10.1097/00003086-198203000-00028.

[26] McAfee PC, Lubicky JP, Werner FW. The use of segmental spinal instrumentation to preserve longitudinal spinal growth. An experimental study. Journal of Bone and Joint Surgery - Series A 1983;65. https://doi.org/10.2106/00004623-198365070-00008.

[27] Mardjetko SM, Hammerberg KW, Lubicky JP, Fister JS. The luque trolley revisited: Review of nine cases requiring revision. Spine (Phila Pa 1976) 1992;17.

[28] Pratt RK, Webb JK, Burwell RG, Cummings SL. Luque trolley and convex epiphysiodesis in the management of infantile and juvenile idiopathic scoliosis. Spine (Phila Pa 1976) 1999;24. https://doi.org/10.1097/00007632-199908010-00007.

[29] Tice A, Aoude A, El-Hawary R, Ouellet J. Modern Luque Trolley Construct for the Management of Early-Onset Scoliosis: The First Ten Patients with a New Gliding Implant with Two-year Follow Up. Spine Deform 2018;6. https://doi.org/10.1016/j.jspd.2018.09.059.

[30] Balioğlu MB, Abul K, Akpolat AO, Özlük AV, Saçık N, Aksay MF, et al. Implant-Related Complications Do Not Interfere with Corrections with the Shilla Technique in Early Onset Scoliosis: Preliminary Results. Children 2023;10. https://doi.org/10.3390/children10060947.

[31] Wijdicks SPJ, Tromp IN, Yazici M, Kempen DHR, Castelein RM, Kruyt MC. A comparison of growth among growth-friendly systems for scoliosis: a systematic review. Spine Journal 2019;19:789–99. https://doi.org/10.1016/j.spinee.2018.08.017.

[32] Akbarnia BA, Marks DS, Boachie-Adjei O, Thompson AG, Asher MA. Dual growing rod technique for the treatment of progressive early-onset scoliosis: A multicenter study. Spine (Phila Pa 1976) 2005;30:S46-57. https://doi.org/10.1097/01.brs.0000175190.08134.73.

[33] Bess S, Akbarnia BA, Thompson GH, Sponseller PD, Shah SA, El Sebaie H, et al. Complications of growing-rod treatment for early-onset scoliosis: Analysis of one hundred and forty patients. Journal of Bone and Joint Surgery - Series A 2010;92:2533–43. https://doi.org/10.2106/JBJS.I.01471.

[34] U.S. FDA. FDA review results in new warnings about using general anesthetics and sedation drugs in young children and pregnant women. US Food and Drug Administration- Drug Safety and Communications 2016:1–11.

[35] Sankar WN, Skaggs DL, Yazici M, Johnston CE, Shah SA, Javidan P, et al. Lengthening of dual growing rods and the law of diminishing returns. Spine (Phila Pa 1976) 2011;36:806–9. https://doi.org/10.1097/BRS.0b013e318214d78f.

[36] Hosseini P, Pawelek J, Mundis G, Yazsay B, Ferguson J, Helenius I, et al. Magnetically-Controlled Growing Rods for Early Onset Scoliosis: A Multicenter Study of 23 Cases with Minimum 2 Years Follow-Up. Spine (Phila Pa 1976) 2016;41:1456–62.

[37] Cheung JPY, Samartzis D, Cheung KMC. A novel approach to gradual correction of severe spinal deformity in a pediatric patient using the magnetically-controlled growing rod. Spine Journal 2014;14:e7–13. https://doi.org/10.1016/j.spinee.2014.01.046.

[38] Lebon J, Batailler C, Wargny M, Choufani E, Violas P, Fron D, et al. Magnetically controlled growing rod in early onset scoliosis: a 30-case multicenter study. European Spine Journal 2017;26:1567–76. https://doi.org/10.1007/s00586-016-4929-y.

[39] Cheung KMC, Cheung JPY, Samartzis D, Mak KC, Wong YW, Cheung WY, et al. Magnetically controlled growing rods for severe spinal curvature in young children: A prospective case series. The Lancet 2012;379:1967–74. https://doi.org/10.1016/S0140-6736(12)60112-3.

[40] Akbarnia BA, Mundis GM, Salari P, Yaszay B, Pawelek JB. Innovation in growing rod technique: A study of safety and efficacy of a magnetically controlled growing rod in a porcine model. Spine (Phila Pa 1976) 2012;37:1109–14. https://doi.org/10.1097/BRS.0b013e318240ff67.

A

[41]   Panagiotopoulou VC, Tucker SK, Whittaker RK, Hothi HS, Henckel J, Leong JJH, et al. Analysing a mechanism of failure in retrieved magnetically controlled spinal rods. European Spine Journal 2017;26:1699–710. https://doi.org/10.1007/s00586-016-4936-z.

[42]   Choi E, Yaszay B, Mundis G, Hosseini P, Pawelek J, Alanay A, et al. Implant Complications After Magnetically Controlled Growing Rods for Early Onset Scoliosis. Journal of Pediatric Orthopaedics 2017;37:e588–92. https://doi.org/10.1097/BPO.0000000000000803.

[43]   Joyce TJ, Smith SL, Rushton PRP, Bowey AJ, Gibson MJ. Analysis of Explanted Magnetically Controlled Growing Rods From Seven UK Spinal Centers. Spine (Phila Pa 1976) 2018;43:E16–22. https://doi.org/10.1097/BRS.0000000000002221.

[44]   Rushton PRP, Smith SL, Kandemir G, Forbes L, Fender D, Bowey AJ, et al. Spinal Lengthening with Magnetically Controlled Growing Rods: Data from the Largest Series of Explanted Devices. Spine (Phila Pa 1976) 2020;45:170–6. https://doi.org/10.1097/BRS.0000000000003215.

[45]   Thakar C, Kieser DC, Mardare M, Haleem S, Fairbank J, Nnadi C. Systematic review of the complications associated with magnetically controlled growing rods for the treatment of early onset scoliosis. European Spine Journal 2018;27:2062–71. https://doi.org/10.1007/s00586-018-5590-4.

[46]   U.S. FDA. Potential Concerns with NuVasive MAGEC System Implants - FDA Safety Communication 2021. https://www.fda.gov/medical-devices/safety-communications/potential-concerns-nuvasive-magec-system-implants-fda-safety-communication (accessed November 24, 2021).

[47]   Medicines and Healthcare products Regulatory Agency. Targeted communication: CE mark suspended for all MAGEC systems manufactured by NuVasive Specialized Orthopedics, Inc. (DSI/2021/007) 2021. https://www.gov.uk/drug-device-alerts/targeted-communication-ce-mark-suspended-for-all-magec-systems-manufactured-by-nuvasive-specialized-orthopedics-inc (accessed November 24, 2021).

[48]   Hothi H. The impact and surgeon perceptions of the suspension of the CE certification of MAGEC devices on clinical practice. Bone Jt Open 2022;3. https://doi.org/10.1302/2633-1462.32.BJO-2021-0144.R2.

[49]   Skaggs D, Chen I. P93. Majority of magnetically controlled growing rods are implanted longer than FDA recommended two years. The Spine Journal 2023;23. https://doi.org/10.1016/j.spinee.2023.06.318.

[50]   Cain T. Spring Design and Manufacture. 1st ed. Special Interest Model Books; 1998.

[51]   Gruca A. The Pathogenesis and Treatment of Idiopathic Scoliosis. Journal of Bone and Joint Surgery - Series A 1958;40-A:570–84.

[52]   Benzel EC, Larson SJ. Operative stabilization of the posttraumatic thoracic and lumbar spine: A comparative analysis of the Harrington distraction rod and the modified Weiss spring. Neurosurgery 1986;19. https://doi.org/10.1227/00006123-198609000-00008.

[53]   de Reuver S, Brink RC, Homans JF, Vavruch L, Tropp H, Kruyt MC, et al. Anterior lengthening in scoliosis occurs only in the disc and is similar in different types of scoliosis. Spine Journal 2020;20:1653–8. https://doi.org/10.1016/j.spinee.2020.03.005.

[54]   Rushton PRP, Smith SL, Forbes L, Bowey AJ, Gibson MJ, Joyce TJ. Force Testing of Explanted Magnetically Controlled Growing Rods. Spine (Phila Pa 1976) 2019;44:233–9. https://doi.org/10.1097/BRS.0000000000002806.

[55]   Poon S, Spencer HT, Fayssoux RS, Sever R, Cho RH. Maximal Force Generated by Magnetically Controlled Growing Rods Decreases With Rod Lengthening. Spine Deform 2018;6:787–90. https://doi.org/10.1016/j.jspd.2018.03.009.

[56]   Yang C, Wang H, Zheng Z, Zhang Z, Wang J, Liu H, et al. Halo-gravity traction in the treatment of severe spinal deformity: a systematic review and meta-analysis. European Spine Journal 2017;26:1810–6. https://doi.org/10.1007/s00586-016-4848-y.

[57]   Yankey KP, Duah HO, Sacramento-Domínguez C, Tutu HO, Owiredu MA, Mahmud R, et al. The Effect of Prolonged Pre-Operative Halo Gravity Traction for Severe Spinal Deformities on the Cervical Spine Radiographs. Global Spine J 2021:219256822199864. https://doi.org/10.1177/2192568221998644.

[58]   Wijdicks SPJ, Lemans JVC, Verkerke GJ, Noordmans HJ, Castelein RM, Kruyt MC. The potential of spring distraction to dynamically correct complex spinal deformities in the growing child. European Spine Journal 2021;30:714–23. https://doi.org/10.1007/s00586-020-06612-3.

[59]   Lemans JVC, Wijdicks SPJ, Castelein RM, Kruyt MC. Spring Distraction System for Dynamic Growth Guidance of Early Onset Scoliosis: 2 Year Prospective Follow-up of 24 Patients. The Spine Journal 2021;21:671–81. https://doi.org/https://doi.org/10.1016/j.spinee.2020.11.007.

[60] Moher D, Liberati A, Tetzlaff J, Altman DG. Preferred reporting items for systematic reviews and meta-analyses: The PRISMA statement. PLoS Med 2009;6:e1000097.

[61] Slim K, Nini E, Forestier D, Kwiatkowski F, Panis Y, Chipponi J. Methodological index for non-randomized studies (Minors): Development and validation of a new instrument. ANZ J Surg 2003;73:712–6.

[62] U.S. FDA. Recommended Content and Format of Non-Clinical Bench Performance Testing Information in Premarket Submissions. 2019. https://www.fda.gov/media/113230/download.

[63] U.S. FDA. Reporting of Computational Modeling Studies in Medical Device Submissions. Appendix II - Computational Solid Mechanics. 2016. https://www.fda.gov/media/87586/download.

[64] Dunn HK, Daniels AU, McBride GG. Intraoperative force measurements during correction of scoliosis. Spine (Phila Pa 1976) 1982;7:448–55. https://doi.org/10.1097/00007632-198209000-00008.

[65] Elfstrom G, Nachemson A. Telemetry recordings of forces in the Harrington distraction rod: a method for increasing safety in the operative treatment of scoliosis patients. Clinical Orthopaedics and Related Research (1976-2007) 1973;93:158–72. https://doi.org/10.1097/00003086-197306000-00016.

[66] Waugh TR. Intravital measurements during instrumental correction of idiopathic scoliosis. Acta Orthop Scand 1966;37:1–87. https://doi.org/10.3109/ort.1966.37.suppl-93.01.

[67] Agarwal A, Goswami A, Vijayaraghavan GP, Srivastava A, Kandwal P, Nagaraja UB, et al. Quantitative Characteristics of Consecutive Lengthening Episodes in Early-onset Scoliosis (EOS) Patients with Dual Growth Rods. Spine (Phila Pa 1976) 2019;44:397–403. https://doi.org/10.1097/BRS.0000000000002835.

[68] Noordeen HM, Shah SA, Elsebaie HB, Garrido E, Farooq N, Al Mukhtar M. In vivo distraction force and length measurements of growing rods: Which factors influence the ability to lengthen? Spine (Phila Pa 1976) 2011;36:2299–303. https://doi.org/10.1097/BRS.0b013e31821b8e16.

[69] Teli M, Grava G, Solomon V, Andreoletti G, Grismondi E, Meswania J. Measurement of forces generated during distraction of growingrods in early onset scoliosis. World J Orthop 2012;3:15–9. https://doi.org/10.5312/wjo.v3.i2.15.

[70] Dibb AT, Nightingale RW, Luck JF, Carol Chancey V, Fronheiser LE, Myers BS. Tension and combined tension-extension structural response and tolerance properties of the human male ligamentous cervical spine. J Biomech Eng 2009;131:081008. https://doi.org/10.1115/1.3127257.

[71] Chazal J, Tanguy A, Bourges M, Gaurel G, Escande G, Guillot M, et al. Biomechanical properties of spinal ligaments and a histological study of the supraspinal ligament in traction. J Biomech 1985;18:167–76.

[72] Yoganandan N, Kumaresan S, Pintar FA. Biomechanics of the cervical spine. Part 2. Cervical spine soft tissue responses and biomechanical modeling. Clinical Biomechanics 2001;16:1–27.

[73] Luck JF, Nightingale RW, Song Y, Kait JR, Loyd AM, Myers BS, et al. Tensile failure properties of the perinatal, neonatal, and pediatric cadaveric cervical spine. Spine (Phila Pa 1976) 2013;38:E1-12. https://doi.org/10.1097/BRS.0b013e3182793873.

[74] Ouyang J, Zhu Q, Zhao W, Xu Y, Chen W, Zhong S. Biomechanical assessment of the pediatric cervical spine under bending and tensile loading. Spine (Phila Pa 1976) 2005;30:E716-23. https://doi.org/10.1097/01.brs.0000192280.53831.70.

[75] Yoganandan N, Pintar FA, Kumaresan S, Gennarelli TA. Pediatric and small female neck injury scale factors and tolerance based on human spine biomechanical characteristics. IRCOBI Conference, Montpellier: 2000, p. 21–3.

[76] Duncan JM. Laboratory note: On the tensile strength of the fresh adult foetus. Br Med J 1874;2:763. https://doi.org/10.1136/bmj.2.729.763.

[77] Nuckley DJ, Linders DR, Ching RP. Developmental biomechanics of the human cervical spine. J Biomech 2013;46:1147–54. https://doi.org/10.1016/j.jbiomech.2013.01.005.

[78] Dong L, Li G, Mao H, Marek S, Yang KH. Development and validation of a 10-year-old child ligamentous cervical spine finite element model. Ann Biomed Eng 2013;41:2538–52. https://doi.org/10.1007/s10439-013-0858-7.

[79] DeWit JA, Cronin DS. Cervical spine segment finite element model for traumatic injury prediction. J Mech Behav Biomed Mater 2012;10:138–50. https://doi.org/10.1016/j.jmbbm.2012.02.015.

[80] Ching RP, Nuckley DJ, Hertsted SM, Eck MP, Mann FA, Sun EA. Tensile Mechanics of the Developing Cervical Spine. Stapp Car Crash J 2001;45:2001-P-375. https://doi.org/10.4271/2001-22-0015.

[81] Pintar F, Mayer R. Child Neck Strength Characteristics Using An Animal Model. Stapp Car Crash J 2000;44:2000-P-362.

A

[82]   Cahill PJ, Marvil S, Cuddihy L, Schutt C, Idema J, Clements DH, et al. Autofusion in the imma-ture spine treated with growing rods. Spine (Phila Pa 1976) 2010;35:E1199–203. https://doi.org/10.1097/BRS.0b013e3181e21b50.

[83]   Williams IV JT, Southerland SS, Souza J, Calcutt AF, Cartledge RG. Cells isolated from adult human skeletal muscle capable of differentiating into multiple mesodermal phenotypes. American Sur-geon 1999;65:22.

[84]   Jebaseelan DD, Jebaraj C, Yoganandan N, Rajasekaran S, Kanna RM. Sensitivity studies of pediatric material properties on juvenile lumbar spine responses using finite element analysis. Med Biol Eng Comput 2012;50:515–22.

[85]   Kumaresan S, Yoganandan N, Pintar FA, Maiman DJ, Kuppa S. Biomechanical study of pediatric human cervical spine: A finite element approach. J Biomech Eng 2000;122:60–71.

[86]   Dreischarf M, Zander T, Shirazi-Adl A, Puttlitz CM, Adam CJ, Chen CS, et al. Comparison of eight published static finite element models of the intact lumbar spine: Predictive power of models im-proves when combined together. J Biomech 2014;47:1757–66.

[87]   Naserkhaki S, Arjmand N, Shirazi-Adl A, Farahmand F, El-Rich M. Effects of eight different lig-ament property datasets on biomechanics of a lumbar L4-L5 finite element model. J Biomech 2018;70:33–42.

[88]   Myklebust JB, Pintar F, Yoganandan N, Cusick JF, Maiman D, Myers TJ, et al. Tensile strength of spinal ligaments. Spine (Phila Pa 1976) 1988;13:526–31.

[89]   Yoganandan N, Pintar FA, Maiman DJ, Cusick JF, Sances A, Walsh PR. Human head-neck biome-chanics under axial tension. Med Eng Phys 1996;18:289–94.

[90]   Yoganandan N, Pintar F, Sances A, Maiman D, Myklebust J, Harris G, et al. Biomechanical inves-tigations of the human thoracolumbar spine. SAE Technical Paper 881331 1988:676–84. https://doi.org/https://doi.org/10.4271/881331.

[91]   Henao J, Labelle H, Arnoux PJ, Aubin CÉ. Biomechanical Simulation of Stresses and Strains Exerted on the Spinal Cord and Nerves During Scoliosis Correction Maneuvers. Spine Deform 2018;6:12–9. https://doi.org/10.1016/j.jspd.2017.04.008.

[92]   Agarwal A, Agarwal AK, Jayaswal A, Goel VK. Outcomes of Optimal Distraction Forces and Fre-quencies in Growth Rod Surgery for Different Types of Scoliotic Curves: An In Silico and In vitro Study. Spine Deform 2017;5:18–26. https://doi.org/10.1016/j.jspd.2016.09.047.

[93]   Agarwal A, Jayaswal A, Goel VK, Agarwal AK. Patient-specific Distraction Regimen to Avoid Growth-rod Failure. Spine (Phila Pa 1976) 2018;43:E221–6.

[94]   Cheung JPY, Bow C, Samartzis D, Kwan K, Cheung KMC. Frequent small distractions with a mag-netically controlled growing rod for early-onset scoliosis and avoidance of the law of diminishing returns. Journal of Orthopaedic Surgery 2016;24:332–7.

[95]   Skaggs DL, Akbarnia BA, Flynn JM, Myung KS, Sponseller PD, Vitale MG. A Classification of Growth Friendly Spine Implants. Journal of Pediatric Orthopaedics 2014;34:260–74. https://doi.org/10.1097/BPO.0000000000000073.

[96]   Ahmad A, Subramanian T, Wilson-Macdonald J, Rothenfluh DA, Nnadi C, Panteliadis P. Quan-tifying the 'law of diminishing returns' in magnetically controlled growing rods. Bone and Joint Journal 2017;99B:1658–64. https://doi.org/10.1302/0301-620X.99B12.BJJ-2017-0402.R2.

[97]   Hill G, Nagaraja S, Akbarnia BA, Pawelek J, Sponseller P, Sturm P, et al. Retrieval and clinical analysis of distraction-based dual growing rod constructs for early-onset scoliosis. Spine Journal 2017;17:1506–18. https://doi.org/10.1016/j.spinee.2017.04.020.

[98]   Agarwal A, Kelkar A, Agarwal AG, Jayaswal D, Jayaswal A, Shendge V. Device-related complica-tions associated with magec rod usage for distraction-based correction of scoliosis. Spine Surg Relat Res 2020;4:148–51. https://doi.org/10.22603/SSRR.2019-0041.

[99]   Agarwal A, Agarwal AK, Jayaswal A, Goel V. Smaller interval distractions may reduce chances of growth rod breakage without impeding desired spinal growth: A finite element study. Spine Deform 2014;2:430–6. https://doi.org/10.1016/j.jspd.2014.08.004.

[100]   Myers MA, Casciani T, Whitbeck GMJ, Puzas EJ. Vertebral Body Osteopenia Associated With Posterolateral Spine Fusion in Humans. Spine (Phila Pa 1976) 1996;21:2368–71.

[101]   Rong T, Shen J, Kwan K, Zhang J, Wang Y, Li S, et al. Vertebral Growth Around Distal Instrumented Vertebra in Patients with Early-Onset Scoliosis Who Underwent Traditional Dual Growing Rod Treatment. Spine (Phila Pa 1976) 2019. https://doi.org/10.1097/BRS.0000000000002957.

[102]   Lippross S, Girmond P, Lüders KA, Austein F, Braunschweig L, Lüders S, et al. Smaller Interverte-bral Disc Volume and More Disc Degeneration after Spinal Distraction in Scoliotic Children. Journal of Clinical Medicine 2021;10. https://doi.org/10.3390/jcm10102124.

[103]   Agarwal A, Agarwal AK, Jayaswal A, Goel VK. Effect of distraction force on growth and biomecha-nics of the spine: A finite element study on normal juvenile spine with dual growth rod instrumen-tation. Spine Deform 2014;2:260–9. https://doi.org/10.1016/j.jspd.2014.03.007.

[104]   Agarwal A, Zakeri A, Agarwal AK, Jayaswal A, Goel VK. Distraction magnitude and frequency affects the outcome in juvenile idiopathic patients with growth rods: Finite element study using a representative scoliotic spine model. Spine Journal 2015. https://doi.org/10.1016/j.spi-nee.2015.04.003.

[105]   Agarwal A, Kodigudla M, Kelkar A, Jayaswal D, Goel V, Palepu V. Towards a validated patient-specific computational modeling framework to identify failure regions in traditional growing rods in patients with early onset scoliosis. North American Spine Society Journal (NASSJ) 2021;5:100043. https://doi.org/10.1016/j.xnsj.2020.100043.

[106]   Schultz A, Andersson GB, Ortengren R, Björk R, Nordin M. Analysis and quantitative myoelectric measurements of loads on the lumbar spine when holding weights in standing postures. Spine (Phila Pa 1976) 1982;7:390–7. https://doi.org/10.1097/00007632-198207000-00009.

[107]   Agarwal A. Mitigating biomechanical complications of growth rods in juvenile idiopathic scoliosis. 2015.

[108]   Shi L, Wang D, Driscoll M, Villemure I, Chu WCW, Cheng JCY, et al. Biomechanical analysis and modeling of different vertebral growth patterns in adolescent idiopathic scoliosis and healthy subjects. Scoliosis 2011;6:1–8. https://doi.org/10.1186/1748-7161-6-11.

[109]   Stokes IAF, Windisch L. Vertebral Height Growth Predominates Over Intervertebral Disc Height Growth in Adolescents With Scoliosis. Spine (Phila Pa 1976) 2006;31:1600–4. https://doi.org/10.1097/01.brs.0000222008.15750.1f.

[110]   Fok J, Adeeb S, Carey J. FEM Simulation of Non-Progressive Growth from Asymmetric Loading and Vicious Cycle Theory: Scoliosis Study Proof of Concept. Open Biomed Eng J 2010;4:162–9. https://doi.org/10.2174/1874120701004010162.

[111]   Agarwal A. Biomechanics of Surgical Intervention Associated with Early-Onset Scoliosis. Early-Onset Scoliosis, CRC Press; 2021, p. 93–106.

[112]   Ahmad AA. Early onset scoliosis and current treatment methods. J Clin Orthop Trauma 2020;11:184–90.

[113]   Lemans JVC, Tabeling CS, Castelein RM, Kruyt MC. Identifying Complications and Failure Modes of Innovative Growing Rod Configurations Using the (Hybrid) Magnetically Controlled Growing Rod and the Spring Distraction System. Spine Deform 2021;9:1679–89.

[114]   Dick JC, Bourgeault CA. Notch sensitivity of titanium alloy, commercially pure titanium, and stainless steel spinal implants. Spine (Phila Pa 1976) 2001;26:1668–72. https://doi.org/10.1097/00007632-200108010-00008.

[115]   Demura S, Murakami H, Hayashi H, Kato S, Yoshioka K, Yokogawa N, et al. Influence of rod con-touring on rod strength and stiffness in spine surgery. Orthopedics 2015;38:e520–3. https://doi.org/10.3928/01477447-20150603-61.

[116]   Lindsey C, Deviren V, Xu Z, Yeh RF, Puttlitz CM. The effects of rod contouring on spinal con-struct fatigue strength. Spine (Phila Pa 1976) 2006;31:1680–7. https://doi.org/10.1097/01.brs.0000224177.97846.00.

[117]   Slivka MA, Fan YK, Eck JC. The effect of contouring on fatigue strength of spinal rods: Is it okay to re-bend and which materials are best? Spine Deform 2013;1:395–400. https://doi.org/10.1016/j.jspd.2013.08.004.

[118]   Yang JS, Sponseller PD, Thompson GH, Akbarnia BA, Emans JB, Yazici M, et al. Growing rod fractu-res: Risk factors and opportunities for prevention. Spine (Phila Pa 1976) 2011;36:1639–44. https://doi.org/10.1097/BRS.0b013e31822a982f.

[119]   Hill G, Nagaraja S, Bridges A, Vosoughi AS, Goel VK, Dreher ML. Mechanical performance of tra-ditional distraction-based dual growing rod constructs. Spine Journal 2019;19:744–54. https://doi.org/10.1016/j.spinee.2018.09.006.

[120]   Luque ER. Paralytic scoliosis in growing children. Clin Orthop Relat Res 1982;163:202–9. https://doi.org/10.1097/00003086-198203000-00030.

[121]   McCarthy RE, Luhmann S, Lenke L, McCullough FL. The shilla growth guidance technique for early-onset spinal deformities at 2-year follow-up: A preliminary report. Journal of Pediatric Ortho-paedics 2014;34:1–7. https://doi.org/10.1097/BPO.0b013e31829f92dc.

[122]   Chorney JML, Kain ZN. Behavioral analysis of children's response to induction of anesthesia. An-esth Analg 2009. https://doi.org/10.1213/ane.0b013e3181b412cf.

A

[123] Matsumoto H, Williams BA, Corona J, Comer JS, Fisher PW, Neria Y, et al. Psychosocial Effects of Repetitive Surgeries in Children With Early-Onset Scoliosis: Are We Putting Them at Risk? Journal of Pediatric Orthopaedics 2014;34:172–8.

[124] Reichel D, Schanz J. Developmental psychological aspects of scoliosis treatment. Pediatr Rehabil 2003;37:293–315. https://doi.org/10.1080/13638490310001644593.

[125] Lemans JVC, Wijdicks SPJ, Koutsoliakos I, Hekman EEG, Agarwal A, Castelein RM, et al. Distraction forces on the spine in early-onset scoliosis: A systematic review and meta-analysis of clinical and biomechanical literature. J Biomech 2021;124:110571. https://doi.org/10.1016/j.jbiomech.2021.110571.

[126] Lemans JVC, Kodigudla M, Kelkar A, Kruyt MC, Goel VK, Agarwal A. Spring Distraction System for Early Onset Scoliosis Provides Continuous Distraction without a Potential Increase in Rod Fractures, Compared to Traditional Growing Rods. Spine Deform 2018;6:819–20.

[127] Rolton D, Thakar C, Wilson-MacDonald J, Nnadi C. Radiological and clinical assessment of the distraction achieved with remotely expandable growing rods in early onset scoliosis. European Spine Journal 2016;25:3371–6. https://doi.org/10.1007/s00586-015-4223-4.

[128] Abolaeha OA, Weber J, Ross LT. Finite element simulation of a scoliotic spine with periodic adjustments of an attached growing rod. Proceedings of the Annual International Conference of the IEEE Engineering in Medicine and Biology Society, EMBS, 2012, p. 5781–5. https://doi.org/10.1109/EMBC.2012.6347308.

[129] Brunette DM, Tengvall P, Textor M, Thomsen P. Titanium in Medicine. Springer; 2001.

[130] Akbarnia BA, Pawelek JB, Cheung KMC, Demirkiran G, Elsebaie H, Emans JB, et al. Traditional growing rods versus magnetically controlled growing rods for the surgical treatment of early-onset scoliosis: A case-matched 2-year study. Spine Deform 2014;2:493–7. https://doi.org/10.1016/j.jspd.2014.09.050.

[131] Dannawi Z, Altaf F, Harshavardhana NS, El Sebaie H, Noordeen H. Early results of a remotely-operated magnetic growth rod in early-onset scoliosis. Journal of Bone and Joint Surgery - Series B 2013;95-B:75–80. https://doi.org/10.1302/0301-620X.95B1.29565.

[132] Hickey BA, Towriss C, Baxter G, Yasso S, James S, Jones A, et al. Early experience of MAGEC magnetic growing rods in the treatment of early onset scoliosis. European Spine Journal 2014;23:61–5. https://doi.org/10.1007/s00586-013-3163-0.

[133] Ugural AC, Fenster SK. Advanced strength and applied elasticity. 2003. https://doi.org/10.1002/qre.4680040324.

[134] Branthwaite MA. Cardiorespiratory consequences of unfused idiopathic scoliosis. Br J Dis Chest 1986;80:360–9. https://doi.org/10.1016/0007-0971(86)90089-6.

[135] Davies G, Reid L. Effect of scoliosis on growth of alveoli and pulmonary arteries and on right ventricle. Arch Dis Child 1971;46:623–32. https://doi.org/10.1136/adc.46.249.623.

[136] Von Elm E, Altman DG, Egger M, Pocock SJ, Gøtzsche PC, Vandenbroucke JP. The Strengthening the Reporting of Observational Studies in Epidemiology (STROBE) Statement: Guidelines for reporting observational studies. J Clin Epidemiol 2008;61:344–9. https://doi.org/10.1136/bmj.39335.541782.ad.

[137] Spurway AJ, Chukwunyerenwa CK, Kishta WE, Hurry JK, El-Hawary R. Sagittal Spine Length Measurement: A Novel Technique to Assess Growth of the Spine. Spine Deform 2016;4:331–7. https://doi.org/10.1016/j.jspd.2016.03.002.

[138] Wijdicks SPJ, Dompeling SD, De Reuver S, Kempen DHR, Castelein RM, Kruyt MC. Reliability and Validity of the Adapted Dutch Version of the Early-Onset Scoliosis-24-Item Questionnaire (EOSQ-24). Spine (Phila Pa 1976) 2019;44:E965–73. https://doi.org/10.1097/BRS.0000000000003017.

[139] Teoh KH, Winson DMG, James SH, Jones A, Howes J, Davies PR, et al. Do magnetic growing rods have lower complication rates compared with conventional growing rods? Spine Journal 2016;16:S40–4. https://doi.org/10.1016/j.spinee.2015.12.099.

[140] Sankar WN, Acevedo DC, Skaggs DL. Comparison of complications among growing spinal implants. Spine (Phila Pa 1976) 2010;35:2091–6. https://doi.org/10.1097/BRS.0b013e3181c6edd7.

[141] Canavese F, Dimeglio A. Normal and abnormal spine and thoracic cage development. World J Orthop 2013;4:167–74. https://doi.org/10.5312/wjo.v4.i4.167.

[142] Wijdicks SPJ, Skov ST, Li H, Castelein RM, Kruyt MC, Bünger C. 3-Year follow-up of a single magnetically controlled growing rod with contralateral gliding system and apical control for early onset scoliosis. Spine Deform 2020;8:751–61. https://doi.org/10.1007/s43390-020-00098-1.

[143] Skov ST, Wijdicks SPJ, Bünger C, Castelein RM, Li H, Kruyt MC. Treatment of early-onset scoliosis with a hybrid of a concave magnetic driver (magnetic controlled growth rod) and a contralateral

passive sliding rod construct with apical control: preliminary report on 17 cases. Spine Journal 2018;18:122–9. https://doi.org/10.1016/j.spinee.2017.06.027.

[144] Pehrsson K, Larsson S, Oden A, Nachemson A. Long-term follow-up of patients with untreated scoliosis: A study of mortality, causes of death, and symptoms. Spine (Phila Pa 1976) 1992;17:1091–6. https://doi.org/10.1097/00007632-199209000-00014.

[145] Redding GJ, Praud JP, Mayer OH. Pulmonary function testing in children with restrictive chest wall disorders. Pediatr Allergy Immunol Pulmonol 2011;24:89–94. https://doi.org/10.1089/ped.2011.0080.

[146] Papastamelos C, Panitch HB, Allen JL. Chest wall compliance in infants and children with neuromuscular disease. Am J Respir Crit Care Med 1996;154:1045–8. https://doi.org/10.1164/ajrccm.154.4.8887605.

[147] Cheung JPY, Yiu K, Kwan K, Cheung KMC. Mean 6-year follow-up of magnetically controlled growing rod patients with early onset scoliosis: A glimpse of what happens to graduates. Neurosurgery 2019;84:1112–23. https://doi.org/10.1093/neuros/nyy270.

[148] Aslan C, Olgun ZD, Ayik G, Karaokur R, Ozusta S, Demirkiran GH, et al. Does Decreased Surgical Stress Really Improve the Psychosocial Health of Early-onset Scoliosis Patients?: A Comparison of Traditional Growing Rods and Magnetically-controlled Growing Rods Patients Reveals Disappointing Results. Spine (Phila Pa 1976) 2019;44:E656–63. https://doi.org/10.1097/BRS.0000000000002938.

[149] Doany ME, Deniz Olgun Z, Kinikli GI, Bekmez S, Kocyigit A, Demirkiran G, et al. Health-Related Quality of Life in Early-Onset Scoliosis Patients Treated Surgically: EOSQ Scores in Traditional Growing Rod Versus Magnetically Controlled Growing Rods. Spine (Phila Pa 1976) 2018;43:148–53. https://doi.org/10.1097/BRS.0000000000002274.

[150] Miladi L, Khouri N, Pradon J, Elie C, Treluyer JM. One-way self-expanding rod for early-onset scoliosis: early results of a clinical trial of 20 patients. European Spine Journal 2021;30. https://doi.org/10.1007/s00586-021-06732-4.

[151] Bowen DJ, Kreuter M, Spring B, Cofta-Woerpel L, Linnan L, Weiner D, et al. How We Design Feasibility Studies. Am J Prev Med 2009. https://doi.org/10.1016/j.amepre.2009.02.002.

[152] McPherson K, Britton A. Preferences and understanding their effects on health. Qual Saf Health Care 2001;10:i61–6. https://doi.org/10.1136/qhc.0100061.

[153] Miladi L, Gaume M, Khouri N, Johnson M, Topouchian V, Glorion C. Minimally invasive surgery for neuromuscular scoliosis. Spine (Phila Pa 1976) 2018;43. https://doi.org/10.1097/BRS.0000000000002588.

[154] Smith JT, Johnston C, Skaggs D, Flynn J, Vitale M. A New Classification System to Report Complications in Growing Spine Surgery: A Multicenter Consensus Study. J Pediatr Orthop 2015;35:798–803.

[155] Matsumoto H, Williams B, Park HY, Yoshimachi JY, Roye BD, Roye DP, et al. The Final 24-Item Early Onset Scoliosis Questionnaires (EOSQ-24): Validity, Reliability and Responsiveness. Journal of Pediatric Orthopaedics 2018;38:144–51. https://doi.org/10.1097/BPO.0000000000000799.

[156] Morrissy RT, Goldsmith GS, Hall EC, Kehl D, Cowie GH. Measurement of the Cobb angle on radiographs of patients who have scoliosis. Evaluation of intrinsic error. Journal of Bone and Joint Surgery - Series A 1990;72. https://doi.org/10.2106/00004623-199072030-00002.

[157] Eekhout I, de Vet HCW, de Boer MR, Twisk JWR, Heymans MW. Passive imputation and parcel summaries are both valid to handle missing items in studies with many multi-item scales. Stat Methods Med Res 2018;27:1128–40. https://doi.org/10.1177/0962280216654511.

[158] Black N. Why we need observational studies to evaluate the effectiveness of health care. Br Med J 1996;312:1215–8. https://doi.org/10.1136/bmj.312.7040.1215.

[159] Abraham NS, Byrne CJ, Young JM, Solomon MJ. Meta-analysis of well-designed nonrandomized comparative studies of surgical procedures is as good as randomized controlled trials. J Clin Epidemiol 2010;63:238–45. https://doi.org/10.1016/j.jclinepi.2009.04.005.

[160] Jacobs WCH, Kruyt MC, Verbout AJ, Oner FC. Spine surgery research: on and beyond current strategies. Spine Journal 2012;12:706–13. https://doi.org/10.1016/j.spinee.2012.08.424.

[161] Seeger BR, D'A Sutherland A, Clark MS. Orthotic management of scoliosis in Duchenne muscular dystrophy. Arch Phys Med Rehabil 1984;65. https://doi.org/10.1097/01241398-198405000-00035.

[162] Li H, Wu J, Song L, Shao S, Chen Z, Wang J, et al. The efficacy of bracing in the treatment of progressive early-onset scoliosis. Sci Rep 2024;14. https://doi.org/10.1038/s41598-024-61030-5.

[163] Harshavardhana NS, Lonstein JE. Results of Bracing for Juvenile Idiopathic Scoliosis*. Spine Deform 2018;6. https://doi.org/10.1016/j.jspd.2017.10.009.

A

[164] De Salvatore S, Oggiano L, Sessa S, Curri C, Fumo C, Costici PF, et al. Patients treated by magnetic growing rods for early-onset scoliosis reach the expected average growth. Spine Deform 2024. https://doi.org/10.1007/s43390-024-00820-3.

[165] Jamnik AA, Shaw KA, Thornberg D, McClung A, Jo CH, Ramo B, et al. Health-related quality of life and clinical outcomes for magnetically controlled growing rod patients after treatment termination. Spine Deform 2024. https://doi.org/10.1007/s43390-023-00801-y.

[166] Teoh KH, Von Ruhland C, Evans SL, James SH, Jones A, Howes J, et al. Metallosis following implantation of magnetically controlled growing rods in the treatment of scoliosis a case series. Bone and Joint Journal 2016. https://doi.org/10.1302/0301-620X.98B12.38061.

[167] Alberghina F, McManus R, Keogh C, Turner H, Moore D, Noël J, et al. The Evaluation of Serum Metal Ion Levels and Metallosis in Graduated Patients With Magnetically Controlled Growing Rods. Journal of Pediatric Orthopaedics 2024;44. https://doi.org/10.1097/BPO.0000000000002526.

[168] Zhang T, Sze KY, Peng ZW, Cheung KMC, Lui YF, Wong YW, et al. Systematic investigation of metallosis associated with magnetically controlled growing rod implantation for early-onset scoliosis: Investigating metallosis in magnetically controlled growing rod surgery. Bone and Joint Journal 2020;102. https://doi.org/10.1302/0301-620X.102B10.BJJ-2020-0842.R1.

[169] Sharma S, Wu C, Andersen T, Wang Y, Hansen ES, Bünger CE. Prevalence of complications in neuromuscular scoliosis surgery: A literature meta-analysis from the past 15 years. European Spine Journal 2013;22. https://doi.org/10.1007/s00586-012-2542-2.

[170] Veldhoen ES, de Vries A, Schlosser TPC, Kruyt MC, van Eijk RPA, Tersmette JM, et al. Short-term effect and effect on rate of lung function decline after surgery for neuromuscular or syndromic scoliosis. Pediatr Pulmonol 2022;57. https://doi.org/10.1002/ppul.25857.

[171] Gaume M, Hajj R, Khouri N, Johnson MB, Miladi L. One-Way Self-Expanding Rod in Neuromuscular Scoliosis: Preliminary Results of a Prospective Series of 21 Patients. JB JS Open Access 2021;6.

[172] Lemans JVC, Tabeling CS, Scholten EP, Stempels HW, Miladi L, Castelein RM, et al. Surgical treatment of neuromuscular Early Onset Scoliosis with a bilateral posterior one-way rod compared to the Spring Distraction System: study protocol for a limited-efficacy Randomized Controlled Trial (BiPOWR). BMC Musculoskelet Disord 2023;24. https://doi.org/10.1186/s12891-022-06048-4.

[173] Moher D, Schulz KF, Altman DG, Lepage L. The CONSORT statement: Revised recommendations for improving the quality of reports of parallel group randomized trials. BMC Med Res Methodol 2001;1. https://doi.org/10.1186/1471-2288-1-2.

[174] Gaumé M, Saghbiny E, Richard L, Thouement C, Vialle R, Miladi L. Pelvic Fixation Technique Using the Ilio-Sacral Screw for 173 Neuromuscular Scoliosis Patients. Children 2024;11. https://doi.org/10.3390/children11020199.

[175] Maloney WJ, Rinsky LA, Gamble JG. Simultaneous correction of pelvic obliquity, frontal plane, and sagittal plane deformities in neuromuscular scoliosis using a unit rod with segmental sublaminar wires: A preliminary report. Journal of Pediatric Orthopaedics 1990;10. https://doi.org/10.1097/01241398-199011000-00007.

[176] Mainard N, Saghbini E, Langlais T, Metaizeau JD, Choufani E, Cunin V, et al. Clinical and radiographic evolution of graduate patients treated with magnetically controlled growing rods: results of a French multicentre study of 90 patients. European Spine Journal 2023;32. https://doi.org/10.1007/s00586-023-07762-w.

[177] Ramo BA, Roberts DW, Tuason D, McClung A, Paraison LE, Moore HG, et al. Surgical site infections after posterior spinal fusion for neuromuscular scoliosis: A thirty year experience at a single institution. Journal of Bone and Joint Surgery - American Volume 2014;96. https://doi.org/10.2106/JBJS.N.00277.

[178] Poe-Kochert C, Shannon C, Pawelek JB, Thompson GH, Hardesty CK, Marks DS, et al. Final fusion after growing-rod treatment for early onset scoliosis is it really final? Journal of Bone and Joint Surgery 2016;98:1913–7. https://doi.org/10.2106/JBJS.15.01334.

[179] Tabeling CS, Lemans JVC, Top A, Scholten EP, Stempels HW, Schlösser TPC, et al. The Spring Distraction System for Growth-Friendly Surgical Treatment of Early Onset Scoliosis: A Preliminary Report on Clinical Results and Safety after Design Iterations in a Prospective Clinical Trial. J Clin Med 2022;11. https://doi.org/10.3390/jcm11133747.

[180] Benson K, Hartz AJ. A Comparison of Observational Studies and Randomized, Controlled Trials. New England Journal of Medicine 2000;342. https://doi.org/10.1056/nejm200006223422506.

[181] Concato J, Shah N, Horwitz RI. Randomized, Controlled Trials, Observational Studies, and the Hierarchy of Research Designs. New England Journal of Medicine 2000;342. https://doi.org/10.1056/nejm200006223422507.

[182] Fernandes P, Weinstein SL. Natural History of Early Onset Scoliosis. J Bone Joint Surg 2007;89:21–33. https://doi.org/10.2106/jbjs.f.00754.

[183] Beaven A, Gardner AC, Marks DS, Mehta JS, Newton-Ede M, Spilsbury JB. Magnetically controlled growing rods: The experience of mechanical failure from a single center consecutive series of 28 children with a minimum follow-up of 2 years. Asian Spine J 2018;12:794–802. https://doi.org/10.31616/ASJ.2018.12.5.794.

[184] Joyce TJ, Smith SL, Kandemir G, Rushton PRP, Fender D, Bowey AJ, et al. The nuvasive MAGEC rod urgent field safety notice concerning locking pin fracture: How does data from an independent explant center compare? Spine (Phila Pa 1976) 2020;45:872–6. https://doi.org/10.1097/BRS.0000000000003439.

[185] Jenks M, Craig J, Higgins J, Willits I, Barata T, Wood H, et al. The MAGEC System for Spinal Lengthening in Children with Scoliosis: A NICE Medical Technology Guidance. Appl Health Econ Health Policy 2014;12:587–99. https://doi.org/10.1007/s40258-014-0127-4.

[186] Polly DW, Ackerman SJ, Schneider K, Pawelek JB, Akbarnia BA. Cost analysis of magnetically controlled growing rods compared with traditional growing rods for early-onset scoliosis in the US: An integrated health care delivery system perspective. ClinicoEconomics and Outcomes Research 2016;8:457–65. https://doi.org/10.2147/CEOR.S113633.

[187] Wong CKH, Cheung JPY, Cheung PWH, Lam CLK, Cheung KMC. Traditional growing rod versus magnetically controlled growing rod for treatment of early onset scoliosis: Cost analysis from implantation till skeletal maturity. Journal of Orthopaedic Surgery 2017;25:1–10. https://doi.org/10.1177/2309499017705022.

[188] Oetgen ME, McNulty EM, Matthews AL. Cost-Effectiveness of Magnetically Controlled Growing Rods: Who Really Benefits? Spine Deform 2019;7:501–4. https://doi.org/10.1016/j.jspd.2018.09.066.

[189] Glattes RC, Bridwell KH, Lenke LG, Kim YJ, Rinella A, Edwards C. Proximal junctional kyphosis in adult spinal deformity following long instrumented posterior spinal fusion: Incidence, outcomes, and risk factor analysis. Spine (Phila Pa 1976) 2005;30:1643–9. https://doi.org/10.1097/01.brs.0000169451.76359.49.

[190] Centers for Disease Control and Prevention. Procedure-associated Module SSI. 2020.

[191] Cheung JPY, Zhang T, Bow C, Kwan K, Sze KY, Cheung KMC. The Crooked Rod Sign: A New Radiological Sign to Detect Deformed Threads in the Distraction Mechanism of Magnetically Controlled Growing Rods and a Mode of Distraction Failure. Spine (Phila Pa 1976) 2020;45:E346–51. https://doi.org/10.1097/BRS.0000000000003268.

[192] Subramanian T, Ahmad A, Mardare DM, Mayers D, Nnadi C, Kieser DC. A six-year observational study of 31 children with early-onset scoliosis treated using magnetically controlled growing rods with a minimum follow-up of two years. Bone and Joint Journal 2018;100B:1187–200. https://doi.org/10.1302/0301-620X.100B9.BJJ-2018-0031.R2.

[193] Teoh KH, Winson DMG, James SH, Jones A, Howes J, Davies PR, et al. Magnetic controlled growing rods for early-onset scoliosis: A 4-year follow-up. Spine Journal 2016;16:S34–9. https://doi.org/10.1016/j.spinee.2015.12.098.

[194] Smith KR, Hunt TR, Asher MA, Anderson HC, Carson WL, Robinson RG. The effect of a stiff spinal implant on the bone-mineral content of the lumbar spine in dogs. JBJS 1991;73:115–23.

[195] Craven TG, Carson WL, Asher MA, Robinson RG. The effects of implant stiffness on the bypassed bone mineral density and facet fusion stiffness of the canine spine. Spine (Phila Pa 1976) 1994;19:1664–73. https://doi.org/10.1097/00007632-199408000-00003.

[196] Murphy RF, Barfield WR, Emans JB, Akbarnia B, Thompson G, Sponseller P, et al. Minimum 5-Year Follow-up on Graduates of Growing Spine Surgery for Early Onset Scoliosis. Journal of Pediatric Orthopaedics 2020;40:e942-46.

[197] Du JY, Poe-Kochert C, Thompson GH, Hardesty CK, Pawelek JB, Flynn JM, et al. Risk Factors for Reoperation Following Final Fusion After the Treatment of Early-Onset Scoliosis with Traditional Growing Rods. J Bone Joint Surg 2020;102:1672–8. https://doi.org/10.2106/JBJS.20.00312.

[198] Williams BA, Matsumoto H, McCalla DJ, Akbarnia BA, Blakemore LC, Betz RR, et al. Development and initial validation of the classification of early-onset scoliosis (C-EOS). Journal of Bone and Joint Surgery 2014;96. https://doi.org/10.2106/JBJS.M.00253.

[199] Pehrsson K, Danielsson A, Nachemson A. Pulmonary function in adolescent idiopathic scoliosis: A 25 year follow up after surgery or start of brace treatment. Thorax 2001;56:388–93. https://doi.org/10.1136/thorax.56.5.388.

A

[200] Loughenbury PR, Tsirikos AI. Current concepts in the treatment of neuromuscular scoliosis: clinical assessment, treatment options, and surgical outcomes. Bone Jt Open 2022;3. https://doi.org/10.1302/2633-1462.31.BJO-2021-0178.R1.

[201] Lavalva S, Adams A, Macalpine E, Gupta P, Hammerberg K, Thompson GH, et al. Serial Casting in Neuromuscular and Syndromic Early-onset Scoliosis (EOS) Can Delay Surgery over 2 Years. Journal of Pediatric Orthopaedics 2020;40. https://doi.org/10.1097/BPO.0000000000001568.

[202] Nakamura N, Uesugi M, Inaba Y, Machida J, Okuzumi S, Saito T. Use of dynamic spinal brace in the management of neuromuscular scoliosis: A preliminary report. Journal of Pediatric Orthopaedics Part B 2014;23. https://doi.org/10.1097/BPB.0000000000000034.

[203] Karol LA. The Natural History of Early-onset Scoliosis. Journal of Pediatric Orthopaedics 2019;39. https://doi.org/10.1097/BPO.0000000000001351.

[204] Caldas JCS, Pais-Ribeiro JL, Carneiro SR. General anesthesia, surgery and hospitalization in children and their effects upon cognitive, academic, emotional and sociobehavioral development - A review. Paediatr Anaesth 2004;14. https://doi.org/10.1111/j.1460-9592.2004.01350.x.

[205] Peiro-Garcia A, Bourget-Murray J, Suarez-Lorenzo I, Ferri-De-Barros F, Parsons D. Early complications in vertical expandable prosthetic titanium rib and magnetically controlled growing rods to manage early onset scoliosis. Int J Spine Surg 2021;15. https://doi.org/10.14444/8048.

[206] Akbarnia BA, Cheung K, Noordeen H, Elsebaie H, Yazici M, Dannawi Z, et al. Next generation of growth-sparing techniques: Preliminary clinical results of a magnetically controlled growing rod in 14 patients with early-onset scoliosis. Spine (Phila Pa 1976) 2013;38. https://doi.org/10.1097/BRS.0b013e3182773560.

[207] Kwan KYH, Alanay A, Yazici M, Demirkiran G, Helenius I, Nnadi C, et al. Unplanned Reoperations in Magnetically Controlled Growing Rod Surgery for Early Onset Scoliosis with a Minimum of Two-Year Follow-Up. Spine (Phila Pa 1976) 2017;42:E1410–4. https://doi.org/10.1097/BRS.0000000000002297.

[208] Wong DC, Nafo W, Lu WW, Chee Cheung KM. A biomechanical study on the effect of lengthening magnitude on spine off-loading in magnetically controlled growing rod surgery: Implications on lengthening frequency. Journal of Orthopaedic Surgery 2021;29. https://doi.org/10.1177/23094990211042237.

[209] Del Mar Pozo-Balado M, Matsumoto H, Vitale MG, Praena-Fernandez JM, Farrington DM. Reliability and validity of the adapted Spanish version of the early-onset scoliosis-24 questionnaire. Spine (Phila Pa 1976) 2016;41. https://doi.org/10.1097/BRS.0000000000001322.

[210] Demirkiran HG, Kinikli GI, Olgun ZD, Kamaci S, Yavuz Y, Vitale MG, et al. Reliability and validity of the adapted Turkish version of the early-onset scoliosis-24-item questionnaire (EOSQ-24). Journal of Pediatric Orthopaedics 2015;35. https://doi.org/10.1097/bpo.0000000000000378.

[211] Ramo BA, McClung A, Jo CH, Sanders JO, Yaszay B, Oetgen ME. Effect of Etiology, Radiographic Severity, and Comorbidities on Baseline Parent-Reported Health Measures for Children with Early-Onset Scoliosis. Journal of Bone and Joint Surgery 2021;103. https://doi.org/10.2106/JBJS.20.00819.

[212] Molland RS, Diep LM, Brox JI, Stuge B, Holm I, Kibsgard TJ. Reliability and Construct Validity of the Adapted Norwegian Version of the Early-Onset Scoliosis 24-item Questionnaire. J Am Acad Orthop Surg Glob Res Rev 2018;2. https://doi.org/10.5435/JAAOSGlobal-D-17-00066.

[213] Matsumoto H, Skaggs DL, Akbarnia BA, Pawelek JB, Hilaire TS, Levine S, et al. Comparing health-related quality of life and burden of care between early-onset scoliosis patients treated with magnetically controlled growing rods and traditional growing rods: a multicenter study. Spine Deform 2021;9. https://doi.org/10.1007/s43390-020-00173-7.

[214] Soliman HAG. Health-related quality of life and body image disturbance of adolescents with severe untreated idiopathic early-onset scoliosis in a developing country. Spine (Phila Pa 1976) 2018;43. https://doi.org/10.1097/BRS.0000000000002686.

[215] Eekhout I, De Vet HCW, Twisk JWR, Brand JPL, De Boer MR, Heymans MW. Missing data in a multi-item instrument were best handled by multiple imputation at the item score level. J Clin Epidemiol 2014;67. https://doi.org/10.1016/j.jclinepi.2013.09.009.

[216] Benjamini Y, Yekutieli D. The control of the false discovery rate in multiple testing under dependency. Ann Stat 2001;29. https://doi.org/10.1214/aos/1013699998.

[217] Copay AG, Subach BR, Glassman SD, Polly DW, Schuler TC. Understanding the minimum clinically important difference: a review of concepts and methods. Spine Journal 2007;7. https://doi.org/10.1016/j.spinee.2007.01.008.

[218] Matsumoto H, Marciano G, Redding G, Ha J, Luhmann S, Garg S, et al. Association between health-related quality of life outcomes and pulmonary function testing. Spine Deform 2021;9. https://doi.org/10.1007/s43390-020-00190-6.

[219] Shaw KA, Ramo B, McClung A, Thornberg D, Yazsay B, Sturm P, et al. Impact of surgical treatment on parent-reported health related quality of life measures in early-onset scoliosis: stable but no improvement at 2 years. Spine Deform 2023;11. https://doi.org/10.1007/s43390-022-00572-y.

[220] Hell AK, Braunschweig L, Behrend J, Lorenz HM, Tsaknakis K, Von Deimling U, et al. Health-related quality of life in early-onset-scoliosis patients treated with growth-friendly implants is influenced by etiology, complication rate and ambulatory ability. BMC Musculoskelet Disord 2019;20. https://doi.org/10.1186/s12891-019-2969-2.

[221] Schlösser TP, Kruyt MC, Tsirikos AI. Surgical management of early-onset scoliosis: indications and currently available techniques. Orthop Trauma 2021;35. https://doi.org/10.1016/j.mporth.2021.09.004.

[222] Hardesty CK, Huang RP, El-Hawary R, Samdani A, Hermida PB, Bas T, et al. Early-Onset Scoliosis: Updated Treatment Techniques and Results. Spine Deform 2018;6. https://doi.org/10.1016/j.jspd.2017.12.012.

[223] Smith JR, Samdani AF, Pahys J, Ranade A, Asghar J, Cahill P, et al. The role of bracing, casting, and vertical expandable prosthetic titanium rib for the treatment of infantile idiopathic scoliosis: A single-institution experience with 31 consecutive patients - Clinical article. J Neurosurg Spine 2009;11. https://doi.org/10.3171/2009.1.SPINE08253.

[224] Dickson RA. Conservative treatment for idiopathic scoliosis. Journal of Bone and Joint Surgery - Series B 1985;67. https://doi.org/10.1302/0301-620x.67b2.3872301.

[225] Lemans JVC, Top A, Tabeling CS, Scholten EP, Stempels HW, Schlösser TPC, et al. Health-related quality of life in early onset scoliosis patients treated with the spring distraction system: what to expect in the first 2 years after surgery. Spine Deform 2023. https://doi.org/10.1007/s43390-023-00777-9.

[226] Johnston CE. Apical control techniques in the management of severe early onset scoliosis. The Growing Spine: Management of Spinal Disorders in Young Children: Third Edition, 2022. https://doi.org/10.1007/978-3-030-84393-9_43.

[227] Lemans JVC, Öner FC, Wijdicks SPJ, Ekkelenkamp MB, Vogely HC, Kruyt MC. The efficacy of intrawound vancomycin powder and povidone-iodine irrigation to prevent surgical site infections in complex instrumented spine surgery. Spine Journal 2019;19. https://doi.org/10.1016/j.spinee.2019.05.592.

[228] Tabeling CS, Lemans JVC, Kruyt MC. Comment on Grabala et al. Radiological Outcomes of Magnetically Controlled Growing Rods for the Treatment of Children with Various Etiologies of Early-Onset Scoliosis-A Multicenter Study. J. Clin. Med. 2024, 13, 1529. J Clin Med 2024;13. https://doi.org/10.3390/jcm13082434.

[229] Grabala P, Gupta MC, Pereira DE, Latalski M, Danielewicz A, Glowka P, et al. Radiological Outcomes of Magnetically Controlled Growing Rods for the Treatment of Children with Various Etiologies of Early-Onset Scoliosis—A Multicenter Study. J Clin Med 2024;13. https://doi.org/10.3390/jcm13061529.

[230] McIntosh AL, Booth A, Oetgen ME. Unplanned return to the operating room (UPROR) occurs in 40% of MCGR patients at an average of 2 years after initial implantation. Spine Deform 2024;12:1823–9. https://doi.org/10.1007/s43390-024-00911-1.

[231] Dubousset J. Scoliosis and its pathophysiology do we understand it? Spine (Phila Pa 1976) 2001;26:1001. https://doi.org/10.1097/00007632-200105010-00002.

[232] Janssen MMA, Vincken KL, Kemp B, Obradov M, De Kleuver M, Viergever MA, et al. Pre-existent vertebral rotation in the human spine is influenced by body position. European Spine Journal 2010;19:1728–34. https://doi.org/10.1007/s00586-010-1400-3.

[233] Kouwenhoven JWM, Smit TH, Van Der Veen AJ, Kingma I, Van Dieën JH, Castelein RM. Effects of dorsal versus ventral shear loads on the rotational stability of the thoracic spine: A biomechanical porcine and human cadaveric study. Spine (Phila Pa 1976) 2007;32:2545–50. https://doi.org/10.1097/BRS.0b013e318158cd86.

[234] Wessels M, Hekman EEG, Kruyt MC, Castelein RM, Homminga JJ, Verkerke GJ. Spinal shape modulation in a porcine model by a highly flexible and extendable non-fusion implant system. European Spine Journal 2016;25:2975–83. https://doi.org/10.1007/s00586-016-4570-9.

[235] Janssen MMA, De Wilde RF, Kouwenhoven JWM, Castelein RM. Experimental animal models in scoliosis research: A review of the literature. Spine Journal 2011;11:347–58. https://doi.org/10.1016/j.spinee.2011.03.010.

A

[236] Purnama KE, Wilkinson MHF, Veldhuizen AG, Van Ooijen PMA, Lubbers J, Burgerhof JGM, et al. A framework for human spine imaging using a freehand 3D ultrasound system. Technology and Health Care 2010;18:1–17. https://doi.org/10.3233/THC-2010-0565.

[237] Sardjono TA, Wilkinson MHF, Veldhuizen AG, Van Ooijen PMA, Purnama KE, Verkerke GJ. Automatic cobb angle determination from radiographic images. Spine (Phila Pa 1976) 2013;38:E1256–62. https://doi.org/10.1097/BRS.0b013e3182a0c7c3.

[238] Meijer GJM, Homminga J, Veldhuizen AG, Verkerke GJ. Influence of interpersonal geometrical variation on spinal motion segment stiffness. Spine (Phila Pa 1976) 2011;36:E929–35. https://doi.org/10.1097/BRS.0b013e3181fd7f7f.

[239] Meijer GJM, Homminga J, Hekman EEG, Veldhuizen AG, Verkerke GJ. The effect of three-dimensional geometrical changes during adolescent growth on the biomechanics of a spinal motion segment. J Biomech 2010;43:1590–7. https://doi.org/10.1016/j.jbiomech.2010.01.028.

[240] Barrios C, Lloris JM, Alonso J, Maruenda B, Burgos J, Llombart-Blanco R, et al. Novel porcine experimental model of severe progressive thoracic scoliosis with compensatory curves induced by interpedicular bent rigid temporary tethering. Journal of Orthopaedic Research 2018;36:174–82. https://doi.org/10.1002/jor.23617.

[241] Bogie R, Roth AK, Willems PC, Weegen vd W, Arts JJ, van Rhijn LW. The Development of a Representative Porcine Early-Onset Scoliosis Model With a Standalone Posterior Spinal Tether. Spine Deform 2017;5:2–10. https://doi.org/10.1016/j.jspd.2016.09.002.

[242] Roth AK, Bogie R, Jacobs E, Arts JJ, Van Rhijn LW. Large animal models in fusionless scoliosis correction research: A literature review. Spine Journal 2013;13:675–88. https://doi.org/10.1016/j.spinee.2013.02.043.

[243] Newton PO, Upasani V V., Farnsworth CL, Oka R, Chambers RC, Dwek J, et al. Spinal growth modulation with use of a tether in an immature porcine model. Journal of Bone and Joint Surgery - Series A 2008;90:2695–706. https://doi.org/10.2106/JBJS.G.01424.

[244] Wessels M, Hekman EEG, Verkerke GJ. Mechanical behavior of a novel non-fusion scoliosis correction device. J Mech Behav Biomed Mater 2013;27:107–14. https://doi.org/10.1016/j.jmbbm.2013.07.006.

[245] McLain RF, Yerby SA, Moseley TA. Comparative morphometry of L4 vertebrae: comparison of large animal models for the human lumbar spine. Spine (Phila Pa 1976) 2002;27:E200–6. https://doi.org/10.1097/00007632-200204150-00005.

[246] Bozkus H, Crawford NR, Chamberlain RH, Valenzuela TD, Espinoza A, Yüksel Z, et al. Comparative anatomy of the porcine and human thoracic spines with reference to thoracoscopic surgical techniques. Surgical Endoscopy and Other Interventional Techniques 2005;19:1652–65. https://doi.org/10.1007/s00464-005-0159-9.

[247] Dath R, Ebinesan AD, Porter KM, Miles AW. Anatomical measurements of porcine lumbar vertebrae. Clinical Biomechanics 2007;22:607–13. https://doi.org/10.1016/j.clinbiomech.2007.01.014.

[248] Smit TH. The use of a quadruped as an in vivo model for the study of the spine - Biomechanical considerations. European Spine Journal 2002;11:137–44. https://doi.org/10.1007/s005860100346.

[249] Sheng SR, Wang XY, Xu HZ, Zhu GQ, Zhou YF. Anatomy of large animal spines and its comparison to the human spine: A systematic review. European Spine Journal 2010;19:46–56. https://doi.org/10.1007/s00586-009-1192-5.

[250] Busscher I, Ploegmakers JJW, Verkerke GJ, Veldhuizen AG. Comparative anatomical dimensions of the complete human and porcine spine. European Spine Journal 2010;19:1104–14. https://doi.org/10.1007/s00586-010-1326-9.

[251] Busscher I, Van Der Veen AJ, Van Dieen JH, Kingma I, Verkerke GJ, Veldhuizen AG. In Vitro biomechanical characteristics of the spine: A comparison between human and porcine spinal segments. Spine (Phila Pa 1976) 2010;35:E35–42. https://doi.org/10.1097/BRS.0b013e3181b21885.

[252] Ouellet J, Odent T. Animal models for scoliosis research: State of the art, current concepts and future perspective applications. European Spine Journal 2013;22:81–95. https://doi.org/10.1007/s00586-012-2396-7.

[253] Schwab F, Patel A, Lafage V, Farcy JP. A porcine model for progressive thoracic scoliosis. Spine (Phila Pa 1976) 2009;34:E397–404. https://doi.org/10.1097/BRS.0b013e3181a27156.

[254] Zheng X, Sun X, Qiu Y, Zhu ZZ, Bin W, Ding YT, et al. A porcine early-onset scoliosis model created using a posterior mini-invasive method a pilot study. J Spinal Disord Tech 2014;27:E294–300. https://doi.org/10.1097/BSD.0000000000000117.

[255] Odent T, Cachon T, Peultier B, Gournay J, Jolivet E, Elie C, et al. Porcine model of early onset scoliosis based on animal growth created with posterior mini-invasive spinal offset tethering A preliminary report. European Spine Journal 2011;20:1869–76. https://doi.org/10.1007/s00586-011-1830-6.

[256]   Sarwahi V, Galina J, Atlas A, Gecelter R, Hasan S, Amaral TD, et al. Scoliosis Surgery Normalizes Cardiac Function in Adolescent Idiopathic Scoliosis Patients. Spine (Phila Pa 1976) 2021. https://doi.org/10.1097/BRS.0000000000004060.

[257]   Castelein RM, Pasha S, Cheng JCY, Dubousset J. Idiopathic Scoliosis as a Rotatory Decompensation of the Spine. Journal of Bone and Mineral Research 2020;35. https://doi.org/10.1002/jbmr.4137.

[258]   Helenius I, Remes V, Yrjönen T, Ylikoski M, Schlenzka D, Helenius M, et al. Harrington and Cotrel-Dubousset Instrumentation in Adolescent Idiopathic Scoliosis: Long-Term Functional and Radiographic Outcomes. Journal of Bone and Joint Surgery - Series A 2003;85. https://doi.org/10.2106/00004623-200312000-00006.

[259]   Wijdicks SPJ, Lemans JVC, Overweg G, Hekman EEG, Castelein RM, Verkerke GJ, et al. Induction of a representative idiopathic-like scoliosis in a porcine model using a multidirectional dynamic spring-based system. Spine Journal 2021;21. https://doi.org/10.1016/j.spinee.2021.03.015.

[260]   Köhn F, Sharifi AR, Simianer H. Modeling the growth of the Goettingen minipig. J Anim Sci 2007;85. https://doi.org/10.2527/jas.2006-271.

[261]   Leary S, Underwood W, Anthony R, Cartner S, Greenacre C, Gwaltney-Brant S, et al. AVMA guidelines for Euthanasia of animals:2020 edition. 2020.

[262]   Pearcy MJ, Tibrewal SB. Axial rotation and lateral bending in the normal lumbar spine measured by three-dimensional radiography. Spine (Phila Pa 1976) 1984. https://doi.org/10.1097/00007632-198409000-00008.

[263]   Willems JM, Jull GA, Ng JKF. An in vivo study of the primary and coupled rotations of the thoracic spine. Clinical Biomechanics 1996. https://doi.org/10.1016/0268-0033(96)00017-4.

[264]   Newton PO, Bartley CE, Bastrom TP, Kluck DG, Saito W, Yaszay B. Anterior Spinal Growth Modulation in Skeletally Immature Patients with Idiopathic Scoliosis: A Comparison with Posterior Spinal Fusion at 2 to 5 Years Postoperatively. J Bone Joint Surg Am 2020;102:769–77. https://doi.org/10.2106/JBJS.19.01176.

[265]   Xu L, Sun X, Du C, Zhou Q, Shi B, Zhu Z, et al. Is Growth-friendly Surgical Treatment Superior to One-stage Posterior Spinal Fusion in 9- to 11-year-old Children with Congenital Scoliosis? Clin Orthop Relat Res 2020;478:2375–86. https://doi.org/10.1097/CORR.0000000000001377.

[266]   Keil LG, Nash AB, Stürmer T, Golightly YM, Lin FC, Stone JD, et al. When is a growth-friendly strategy warranted? A matched comparison of growing rods versus primary posterior spinal fusion in juveniles with early-onset scoliosis. Journal of Pediatric Orthopaedics 2021. https://doi.org/10.1097/BPO.0000000000001926.

[267]   Lemans JVC, Kodigudla MK, Kelkar A V., Jayaswal D, Castelein RM, Kruyt MC, et al. Finite Element Comparison of the Spring Distraction System and the Traditional Growing Rod for the Treatment of Early Onset Scoliosis. Spine (Phila Pa 1976) 2022;47:E456–65. https://doi.org/10.1097/BRS.0000000000004297.

[268]   Alanay A, Yucekul A, Abul K, Ergene G, Senay S, Ay B, et al. Thoracoscopic Vertebral Body Tethering for Adolescent Idiopathic Scoliosis: Follow-up Curve Behavior According to Sanders Skeletal Maturity Staging. Spine (Phila Pa 1976) 2020;45:E1483–92. https://doi.org/10.1097/BRS.0000000000003643.

[269]   Andry N. L'orthopédie ou l'art de prévenir et de corriger dans les enfants les difformités du corps. vol. 2. 1741.

[270]   Nachemson A. A long term follow-up study of non-treated scoliosis. Acta Orthop 1968;39. https://doi.org/10.3109/17453676808989664.

[271]   Bauer JM, Yorgova P, Neiss G, Rogers K, Sturm PF, Sponseller PD, et al. Early Onset Scoliosis: Is there an Improvement in Quality of Life with Conversion from Traditional Growing Rods to Magnetically Controlled Growing Rods? Journal of Pediatric Orthopaedics 2019;39:E284–8. https://doi.org/10.1097/BPO.0000000000001299.

[272]   Elefteriou F, Kolanczyk M, Schindeler A, Viskochil DH, Hock JM, Schorry EK, et al. Skeletal abnormalities in neurofibromatosis type 1: Approaches to therapeutic options. Am J Med Genet A 2009;149. https://doi.org/10.1002/ajmg.a.33045.

[273]   Wilkinson JT, Songy CE, Bumpass DB, McCullough FL, McCarthy RE. Curve Modulation and Apex Migration Using Shilla Growth Guidance Rods for Early-onset Scoliosis at 5-Year Follow-up. Journal of Pediatric Orthopaedics 2019;39. https://doi.org/10.1097/BPO.0000000000000983.

[274]   Heijboer RRO, Heemskerk JL, Vorrink SNW, Kempen DHR. The Prevalence of Cancer in Dutch Female Patients with Idiopathic Scoliosis Compared with the General Population. J Clin Med 2024;13. https://doi.org/10.3390/jcm13092616.

A

[275]   Simony A, Hansen EJ, Christensen SB, Carreon LY, Andersen MO. Incidence of cancer in adolescent idiopathic scoliosis patients treated 25 years previously. European Spine Journal 2016;25. https://doi.org/10.1007/s00586-016-4747-2.

[276]   Iwasaka-Neder J, Bedoya MA, Connors J, Warfield S, Bixby SD. Morphometric and clinical comparison of MRI-based synthetic CT to conventional CT of the hip in children. Pediatr Radiol 2024. https://doi.org/10.1007/s00247-024-05888-7.

[277]   Costa L, Schlosser TPC, Seevinck P, Kruyt MC, Castelein RM. The three-dimensional coupling mechanism in scoliosis and its consequences for correction. Spine Deform 2023;11. https://doi.org/10.1007/s43390-023-00732-8.

[278]   Yilgor C, Efendiyev A, Akbiyik F, Demirkiran G, Senkoylu A, Alanay A, et al. Metal Ion Release During Growth-Friendly Instrumentation for Early-Onset Scoliosis: A Preliminary Study. Spine Deform 2018;6. https://doi.org/10.1016/j.jspd.2017.06.005.

[279]   Urban RM, Jacobs JJ, Tomlinson MJ, Gavrilovic J, Black J, Peoc'h M. Dissemination of wear particles to the liver, spleen, and abdominal lymph nodes of patients with hip or knee replacement. Journal of Bone and Joint Surgery 2000;82. https://doi.org/10.2106/00004623-200004000-00002.

[280]   Martin S, Cobetto N, Larson AN, Aubin C-E. Biomechanical modeling and assessment of lumbar vertebral body tethering configurations. Spine Deform 2023;11:1041–8. https://doi.org/10.1007/s43390-023-00697-8.

[281]   Jayaswal D, Kodigudla M, Kelkar A, Goel V, Palepu V. Validation of a patient-specific finite element analysis framework for identification of growing rod-failure regions in early onset scoliosis patients. Spine Deform 2024;12:941–52. https://doi.org/10.1007/s43390-024-00846-7.

[282]   Kok J, Shcherbakova YM, Schlösser TPC, Seevinck PR, van der Velden TA, Castelein RM, et al. Automatic generation of subject-specific finite element models of the spine from magnetic resonance images. Front Bioeng Biotechnol 2023;11. https://doi.org/10.3389/fbioe.2023.1244291.

[283]   ARKIN AM, KATZ JF. The effects of pressure on epiphyseal growth; the mechanism of plasticity of growing bone. J Bone Joint Surg Am 1956;38 A. https://doi.org/10.2106/00004623-195638050-00009.

[284]   Roser MJ, Askin GN, Labrom RD, Zahir SF, Izatt M, Little JP. Vertebral body tethering for idiopathic scoliosis: a systematic review and meta-analysis. Spine Deform 2023;11. https://doi.org/10.1007/s43390-023-00723-9.

[285]   Tromp IN, Foolen J, van Doeselaar M, Zhang Y, Chan D, Kruyt MC, et al. Comparison of annulus fibrosus cell collagen remodeling rates in a microtissue system. Journal of Orthopaedic Research 2021;39. https://doi.org/10.1002/jor.24921.

[286]   Bushell GR, Ghosh P, Taylor TKF, Sutherland JM. The collagen of the intervertebral disc in adolescent idiopathic scoliosis. Journal of Bone and Joint Surgery - Series B 1979;61. https://doi.org/10.1302/0301-620x.61b4.500764.

[287]   de Reuver S, Homans JF, Houben ML, Schlösser TPC, Ito K, Kruyt MC, et al. Early Sagittal Shape of the Spine Predicts Scoliosis Development in a Syndromic (22q11.2DS) Population: A Prospective Longitudinal Study. J Bone Joint Surg Am 2024;106:2256–63. https://doi.org/10.2106/JBJS.23.01096.

[288]   Lai KKL, Lee TTY, Lau HHT, Chu WCW, Cheng JCY, Castelein RM, et al. Monitoring of Curve Progression in Patients with Adolescent Idiopathic Scoliosis Using 3-D Ultrasound. Ultrasound Med Biol 2024;50. https://doi.org/10.1016/j.ultrasmedbio.2023.11.011.

Appendix III: Publication List

Publications which form the basis of this thesis:

- Lemans JVC, Wijdicks SPJ, Koutsoliakos I, et al. Distraction forces on the spine in early-onset scoliosis: A systematic review and meta-analysis of clinical and biomechanical literature. J Biomech. 2021;124:110571

- Wijdicks SPJ, Lemans JVC, Verkerke GJ, Noordmans HJ, Castelein RM, Kruyt MC. The potential of spring distraction to dynamically correct complex spinal deformities in the growing child. European Spine Journal. 2021;30(3):714-723

- Lemans JVC, Wijdicks SPJ, Castelein RM, Kruyt MC. Spring Distraction System for Dynamic Growth Guidance of Early Onset Scoliosis: 2 Year Prospective Follow-up of 24 Patients. The Spine Journal. 2021;21(4):671-681

- Lemans JVC, Tabeling CS, Castelein RM, Kruyt MC. Identifying Complications and Failure Modes of Innovative Growing Rod Configurations Using the (Hybrid) Magnetically Controlled Growing Rod and the Spring Distraction System. Spine Deform. 2021;9:1679-1689

- Wijdicks SPJ, Lemans JVC, Overweg G, et al. Induction of a representative idiopathic-like scoliosis in a porcine model using a multidirectional dynamic spring-based system. Spine Journal. 2021;21(8)

- Navarro-Ramirez R, Ferland CE, Miladi L, et al. Other posterior growth-friendly systems. In: The Growing Spine: Management of Spinal Disorders in Young Children: Third Edition; 2022. doi:10.1007/978-3-030-84393-9_46

- Lemans JVC, Kodigudla MK, Kelkar AV, et al. Finite Element Comparison of the Spring Distraction System and the Traditional Growing Rod for the Treatment of Early Onset Scoliosis. Spine (Phila Pa 1976). 2022;47(10):E456-E465

- Lemans JVC, Wijdicks SPJ, Overweg G, et al. Three-dimensional correction of scoliosis by a double spring reduction system as a dynamic internal brace: a pre-clinical study in Göttingen minipigs. Spine Journal. 2022;23(4):599-608

- Tabeling CS, Lemans JVC, Top A, et al. The Spring Distraction System for Growth-Friendly Surgical Treatment of Early Onset Scoliosis: A Preliminary Report on Clinical Results and Safety after Design Iterations in a Prospective Clinical Trial. J Clin Med. 2022;11(13)

- Lemans JVC, Tabeling CS, Scholten EP, et al. Surgical treatment of neuromuscular Early Onset Scoliosis with a bilateral posterior one-way rod compared to the Spring Distraction System: study protocol for a limited-efficacy Randomized Controlled Trial (BiPOWR). BMC Musculoskelet Disord. 2023;24(1)

- Lemans JVC, Top A, Tabeling CS, et al. Health-related quality of life in early onset scoliosis patients treated with the spring distraction system: what to expect in the first 2 years after surgery. Spine Deform 12, 489–499 (2024)

- Lemans JVC, Tabeling CS, Stadhouder A et al. One Year Results of the Randomized BiPOWR Trial Comparing the Spring Distraction System (SDS) and the One Way Self-Expanding Rod (OWSER) for the Correction of Neuromuscular and Syndromic Early Onset Scoliosis. Accepted in JPOSNA.

A

Manuscripts not included in this thesis

- Govaert GAM, Bosch P, IJpma FFA, et al. High diagnostic accuracy of white blood cell scintigraphy for fracture related infections: Results of a large retrospective single-center study. Injury. 2018;49(6). doi:10.1016/j.injury.2018.03.018

- Lemans JVC, Wijdicks SPJ, Boot W, et al. Intrawound Treatment for Prevention of Surgical Site Infections in Instrumented Spinal Surgery: A Systematic Comparative Effectiveness Review and Meta-Analysis. Glob Spine J. 2019;9(2). doi:10.1177/2192568218786252

- Lemans JVC, Öner FC, Wijdicks SPJ, Ekkelenkamp MB, Vogely HC, Kruyt MC. The efficacy of intra-wound vancomycin powder and povidone-iodine irrigation to prevent surgical site infections in complex instrumented spine surgery. Spine J. 2019;19(10). doi:10.1016/j.spinee.2019.05.592

- Lemans JVC, Hobbelink MGG, IJpma FFA, et al. The diagnostic accuracy of 18 F-FDG PET/CT in diagnosing fracture-related infections. Eur J Nucl Med Mol Imaging. 2019;46(4). doi:10.1007/s00259-018-4218-6

- Shah A, Lemans JVC, Zavatsky J, et al. Spinal balance/alignment-clinical relevance and biomechanics. J Biomech Eng. 2019;141(7). doi:10.1115/1.4043650

- Van Dijk B, Lemans JVC, Hoogendoorn RM, et al. Treating infections with ionizing radiation: A historical perspective and emerging techniques. Antimicrob Resist Infect Control. 2020;9(1). doi:10.1186/s13756-020-00775-w

- De Reuver S, Costa L, Van Rheenen H, et al. Disc and Vertebral Body Morphology from Birth to Adulthood. Spine (Phila Pa 1976). 2022;47(7). doi:10.1097/BRS.0000000000004278

Letters to the editor:

- Lemans JVC, Muijs SPJ, Kruyt MC. Letter to the editor regarding: Intrawound application of vancomycin changes the responsible germ in elective spine surgery without significant effect on the rate of infection: a randomized prospective study. Musculoskelet Surg. 2019;103(3). doi:10.1007/s12306-019-00596-0

- Lemans JVC, Castelein RM, Kruyt MC. Letter to the editor regarding "Growth-preserving instrumentation in early-onset scoliosis patients with multi-level congenital anomalies." Spine Deform. 2021;9(5). doi:10.1007/s43390-020-00249-4

- Tabeling CS, Lemans JVC, Castelein RM, Kruyt MC. Letter to the editor regarding "Is rod diameter associated with the rate of rod fracture in patients treated with magnetically controlled growing rods? Spine Deform. 2021;9(4). doi:10.1007/s43390-021-00306-6

- Lemans JVC, Schlösser TPC, Castelein RM, Kruyt MC. Comment on Burgos et al. Fusionless All-Pedicle Screws for Posterior Deformity Correction in AIS Immature Patients Permit the Restoration of Normal Vertebral Morphology and Removal of the Instrumentation Once Bone Maturity Is Reached. J. Clin. Med. 2023, 12, 2408. J Clin Med. 2023;12(14). doi:10.3390/jcm12144677

Appendix IV: Dankwoord

Dit werk was niet mogelijk geweest zonder de hulp en ondersteuning van een gigantische groep mensen. Hieronder bedank ik er enkelen.

Prof. dr. Kruyt, beste Moyo. Wat heb ik ontzettend veel van je geleerd. Je bent one-of-a-kind. Een creatieve, volhardende, niet te stoppen trein vol met ideeën, die zich niet tegen laat houden door het stroperige moeras van regelgeving. Je bent geen fan van onzinnige regels en bureaucratie en weet als geen ander hoe je daar op een slimme manier mee om kan gaan. Dank voor de vele brainstormsessies, je kritische blik en voor het feit dat je me altijd veel ruimte hebt geboden om mijn eigen projecten vorm te geven. Ik hoop van harte dat we samen nog ontzettend veel onderzoek gaan doen!

Prof. dr. Castelein, beste René. Je bent een bron van enthousiasme en weet elk project en elke presentatie met flair te brengen. Je had bij elk project precies door wat de kernboodschap was en hoe we deze het beste tot zijn recht konden laten komen. En natuurlijk bedankt voor de fantastische dagen in Kroatië, waar (na een aantal glazen Dingač) elk diner eindigde met gepassioneerde discussies over scoliose. Ik ben trots dat ik één van de laatste provendi ben die jou als promotor heeft.

Sebastiaan, jij bent met Moyo en René het SDS avontuur begonnen. Bedankt voor het me wegwijs maken in de wereld van SDS. Bijna alle projecten die ik heb gedaan waren alleen mogelijk door het fantastische voorwerk dat door jou is gedaan. **Casper,** je bent begonnen als student bij een SDS project, en inmiddels een fantastische opvolger. We hebben samen veel varkens geopereerd, congressen bezocht en ontzettend veel lol gehad op Q. Ik kijk uit naar jouw verdediging over een tijdje.

Ontzettend bedankt alle andere onderzoekers van Q en het Hubrecht: **Abdi, Anneli, Bas, Bruce, Chella, Chien, Dineke, Dunja, Erin, Esmee, Eva, Floris, Jasmijn, Jasper, Jelle, Joëll, Jonneke, Karlijn, Lorenzo, Margo, Margot, Mattie, Mechteld, Milou, Paul, Peter, Razmara, Rob, Ruben, Steven** en **Willem-Paul.** Jullie gaven de onderzoeksdagen kleur. Van ontelbare potjes Nations League minipingpong, tot vele middagen Hideout en natuurlijk ontelbare hitjes met karaoke. Hierbij ook nog een kort excuus voor de gehele Q3 gang, die (toen ik gelukkig op vakantie was) een tijdje is afgesloten door de politie en het Openbaar Ministerie, omdat men niet wist of de wervels die ik had bewaard in de (niet-daarvoor-bedoelde) consumentenvriezer van mensen afkomstig waren of van varkens. Dank Casper, voor je optreden als forensisch expert hierbij, waardoor de verwarring vlot opgehelderd kon worden en alles met een (wel vrij forse) sisser afliep.

A

Bedankt **Pauline** voor het ondersteunen bij de GRADS en BiPOWR studie. En natuurlijk bedankt **Hilde,** voor het bijhouden van alle plannings- en financiële overzichten. Jij hebt me meer dan eens gewezen op aanstaande deadlines van financieringsrapporten of monitorafspraken. En daarnaast ook bedankt voor de gezelligheid buiten werk, met als hoogtepunten de vele keren SinterQlaas die je organiseerde en natuurlijk de dronken karaokeavond in Linköping (waar ik helaas niet heel veel meer van weet). Superveel succes ook met jouw promotietraject.

Dank aan alle studenten, die ontelbare Cobb-hoeken en T1-S1 lengtes hebben gemeten, dag in, dag uit. Speciale dank voor **Isabelle,** ik vond het ontzettend leuk om je te begeleiden. Superleuk dat we samen naar congres konden in Salt Lake City. En ontzettend fijn dat het manuscript nu eindelijk af is!

A special thanks are in order for the fantastic team at E-CORE in Toledo, Ohio. To the late **dr. Goel,** thank you for your stellar guidance in the complex field of finite element analysis. You are one of the fathers of spinal finite element analysis, and with your passing, the world has lost a biomechanical giant. Thank you **Aakash, Manoj, Amey, Daksh and Anoli,** you helped me out when I (time and time again) did not understand anything of Abacus. And thank you, not only for the work we did together, but also for the fun times after work. You guys treated me like family when I was so far from home and for that, I am eternally grateful.

Dank aan alle collega AIOS en ANIOS tijdens mijn klinische werk, door jullie is elke dag zaal, poli of OK een feest. Speciale dank voor Team Libero in het St. Antonius Ziekenhuis, **Arthur, Angélica, Fien en Emma.** Jullie zijn toppers en ik ben enorm blij dat ik jullie nog regelmatig zie.

Dank voor de orthopeden in het St. Antonius ziekenhuis, waar ik de basis heb gelegd voor mijn orthopedische kennis en kunde. Ik ben ontzettend dankbaar dat ik mijn opleiding tot orthopeed bij jullie voort ga zetten. En dank voor de chirurgen in het Diakonessenhuis, die tijdens mijn vooropleiding, opnieuw hebben bewezen dat je iedere (orthopedische) aap kunt leren opereren.

Dank aan al mijn vrienden. **Andel, Anniek, Claudia, Maria, Michelle, Mick, Nick, Renz, Simone** en **Wout.** Al sinds het begin van de studie mijn beste vrienden. Ik hoop dat we als Kingsday nog vele festivals gaan bezoeken. En **Daan, Elian, Karlijn, Marc, Milou, Onno en Wout,** dank voor alle geweldige etentjes en mini-Beco's, laten we dit nog jaren volhouden!

Dank aan mijn paranimfen, **Chien** en **Mick.** Jullie hebben ervoor gezorgd dat deze laatste loodjes niet nóg zwaarder waren. Ik heb heel veel zin in jullie verdediging aankomende maanden.

Mama en papa, dank voor jullie continue steun gedurende het hele traject. Het was niet altijd makkelijk, zeker niet toen papa plotseling ziek werd en geopereerd moest worden. Maar ook daar zijn we goed uitgekomen en ik ben ontzettend blij dat jullie allebei bij mijn verdediging kunnen zijn. Ik hoop dat jullie trots zijn. Ook dank aan de schoonfamilie, **Helma, Arthur, Lotte, Hans, Maartje** en **Aad.** Jullie zijn altijd welkom in het mooie Utrecht.

En als laatste natuurlijk ontzettend bedankt lieve **Ilse.** Na een paar dates ben je me op komen zoeken in Toledo, en sindsdien ben ik ontzettend blij dat wij samen zijn! Zonder jou had ik dit nooit af kunnen maken (en niet alleen omdat jij een epidemiologische topper bent). Ik kan niet wachten op het moment dat jij je proefschrift gaat verdedigen. Ik hou ontzettend van je, en heb ontzettend veel zin om binnenkort met jou in ons nieuwe huisje te gaan wonen. Je bent de liefde van mijn leven.
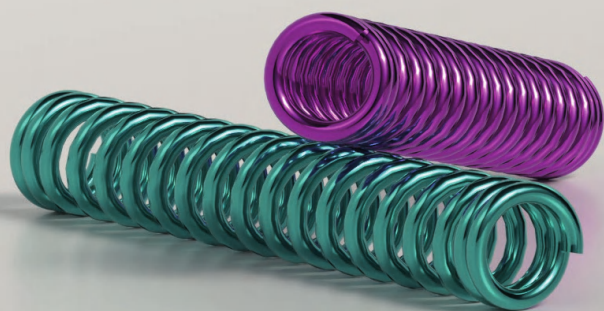
A

Appendix V: Curriculum Vitae

Justin Lemans was born on May 6, 1993 in Utrecht. Following high school, he studied Medicine at Utrecht University. During his Bachelor in Medicine, he started his scientific career at the department of Orthopedic Surgery of UMC Utrecht. Under supervision of prof. Kruyt, he was at the forefront of Dutch research on intra-wound treatments to prevent deep surgical site infections in spinal surgery. With several publications on the intrawound application of vancomycin powder and povidone-iodine solution, he helped to change infection prevention guidelines at UMC Utrecht. The practice of using intra-wound vancomycin powder has now become commonplace around the world. Simultaneously, he performed research in the field of Trauma Surgery under dr. Govaert, with whom he investigated the efficacy of nuclear imaging modalities to diagnose fracture-related infections.

After finishing his Master in Medicine in 2018, he performed a research fellowship at the University of Toledo (Ohio) at the renowned computational biomechanics laboratory of the late dr. Goel (E-CORE), where he learned to use finite element analysis to evaluate implants used in scoliosis surgery.

Following his research fellowship, he performed his PhD research at UMC Utrecht to investigate novel implants to treat Early Onset Scoliosis, with prof. Kruyt and prof. Castelein as his supervisors. During this time, he assisted in the valorization process of the Spring Distraction System, and coordinated several prospective, clinical studies. He combined these clinical investigations, with biomechanical research and was also involved in several animal studies in Göttingen minipigs.

During his time at UMC Utrecht, he has acquired several prestigious research grants, has authored more than 20 publications, and has given many presentations at both national and international conferences. He also co-authored a book chapter in the most recent edition of The Growing Spine (3rd edition).

In 2024, Justin started his residency in Orthopaedic Surgery in ROGO Midden-West. He lives in the city of Utrecht, together with his beautiful girlfriend Ilse and his two cats, Emmy and Oscar.

Justin Lemans

2025